

Stereoselective and Economical Methods for Chemical Synthesis of Essential Medicines

by

Sarah Jane Mear

B.S., University of North Carolina at Chapel Hill (2015)

Submitted to the Department of Chemistry
in partial fulfillment of the requirements for the degree of

Doctor of Philosophy in Chemistry

at the

MASSACHUSETTS INSTITUTE OF TECHNOLOGY

May 2022

© Massachusetts Institute of Technology 2022. All rights reserved.

Author
Department of Chemistry
April 12, 2022

Certified by.....
Timothy F. Jamison
Associate Provost and Robert Robinson Taylor Professor of Chemistry
Thesis Supervisor

Accepted by
Adam Willard
Associate Professor
Graduate Officer

This doctoral thesis has been examined by a Committee of the
Department of Chemistry as follows:

Assistant Professor Alison Wendlandt.....
Thesis Committee Chair
Green C. D. Assistant Professor of Chemistry

Professor Timothy F. Jamison.....
Thesis Supervisor
Associate Provost and Robert Robinson Taylor Professor of Chemistry

Professor Professor Rick Lane Danheiser.....
Thesis Committee Member
A. C. Cope Professor of Chemistry

Stereoselective and Economical Methods for Chemical Synthesis of Essential Medicines

by

Sarah Jane Mear

Submitted to the Department of Chemistry
on April 12, 2022, in partial fulfillment of the
requirements for the degree of
Doctor of Philosophy in Chemistry

Abstract

Executive Summary: Innovation in synthetic chemistry enables pharmaceutical research and development by allowing the exploration of diverse chemical space during drug discovery, and by encouraging the development of economical and sustainable solutions in active pharmaceutical ingredient (API) manufacturing. For a given API, a single stereoisomer often displays preferable chemical and pharmacological properties including potency, stability, solubility, or toxicity. Methods for diastereo- or enantioselective synthesis are highly desirable, for exploration of biological properties of different stereoisomers, or for driving efficiency during drug manufacturing. In this thesis, synthesis of small molecule drugs emtricitabine, lamivudine, bedaquiline, and diazepam was investigated. Stereoselective strategies and cost-of-goods reduction more broadly are described. Lastly, a perspective on reproductive health safety in the chemical laboratory is presented.

Chapter 1: Diazotization of *S*-Sulfonyl-Cysteines. We report the synthesis of enantiomerically enriched β -thio- α -hydroxy and α -chloro carboxylic acid and ester building blocks by diazotization of *S*-sulfonyl-cysteines. Within these pharmaceutically-relevant building blocks, the thiosulfonate protecting group demonstrated resistance to oxidation and attenuation of sulfur's nucleophilicity. The key transformation was optimized by a 2^2 factorial design of experiment, highlighting the unique reactivity of cysteine derivatives in comparison with aliphatic amino acids.

Chapter 2: Synthesis of Emtricitabine and Lamivudine by Chlorotrimethylsilane-Sodium Iodide-Promoted Vorbrüggen Glycosylation. By simply adding water and sodium iodide (NaI) to chlorotrimethylsilane (TMSCl), promotion of a Vorbrüggen glycosylation en route to essential HIV drugs emtricitabine (FTC) and lamivudine (3TC) is achieved. TMSCl–NaI in wet solvent (0.1 M water) activates a 1,3-oxathiolanyl acetate donor for *N*-glycosylation of silylated cytosine derivatives, leading to *cis* oxathiolane products with up to 95% yield and >20:1 d.r.. This telescoped sequence is followed by recrystallization and borohydride reduction, resulting in rapid synthesis of (\pm)-FTC/3TC from a tartrate diester.

Chapter 3: Diastereoselectivity is in the Details: Minor Changes Yield Major Im-

improvements to the Synthesis of Bedaquiline. Bedaquiline is a crucial drug in the global fight against tuberculosis, yet its high price places it out of reach for many patients. Herein, we describe improvements to the key industrial lithiation-addition sequence that enable a higher yielding and therefore more economical synthesis of bedaquiline. A focus on reproducibility and mechanistic understanding led to optimized conditions that double the previously reported yields of racemic bedaquiline simply by changing the lithium amide base and including a salt additive. We anticipate facile implementation of these improvements on manufacturing scale that will increase throughput of this essential medication.

Chapter 4: Synthesis of a Key Precursor to Benzodiazepines by Copper Hydride Reduction of 2,1-benzo[*c*]isoxazole. Benzodiazepines are used broadly for the treatment of anxiety disorders and for general anaesthesia. Herein we describe a new method for synthesis of diazepam precursor 2-amino-5-chlorobenzophenone by *N,O*-reduction of 5-chloro-3-phenylbenzo[*c*]isoxazole using copper hydride. The desired compound is prepared in >80% isolated yield by optimizing reaction parameters to prevent overreduction of the product. We outline future directions including continuous flow processing and purification by recrystallization.

Chapter 5: A Call for Increased Focus on Reproductive Health within Lab Safety Culture. The approach to reproductive health and safety in academic laboratories requires increased focus and a shift in paradigm. Our analysis of the current guidance from more than 100 academic institutions' Chemical Hygiene Plans (CHPs) indicates that the burden to implement laboratory reproductive health and safety practices is often placed on those already pregnant or planning conception. We also found inconsistencies in the classification of potential reproductive toxins by resources generally considered to be authoritative, adding further confusion. In the interest of human health and safe laboratory practice, we suggest straightforward changes that institutions and individual laboratories can make to address these present deficiencies: Provide consistent and clear information to laboratory researchers about reproductive health and normalize the discussion of reproductive health among all researchers. Doing so will promote safer and more inclusive laboratory environments.

Portions of this thesis have been reprinted, adapted, or both, with permission from the respective publishers:

- Chapter 1 adapted with permission from Mear, S. J.; Jamison, T. F. Diazotization of *S*-Sulfonyl-cysteines. *J. Org. Chem.* **2019**, *84*, 15001–15007. DOI: 10.1021/acs.joc.9b02630. Copyright 2019 American Chemical Society. S.J.M. carried out all aspects of this investigation under the mentorship of T.F.J.
- Chapter 2 adapted with permission from Mear, S. J.; Nguyen, L. V.; Rochford, A. J.; Jamison, T. F. Synthesis of (\pm)-Lamivudine and (\pm)-Emtricitabine by Chlorotrimethylsilane-Sodium Iodide Promoted Vorbrüggen Reaction. *J. Org. Chem.* **2022**, *87*, 2887–2897. DOI: 10.1021/acs.joc.1c02772. Copyright 2022 American Chemical Society. S.J.M. led this investigation with strategic guidance from T.F.J. and L.V.N.; A.J.R. synthesized compounds for the substrate scope and synthesis, and contributed to the purification and recrystallization strategy for **17**.
- Chapter 3 is described in the following pre-print article: Mear, S. J.*; Lucas, T.*; Ahlqvist, G. P.*; Robey, J. M. S.; Dietz, J.-P.; Khairnar, P. V.; Maity, S.; Williams, C. L.; Snead, D. R.; Nelson, R. C.; Opatz, T.; Jamison, T. F. Diastereoselectivity is in the Details: Minor Changes Yield Major Improvements to the Synthesis of Bedaquiline. *ChemRxiv* **2022**, *Pre-print*, DOI: 10.26434/chemrxiv-2022-cp3g8. S.J.M., T.L., and G.P.A. contributed equally to the writing of the manuscript. S.J.M. contributed to mechanism (NMR studies), base screen, salt additives, continuous flow, reaction time/temp., and chiral amines. T.L. contributed to mechanism, synthesis of starting material, salt additive effects, scale-up, isolation, and characterization. G.P.A. contributed to mechanism, base screen, and design/implementation of continuous flow. J.M.S.R contributed to mechanism and characterization of side products. J.-P.D. contributed to salt additives. P.V.K. and S.M. validated effects of salt additives and contributed scale-up to 5 and 10 g scale. C.L.W. contributed to screening of secondary amines.
- Chapter 5 adapted with permission from McGeough, C. P.*; Mear, S. J.*; Jamison, T. F. A Call for Increased Focus on Reproductive Health within Lab Safety Culture. *J. Am. Chem. Soc.* **2021**, *143*, 12422–12427. *contributed equally. DOI: 10.1021/jacs.1c03725. Copyright 2021 American Chemical Society.

Thesis Supervisor: Timothy F. Jamison

Title: Associate Provost and Robert Robinson Taylor Professor of Chemistry

Acknowledgments

The care taken in the writing of this thesis is intended to reflect appreciation for my mentors, colleagues, friends, and family, to whom I am forever indebted and whom I acknowledge only glibly here:

My thesis advisor for fostering a productive research environment and for teaching valuable scientific, professional, and decision-making skills.

My thesis committee members for strengthening the department with their teaching abilities and exemplary research programs, and for offering constructive advice throughout my graduate education.

My labmates and friends in MIT chemistry for accompanying me on the research journey as we have developed the emotional endurance that experimental science demands. Shout-out to the TH*GS.

Colleagues at the MIT Department of Chemistry Instrumentation Facility for teaching responsible analytical instrumentation stewardship.

MIT-EHS and Facilities colleagues for maintaining safe lab operations.

The Department of Chemistry Education Office (Chem-Ed) for supporting many practical and social aspects of graduate student life.

MIT student groups including the Chemistry Graduate Student Council, MIT WIC+, and Graduate Housing for providing valuable peer-to-peer connections.

My husband and my daughter who bring me great joy.

Collaborators at the Medicines for All Institute for years of thrilling science.

My parents for prioritizing education and teaching how to balance competing responsibilities of work and family.

Each of my former teachers and mentors who have paved the way for this long-haul journey of scientific education.

*“The skill I was learning was a crucial one,
the patience to read things I could not yet understand.”*
— Tara Westover, *Educated*

*"I have fought the good fight,
I have finished the race,
I have kept the faith."*
— 2 Timothy 4:7

Contents

Title Page	1
Signature Page	3
Abstract	5
Acknowledgements	9
Quotes Page	11
1 Diazotization of <i>S</i>-Sulfonyl-cysteines	19
1.1 Introduction	19
1.2 Results and Discussion	19
1.3 Conclusion	28
1.4 Experimental Section	29
1.4.1 General Remarks	29
1.4.2 Safety Considerations	30
1.4.3 Reaction Optimization	31
1.4.4 Synthesis of Numbered Compounds	35
1.5 Enantiomeric Ratio Analysis by HPLC	45
1.6 2D NMR Data for L-Cystine Diazotization Products	48
1.7 X-Ray Crystallographic Data	49
1.8 ^1H and $^{13}\text{C}\{^1\text{H}\}$ NMR Spectra	51
1.9 References	74

2	Synthesis of Emtricitabine and Lamivudine by Chlorotrimethylsilane–Sodium Iodide-Promoted Vorbrüggen Glycosylation	77
2.1	Introduction	77
2.2	Results and Discussion	78
2.3	Conclusion	91
2.4	Experimental Section	91
2.4.1	General Methods	91
2.4.2	Synthesis of Starting Materials	94
2.4.3	NMR Assay for Glycosyl Iodide Formation Promoted by TMSCl–NaI	96
2.4.4	General Procedure for Optimization of TMSCl–NaI-Promoted Glycosylation	97
2.4.5	Synthesis of Nucleoside Analogs on 1.0 mmol Scale	99
2.4.6	Synthesis of Derivatives for Mechanistic Investigation	102
2.4.7	Synthesis of (±)-FTC/3TC	109
2.5	¹ H and ¹³ C{ ¹ H} NMR Spectra	116
2.6	References	152
3	Diastereoselectivity is in the Details: Minor Changes Yield Major Improvements to the Synthesis of Bedaquiline	155
3.1	Introduction	155
3.2	Results and Discussion	157
3.2.1	Mechanistic Investigation of the Lithiation/1,2-Addition	161
3.2.2	Optimizing for Maximum Yield of Bedaquiline	168
3.2.3	Enantioselective Synthesis of Bedaquiline by Asymmetric Lithiation-Addition	176
3.3	Conclusion	180
3.4	Experimental Section	181
3.4.1	General Experimental Details	181

3.4.2	Synthesis of Starting Materials and Reagents	183
3.4.3	General Procedure: Early Attempts to Reproduce Precedence for Synthesis of 1	185
3.4.4	Influence of Step 2 (1,2-Addition) Temperature on Yield of 1 .	186
3.4.5	Unified Procedure: Baseline for Reaction Optimization Across Research Sites	187
3.4.6	Assay for Recovery of 3 after Benzylic Deprotonation with Lithium Amide Base	188
3.4.7	Reverse Reaction at $-78\text{ }^{\circ}\text{C}$ and Room Temperature Using LDA	189
3.4.8	Reaction of 3a with 2-d₂	189
3.4.9	^1H NMR Characterization of 3a at $-78\text{ }^{\circ}\text{C}$	190
3.4.10	Variable Temperature ^1H NMR Experiment for Reaction Mix- ture Containing 3a	191
3.4.11	Quantification of Formation of 3a by ^1H NMR	192
3.4.12	General Procedure: Screening Secondary Amine Bases	193
3.4.13	General Procedure: Screening Salt Additives	194
3.4.14	General Procedure: Screening LiBr Stoichiometry and LiBr + Secondary Amine Bases	194
3.4.15	Reaction Screening in Continuous Flow	195
3.4.16	General Procedures for Synthesis of 1 on 1–10 g scale	197
3.4.17	General Procedure: Enantioselective Synthesis of Bedaquiline Using Chiral Secondary Amine Bases	201
3.4.18	Supplementary Tables	204
3.5	^1H and $^{13}\text{C}\{^1\text{H}\}$ NMR Spectra	212
3.5.1	Synthesis of Materials 3 and 2·HCl by WuXi AppTech	239
3.6	References	244
4	Synthesis of a Key Precursor to Benzodiazepines by Copper Hydride	
	Reduction of 2,1-Benzo[<i>c</i>]isoxazoles	247
4.1	Introduction	247

4.2	Results and Discussion	250
4.2.1	Feasibility and Side Product Identification	250
4.2.2	Investigation of Monodentate Phosphine Ligands	252
4.2.3	Investigation of Additives, Copper Catalyst Source and Ligand Stoichiometry	254
4.2.4	Reaction Optimization: Temperature, Additives, and Silane Stoichiometry	256
4.2.5	Implementation in Continuous Flow	258
4.2.6	Batch Scale-Up and Purification	264
4.2.7	Conclusion	270
4.3	Experimental Section	272
4.3.1	General Methods	272
4.3.2	General Procedures for Reaction Optimization and Synthesis	273
4.3.3	General Procedure for Initial Screening and Feasibility Assess- ment	274
4.3.4	General Procedure for Investigation of Monodentate Phosphine Ligands	275
4.3.5	General Procedure for Screening Monodentate Phosphine Lig- and Stoichiometry	276
4.3.6	General Procedure for Investigation of Additives and Copper Catalyst Source	277
4.3.7	General Procedure for Screening Temperature, Additives, and Silane Stoichiometry	278
4.3.8	Continuous Flow Trial 1	279
4.3.9	Continuous Flow Trial 2	280
4.3.10	Representative Procedure for Synthesis of (2-amino-5-chlorophenyl)(phenyl)methanone (1) on 2 mmol Scale	280
4.4	^1H and $^{13}\text{C}\{^1\text{H}\}$ NMR Spectra	281

4.5	References	287
5	A Call for Increased Focus on Reproductive Health within Lab Safety Culture	289
5.1	Introduction	289
5.2	Analysis and Perspective	290
5.3	Conclusion	297
	5.3.1 Supporting Figures and Tables	299
	5.3.2 Abbreviations	305
5.4	References	305

Chapter 1

Diazotization of *S*-Sulfonyl-cysteines

1.1 Introduction

Diazotization of naturally-occurring α -amino acids yields enantiomerically enriched α -hydroxy or α -chloro acids, useful building blocks in medicinal chemistry,¹⁻⁴ total synthesis of natural products,⁵⁻⁷ and polymer chemistry.⁸⁻¹¹ Although α -hydroxy and α -chloro acids are commonly prepared by the diazotization of α -amino acids,^{7,12-15} cysteine remains an elusive substrate in this transformation due to the chemically sensitive sulfur atom. Cysteine derivatives offer many opportunities for synthesis and are prominently featured in the selective modification of polypeptides and in drug delivery.¹⁶⁻¹⁹ Herein we report that protection of the sulfur in cysteine as a thiosulfonate enables the synthesis of enantiomerically enriched β -thio- α -hydroxy and α -chloro acids by diazotization (Figure 1-1a).

1.2 Results and Discussion

We were inspired to investigate the synthesis of β -thio- α -hydroxy acids by diazotization of cysteine after the observation of Humber et al.'s use of α -hydroxy acid **1** as an intermediate in the synthesis of nucleoside reverse transcriptase inhibitor lamivudine (**2**) (Figure 1-1b).² In this report, the enantiomerically enriched intermediate was prepared from racemic chlorohydrin, requiring chiral resolution with (-)-brucine.²⁰ A

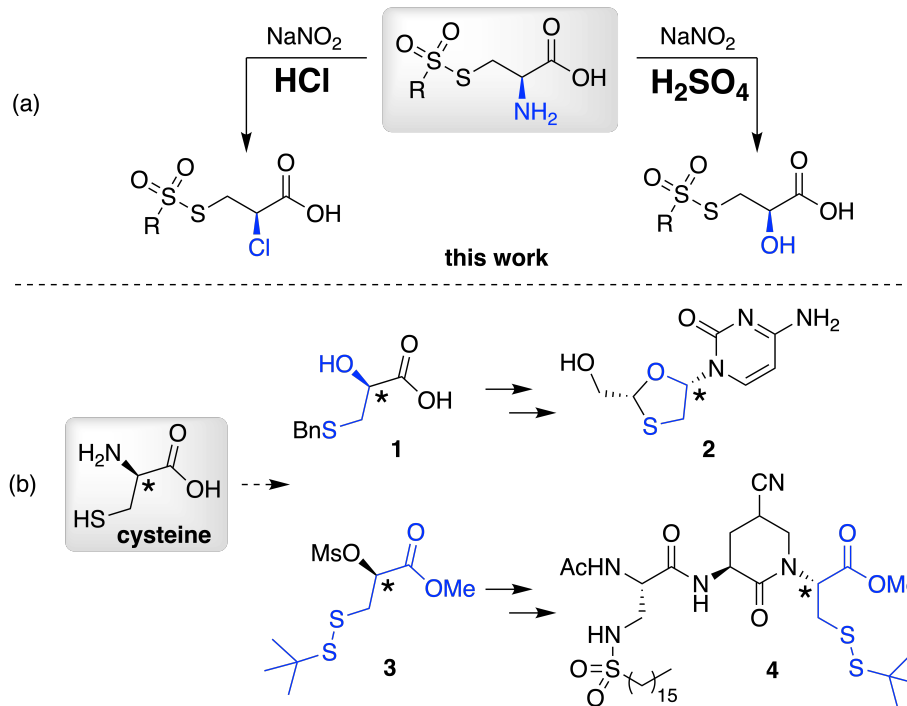
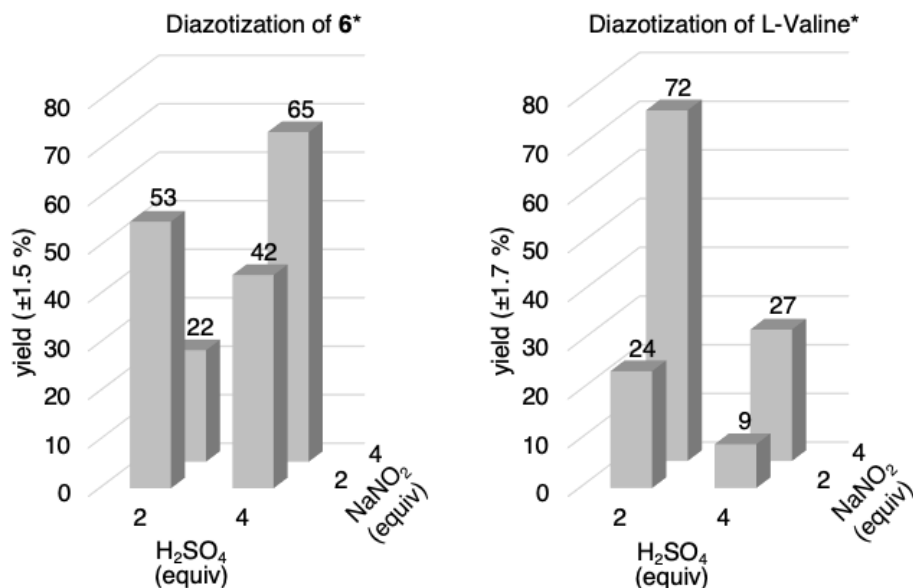
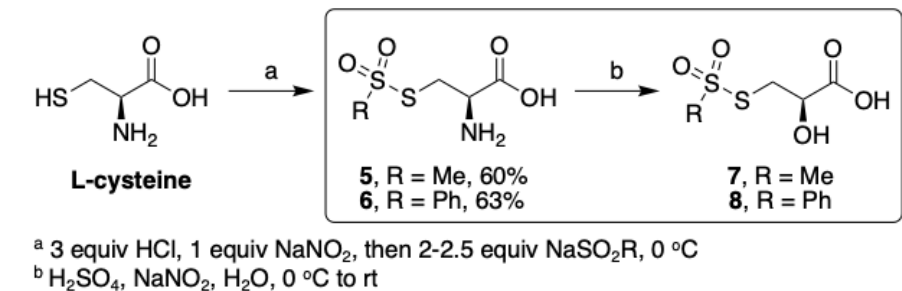


Figure 1-1: (a) General scheme for the diazotization of *S*-sulfonyl-cysteines and (b) applications in synthesis.^{2,3}

similar β -thio- α -hydroxy acid derivative **3** was used by Biel et al. in the synthesis of acyl protein thioesterase inhibitor **4**.³ We concluded from these examples that enabling the diazotization of cysteine could allow synthesis of similar sulfur-containing enantiomerically enriched building blocks from the chiral pool.

In 2004, Deechongkit et al. demonstrated synthesis of enantiomerically enriched α -hydroxy acids by diazotization of seven of the naturally occurring amino acids, describing cysteine as a limitation in the scope due to the acidic and oxidizing reaction conditions.¹⁵ Stuhr-Hansen et al. and Matthes et al. have reported diazotization of *S*-benzyl-cysteine derivatives with 8% and 57% yields; however, the enantiomeric ratio of the products was not reported in either case and further elaboration of the sidechain was not demonstrated.^{7,13} Given this precedent, we first investigated diazotization of cysteine using the common benzyl thioether protecting group, but obtained less than 10% yield of the desired α -hydroxy product and observed a complex mixture of products, including debenzylated species (¹H NMR). Thioester protecting groups were also not viable due to known *S*-to-*N* acyl migration pathways.²¹ We learned



*General screening procedure provided in the experimental section. Amino acid concentration 0.08 M post-reagent mixing. Acetone cosolvent (2:1 aq/organic post-reagent mixing). Yields determined by integration of α -proton in ¹H NMR using benzyl benzoate as internal standard. Yields are averages of triplicate runs.

Figure 1-2: Synthesis of *S*-sulfonyl-cysteines and results for DoE optimization of diazotization of **6** (left) versus control substrate valine (right).

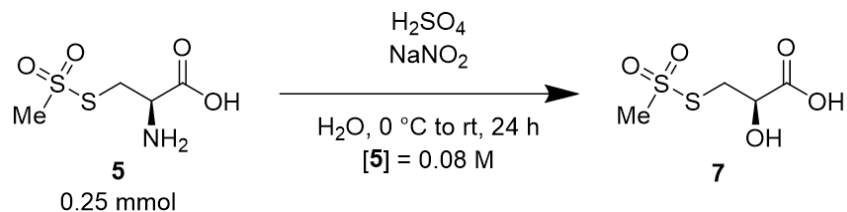
in the course of these investigations that disulfides are oxidized by nitrogen oxides to thiosulfonates by an established mechanism.²² We therefore hypothesized that an *S*-sulfonyl protecting group may prevent undesired oxidation of the substrate. *S*-sulfonyl-cysteines **5** and **6** were prepared on multigram scale by slight modification of reported procedures (Figure 1-2).^{23,24}

Our initial investigations into the diazotization of **5** with two equivalents of nitrite, four equivalents of sulfuric acid and 24 h reaction time produced the targeted α -hydroxy acid **7** in 33% yield, according to ¹H NMR (Figure 1-2). This promising result demonstrated that the thiosulfonate was more stable to the acidic and oxidizing

reaction conditions than the other thiol protecting groups tested. In the diazotization of **6**, benzenesulfonic acid was observed by ESI-MS as a side product, presumably by hydrolysis of the thiosulfonate. Derivatization of the products and separation of the enantiomers by HPLC using a column with a chiral stationary phase demonstrated that the reaction proceeds with >96:4 er (see Experimental Section), despite the nucleophilic β -thio substituent. These results demonstrated that the sulfonyl protecting group provides resistance to oxidation, and also controls the undesired nucleophilicity of the β -substituent.

Initial reaction optimization with **5** and **6** by a one-factor-at-a-time approach led to yields ranging from 19–54%, as determined by ^1H NMR (see Tables 1.1 and 1.2 on page 23). Reaction time of 4 h, higher dilution of starting material to 0.08 M, and use of acetone as cosolvent (with **6**) gave improved yields while minimizing formation of impurities. We hypothesized that the molar ratio of acid and nitrite employed would affect the yield based on the reported mechanism for diazonium formation, which proceeds via generation of the reactive nitrosyl cation from nitrite and two acidic protons. To investigate this possible variable interaction effect, we performed a two-level, two-factor design of experiment (2^2 DoE) investigating the stoichiometry of acid and nitrite in the diazotization reaction of **6**.²⁵ To compare the results of this study with an amino acid less prone to oxidation, we performed the same DoE on the aliphatic amino acid valine. The results are summarized in Figure 1-2.

The results of the DoE indicated that the stoichiometry of both reagents must be considered in combination to maximize the yield. For cysteine, the yield was maximized when equimolar amounts of the two reagents were employed, while lower yields were observed with an excess of either reagent (Figure 1-2). For valine, an inverse trend was observed and the yield was maximized when an excess of nitrite was used (Figure 1-2). This demonstrated that the optimal conditions for diazotization of cysteine derivatives are not obvious based on results for other amino acids. Since a 1:1 molar ratio of $\text{NaNO}_2:\text{H}_2\text{SO}_4$ gave the highest yield, we varied the equivalents of nitrite, keeping the 1:1 ratio constant (Figure 1-3). We determined that 4 equivalents of nitrite is optimal for the diazotization of this substrate; lower yields were observed

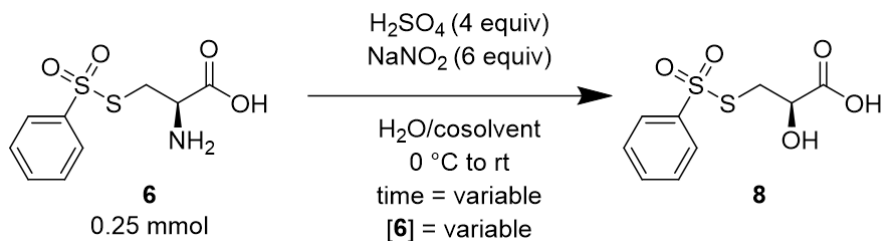


entry	NaNO ₂ (equiv)	H ₂ SO ₄ (equiv)	AY 7 (%) [†]
1*	1	4	19
2	2	4	33
3	4	8	49
4	6	12	37

*minimal amount acid required to dissolve **5**.

[†]AY = assay yield by ¹H NMR, benzyl benzoate internal standard.

Table 1.1: Initial reaction optimization for diazotization of **5**.



entry	[6]	cosolvent	time (h)	AY 8 (%)	observation
1	0.08	THF	24	20	complex mixture
2	0.08	acetone	24	54	complex mixture vs. entry 8/9
3	0.08	1,4-dioxane	24	53	difficult to remove solvent
4	0.17	acetone	24	49	lower yield than entry 2
5	0.33	acetone	24	41	lower yield than entry 2
6	0.08	acetone	1	36	
7	0.08	acetone	2	43	
8	0.08	acetone	4	47	
9	0.08	acetone	6	47	

AY = assay yield determined by ¹H NMR using benzyl benzoate as internal standard

Table 1.2: Initial reaction optimization for diazotization of **6**.

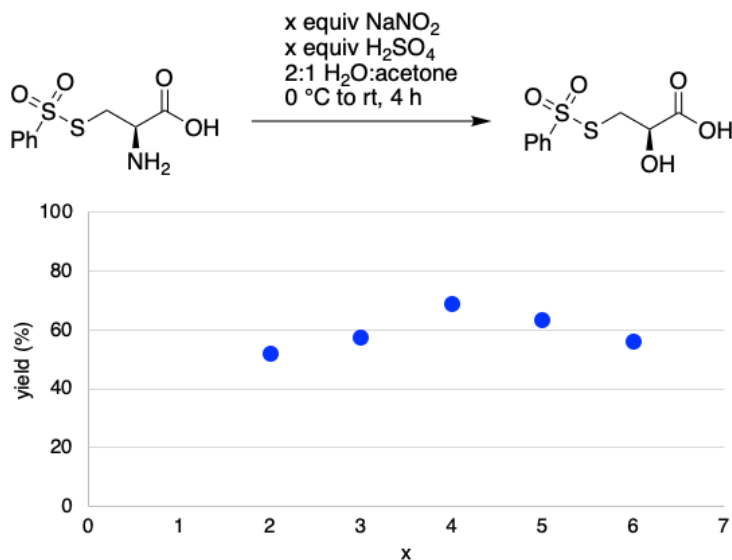


Figure 1-3: Diazotization of *S*-phenylsulfonyl-L-cysteine with varying equivalents of nitrite and 1:1 ratio of NaNO₂/H₂SO₄.

when the stoichiometry of nitrite relative to the amino acid was increased or decreased.

To demonstrate the utility of this method, the diazotization was performed on 1 mmol scale and the resulting products were isolated and characterized (Figure 1-4). The *S*-mesyl derivative **7** was sufficiently pure after aqueous workup, and 59% yield was obtained requiring no further purification. We observed an approximate 10% improvement in mass balance when saturated sodium sulfate solution was added to the reaction mixture before workup to provide a salting-out effect.²⁶ The *S*-phenylsulfonyl derivative **9** was prepared by a two-step procedure after esterification to form the methyl ester, which was purified by column chromatography. The allyl ester derivatives **10** and **11** were prepared by Fischer esterification; yields were limited by heat-sensitivity of **7** and **8**. By replacing sulfuric acid with hydrochloric acid in the diazotization of **6**, we found that α -chloro acid **12** is prepared; the methyl ester **13** was isolated by column chromatography after a two-step procedure involving methylation of **12** with trimethylsilyldiazomethane (see Safety Considerations). Furthermore, by reaction of the thiosulfonate **9** with a thiol and triethylamine, mixed disulfide product **14** is prepared in a single step. Synthesis of **14** demonstrates a new synthetic route to medically relevant building block **3** from chiral pool precursor L-cysteine.

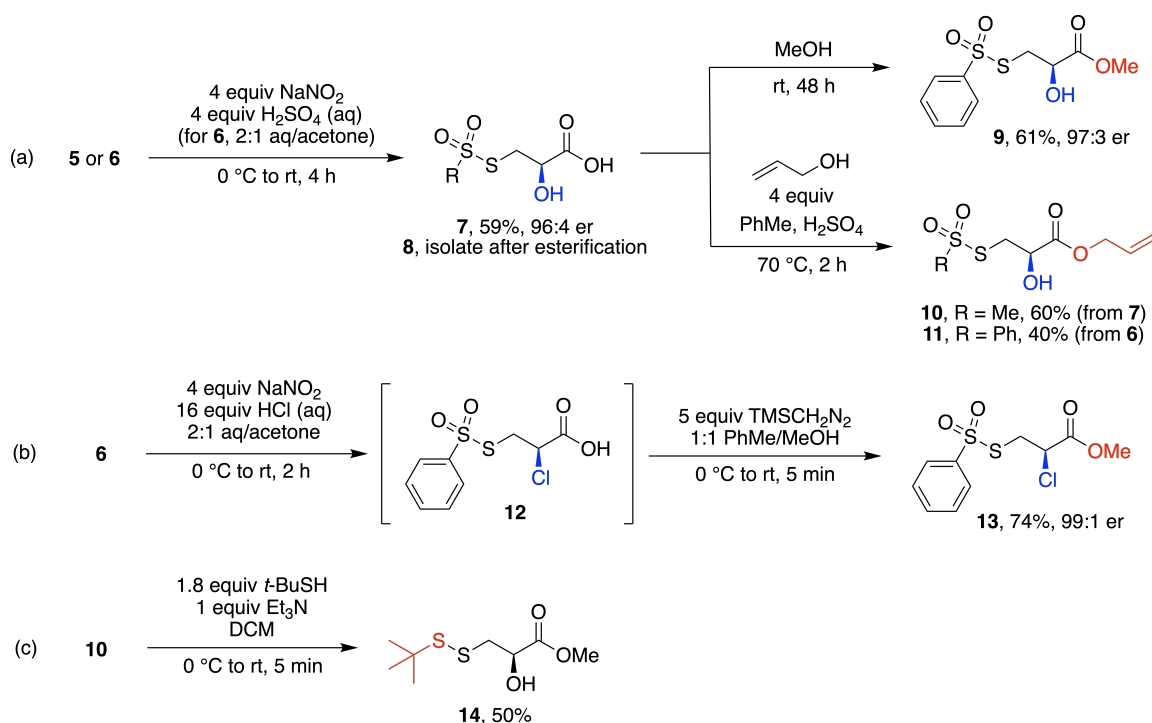


Figure 1-4: Isolated yields of cysteine diazotization products and derivatives on 1 mmol scale or greater.

The stereochemical fidelity of this transformation is notable when compared with the diazotization of other β -substituted amino acids such as *O*-benzyl-L-serine, for which the hydroxy-acid derivative has been prepared previously with 80:20 er.¹² In the course of exploratory investigations with the disulfide cystine, we observed formation of thiirane carboxylic acid and acrylic acid in 51% and 19% yields after diazotization. We believe that the thiirane forms by nucleophilic displacement of the diazonium by sulfur. The observed thiirane product provides indirect evidence of the problematic nucleophilicity of the β -thio substituent. We propose that the successful diazotization of *S*-sulfonyl-cysteines results from minimization of this undesired substitution pathway.

We obtained a crystal structure of allyl ester derivative **11**, and observed the thiosulfonate in a gauche conformation with a C–S–S–C dihedral angle of 64.33° (Figure 1-5). Existing theoretical and spectroscopic studies of dimethylthiosulfonate derivatives also demonstrate a preference for the gauche conformation.^{27,28} In these examples, the favored conformation is influenced by the electronic nature of the sul-

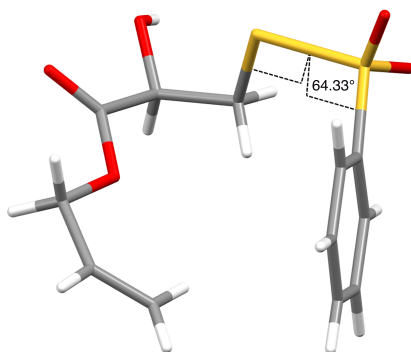


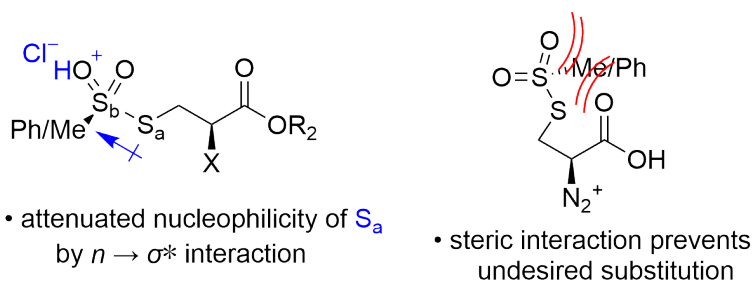
Figure 1-5: Crystal structure of **11** showing a gauche conformation about the thiosulfonate S-S bond.

fonyl R-group. We rationalize the observation of this gauche conformation with a stabilizing $n \rightarrow \sigma^*$ interaction; the gauche conformation is stabilized by delocalization of a sulfenyl lone pair into the antibonding orbital of the adjacent S-C bond.

Figure 1-6 illustrates how the gauche effect and $n \rightarrow \sigma^*$ interaction in thiosulfonates could contribute to the stereochemical fidelity of this transformation by minimizing undesired substitution pathways. After diazotization, an episulfonium may form competitively with the α -lactone by substitution at the α -position. Any variation in the sequence of substitution events could lead to erosion in *er*. Likewise, preventing episulfonium formation should improve *er* (blue pathway). We propose that the $n \rightarrow \sigma^*$ interaction decreases the nucleophilicity of the sulfenyl sulfur, destabilizing the undesired episulfonium and favoring the α -lactone pathway.

This gauche effect can help rationalize the higher enantiomeric ratio of the products observed in preparation of the α -chloro derivative **13**; hydrochloric acid likely protonates the thiosulfonate oxygens to a greater extent than sulfuric acid, increasing the extent of the $n \rightarrow \sigma^*$ interaction. Alternatively, the steric bulk of the thiosulfonate may also contribute to the stereochemical fidelity of this transformation. Repulsive interactions between the sulfonyl oxygens and the carbonyl oxygen could minimize undesired nucleophilic substitution at the α -position after diazonium formation (Figure 1-6a).

(a) Conformational analysis of the thiosulfonate protecting group



(b) Proposed mechanism for erosion in er by competing substitution pathways

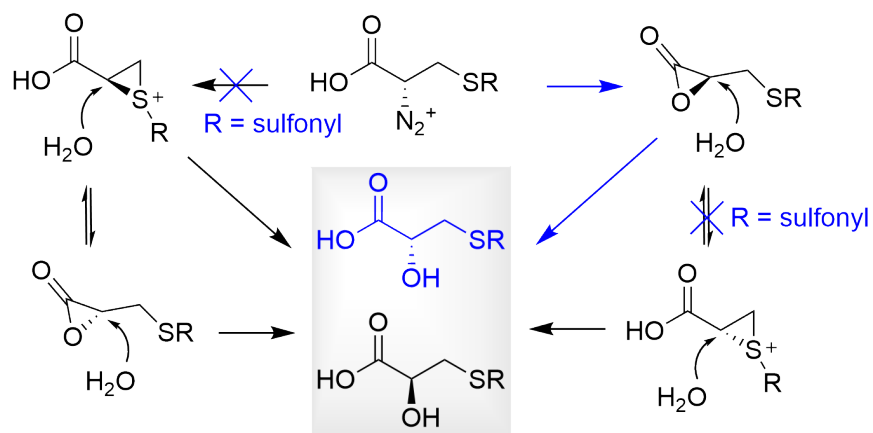


Figure 1-6: Mechanistic rationale for retention of configuration and stereochemical fidelity in the diazotization of *S*-sulfonyl-cysteines.

1.3 Conclusion

In conclusion, we have enabled preparation of enantiomerically enriched sulfur-containing α -hydroxy and α -chloro acid building blocks by diazotization of *S*-sulfonyl-cysteines. Key to the success of this investigation was the use of a thiosulfonate protecting group and optimization of the reaction conditions by a 2^2 factorial DoE. We posit that the thiosulfonates protecting group enables this transformation by rendering the sulfur in cysteine resistant to the oxidizing reaction conditions, and by attenuating sulfur's nucleophilicity.

1.4 Experimental Section

1.4.1 General Remarks

Reagents were used as supplied commercially without further purification. Solvents were dried and sparged with Argon using a solvent purification system prior to use. Reactions were run under inert atmosphere except where otherwise noted. Thin-layer chromatography (TLC) was performed using 0.2 mm coated glass silica gel plates and visualized using either ultraviolet light or staining with KMnO_4 solution. Purification by column chromatography over silica gel was performed on a Biotage Isolera flash chromatography system using SNAP KP-Sil or RediSep Rf Gold normal-phase columns. All NMR spectra were collected on Bruker instruments. Spectra reported with field strength 400 MHz were collected using a two-channel Bruker Avance-III HD Nanobay spectrometer operating at 400.09 MHz. Spectra reported with field strength 500 MHz were collected using a three-channel Bruker Avance Neo spectrometer operating at 500.34 MHz. Both spectrometers were equipped with a 5 mm liquid-nitrogen cooled Prodigy broad band observe (BBO) cryoprobe. Chemical shifts (δ) are reported in units of ppm, relative to the residual solvent peak, which was adjusted to match reported values.²⁹ Individual peaks are assigned multiplicity with the definitions: s = singlet, d = doublet, t = triplet, q = quartet, m = multiplet. Reported NMR data follow the general format: Nuclei NMR (resonance frequency, reference solvent) chemical shift (multiplicity, coupling constants, integration). High-resolution mass spectrometry data was recorded using an Agilent Technologies 6545 Q-TOF LC/MS. Samples were directly injected using a mobile phase of 0.1% formic acid in acetonitrile. Infrared (IR) resonances were observed using an Agilent Cary 630 FTIR spectrometer. IR samples were prepared as solutions in dichloromethane then loaded onto a diamond surface, with the exception of compounds **5** and **6** which were observed in solid form. Enantiomeric ratio was assessed by HPLC using an Agilent 1290 Infinity II series instrument equipped with a chiral column. For each compound, a racemic standard was prepared to identify retention times for each enantiomer. Method details are described separately for each compound. Optical rotation was

measured using a Jasco Model 1010 Polarimeter configured with a standard 589 nm Sodium D line at ambient temperature of 23 °C (c = grams of material / 100 mL) and a standard glass cell of 3 mm width and 1 dm length.

1.4.2 Safety Considerations

Mixing solutions of sodium nitrite with solutions of strong acid (hydrochloric acid or sulfuric acid) may generate noxious NO_x fumes. Take care to mix these reagents slowly, use the indicated quantities of each reagent according to the reported procedures, and always perform reactions in a working fume hood. This safety precaution is relevant to the preparation of compounds **5**, **6**, and all diazotization products.

Methylating agent trimethylsilyldiazomethane (TMSCH_2N_2) should be used with great caution. Carefully review safety documentation prior to use and always perform reaction in a fume hood with proper personal protective equipment. Increasing the scale beyond what is reported herein is not recommended by the authors. Take care when washing syringes and needles used for reagent addition, as gas evolution will occur. This safety recommendation is relevant to the preparation of compounds **9** and **13**.

1.4.3 Reaction Optimization

General Screening Procedure for Amino Acid Diazotization

All optimization data reported for amino acid diazotizations of cysteine derivatives and valine was collected according to the following general procedure: Amino acid starting material (0.25 mmol) was dissolved in aqueous acid (0.5–2 M stock solution, stoichiometry as indicated) and added to a 2-dram glass vial equipped with a magnetic stirrer. Cosolvent and/or additional DI water was added to achieve indicated cosolvent mixture and starting material concentration, and the mixture was cooled in an ice-water bath for 5 minutes. A 1 M aqueous solution of sodium nitrite (as indicated) was added with stirring. The vial was *not* capped, but left open to ambient atmosphere. The reaction was allowed to warm slowly to room temperature and stirred for the indicated reaction time (1–24 h). Ethyl acetate (1.5 mL) was added directly to the vial. The vial was shaken vigorously, then the layers were allowed to separate. The organic layer was separated, and this extraction procedure was repeated 4 times. The combined organic fractions were dried (MgSO_4), then filtered through cotton. Benzyl benzoate (0.25 mmol) was added, then the solvent was removed under reduced pressure. The resulting mixture was analyzed by ^1H NMR with a 25-second relaxation delay in $(\text{CD}_3)_2\text{SO}$ to calculate an assay yield for the transformation. The results of optimization experiments are tabulated and summarized herein.

2² Design of Experiment (DoE)

For more information on the use of DoE in organic synthesis, see the cited book by Rolf Carlson.²⁵ The factors tested in this DoE are defined in Table 1.3.

Factors	Levels		
	(-) level	(+) level	
A	equiv sulfuric acid	2	4
B	equiv nitrite	2	4

Table 1.3: Variables and experimental domain for 2² factorial design of experiment: diazotization of amino acids.

Label	Factors		Yield (%)			
	A	B	trial 1	trial 2	trial 3	mean
1	-	-	53	55	50	53
a	+	-	42	46	39	42
b	-	+	24	18	23	22
ab	+	+	65	64	66	65

Table 1.4: Sign table and results of 2² factorial design for *S*-phenylsulfonyl-L-cysteine.

The main effect of A is defined as half the average of the observed difference in response when A is varied from the low level to the high level when factor B is held constant. Therefore the main effect for A is calculated as follows:

$$A = 1/2 * [(a - 1) + (ab - b)]/2 \quad (1.1)$$

or by using the matrix in Table 1.5. Therefore the main effect for A (sulfuric acid) is 8.0. The main effect for B (nitrite) is calculated analogously and found to be -2.0.

An interaction effect between factors A and B in a 2² DOE is defined as half of the difference of the effects of A when they are determined with factor B on its high, respectively its low level.

$$AB = 1/2 * [A_{B+} - A_{B-}] \text{ or } AB = 1/2 * [(ab - b) - (a - 1)] \quad (1.2)$$

or by using the matrix in Table 1.5. Therefore the interaction effect AB is 14.

Results of the same analysis for L-valine diazotization are summarized below.

I	A	B	AB	
1	-1	-1	1	53
1	1	-1	-1	42
1	-1	1	-1	22
1	1	1	1	65
	32	-8	54	Total
	8.0	-2.0	14	Total/4

Table 1.5: Calculation of main effects and interaction effect in diazotization of *S*-phenylsulfonyl-L-cysteine.

Label	Factors		Yield (%)			
	A	B	trial 1	trial 2	trial 3	mean
1	-	-	20	27	26	24
a	+	-	9	10	8	9
b	-	+	68	76	72	72
ab	+	+	26	31	25	27

Table 1.6: Sign table and results of replicated 2^2 factorial design for L-valine.

I	A	B	AB	Yield (%)
1	-1	-1	1	24
1	1	-1	-1	9
1	-1	1	-1	72
1	1	1	1	27
	-60	66	-30	Total
	-15	17	-7.5	Total/4

Table 1.7: Calculation of main effects and interaction effect in diazotization of L-valine

To draw conclusions on the significance of the estimated effects they must be compared to an estimate of the experimental error variation. An estimate of the experimental error variance can be obtained from a residual sum of squares as

$$s^2 = SSE/(n - p) = SSE/5 \quad (1.3)$$

where n is the number of runs in the experimental design, and p is the number of parameters ($12 - 4 = 8$ degrees of freedom). For cysteine: $s^2 = 84/8 = 7.6$. The variance is calculated as s^2/n , so the variance is $7.6/12 = 0.64$. The standard error therefore is $standard\ error = \sqrt{0.645} = 0.80$. The critical t-value at the 95% confidence level for 8 degrees of freedom is $t^{Crit} = 1.86$. The confidence limits of

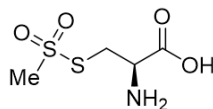
the estimated parameters is then: *confidence limits* = $\pm t^{Crit} * \text{standard error}$ = $1.86 * 0.80 = \pm 1.5$. Performing the same analysis for the DOE with L-valine gives a confidence limit of ± 1.7 . The observed effects are summarized in Table 1.8.

cysteine	
Main effects	Two-factor interaction
A = 8.0 ± 1.5	AB = 14 ± 1.5
B = -2.0 ± 1.5	
valine	
Main effects	Two-factor interaction
A = -15 ± 1.7	AB = -7.5 ± 1.7
B = 17 ± 1.7	

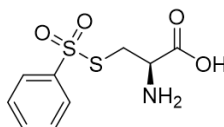
Table 1.8: Calculated effects with confidence intervals. A = equivalents H_2SO_4 ; B = equivalents NaNO_2 .

These calculated main effects give a numerical value to the trend described in the text. For cysteine, increased amounts of sulfuric acid (positive A value) are beneficial, and increased amounts of nitrite are detrimental (negative B value). For valine, the opposite is observed: increased amounts of sulfuric acid is detrimental, while increased stoichiometry of nitrite is beneficial. Additionally, comparing the two-factor interaction shows that this interaction is more significant for cysteine than for valine.

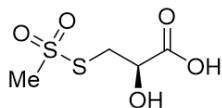
1.4.4 Synthesis of Numbered Compounds



Synthesis of *S*-(methylsulfonyl)-L-cysteine, (5). L-cysteine hydrochloride monohydrate (7.02 g, 40.0 mmol) was dissolved in aqueous 2 N HCl (40 mL) in a 250-mL Erlenmeyer flask, then cooled in an ice-water bath. Note: precisely 3 equiv of HCl are required, so if L-cysteine is used in place of HCl salt, use 40 mL of 3 N HCl. With stirring, sodium nitrite (2.76 g, 40 mmol) dissolved in DI water (20 mL) was added dropwise, and the deep red solution was stirred open to ambient atmosphere for 40 min. Sodium methane sulfinate (8.17 g, 80.0 mmol) dissolved in DI water (20 mL) was added by pipette, rapidly, with stirring. Additional DI water (2 mL) was used to complete the transfer. The solution was stirred on ice for 3.5 h, replenishing ice as needed, then additional sodium methane sulfinate (2.04 g, 20.0 mmol) dissolved in 20 mL DI water was added rapidly. The solution was stirred for a further 30 min, until the red color disappeared. The resulting suspension was filtered using a sintered glass funnel (medium porosity). Washing the isolated solid with DI water, acetone, and diethyl ether (60 mL each), followed by drying under high vacuum afforded the title compound as a fine white powder (4.76 g, 23.9 mmol, 60%). ^1H NMR (400 MHz, D_2O) δ 4.47 (dd, $J = 6.8, 4.5$ Hz, 1H), 3.85 (dd, $J = 15.7, 4.5$ Hz, 1H), 3.74 (dd, $J = 15.7, 6.8$ Hz, 1H), 3.55 (s, 3H). $^{13}\text{C}\{^1\text{H}\}$ NMR (100 MHz, D_2O) δ 169.5, 52.6, 49.6, 34.8. HRMS (ESI-QTOF) m/z : $[\text{M}+\text{Na}]^+$ Calcd for $\text{C}_4\text{H}_9\text{NO}_4\text{S}_2\text{Na}$ 221.9865; Found 221.9871. IR 3243, 3035, 2987, 2913, 2802, 2621, 2103, 1991, 1578, 1490, 1404, 1342, 1290, 1254, 1192, 1117, 1044, 956, 888, 856, 801, 753, 693 cm^{-1} . Specific Rotation $[\alpha]_D^{23} = -48.7$ (c 1.1, H_2O).

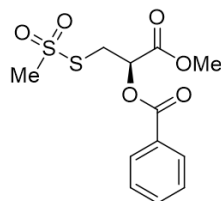


Synthesis of *S*-(phenylsulfonyl)-L-cysteine, (6). L-cysteine hydrochloride monohydrate (5.27 g, 30.0 mmol) was dissolved in aqueous 2 N HCl (30 mL) in a 250-mL Erlenmeyer flask, then cooled in an ice-water bath. Note: precisely 3 equiv of HCl are required, so if L-cysteine is used in place of HCl salt, use 40 mL of 3 N HCl. With stirring, sodium nitrite (2.07 g, 3.0 mmol) dissolved in DI water (20 mL) was added dropwise, and the deep red solution was stirred open to ambient atmosphere for 40 min, then a solution of sodium benzene sulfinate (9.85 g, 60.0 mmol) in DI water (20 mL) was added dropwise with stirring. Solids immediately start to form. The solution was warmed to room temperature to disperse solids (the product began collecting on the magnetic stirrer). Stirring was continued at room temperature until all of red color disappeared, about 3 h. The suspension was briefly cooled in an ice bath, then filtered using a sintered glass funnel (medium porosity, note that filtering will take hours if fine porosity is used), and washed with approximately DI water, acetone, and diethyl ether (60 mL each) to afford the title compound as a fluffy white solid (4.97 g, 19.0 mmol, 63%). ¹H NMR (400 MHz, CD₃OD) δ 8.01 (dd, *J* = 7.7, 1.7 Hz, 2H), 7.80 (t, *J* = 7.4 Hz, 1H), 7.70 (t, *J* = 7.7 Hz, 2H), 4.36 (dd, *J* = 7.0, 4.9 Hz, 1H), 3.59 (dd, *J* = 15.3, 5.0 Hz, 1H), 3.54 (dd, *J* = 15.3, 7.0 Hz, 1H). ¹³C{¹H} NMR (100 MHz, CD₃OD) δ 169.4, 144.7, 135.9, 131.0, 128.3, 53.4, 35.8. HRMS (ESI-QTOF) *m/z*: [M+Na]⁺ Calcd for C₉H₁₁NO₄S₂Na 284.0022; Found 284.0022. IR 3276, 2973, 2923, 2688, 2199, 2117, 1932, 1617, 1577, 1437, 1396, 1349, 1311, 1255, 1187, 1140, 1069, 929, 848, 757, 717, 684 cm⁻¹. Specific Rotation [α]_D²³ = -97.1 (*c* 0.10, MeOH).

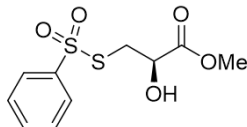


Synthesis of (*R*)-2-hydroxy-3-((methylsulfonyl)thio)propanoic acid, (7).

Amino acid **5** (199.2 mg, 1.0 mmol) was dissolved in aqueous 0.5 M sulfuric acid (8 mL) in a 50-mL roundbottom flask and cooled in an ice-water bath. The reaction was run open to ambient atmosphere. After stirring for 5 min, a solution of sodium nitrite (276 mg, 4.0 mmol) in DI water (3 mL) was added dropwise with stirring. Additional DI water (1 mL) was used to complete the transfer. The solution was warmed to room temperature gradually over 4 h. The reaction mixture was transferred to a separatory funnel and saturated sodium sulfate solution (8 mL) was added. The aqueous layer was extracted four times with ethyl acetate (4 x 5 mL). The combined organic extracts were dried with MgSO₄ then filtered using a sintered glass funnel (medium porosity). The solvent was removed under reduced pressure at 30 °C, then concentrated three times with hexanes and dried under high vacuum to yield the title compound as a waxy yellow solid (119 mg, 0.59 mmol, 59%, 96:4 er). ¹H NMR (400 MHz, (CD₃)₂SO) δ 4.34 (dd, *J* = 6.9, 4.3 Hz, 1H), 3.53 (s, 3H), 3.52 (dd, *J* = 13.8, 4.3 Hz, 1H), 3.41 (dd, *J* = 13.8, 7.0 Hz, 1H). ¹³C{¹H} NMR (100 MHz, (CD₃)₂SO) δ 173.2, 69.0, 50.4, 40.1. HRMS (ESI-QTOF) *m/z*: [M+Na]⁺ Calcd for C₄H₈O₅S₂Na 222.9705; Found 222.9702. IR 3412, 3010, 2931, 2612, 1734, 1430, 1403, 1306, 1280, 1227, 1167, 1127, 1079, 1005, 956, 914, 860, 776, 742 cm⁻¹. Specific Rotation [α]_D²³ = -33.5 (*c* 0.23, MeOH).

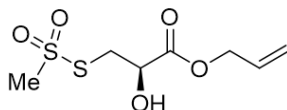


Synthesis of (*R*)-1-methoxy-3-((methylsulfonyl)thio)-1-oxopropan-2-yl benzoate, (7b). The hydroxy acid **7** was derivatized as described for Chiral HPLC analysis: **7** (50 mg, 0.25 mmol) was dissolved in dry methanol (2 mL), heated to 60 °C and stirred overnight. The solvent was removed under reduced pressure. The crude residue was diluted with ethyl acetate, and washed with dilute sodium bicarbonate, then dried (MgSO₄). The solvent was removed under reduced pressure. The resulting oil (ca. 0.23 mmol) was dissolved in 5 mL dry dichloromethane in a flame-dried round-bottom flask, then cooled in an ice-water bath. To the solution was added triethylamine (39 μL, 0.28 mmol), followed by benzoyl chloride (32 μL, 0.28 mmol) and 4-dimethylaminopyridine (5.6 mg, 0.05 mmol). The mixture was warmed to room temperature overnight, then quenched with NH₄Cl (aq). The layers were separated, and the aqueous layer was extracted three times with dichloromethane. The combined organic extracts were washed with dilute HCl, then dried with MgSO₄. The resulting residue was purified by flash column chromatography (7-40% EtOAc/hexanes, R_f = 0.14, 25% EtOAc/hexanes). Sample was used for analytical purposes; yield was not determined. ¹H NMR (400 MHz, CDCl₃) δ 8.11–8.05 (m, 2H), 7.68–7.56 (m, 1H), 7.48 (dd, *J* = 8.5, 7.1 Hz, 2H), 5.65 (dd, *J* = 7.0, 4.1 Hz, 1H), 3.86 (dd, *J* = 14.8, 4.1 Hz, 1H), 3.82 (s, 3H), 3.74 (dd, *J* = 14.8, 7.1 Hz, 1H), 3.37 (s, 3H). ¹³C{¹H} NMR (100 MHz, CDCl₃) δ 168.2, 165.5, 134.0, 130.1, 128.7, 128.7, 71.2, 53.2, 51.2, 37.2. HRMS (ESI-QTOF) *m/z*: [M+H]⁺ Calcd for C₁₂H₁₅O₆S₂ 319.0305; Found 319.0307. IR 3007, 1754, 1726, 1601, 1452, 1319, 1268, 1177, 1134, 1109, 1071, 1026, 957, 745, 713 cm⁻¹. Specific Rotation [α]_D²³ = +28.9 (*c* 1.7, CHCl₃). Enantiomeric Ratio 96:4. HPLC chromatograms and method information for assessment of enantiomeric ratio vide infra.



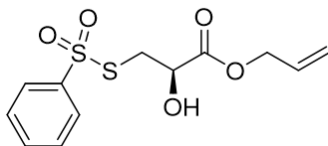
Synthesis of methyl (*R*)-2-hydroxy-3-((phenylsulfonyl)thio)propanoate, (9**).**

Amino acid **6** (261 mg, 1.00 mmol) was dissolved in aqueous 1 M H₂SO₄ (4 mL) in a 50-mL roundbottom flask equipped with a magnetic stirrer. The reaction was run open to ambient atmosphere. The mixture was cooled in an ice-water bath, then acetone (4 mL) was added. NaNO₂ (276 mg, 4.00 mmol) was dissolved in DI water (3 mL), then added dropwise, using additional DI water for rinsing (1 mL). The solution was warmed to room temperature gradually over 4 h. The reaction mixture was transferred to a separatory funnel. An aqueous solution of saturated sodium sulfate was added (8 mL) to aid recovery of the product from the aqueous layer, then extracted with ethyl acetate (4 x 5 mL) was performed. The combined organic extracts were dried with MgSO₄, then filtered using a sintered glass funnel (medium porosity). The solvent was removed under reduced pressure. The resulting yellow oil containing **8** was dissolved in dry methanol in a flame-dried roundbottom flask and stirred for 48 h at room temperature. The solvent was removed under reduced pressure and the resulting residue was purified by flash column chromatography (7–40% EtOAc/hexanes) to yield a yellow oil (168 mg, 0.61 mmol, 61%, 97:3 er). Alternatively, the crude oil containing **8** was methylated with TMSCH₂N₂ (see Safety Consideration, S4) according to a general procedure¹² and purified analogously (143.2 mg, 0.52 mmol, 52%). ¹H NMR (500 MHz, CDCl₃) δ 8.02–7.84 (m, 2H), 7.70–7.61 (m, 1H), 7.55 (dd, *J* = 8.4, 7.0 Hz, 2H), 4.42 (dd, *J* = 6.3, 4.1 Hz, 1H), 3.75 (s, 3H), 3.49 (dd, *J* = 14.0, 4.1 Hz, 1H), 3.30 (dd, *J* = 14.0, 6.3 Hz, 1H), 3.23 (s, 1H). ¹³C{¹H} NMR (125 MHz, CDCl₃) δ 172.4, 144.5, 134.0, 129.5, 127.1, 69.2, 53.2, 39.7. HRMS (ESI-QTOF) *m/z*: [M+Na]⁺ Calcd for C₁₀H₁₂O₅S₂Na 299.0018; Found 299.0023. IR 3487, 3065, 2955, 1736, 1447, 1404, 1322, 1218, 1179, 1134, 1096, 1076, 1013, 969, 847, 755, 716, 685 cm⁻¹. Specific Rotation [α]_D²³ = +7.8 (*c* 0.57, CHCl₃). Enantiomeric Ratio 97:3. HPLC chromatograms and method information for assessment of enantiomeric ratio, vide infra.



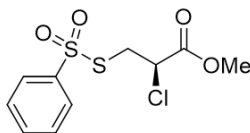
Synthesis of allyl (*R*)-2-hydroxy-3-((methylsulfonyl)thio)propanoate, (10).

Hydroxy acid **7** (2.12 g, 10.6 mmol) was suspended in dry toluene (10 mL) in a flame-dried 50-mL round bottom flask. Allyl alcohol (2.9 mL, 42 mmol) was added with stirring. Concentrated H₂SO₄ (4 drops with a glass pipette) was added, and the reaction was heated to 70 °C. Note that the thiosulfonate degrades when heated to refluxing temperatures, or above approx. 85 °C. A reflux condenser was attached and the reaction was stirred for 2 h, turning pale yellow in color. The reaction mixture was transferred to a separatory funnel and diluted with ethyl acetate, then washed with half-saturated NaHCO₃. The aqueous layer was extracted with ethyl acetate, then the combined organic layers were washed with brine and dried with MgSO₄. The solvent was removed under reduced pressure, and the resulting oil was purified by flash column chromatography on silica gel (10–100% EtOAc/hexanes, R_f = 0.38, 50:50 EtOAc/hexanes) to yield the title compound as a yellow oil (1.49 g, 6.20 mmol 60%). ¹H NMR (400 MHz, CDCl₃) δ 5.90 (ddt, *J* = 16.6, 10.4, 5.9 Hz, 1H), 5.39–5.25 (m, 2H), 4.69 (dt, *J* = 6.0, 1.3 Hz, 2H), 4.56 (dd, *J* = 6.0, 3.8 Hz, 1H), 3.66 (dd, *J* = 14.8, 3.8 Hz, 1H), 3.53 (dd, *J* = 14.8, 5.9 Hz, 1H), 3.42 (s, 3H), 3.39 (s, 1H). ¹³C{¹H} NMR (100 MHz, CDCl₃) δ 171.8, 130.9, 120.0, 69.9, 67.1, 50.9, 40.2. HRMS (ESI-QTOF) *m/z*: [M+Na]⁺ Calcd for C₇H₁₂O₅S₂Na 263.0018; Found 263.0022. IR 3477, 3011, 2930, 1735, 1648, 1449, 1411, 1312, 1185, 1128, 1093, 995, 956, 744 cm⁻¹. Specific Rotation [α]_D²³ = -56.2 (*c* 2.5, CHCl₃).



Synthesis of allyl (*R*)-2-hydroxy-3-((phenylsulfonyl)thio)propanoate, (11).

The title compound was prepared by the method described for **10**, starting from the crude hydroxy acid intermediate **8** described in the preparation of **9** on approximately 3.2 mmol scale. The crude oil was purified by flash column chromatography ($R_f = 0.49$, 50:50 EtOAc/hexanes) to yield the title compound as a pearly yellow solid (381 mg, 40% over 2 steps from **6**). A single crystal was grown for X-ray analysis by dissolving the material in a minimal amount of diethyl ether, layering with hexanes, and allowing to stand at room temperature for 48 hours. ^1H NMR (500 MHz, CDCl_3) δ 7.97–7.91 (m, 2H), 7.69–7.62 (m, 1H), 7.56 (dd, $J = 8.5, 7.1$ Hz, 2H), 5.90 (ddt, $J = 16.4, 10.4, 5.9$ Hz, 1H), 5.42–5.26 (m, 2H), 4.67 (qdt, $J = 12.9, 5.9, 1.4$ Hz, 2H), 4.45 (dd, $J = 6.3, 4.1$ Hz, 1H), 3.51 (dd, $J = 14.1, 4.1$ Hz, 1H), 3.34 (dd, $J = 14.0, 6.3$ Hz, 1H), 2.77 (s, 1H). $^{13}\text{C}\{^1\text{H}\}$ NMR (125 MHz, CDCl_3) δ 171.8, 144.6, 134.1, 131.1, 129.5, 127.2, 119.9, 69.3, 67.1, 39.8. HRMS (ESI-QTOF) m/z : $[\text{M}+\text{Na}]^+$ Calcd for $\text{C}_{12}\text{H}_{14}\text{O}_5\text{S}_2\text{Na}$ 325.0175; Found 325.0177. IR 3482, 3067, 2948, 1736, 1648, 1582, 1447, 1415, 1322, 1243, 1203, 1139, 1095, 1075, 997, 937, 755, 715, 684 cm^{-1} . Specific Rotation $[\alpha]_D^{23} = +6.3$ (c 0.54, CHCl_3) Melting Point Range 39–42 $^\circ\text{C}$.

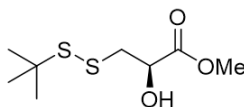


Synthesis of methyl (*R*)-2-chloro-3-((phenylsulfonyl)thio)propanoate, (13**).**

Amino acid **6** (261 mg, 1.00 mmol) was dissolved in aqueous 4 M HCl (4 mL) in a 25-mL roundbottom flask. The mixture was cooled in an ice-water bath, then acetone (4 mL) was added. Solid NaNO₂ (276 mg, 4.00 mmol) was added in portions with stirring. The solution was gradually warmed to rt over 2 h. The reaction mixture was transferred to a separatory funnel and diluted with saturated aqueous Na₂SO₄ (8 mL) to aid recovery of the product from the aqueous layer. The aqueous mixture was extracted with ethyl acetate (4 x 5 mL). The combined organic layers were dried with MgSO₄, then filtered into a flame-dried 100 mL roundbottom flask and concentrated under reduced pressure.

The resulting yellow oil containing **12** was suspended in 1:1 anhydrous MeOH–toluene (14 mL) and cooled in an ice-water bath. The mixture was capped with a rubber septum and vented with a needle. A solution of TMSCH₂N₂ (2.0 M in diethyl ether) was added dropwise through the septum until gas evolution ceased and yellow color persisted (approx. 2.5 mL, 5 mmol). The mixture was stirred for 5 min at room temperature, and quenched with 10% aq. AcOH (10 mL). The biphasic mixture was carefully transferred to a separatory funnel and aqueous 4 M HCl (1 mL) was added. The aqueous phase was extracted with EtOAc (4 x 20 mL). The combined organic fractions were dried with MgSO₄ and concentrated under reduced pressure at 40 °C, then diluted with toluene and concentrated twice more. The resulting oil was purified by flash column chromatography over silica gel (4–40% EA/hexanes, R_f = 0.4 in 50:50 EtOAc/hexanes) to yield the title compound as a yellow oil (219 mg, 0.74 mmol, 74%, 99:1 er). ¹H NMR (400 MHz, CDCl₃) δ 8.01–7.84 (m, 2H), 7.75–7.65 (m, 1H), 7.59 (t, *J* = 7.6 Hz, 2H), 4.52 (dd, *J* = 8.8, 5.8 Hz, 1H), 3.80 (s, 3H), 3.56 (dd, *J* = 14.7, 8.7 Hz, 1H), 3.36 (dd, *J* = 14.7, 5.8 Hz, 1H). ¹³C{¹H} NMR (100 MHz, CDCl₃) δ 168.3, 144.2, 134.4, 129.7, 127.2, 53.6, 53.5, 38.7. HRMS (ESI-QTOF) *m/z*: [M+Na]⁺ Calcd for C₁₀H₁₁ClO₄S₂Na 316.9679; Found 316.9678. IR 3064, 2999, 2956,

1742, 1582, 1447, 1404, 1325, 1275, 1226, 1198, 1139, 1077, 999, 972, 892, 834, 754, 715, 684 cm⁻¹. Specific Rotation $[\alpha]_D^{23} = +80.1$ (*c* 0.92, CHCl₃). Enantiomeric Ratio 99:1. HPLC chromatograms and method information for assessment of enantiomeric ratio, vide infra.



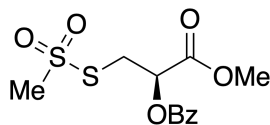
Synthesis of methyl (*R*)-3-(*tert*-butylsulfanyl)-2-hydroxypropanoate, (14).

Thiosulfonate **9** (276 mg, 1.00 mmol) was dissolved in CH₂Cl₂ (15 mL) in a flame-dried 50-mL roundbottom flask equipped with a magnetic stirrer. The solution was cooled in an ice-water bath and 2-methyl-2-propanethiol (200 μL, 1.8 mmol) was added. The solution was warmed to room temperature, and triethylamine (140 μL, 1.0 mmol) was added. The pale yellow mixture was stirred for 5 min, then diluted with CH₂Cl₂ and transferred to a separatory funnel. The organic layer was washed with aqueous 1 M HCl (10 mL). The aqueous layer was extracted with CH₂Cl₂, then the combined organic layers were washed with brine (10 mL) and dried with MgSO₄. The solvent was removed under reduced pressure, and the resulting clear oil was purified by flash column chromatography over silica gel (3–35% EtOAc/hexanes, *R_f* = 0.43, 30:70 EtOAc/hexanes) to yield the title compound as a clear oil (120.4 mg, 0.50 mmol, 50%). ¹H NMR (400 MHz, CDCl₃) δ 4.49 (td, *J* = 6.3, 4.0 Hz, 1H), 3.82 (s, 3H), 3.17 (dd, *J* = 13.7, 4.0 Hz, 1H), 3.06 (d, *J* = 6.2 Hz, 1H), 3.02 (dd, *J* = 13.7, 6.4 Hz, 1H), 1.34 (s, 9H). ¹³C{¹H} NMR (100 MHz, CDCl₃) δ 173.4, 69.5, 52.7, 48.1, 44.9, 29.8. HRMS (ESI-QTOF) *m/z*: [M+Na]⁺ Calcd for C₈H₁₆O₃S₂Na 247.0433; Found 247.0434. IR 3448, 2962, 1724, 1456, 1362, 1217, 1164, 1088, 1018, 914, 832, 768, 669 cm⁻¹. Specific Rotation $[\alpha]_D^{23} = +10.0$ (*c* 0.48, CHCl₃).

Diazotization of L-cystine: Synthesis of thiirane-2-carboxylic acid and acrylic acid. L-cystine (60 mg, 0.25 mmol) was dissolved in aqueous 0.5 M sulfuric acid (2 mL) in a 2-dram vial then cooled in an ice-water bath. The reaction was run open to ambient atmosphere. Sodium nitrite (1 mL of a 1 M aqueous solution) was added dropwise with stirring. The mixture was warmed to room temperature overnight. Saturated sodium sulfate (1 mL) was added, then the mixture was extracted 4 times with diethyl ether. The combined organic fractions were dried with MgSO₄ and filtered, then concentrated under reduced pressure (200 Torr, room temperature). Note that material was not dried under high vacuum, because this results in polymerization and loss of acrylic acid. For yield determination, benzyl benzoate (23.7 μ L, 0.13 mmol) was added as an NMR internal standard, the mixture was suspended in (CD₃)₂SO, and analyzed by ¹H NMR using a 25 s relaxation delay. A mixture of two products was observed: thiirane-2-carboxylic acid (ca. 51%) and acrylic acid (ca. 19%), as identified by ¹H NMR relative to reported spectra.^{30,31} The mixture of products could not be separated, due to instability of the material upon concentration (likely polymerization). Tabulated correlations observed by ¹H-¹H COSY and ¹H-¹³C HSQC NMR are included, vide infra. *Thiirane-2-carboxylic acid*: ¹H NMR (400 MHz, (CD₃)₂SO) δ 12.90 (s, 1H), 3.42 (t, J = 5.6 Hz, 1H), 2.70 (d, J = 5.6 Hz, 2H). ¹³C{¹H} NMR (100 MHz, (CD₃)₂SO) 171.4, 29.2, 23.5. HRMS (ESI-QTOF) m/z : [M-H]⁻ Calcd for C₃H₃O₂S 102.9859; Found 102.9693. *acrylic acid*: ¹H NMR (400 MHz, (CD₃)₂SO) δ 12.90 (s, 1H), 6.26 (dd, J = 17.3, 1.8 Hz, 1H), 6.08 (dd, J = 17.3, 10.3 Hz, 1H), 5.88 (dd, J = 10.3, 1.8 Hz, 1H). ¹³C{¹H} NMR (100 MHz, (CD₃)₂SO) 166.9, 130.7, 129.5.

1.5 Enantiomeric Ratio Analysis by HPLC

Chiral HPLC analysis of **7b**



Column	CHIRALCEL OD-H
Dimensions	4.6 mm ϕ x 250 mm λ
Particle Size	5 μ m
Flow Rate	1.0 mL/min
Mobile Phase	200:800 isopropanol/hexanes

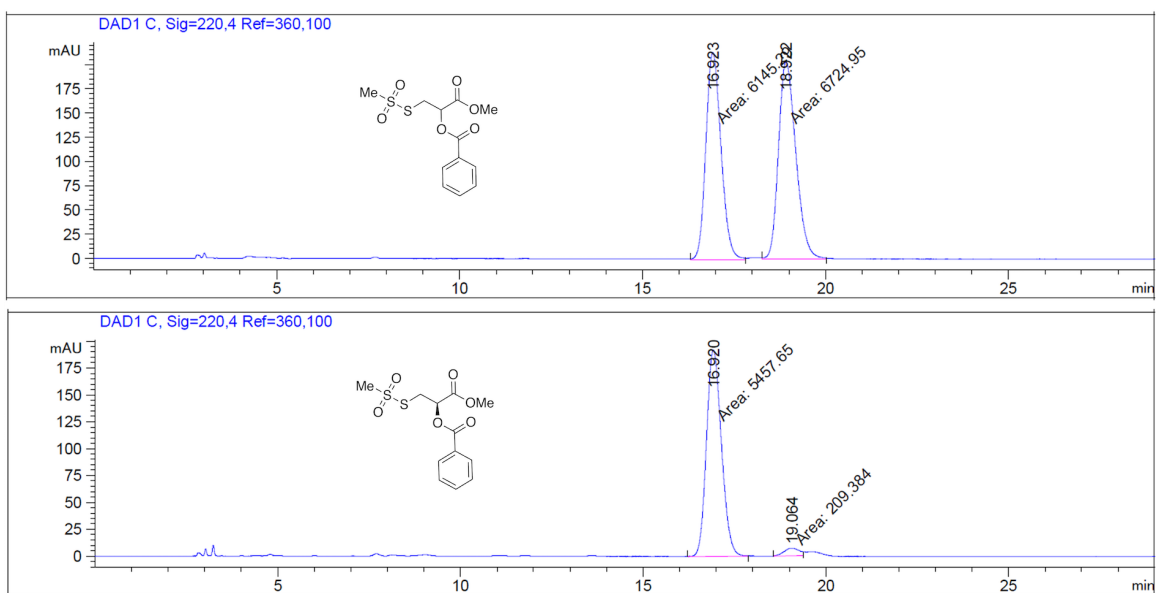
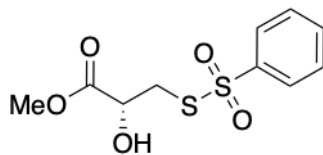


Figure 1-7: HPLC UV trace for compound **7b** versus racemic standard showing 96:4 er.

Chiral HPLC Analysis of **9**



Column	CHIRALCEL OD-H
Dimensions	4.6 mm ϕ x 250 mm λ
Particle Size	5 μ m
Flow Rate	1.0 mL/min
Mobile Phase	200:800 isopropanol/hexanes

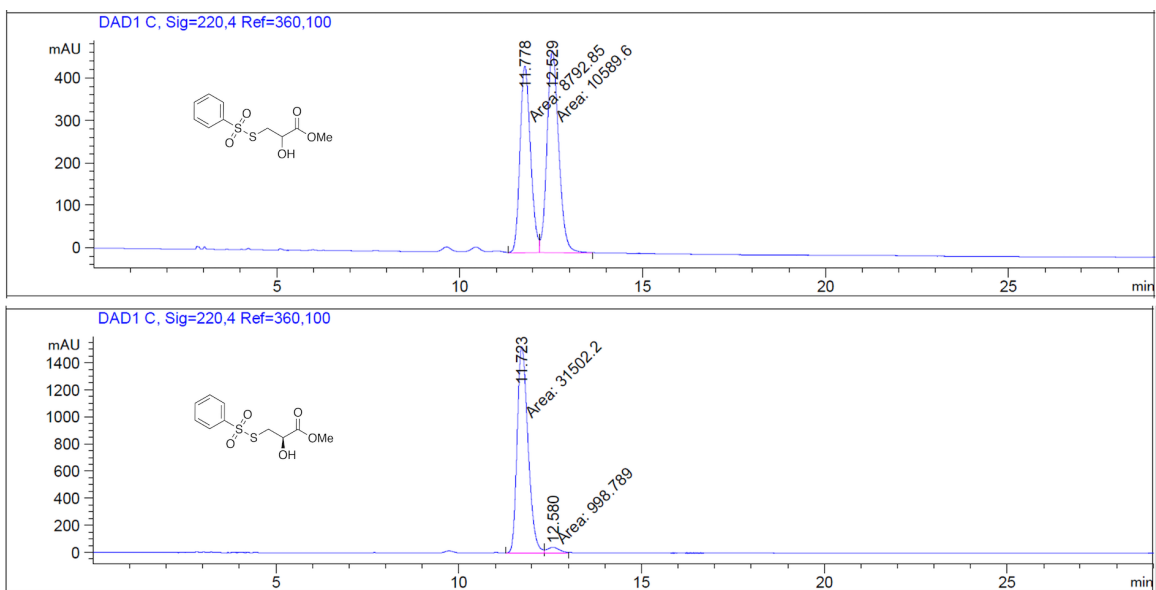
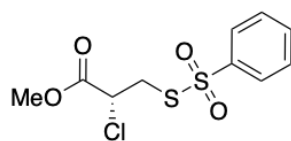


Figure 1-8: HPLC UV trace for compound **9** versus racemic standard showing 97:3 er.

Chiral HPLC Analysis of **13**



Column	CHIRALPAK AD-H
Dimensions	4.6 mm ϕ x 250 mm λ
Particle Size	5 μ m
Flow Rate	1.00 mL/min
Mobile Phase	200:900:2:1 EtOH/hexanes/diethylamine/AcOH

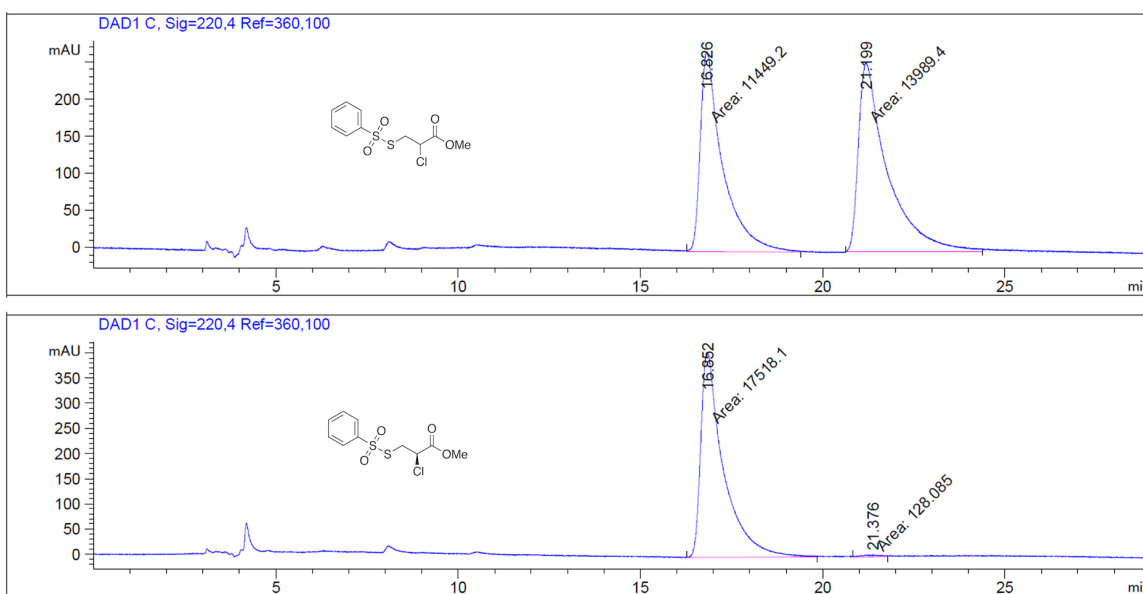


Figure 1-9: HPLC UV trace for compound **13** versus racemic standard.

1.6 2D NMR Data for L-Cystine Diazotization Products

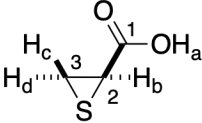
			
Carbon Number	^{13}C signal (ppm)	^1H - ^{13}C HSQC correlation (ppm)	^1H - ^1H COSY correlation
1	171.4		
2	29.2	H_b , 3.42	H_c , H_d
3	23.5	H_c , H_d 2.70	H_b

Table 1.9: ^1H and ^{13}C NMR peak assignments and 2D correlations for thirane carboxylic acid.

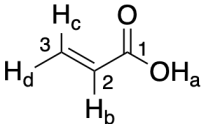
			
Carbon Number	^{13}C signal (ppm)	^1H - ^{13}C HSQC correlation (ppm)	^1H - ^1H COSY correlation
1	166.9		
2	130.7	H_b , 6.08	H_c , H_d
3	129.5	H_c , 6.26 H_d , 5.88	H_b H_b

Table 1.10: ^1H and ^{13}C NMR peak assignments and 2D correlations for acrylic acid.

1.7 X-Ray Crystallographic Data

Empirical formula:	C ₁₂ H ₁₄ O ₅ S ₂
a:	5.428 Å
b:	15.577 Å
c:	15.884 Å
α (alpha):	90.00 °
β (beta):	90.00 °
γ (gamma):	90.00 °
Volume:	1343.02 Å ³
Space group:	P212121
Calculated density:	1.495 g/cm ³
Color:	colourless
Z:	4
Temperature:	-173.0 °C
Formula weight:	302.372 g/mole
R(F):	0.0215
R _w (F ²):	0.0545
Chirality at C2:	R

Table 1.11: Structure Factor data for **11** (CCDC 1949213)

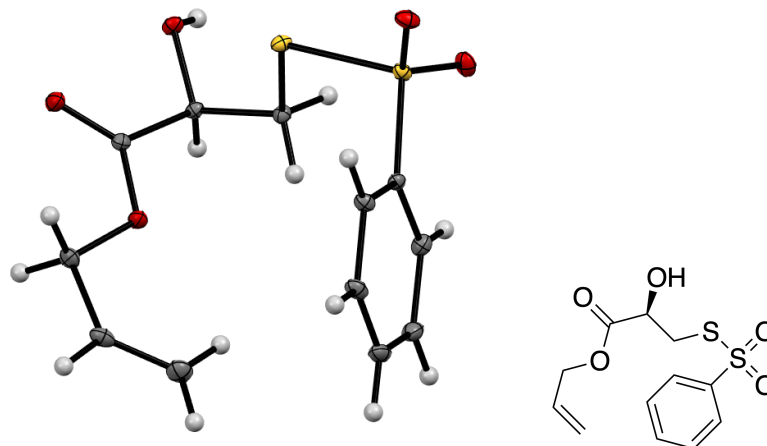
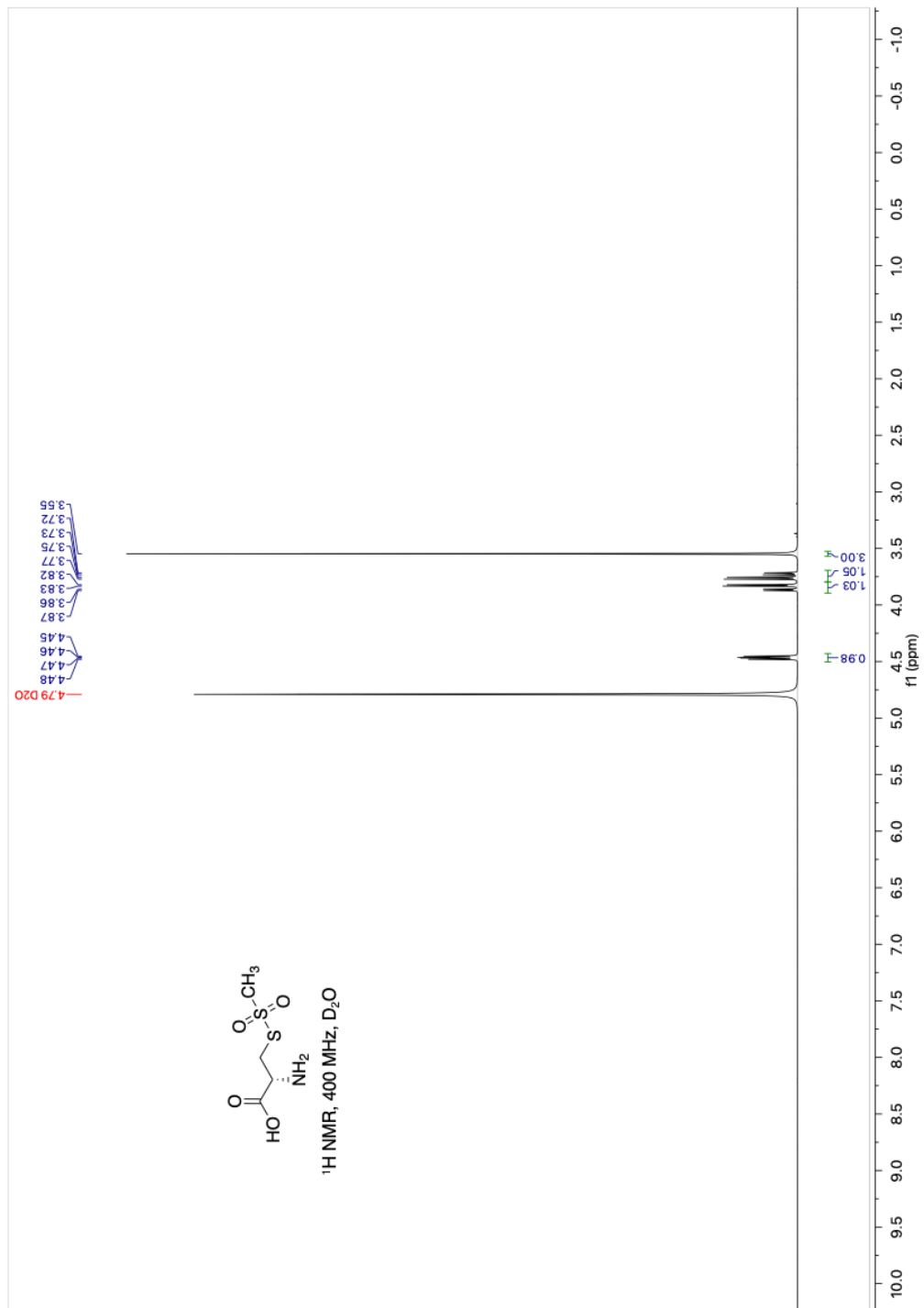
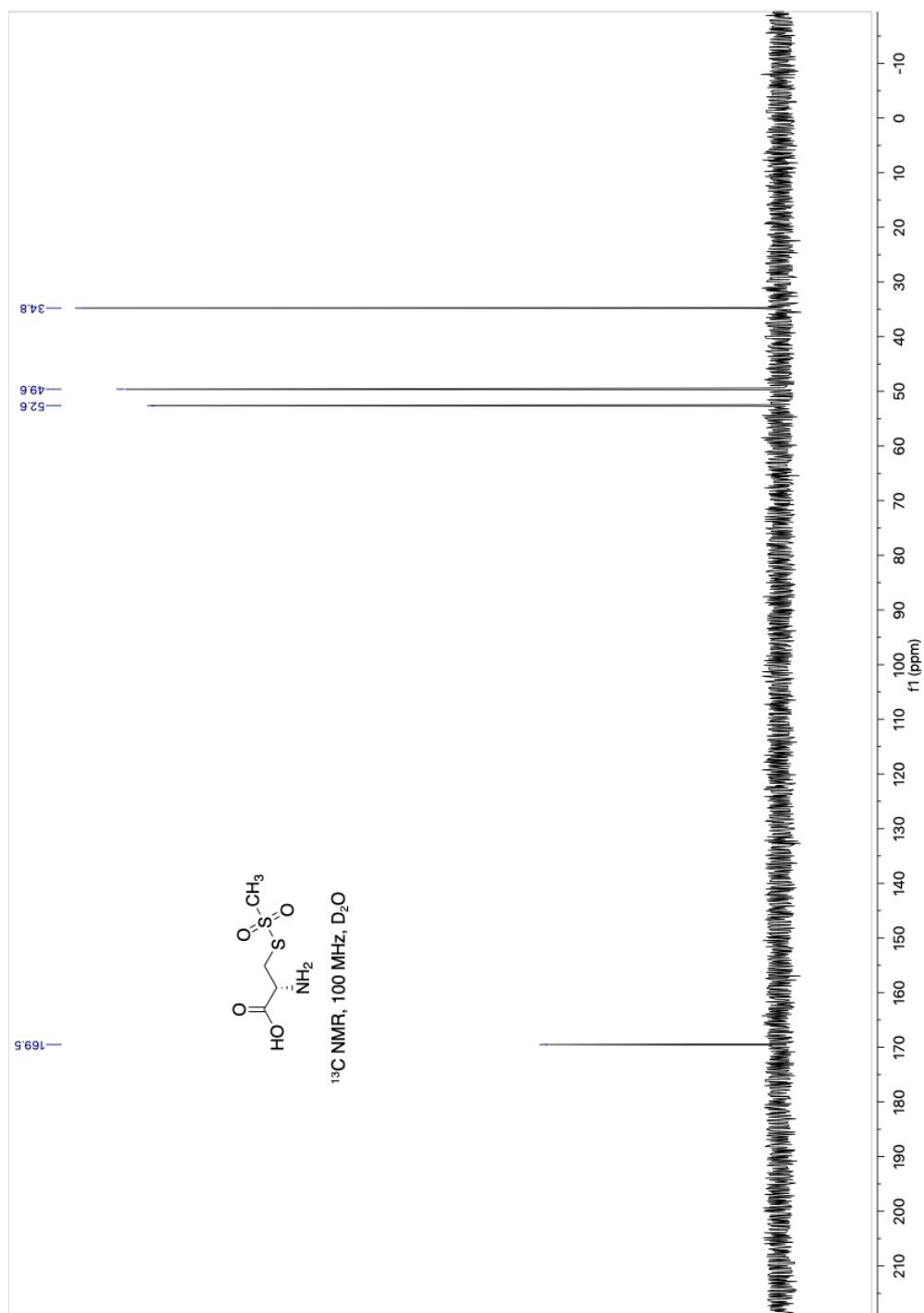


Figure 1-10: Oak Ridge Thermal Ellipsoid Plot (ORTEP) rendering of X-ray crystal structure of compound **11** with 30% ellipsoid probability (CCDC 1949213). Color code: grey for carbon, white for hydrogen, red for oxygen, yellow for sulfur. The crystals were grown by dissolving the purified compound in a minimal amount of diethyl ether and layering with hexanes at room temperature. Dataset was collected in the MIT X-Ray Diffraction Facility by Dr. Peter Müller using a Bruker defrac-tometer coupled to a Bruker Photon II detector. Additional crystal information and experimental parameters are provided in Table 1.11.

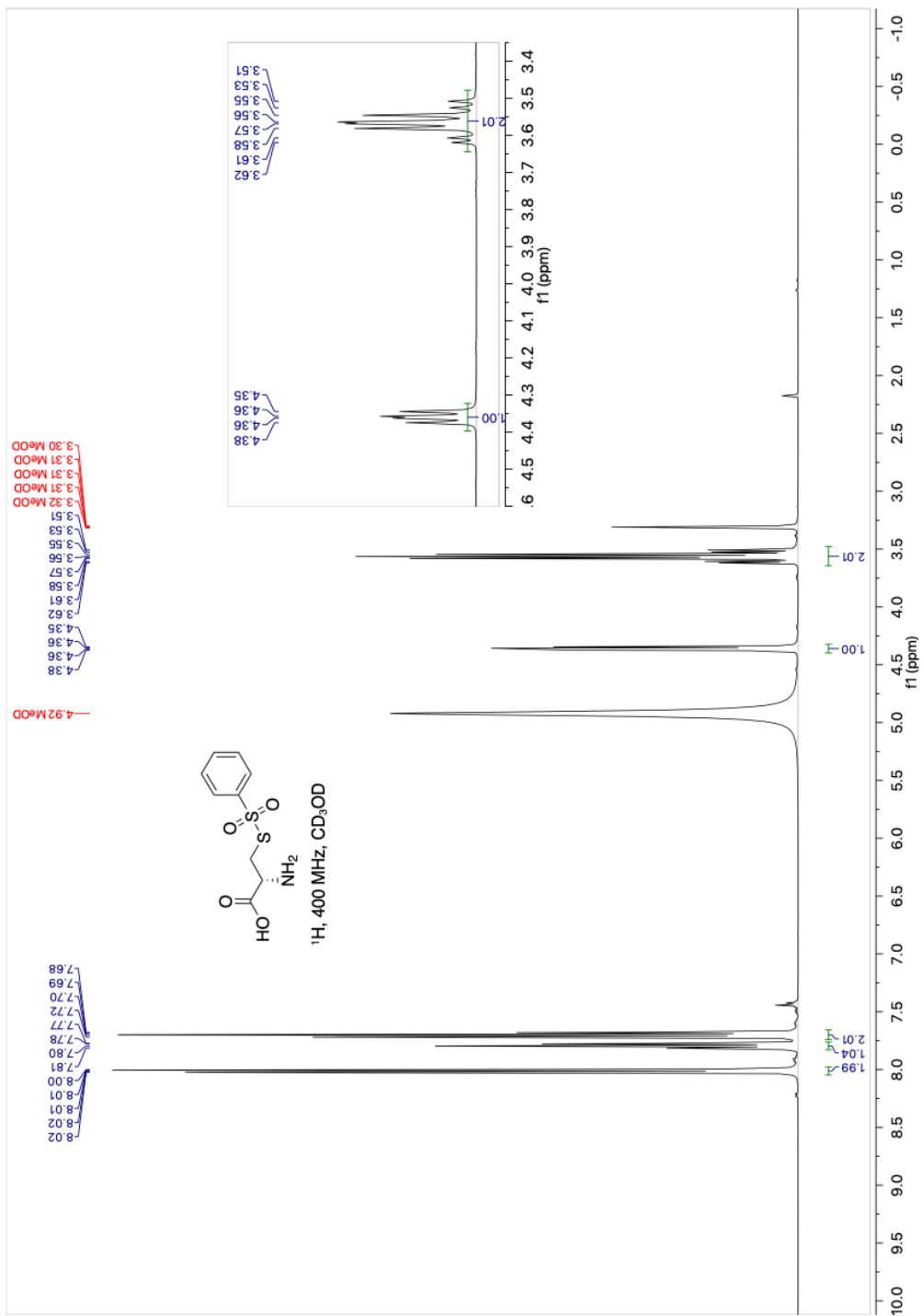
1.8 ^1H and $^{13}\text{C}\{^1\text{H}\}$ NMR Spectra



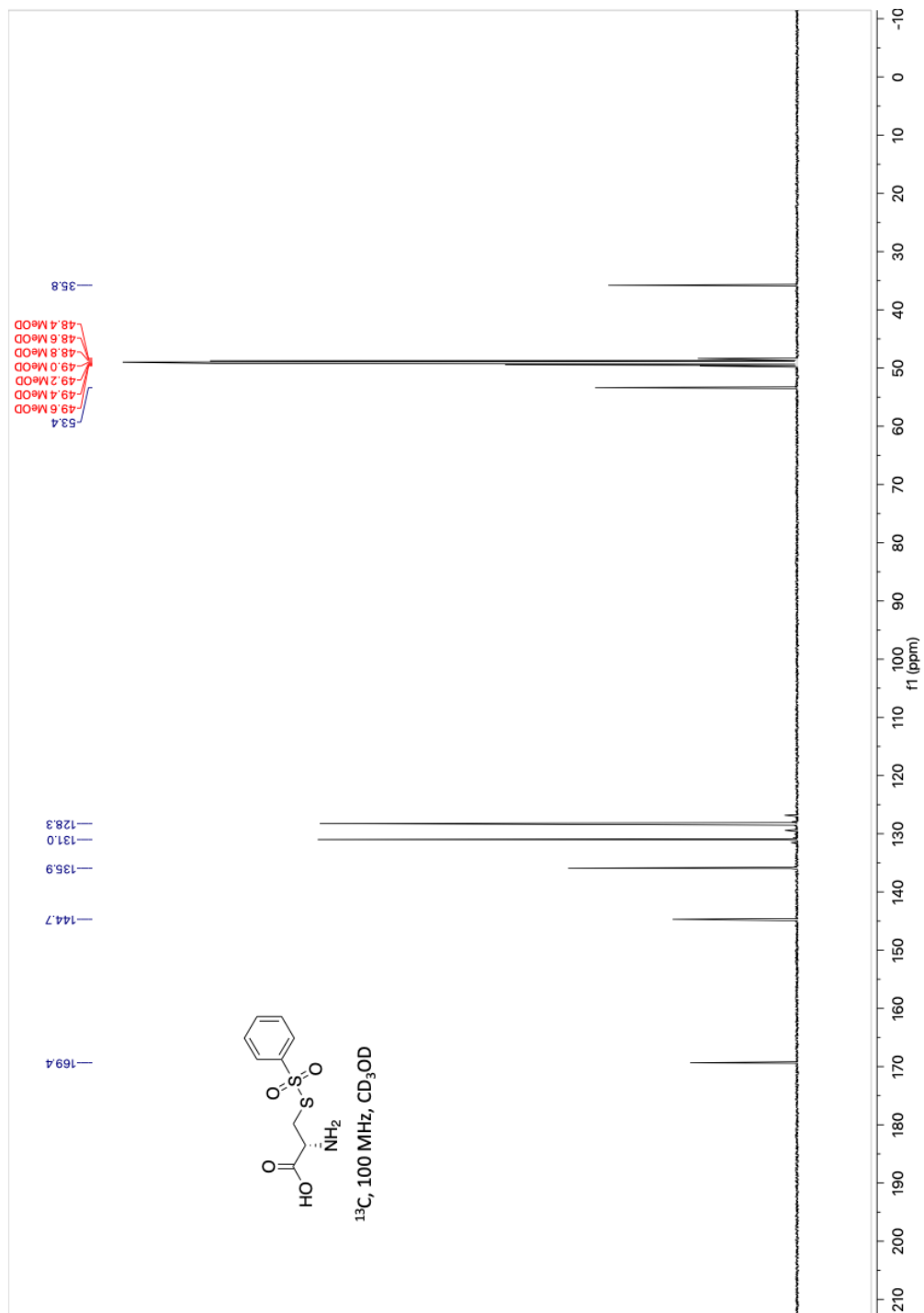
¹H NMR spectrum for 5



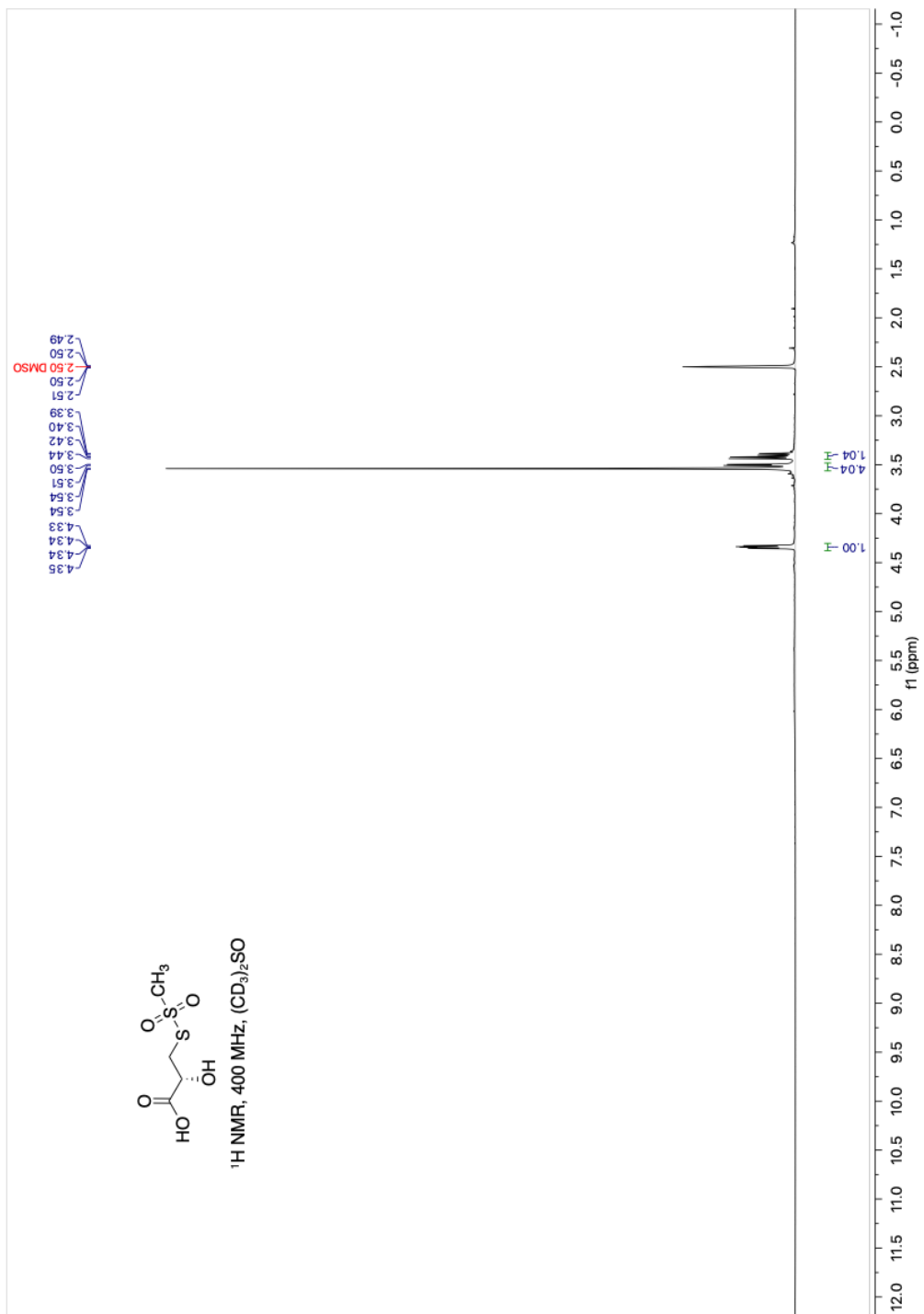
$^{13}\text{C}\{^1\text{H}\}$ NMR spectrum for 5



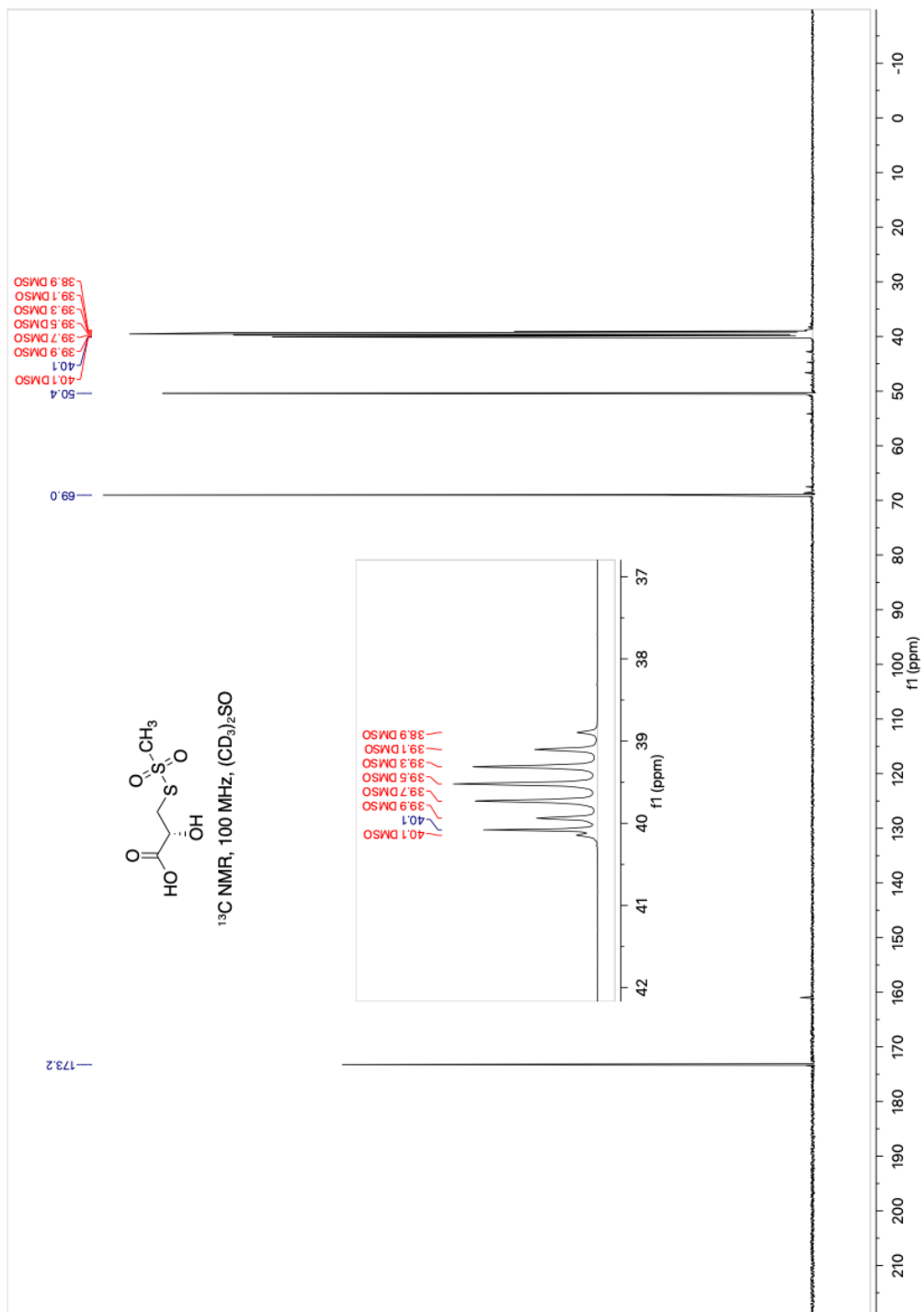
¹H NMR spectrum for **6**



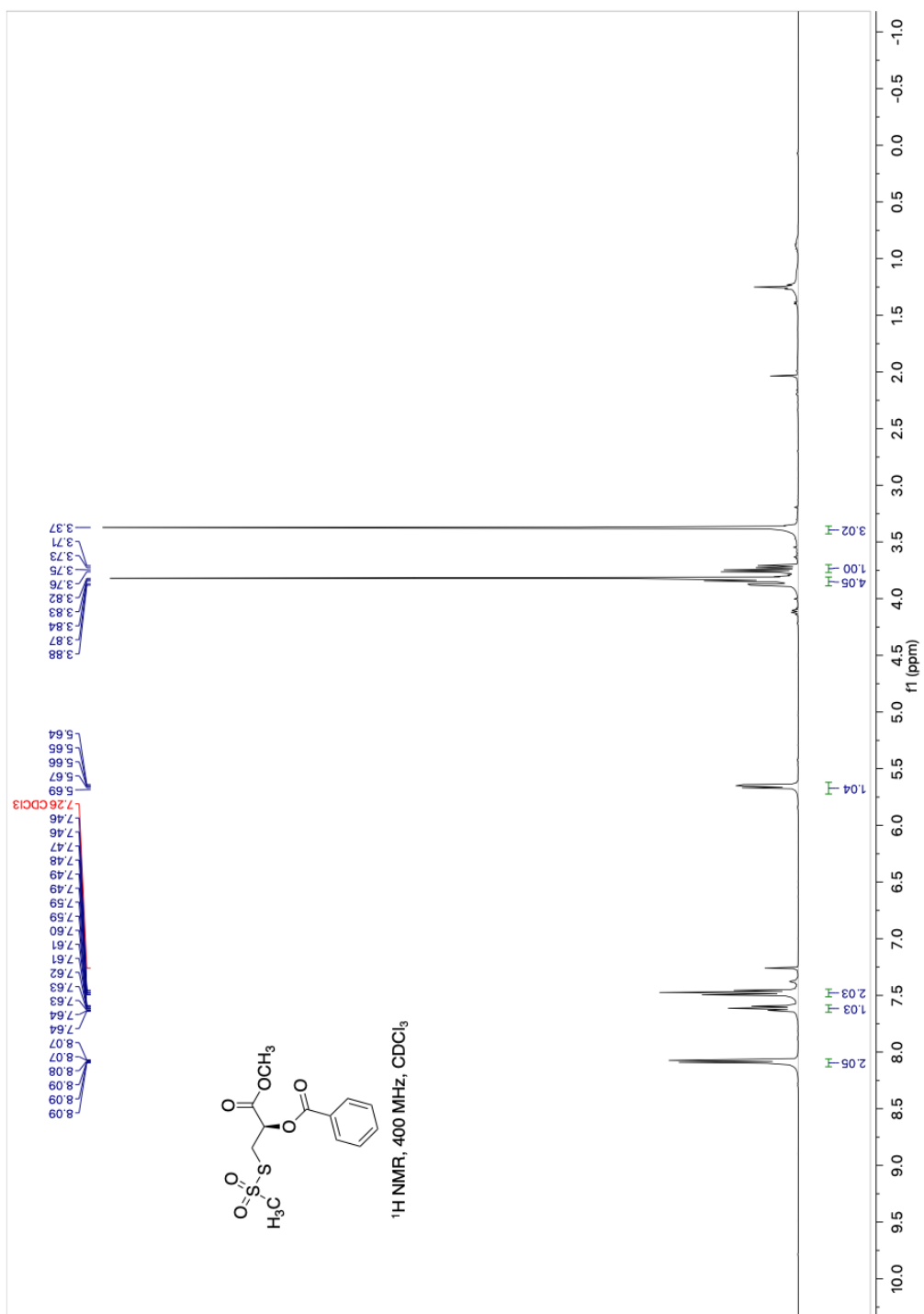
$^{13}\text{C}\{^1\text{H}\}$ NMR spectrum for **6**

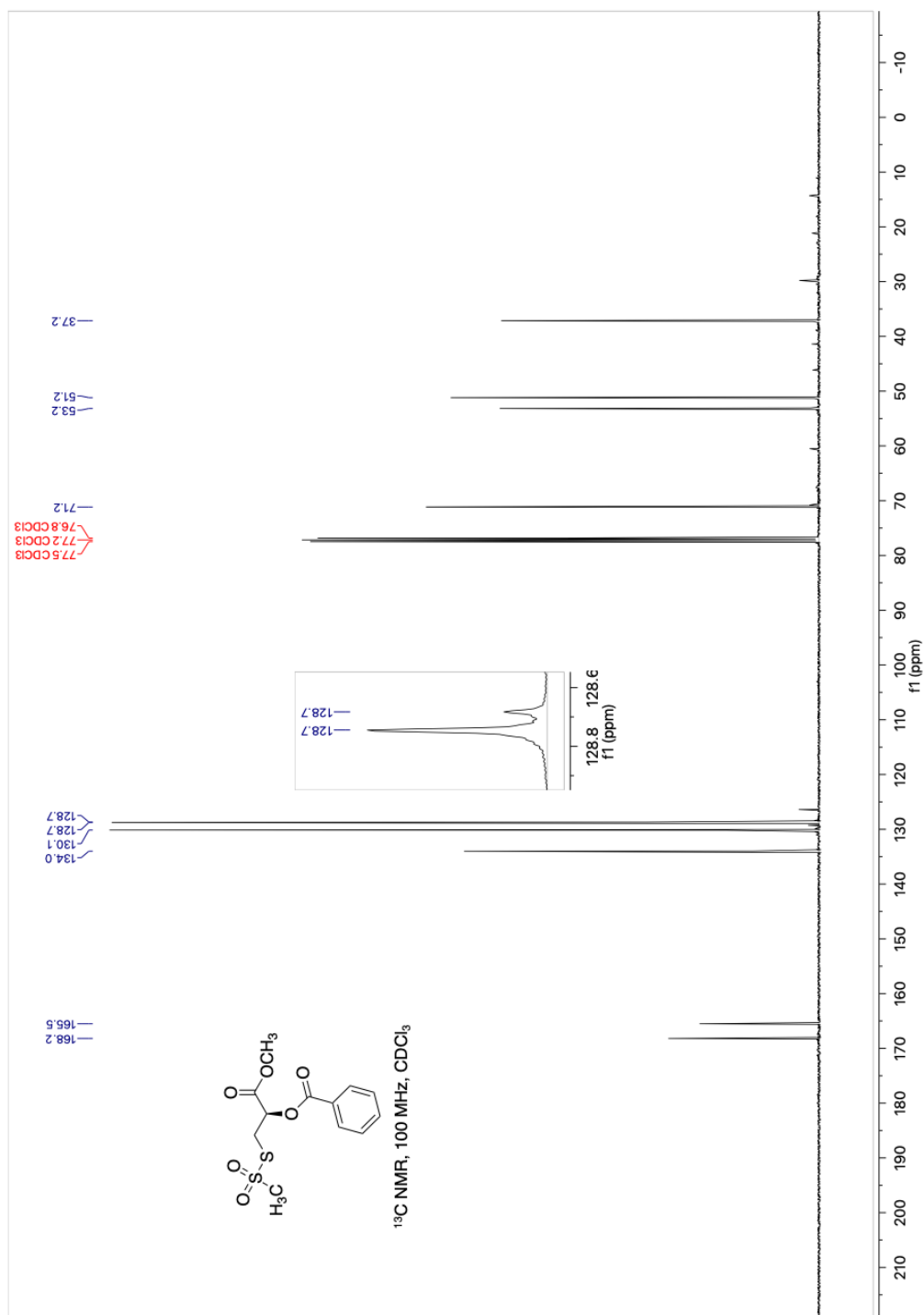


¹H NMR spectrum for **7**

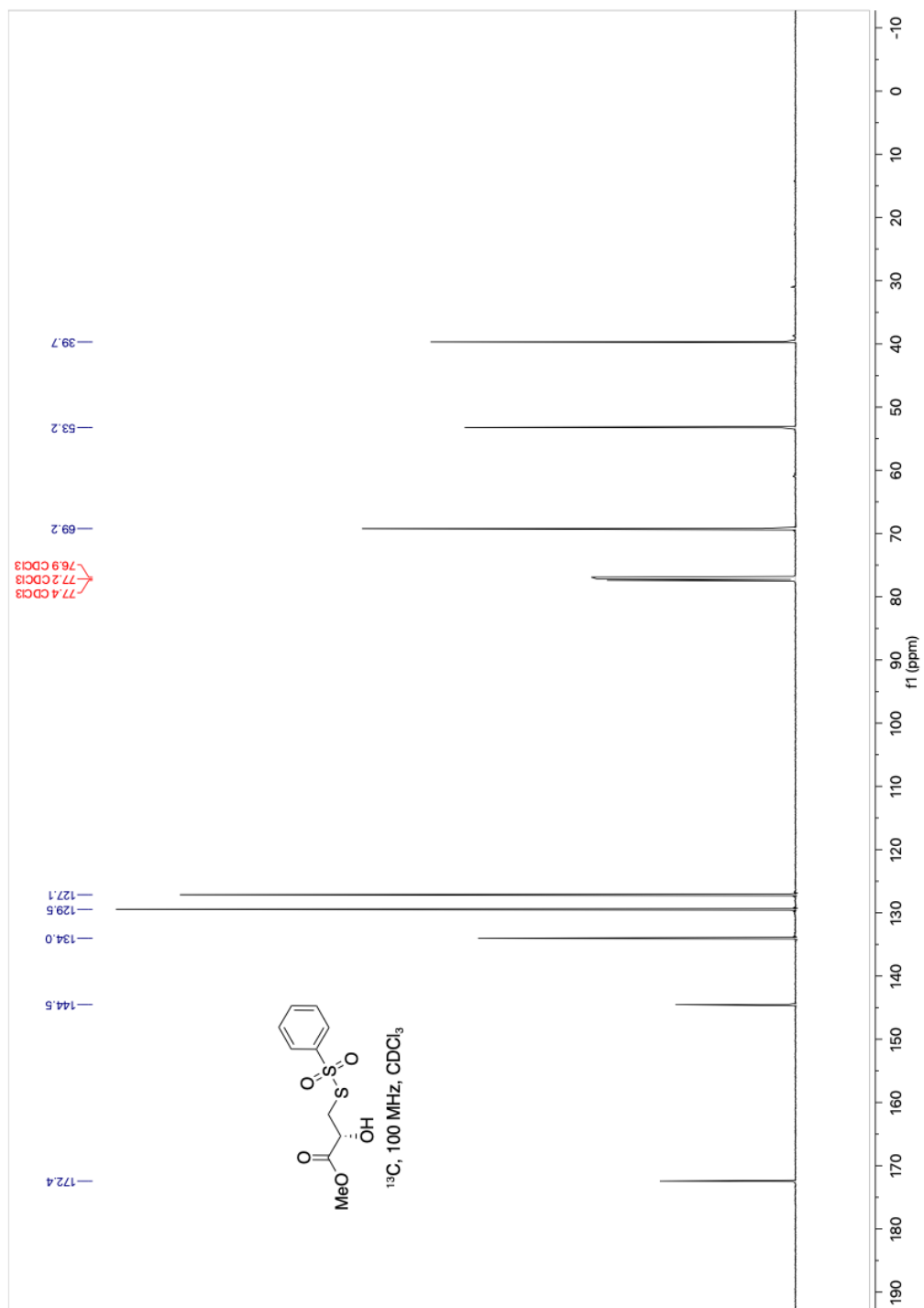


¹³C{¹H} NMR spectrum for **7**

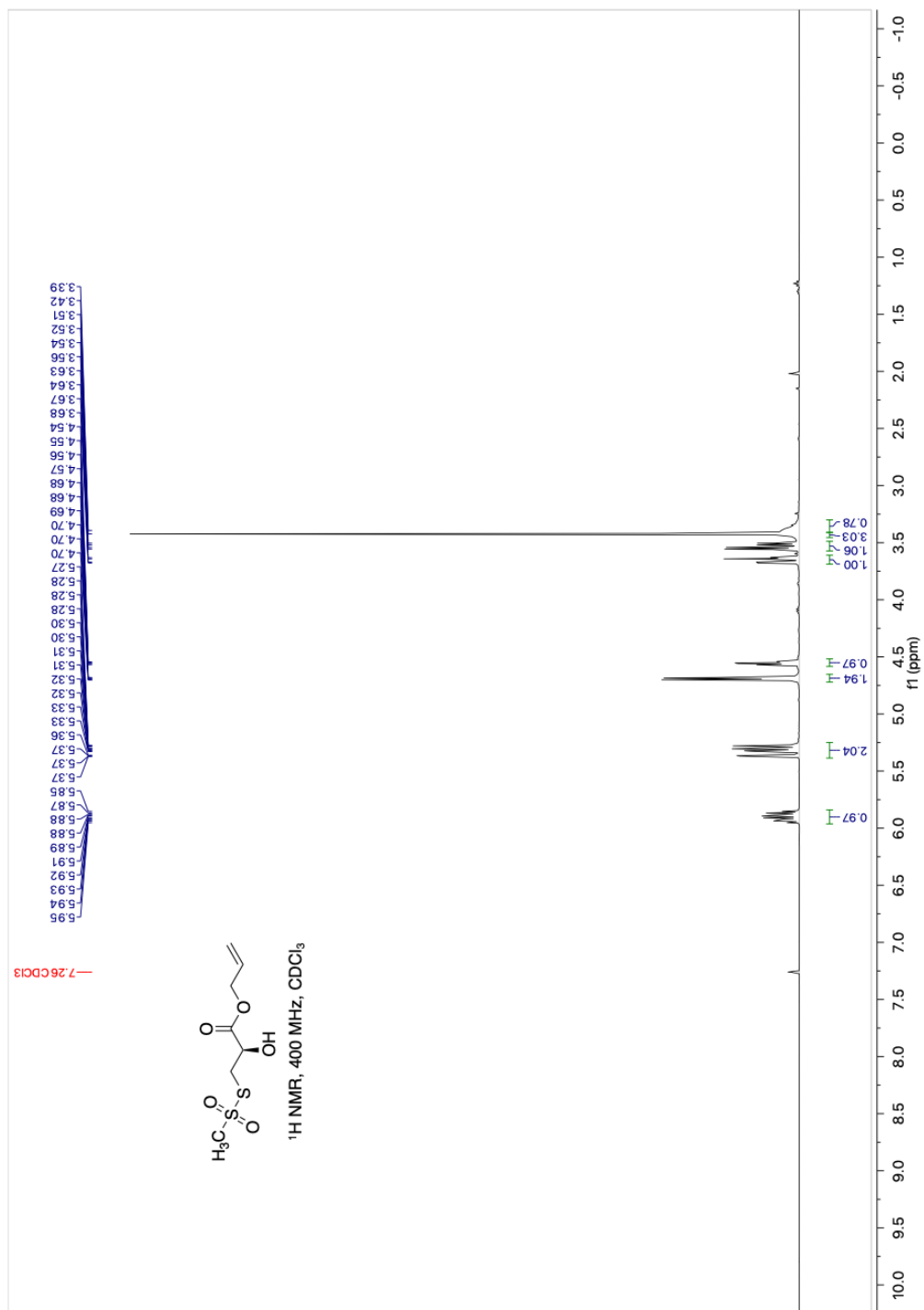




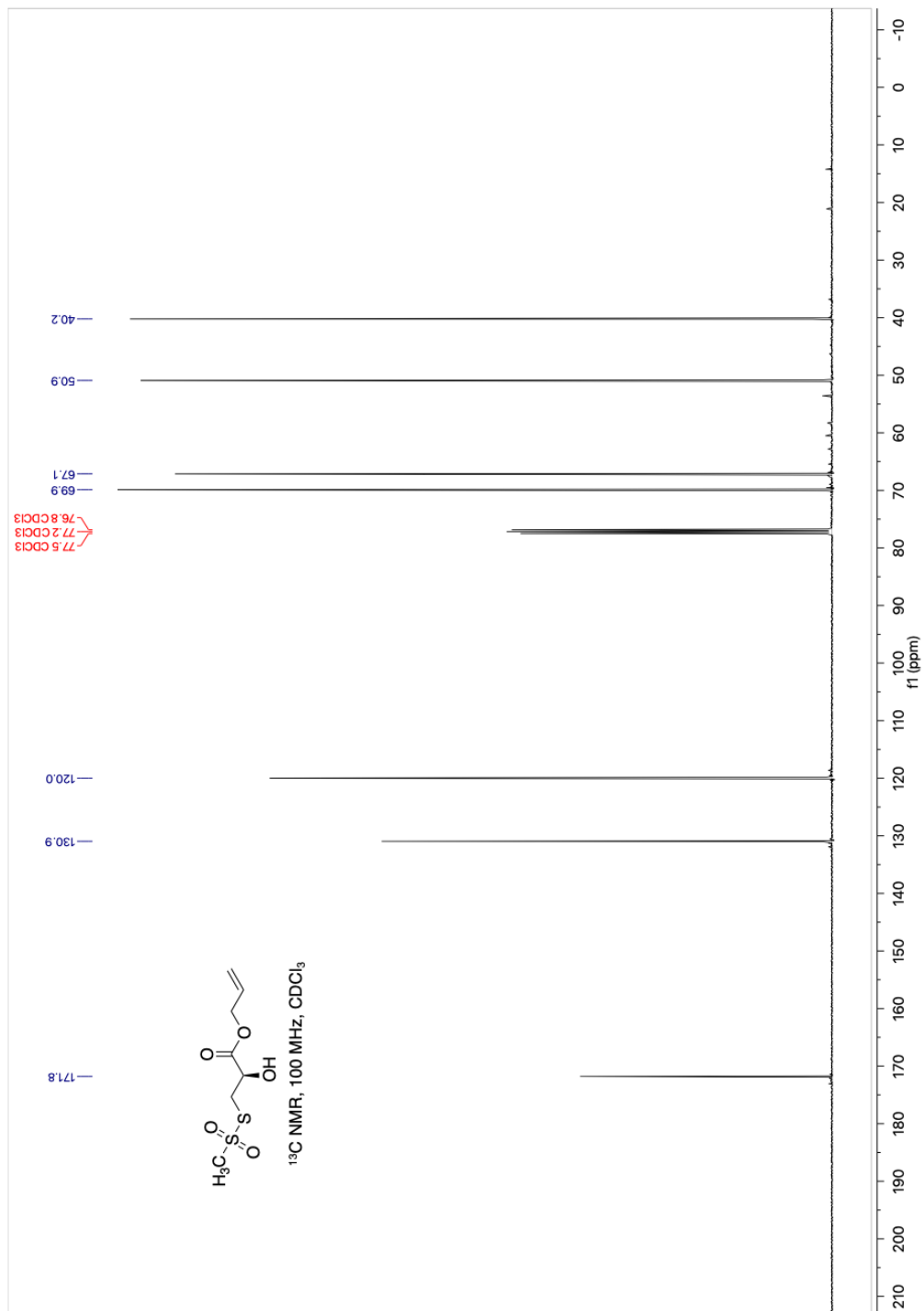
¹³C{¹H} NMR spectrum for **7b**



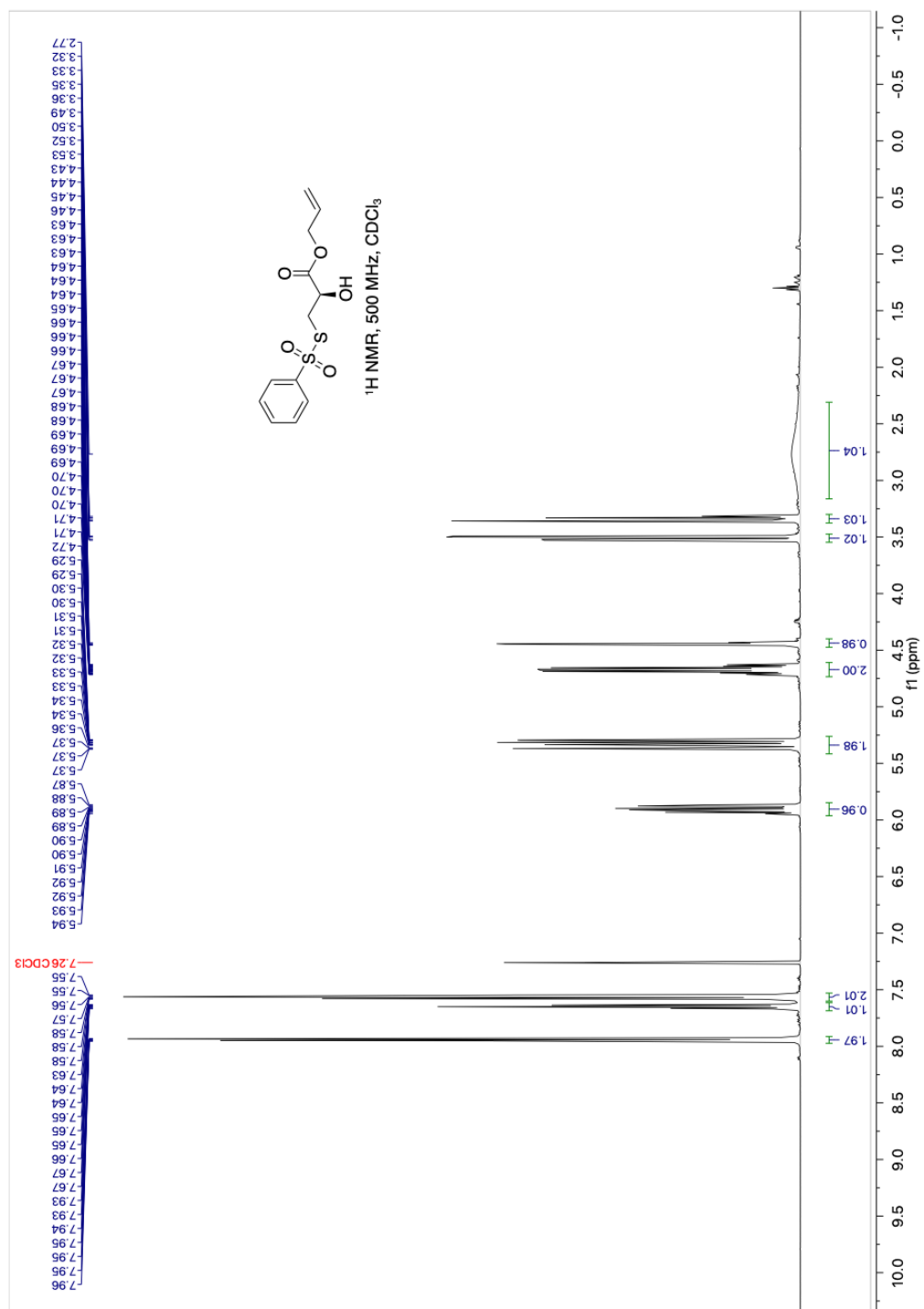
$^{13}\text{C}\{^1\text{H}\}$ NMR spectrum for **9**



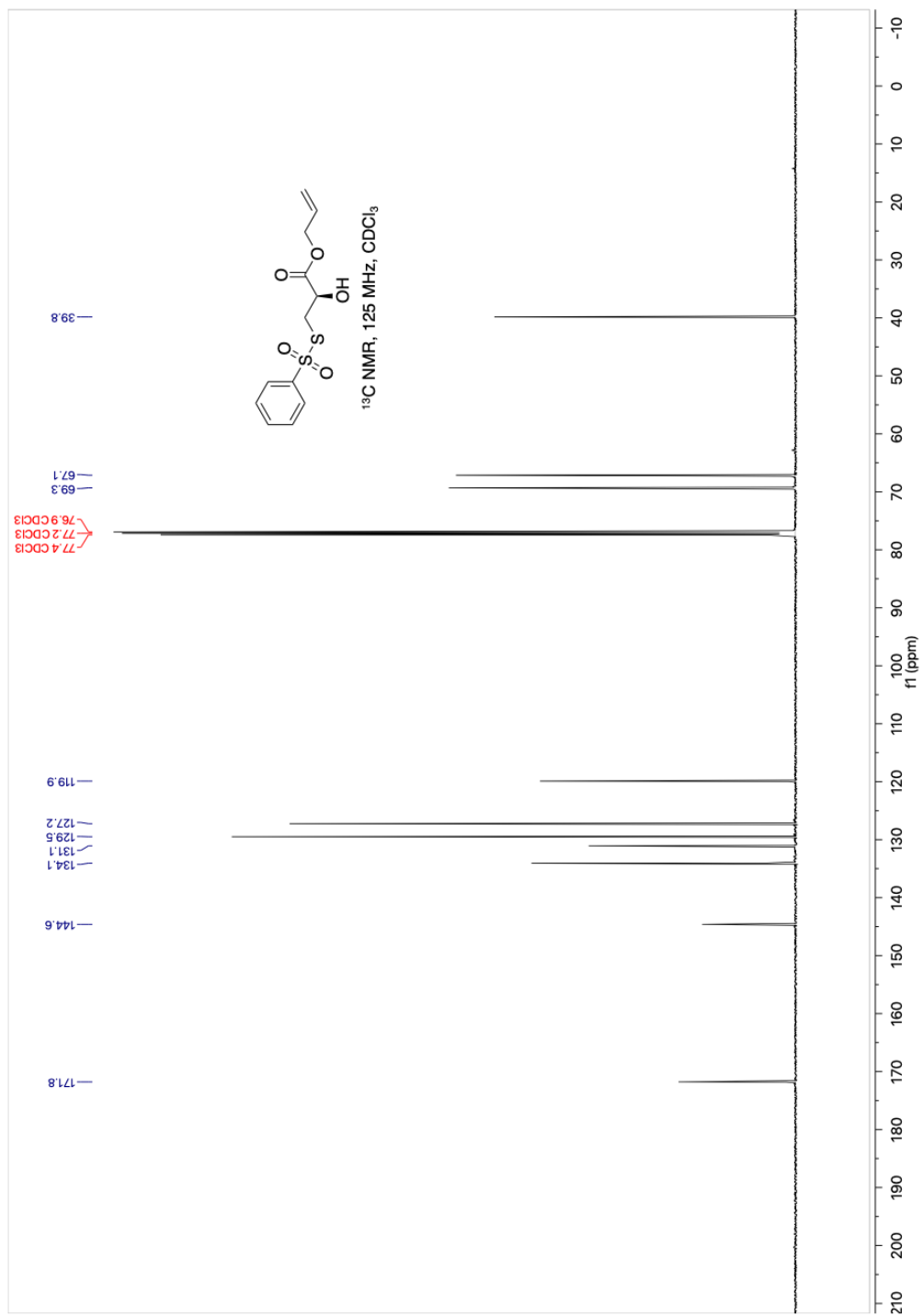
¹H NMR spectrum for **10**



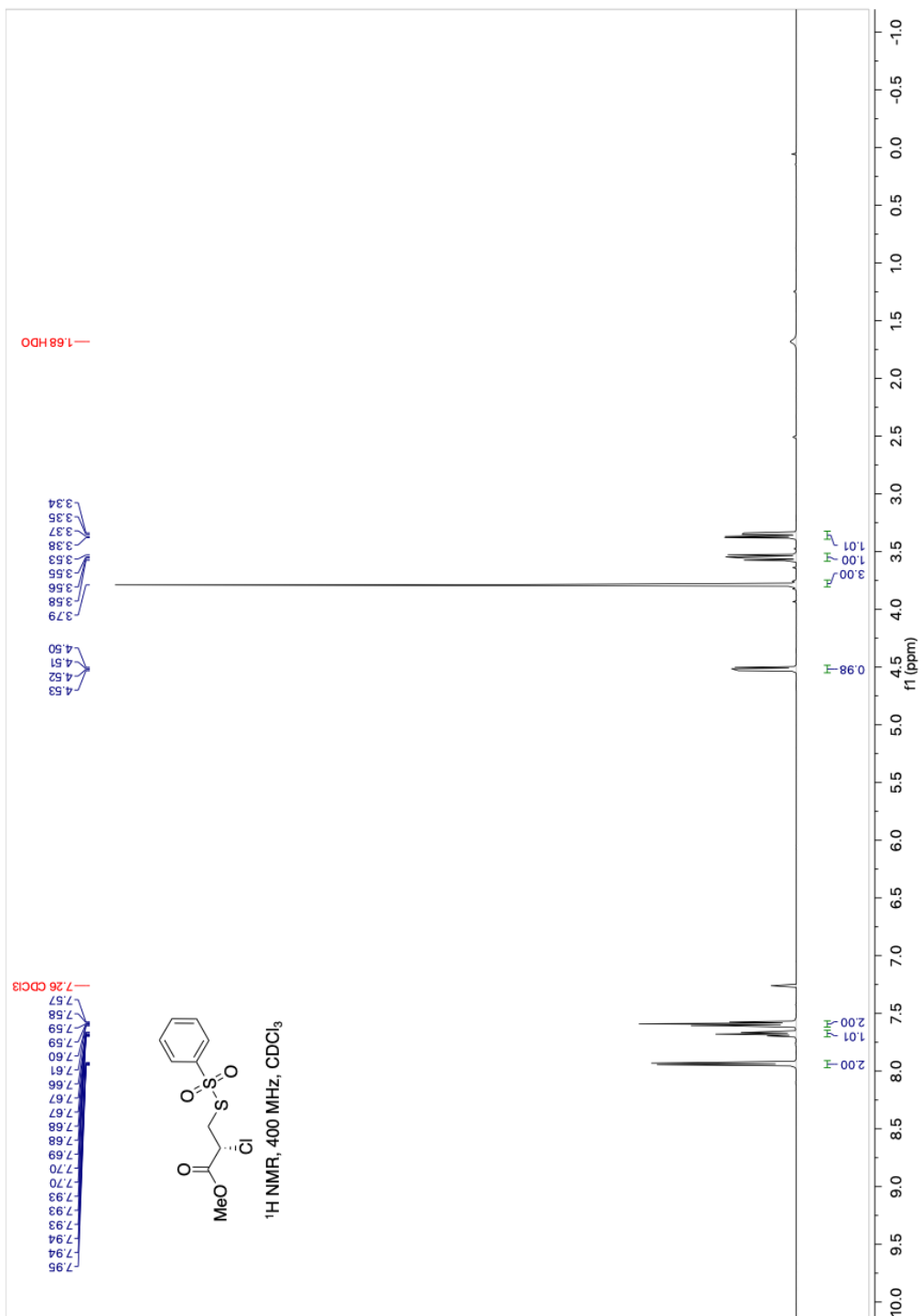
$^{13}\text{C}\{^1\text{H}\}$ NMR spectrum for **10**



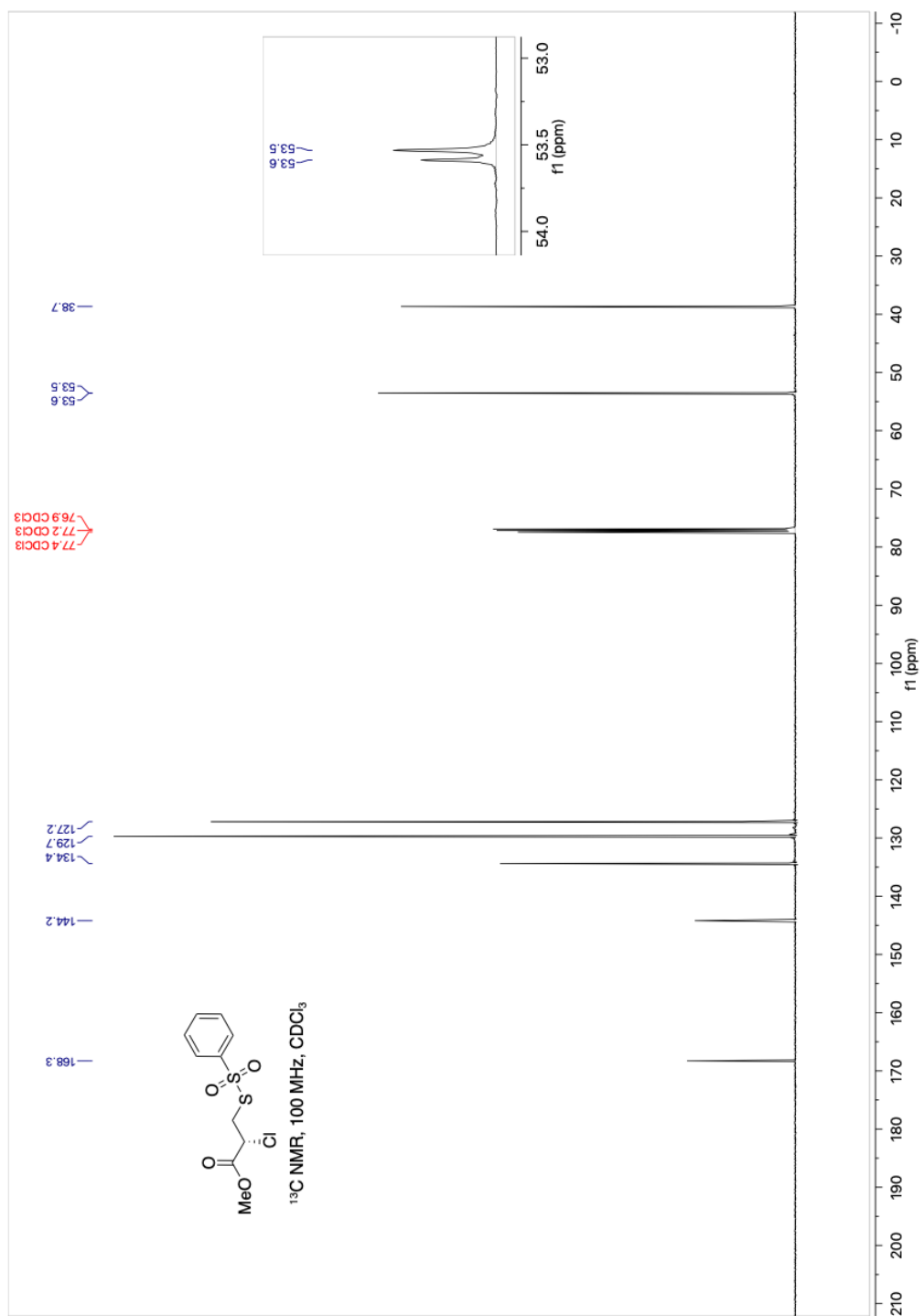
¹H NMR spectrum for **11**



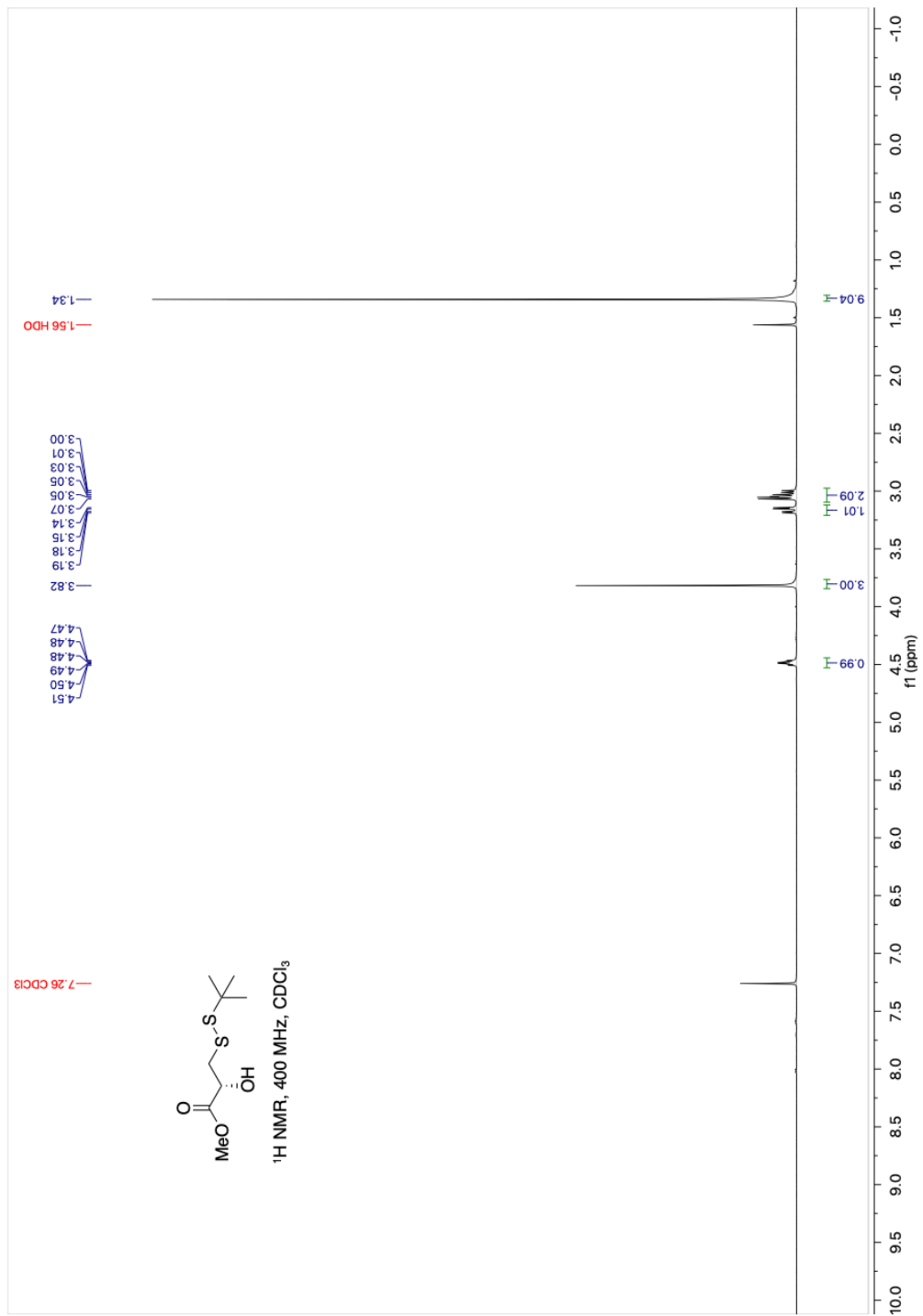
$^{13}\text{C}\{^1\text{H}\}$ NMR spectrum for **11**



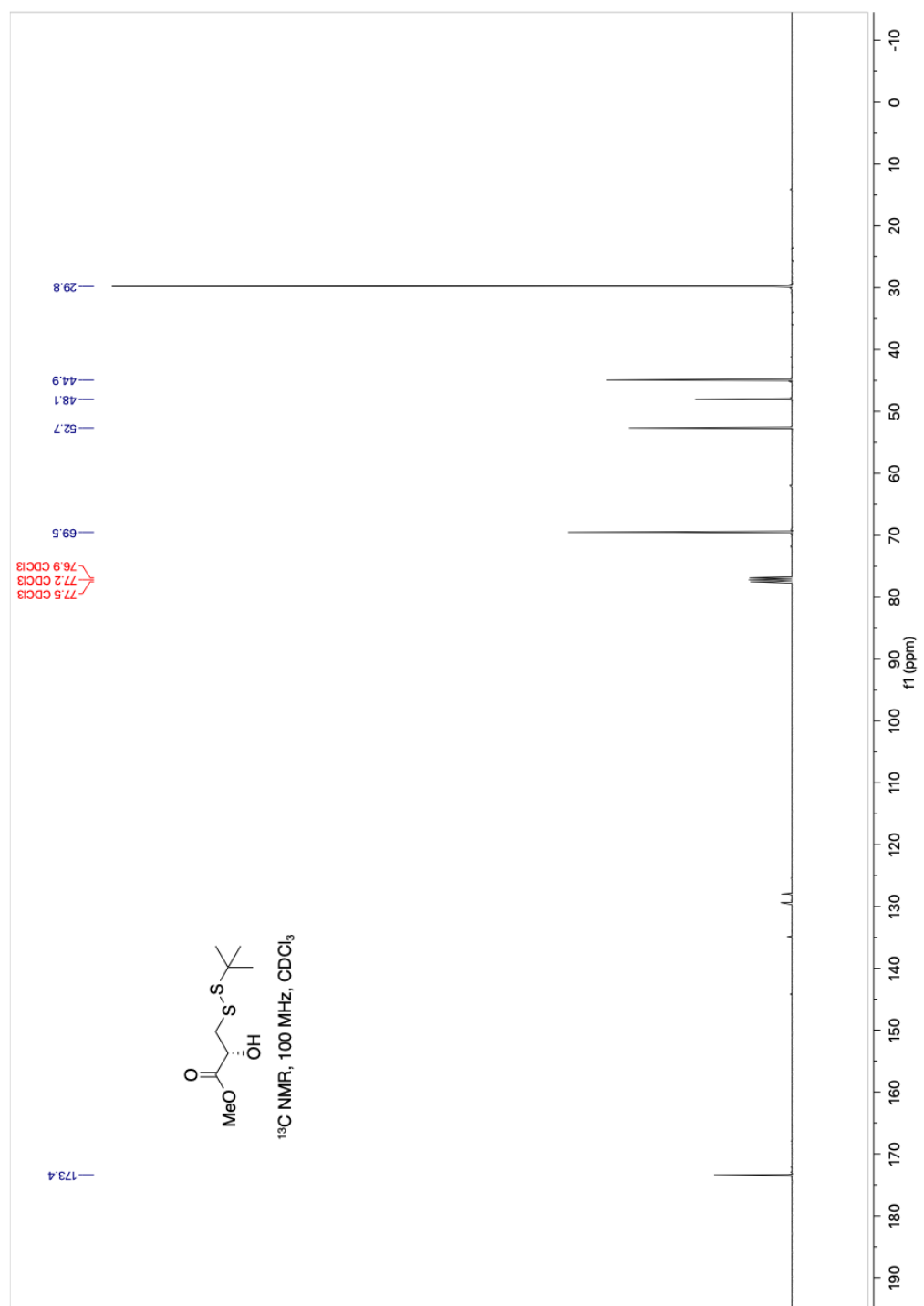
¹H NMR spectrum for **13**



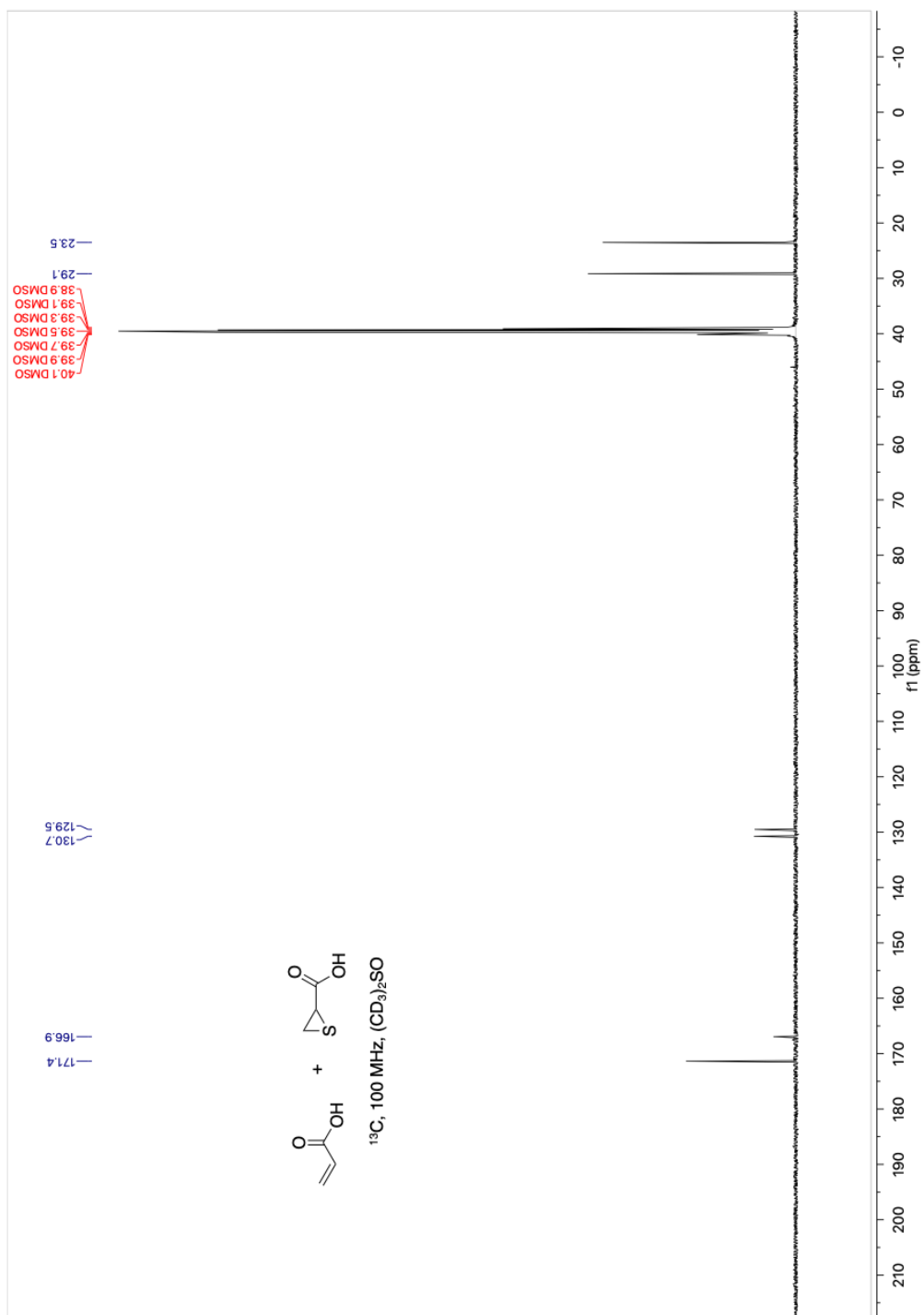
¹³C{¹H} NMR spectrum for **13**



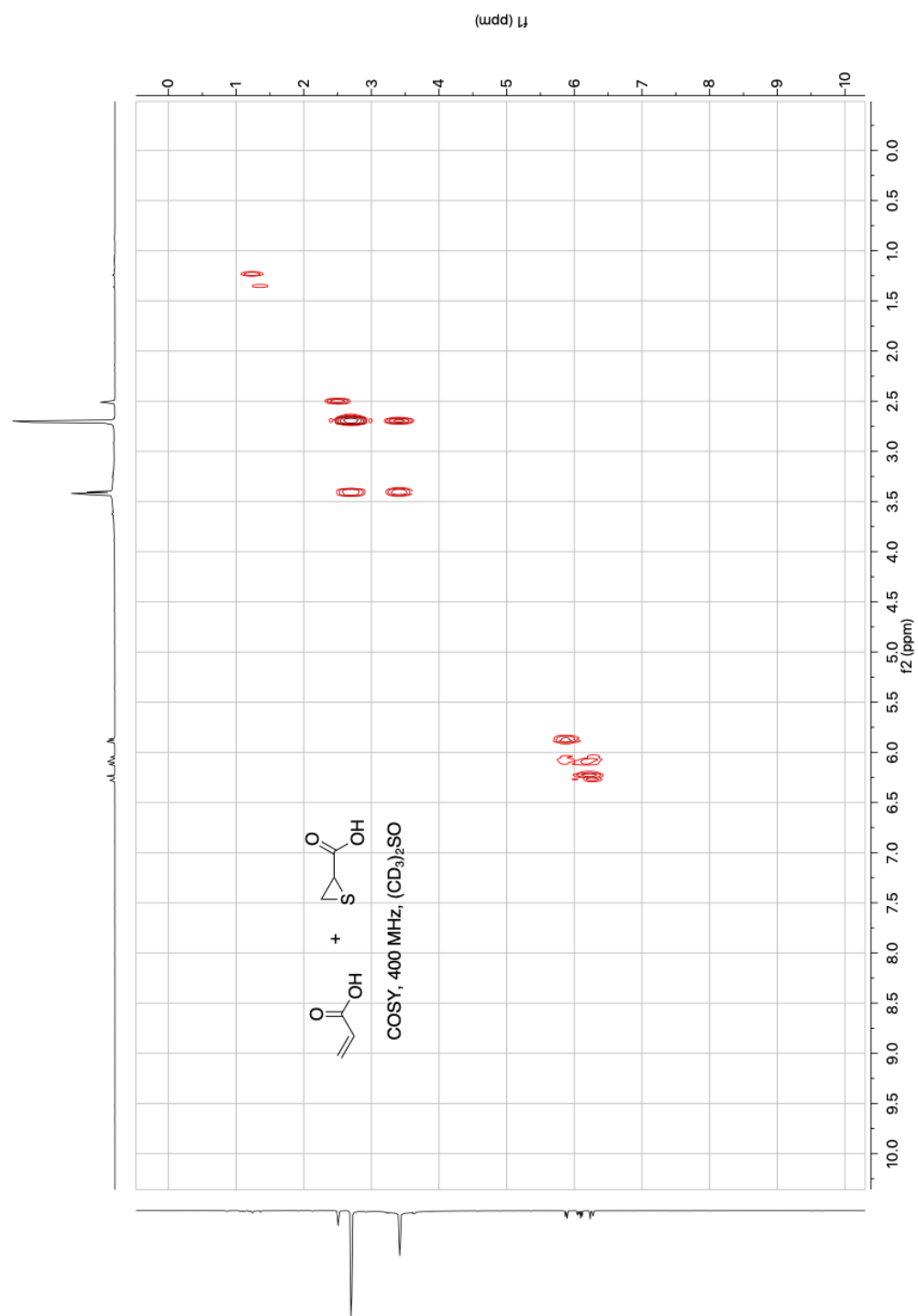
$^1\text{H NMR}$ spectrum for 14



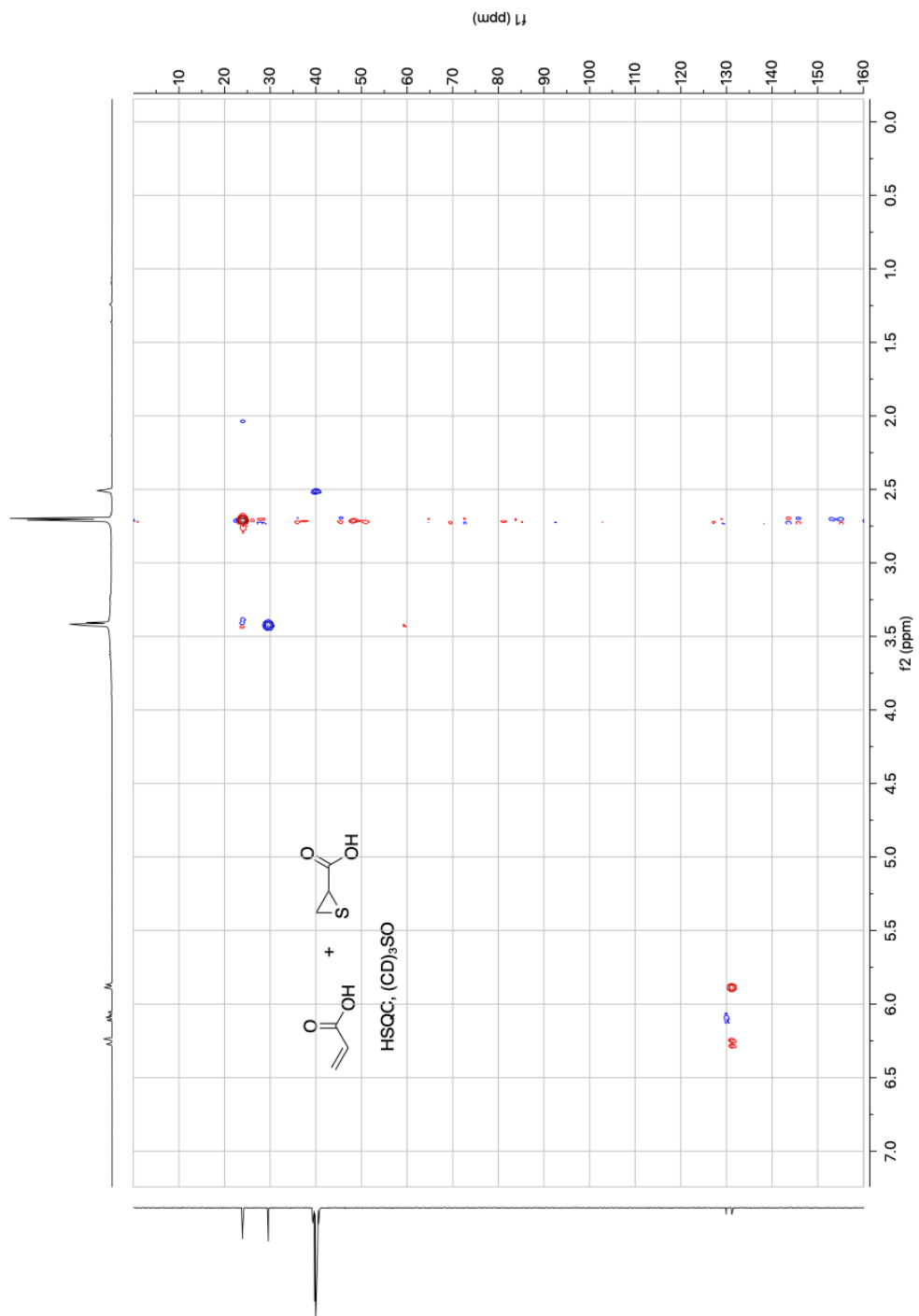
$^{13}\text{C}\{^1\text{H}\}$ NMR spectrum for 14



$^{13}\text{C}\{^1\text{H}\}$ NMR spectrum for thirane-2-carboxylic acid and acrylic acid.



NMR-COSY spectrum for thirane-2-carboxylic acid and acrylic acid. See tabulated correlations, Tables 1.9 and 1.10.



NMR-HSQC spectrum for thirane-2-carboxylic acid and acrylic acid. See tabulated correlations, Tables 1.9 and 1.10.

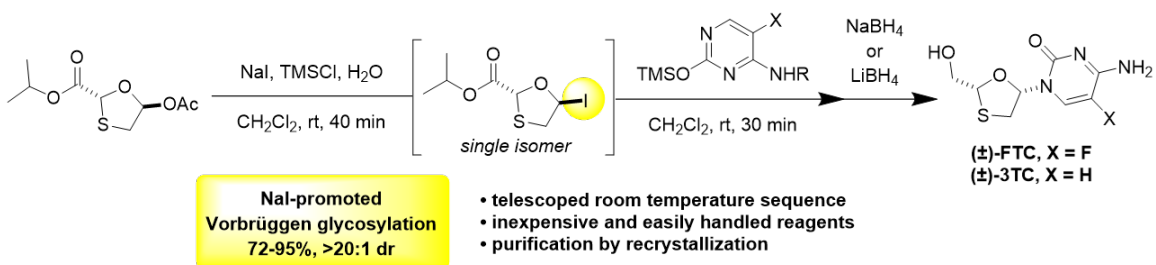
1.9 References

- [1] Coppola, G. M.; Schuster, H. F. *α -Hydroxy Acids in Enantioselective Syntheses*; Wiley-VCH Verlag GmbH & Co. KGaA: Weinheim, Germany, 2002.
- [2] Humber, D. C.; Jones, M. F.; Payne, J. J.; Ramsay, M. V. J.; Zacharie, B.; Jin, H.; Siddiqui, A.; Evans, C. A.; Tse, H. L. A.; Mansour, T. S. *Tetrahedron Lett.* **1992**, *14*, 4625–4628.
- [3] Biel, M.; Deck, P.; Giannis, A.; Waldmann, H. *Chem. Eur. J.* **2006**, *12*, 4121–4143.
- [4] Raza, A. R.; Saddiqa, A.; Çakmak, O. *Chirality* **2015**, *27*, 951–957.
- [5] Hu, D. X.; Bielitz, M.; Koos, P.; Ley, S. V. *Tetrahedron Lett.* **2012**, *53*, 4077–4079.
- [6] Lücke, D.; Dalton, T.; Ley, S. V.; Wilson, Z. E. *Chem. Eur. J.* **2016**, *22*, 4206–4217.
- [7] Matthes, D.; Richter, L.; Müller, J.; Denisiuk, A.; Feifel, S. C.; Xu, Y. *Chem. Commun.* **2012**, *48*, 5674–5676.
- [8] Albertsson, A.-C.; Varma, I. K. *Biomacromolecules* **2003**, *4*, 1466–1486.
- [9] Rasal, R. M.; Janorkar, A. V.; Hirt, D. E. *Prog. Pol. Sci.* **2010**, *35*, 338–356.
- [10] Lu, Y.; Yin, L.; Zhang, Y.; Zhonghai, Z.; Xu, Y.; Tong, R.; Cheng, J. *ACS Macro Lett.* **2012**, *1*, 441–444.
- [11] Sokolsky-Papkov, M.; Agashi, K.; Olaye, A.; Shakesheff, K.; Domb, A. J. *Adv. Drug Deliv. Rev.* **2007**, *59*, 187–206.
- [12] Hu, D. X.; O'Brien, M.; Ley, S. V. *Org. Lett.* **2012**, *14*, 4246–4249.
- [13] Stühr-Hansen, N.; Padrah, S.; Strømgaard, K. *Tetrahedron Lett.* **2014**, *55*, 4149–4151.
- [14] Koppenhoefer, B.; Schurig, V. *Org. Synth.* **1988**, *66*, 151.
- [15] Deechongkit, S.; You, S.-L.; Kelly, J. W. *Org. Lett.* **2004**, *6*, 497–500.
- [16] Muhl, C.; Schäfer, O.; Bauer, T.; Räder, H.-J.; Barz, M. *Macromolecules* **2018**, *51*, 8188–8196.
- [17] Schäfer, O.; Huesmann, D.; Muhl, C.; Barz, M. *Chem. Eur. J.* **2016**, *22*, 18085–18091.
- [18] Rojas, A. J.; Pentelute, B. L.; Buchwald, S. L. *Org. Lett.* **2017**, *19*, 4263–4266.

- [19] Hanaya, K.; Ohata, J.; Miller, M. K.; Mangubat-Medina, A. E.; Swierczynski, M. J.; Yang, D. C.; Rosenthal, R. M.; Popp, B. V.; Ball, Z. T. *Chem. Commun.* **2019**, *55*, 2841–2844.
- [20] Hope, D. B.; Wälti, M. *J. Chem. Soc. C* **1970**, *18*, 2475–2478.
- [21] Burke, H. M.; McSweeney, L.; Scanlan, E. M. *Nat. Commun.* **2017**, *8*, 15655.
- [22] Oae, S.; Fukushima, D.; Kim, Y. H. *Chem. Lett.* **1978**, *7*, 279–280.
- [23] Leonov, A.; Voigt, B.; neda, F. R.-C.; Sakhaii, P.; Griesinger, C. *Chem. Eur. J.* **2005**, *11*, 3342–3348.
- [24] Huesmann, D.; Schäfer, O.; Braun, L.; Klinker, K.; Reuter, T.; Barz, M. *Tetrahedron Lett.* **2016**, *57*, 1138–1142.
- [25] Carlson, R. *Design and optimization in organic synthesis*, 1st ed.; Elsevier Science B.V.: Amsterdam, The Netherlands, 1992.
- [26] Hyde, A. M.; Zultanski, S. L.; Waldman, J. H.; Zhong, Y.-L.; Shevlin, M.; Peng, F. *Org. Process Res. Dev.* **2017**, *21*, 1355–1370.
- [27] Lestard, M. E. D.; Ramos, L. A.; e. Tuttolomondo, M.; Ulic, S. E.; Altabef, A. B. *Vib. Spectrosc.* **2012**, *59*, 40–46.
- [28] Galván, J. E.; Aguilar, E. C.; Lestard, M. E. D.; Tuttolomondo, M. E.; Ulic, S. E.; Altabef, A. B. *Inorg. Chim. Acta* **2017**, *455*, 254–261.
- [29] Fulmer, G. R.; Miller, A. J. M.; Sherden, N. H.; Gottlieb, H. E.; Nudelman, A.; Stoltz, B. M.; Bercaw, J. E.; Goldberg, K. I. *Organometallics* **2010**, *29*, 2176–2179.
- [30] Maycock, C. D.; Stoodley, R. J. *J. Chem. Soc. Perk. T. 1* **1979**, 1852–1857.
- [31] Yu, H.; Ru, S.; Dai, G.; Zhai, Y.; Lin, H.; Han, S.; Wei, Y. *Angew. Chem. Int. Ed.* **2017**, *56*, 3867–3871.

Chapter 2

Synthesis of Emtricitabine and Lamivudine by Chlorotrimethylsilane–Sodium Iodide-Promoted Vorbrüggen Glycosylation



2.1 Introduction

Emtricitabine (FTC) and lamivudine (3TC) comprise key components of most combination therapies used for treatment of HIV infection.¹ These active ingredients contain subtle structural complexities, most notably the *cis* configuration about the 2',3'-dideoxy framework and the epimerizable thioacetal of the oxathiolane. Both

FTC and 3TC display opposite geometry relative to naturally occurring nucleosides and are dosed in enantiopure form due to the higher toxicity of their enantiomers.¹ Merely two approaches prepare these targets from chiral building blocks while the majority of reported synthetic strategies employ either chemical or enzymatic kinetic resolution of (\pm)-FTC and (\pm)-3TC for isolation of the desired enantiomer (Figure 2-1).² Chemical resolution strategies which are enacted prior to *N*-glycosylation include a longstanding route invented by GlaxoSmithKline (GSK) and a recent report by Medicines for All (M4All).^{3,4} Successful strategies for enzymatic resolution (DKR) of early intermediates include ester cleavage or acetylation of intermediates, yet these approaches achieve poor diastereoselectivity in subsequent *N*-glycosylation.^{5,6} Resolution after *N*-glycosylation constitutes another viable strategy.⁷⁻¹⁶ Herein, we report a method for chlorotrimethylsilane–sodium iodide-promoted Vorbrüggen glycosylation en route to FTC and 3TC, and apply the optimized method to a synthesis of diastereomerically pure (\pm)-FTC and (\pm)-3TC suitable for chiral resolution.

Formation of an anomeric iodide to react with a silylated pyrimidine by a Vorbrüggen glycosylation has emerged as an effective strategy for achieving selective formation of the desired *cis* oxathiolane with chiral glycosyl donor **3** (Figure 2-1).^{3,11,17} Precedented methods include the use of iodotrimethylsilane (TMSI) or I₂–triethylsilane (in situ generation of HI) to access the iodide. These reagents are effective yet exhibit disadvantages including cost and instability. The more inexpensive polymethylhydrosiloxane (PMHS) replaces triethylsilane for a cost-effective option, although separation of the product from polymeric siloxanes remains problematic. We sought to develop a promoter system for this desirable Vorbrüggen glycosylation which would provide improved ease of handling and use economical reagents.

2.2 Results and Discussion

Considering the precedence of chlorotrimethylsilane (TMSCl) in combination with sodium iodide in acetonitrile (MeCN) for the dealkylation of ethers and esters, we hypothesized that treatment of **3** with TMSCl and NaI would lead directly to iodide

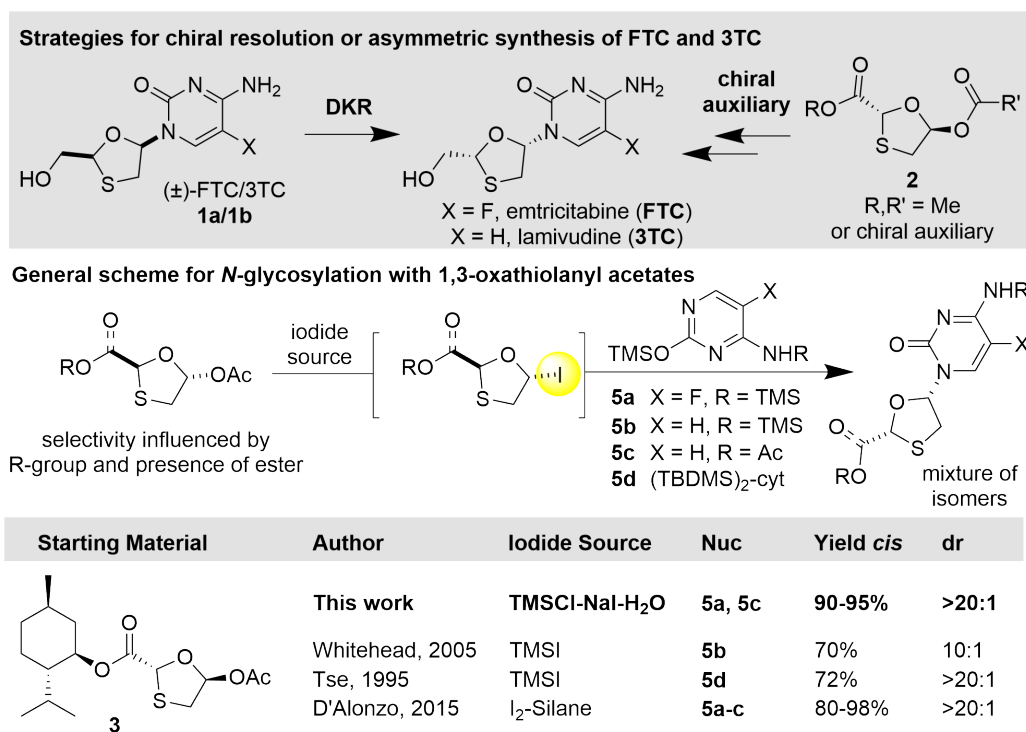


Figure 2-1: Strategies for synthesis of FTC/3TC and contextualization of TMSCl–NaI method with precedent. ? ? ? ?

4.¹⁸ We assayed the formation of **4** by ¹H NMR after treatment of **3** with TMSCl–NaI, monitoring the anomeric proton of **4** which possesses a diagnostic chemical shift of 7.2 ppm and coupling constant of 4.2 Hz (Figure 2-2). Preliminary experiments encouragingly showed formation of **4** using TMSCl–NaI both in MeCN and CH₂Cl₂. In a control experiment no conversion was observed in absence of NaI, but formation of **4** (87% conversion) was obtained upon late addition of the salt to the mixture.

The formation of **4** via activation of **3** with TMSCl–NaI was telescoped into a two-step sequence to assay the glycosylation of silylated 5-fluorocytosine (**5a**). It was found that water content and solvent have remarkable effects on yield and diastereoselectivity, respectively (Table 2.1). An initial test of TMSCl–NaI in MeCN showed conversion of intermediate **4** to desired product **6a**, with moderate diastereoselectivity (Table 2.1, entry 1). Suspecting that adventitious water was introduced into the reaction by NaI, extra care was taken to exclude water in a second trial. Surprisingly, lower yield and lower conversion were observed, indicating that the desired

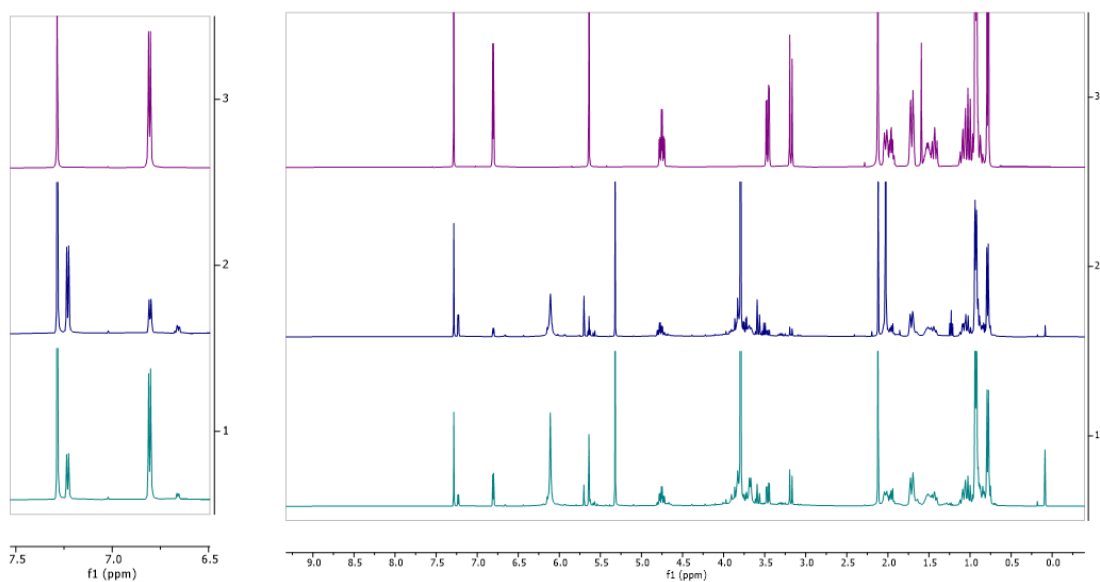
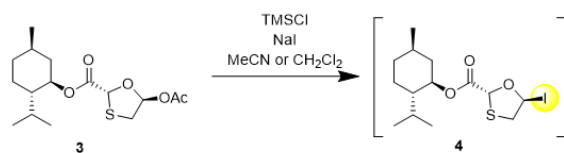


Figure 2-2: ^1H NMR spectra for assay of formation of **4**. (3) Compound **3** in CDCl_3 (2) Compound **3** + TMSCl + NaI + MeCN (1) Compound **3** + TMSCl + NaI + CH_2Cl_2 . Additional experimental details described in Experimental Section. Compound **4** resonance at 7.2 ppm.

transformation is promoted by water (Table 2.1, entry 2). By doping explicit quantities of water into the reaction, we observed complete conversion to product with similar d.r. (Table 2.1, entry 3). Improvement of diastereoselectivity was achieved by switching from MeCN to CH₂Cl₂ as solvent, albeit with drastic loss in conversion (Table 2.1, entry 5). We explored the use of 2-MeTHF as solvent, however reduced mass balance was observed (Table 2.1, entry 4). Other solvents were evaluated and deemed ineffective due to either poor solubility of the nucleobase or incompatibility with the reaction conditions. Introduction of water by pre-saturation of CH₂Cl₂ with water (wet CH₂Cl₂) gave nearly quantitative yield with dramatic improvement in d.r. (Table 2.1, entry 6). Wet CH₂Cl₂ was prepared by shaking CH₂Cl₂ and water in a separatory funnel, and Karl-Fischer titration indicated 0.10–0.12 M water. Altering the stoichiometric ratio of TMSCl and NaI led to no observable change, and lower yield was observed with decreased stoichiometry of TMSCl and NaI relative to **3** (Table 2.1, entries 7–10). In a control experiment where NaI was excluded no product was observed, with high recovery of starting material (Table 2.1, entry 11).

Upon closer investigation of the effect of water stoichiometry on yield of the glycosylation reaction, we observed that yield was proportional to the stoichiometry of water added (Figure 2-3), and at least one equivalent of water relative to **3** was required to achieve high conversion. Therefore, maximum conversion of **3** is achieved by maintaining a reaction concentration below the maximum solubility of water in CH₂Cl₂, or approximately 0.1 M. We reason that water acts as a proton donor for the in situ generation of HI (Figure 2-4). We hypothesize that water first hydrolyzes TMSCl to TMSOH and HCl, which then reacts with NaI to produce HI and NaCl. Hexamethyldisiloxane is formed by reaction of TMSOH and TMSCl or by condensation of TMSOH, which could serve as a thermodynamic driving force for formation of HI. The direct reaction of TMSCl with NaI to form TMSI followed by hydrolysis is also possible and we suspect that both pathways participate. Following the addition of **3**, HI ionizes the anomeric acetate, leading to an oxonium ion which is trapped by the iodide as the thermodynamically preferred *trans* isomer **4**.

entry	TMSCl-NaI	solvent	water (mmol)	3 (%) ^a	6a + 6b (%) ^b	d.r. (6a:6b)
1	0.4/0.4	MeCN	–	51	44	8.4:1
2 ^b	0.4/0.5	MeCN	<5 ppm	50	14	8.6:1
3 ^c	0.4/0.4	MeCN	0.1	5	92	8.2:1
4 ^d	0.4/0.4	2-MeTHF	0.2	3	75	>20:1
5	0.4/0.4	CH ₂ Cl ₂	<5 ppm	93	5	>20:1
6	0.4/0.4	wet CH ₂ Cl ₂	0.2	<1	>95(81)	>20:1
7	0.4/0.8	wet CH ₂ Cl ₂	0.2	<1	>95	>20:1
8	0.8/0.4	wet CH ₂ Cl ₂	0.2	0	>95	>20:1
9	0.26/0.26	wet CH ₂ Cl ₂	0.2	2	92	>20:1
10	0.24/0.24	wet CH ₂ Cl ₂	0.2	3	84(71)	>20:1
11	0.4/0	wet CH ₂ Cl ₂	0.2	87	0	–

^a Yield determined by ¹H NMR analysis of 1,3,5-trimethoxybenzene as internal standard, isolated yields in parentheses.

^b [**3**] = 0.04 M

^c Water (1.8 μL, 0.1 mmol) added by microliter syringe.

^d α,α,α-trifluorotoluene was also evaluated but deemed ineffective due to insolubility of **5a**.

Table 2.1: Reaction optimization for TMSCl-NaI promoted Vorbrüggen glycosylation

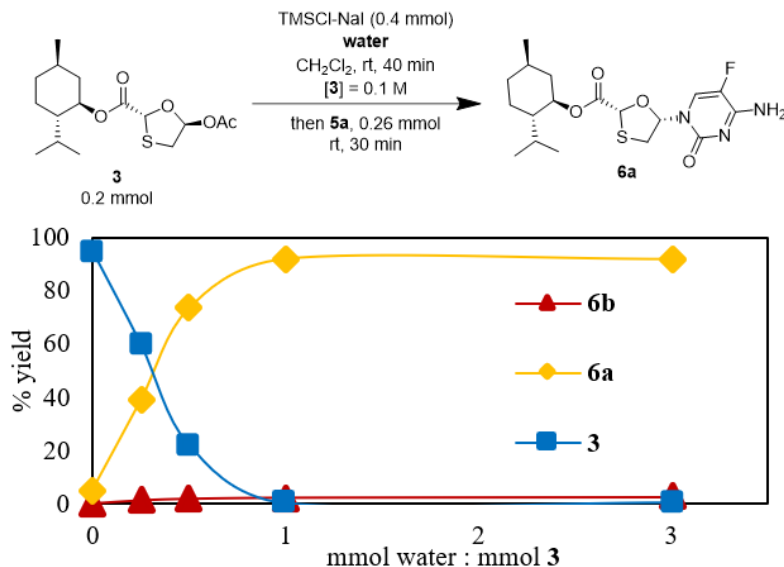
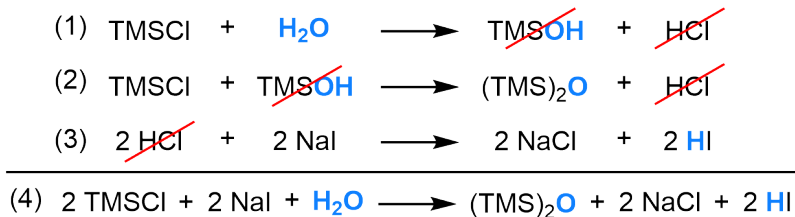


Figure 2-3: Effect of water stoichiometry in the activation of **3** with TMSCl–NaI–H₂O for *N*-glycosylation. Yield determined by ¹H NMR.

We envisioned that a more nonpolar proton donor such as an alcohol or silanol could replace water in the TMSCl–NaI–H₂O reagent system to allow for higher reaction concentrations. Isopropanol afforded slow conversion of **3** and poor mass balance, which was rationalized with the undesired reaction of iodide **4** with isopropanol (Table 2.2, entry 2). Methanol gave rapid and higher conversion, but the mass balance remained poor (Table 2.2, entry 3). Trimethylsilanol (TMSOH, entry 4) showed rapid conversion of **3** and improved mass balance, while triisopropylsilanol (*i*-Pr₃SiOH, entry 5) showed the highest selectivity for the desired *N*-glycosylated product.

Despite the suitability of TMSOH or *i*-Pr₃SiOH as proton donors in this TMSCl–NaI–ROH reagent system, we proceeded to scale-up and isolation with the TMSCl–NaI–H₂O combination which afforded the highest conversion and yield. Accordingly, we found that *N*-glycosylation of pyrimidines 5-fluorocytosine and *N*-acetyl cytosine with **3** is achievable on 1 mmol scale, yielding FTC and 3TC precursors **6** and **7** with high yield and diastereoselectivity (Figure 2-5). The use of unprotected cytosine in place of *N*-acyl cytosine gave low yields due to the insolubility of **5b**. These findings are directly applicable to the prominent chiral auxiliary-based manufacturing routes

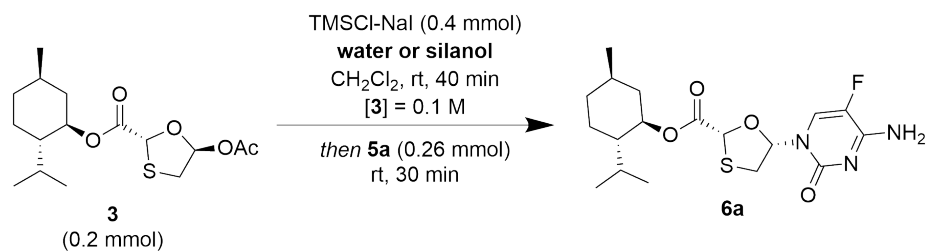
A : Fate of water in TMSCl/NaI/H₂O mixture



B : Rationale for replacement of water with silanol



Figure 2-4: Rationale for the role of water in chlorotrimethylsilane–sodium iodide-promoted glycosylation.



entry	ROH	<i>t_{rxn}</i> (min)	3 (%) ^a	6a + 6b (d.r.) (%) ^a
1	H ₂ O, 0.2	40	1	>99 (44:1)
2	<i>i</i> PrOH, 0.4	165	46	22 (21:1)
3	MeOH, 0.4	90	1	34 (34:1)
4	TMSOH, 0.4	40	2	90 (44:1)
5	<i>i</i> Pr ₃ SiOH, 0.4	90	2	96 (31:1)

^a Determined by ¹H NMR analysis using 1,3,5-trimethoxybenzene as internal standard, d.r. in parentheses as a ratio of **6a**:**6b**.

Table 2.2: Assay for TMSCl–NaI–ROH promoted Vorbrüggen glycosylation

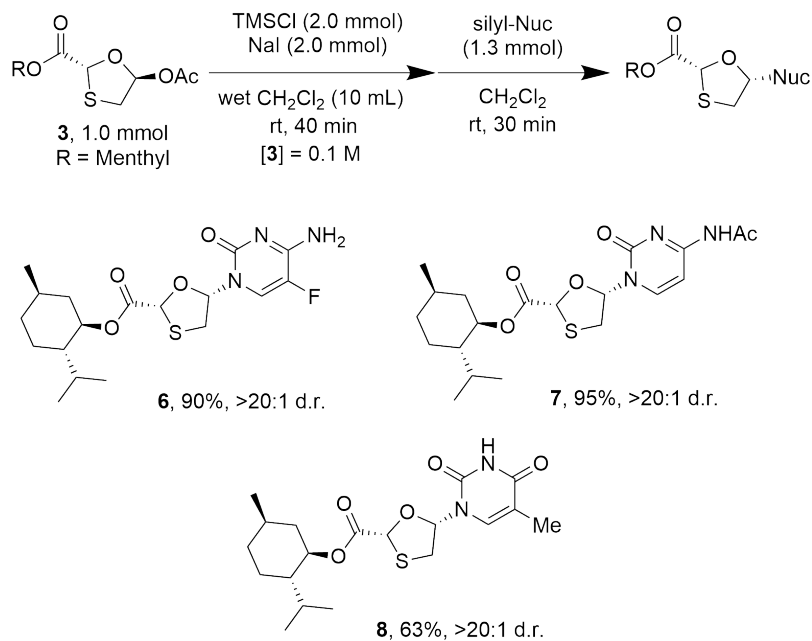


Figure 2-5: Synthesis of nucleoside analogs on 1 mmol scale by TMSCl–NaI promoted Vorbrüggen glycosylation.

to FTC and 3TC which proceed via chiral intermediate **3**.¹⁹ Interestingly, thymine derivative **8** was also synthesized without issue (Figure 2-5). We explored the applicability of this method to 2-deoxyribofuranose derivatives, however low diastereoselectivity was observed with these substrates, highlighting the unique reactivity of 1,3-oxathiolanyl acetates. A variety of 2'-deoxynucleosides are commercially available and several strategies have been reported for their synthesis including deoxygenation of native nucleosides, the use of 3' directing groups, and glycosylation with thioglycoside donors, so we did not explore this further.^{20–22}

In addition to the relevance of this method for synthesis of FTC and 3TC by a chiral auxiliary strategy, we envisioned that this method could bolster an improved route to (±)-FTC/3TC. Numerous strategies exist for resolution to the enantiopure active pharmaceutical ingredients (Figure 2-9 on page 93). We find that a key inefficiency in the existing routes is the glycosylation step. Commonly, a protected primary alcohol intermediate similar to **12** is accessed, followed by glycosylation using TMSOTf, TMSI, or SnCl₄, which yields glycosylated products such as **14** with approximately 1:1 d.r.^{5,6,8,9} We proposed a different synthetic strategy to access (±)-

FTC/3TC via an achiral ester (Figure 2-6, top), by analogy to the precedented HI-promoted glycosylation using menthyl ester **3**.^{3,17}

The widely reported mechanistic rationale for diastereoselective glycosylation of **3** states that menthyl ester **3** stabilizes the *trans* isomer of iodide **4** by anchimeric assistance.^{3,17} Intermediate **4** then reacts in an S_N2-like glycosylation event to form product **7** with selectivity for the desired *cis* isomer. We reasoned that a simple achiral ester could have a similar effect on diastereoselectivity, allowing rapid access to (±)-FTC/3TC without the menthol auxiliary. We designed a series of three model substrates to elucidate the role of the alcohol protecting group in determining the diastereoselectivity of an HI-promoted *N*-glycosylation event (Figure 2-6, compounds **3**, **9**, **12**). Ethyl ester **9** was prepared analogously to the GSK manufacturing route using commercially available ethyl glyoxylate (see Experimental Section). Meanwhile, model substrate **12** was prepared from ethylene glycol via a 5-step sequence (see Experimental Section): monosilylation of ethylene glycol to yield **21** followed by a Swern oxidation resulted in synthesis of aldehyde **22**. Condensation with thioglycolic acid by refluxing in toluene led to formation of oxathiolanone **23** which was reduced with DIBAL-H and acetylated to yield model substrate **12**. After exposing these model substrates to reported conditions for HI-promoted glycosylation with I₂-triethylsilane, we observed high diastereoselectivity with esters **3** and **9** and low selectivity with silyl ether **12** (Figure 2-6). We were pleased to find that a simple achiral ester is sufficient to promote this highly diastereoselective glycosylation event, and can provide improved access to the *cis* oxathiolane product when compared with other alcohol protecting groups.

Following this mechanistic observation, we sought to develop the proposed route to (±)-FTC/3TC. Optimally, the glyoxylate ester was prepared by diol cleavage of diisopropyl tartrate and the resulting mixture was telescoped directly to oxathiolane formation with dithiane diol to yield hydroxyoxathiolane **15** (Figure 2-7).²³ The isopropyl group improved the solubility profile of the substrate in subsequent steps relative to the corresponding ethyl or methyl ester. Crude hydroxyoxathiolane **15** was directly acetylated and delivered glycosyl donor **16** in 3 steps from tartrate with-

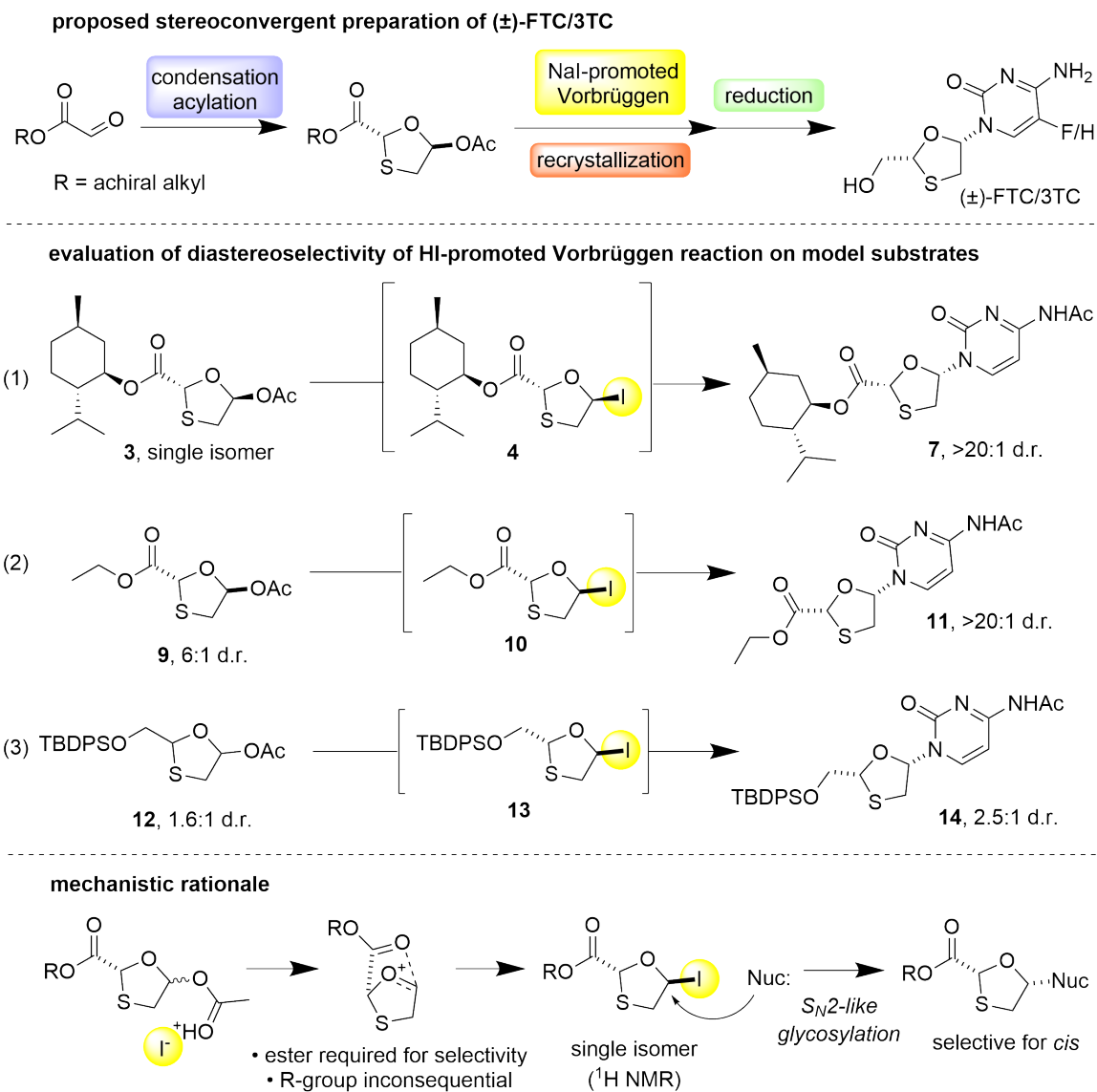
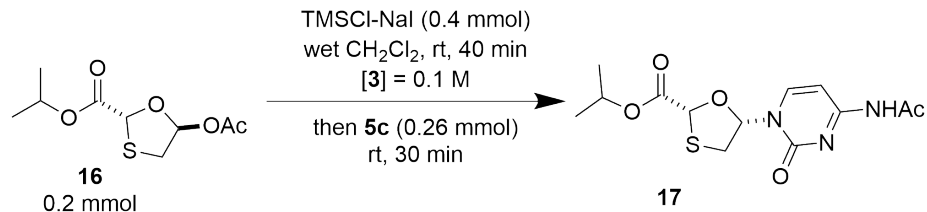


Figure 2-6: Proposed route to FTC/3TC and mechanistic investigation of HI-promoted Vorbrüggen glycosylation using I₂-triethylsilane.



entry	TMSCl-NaI (mmol)	solvent	16 (%) ^a	17 (%) ^a	d.r. (<i>cis:trans</i>)
1 ^b	0.4/0.5	MeCN ^b	41	60	10:1
2	0.4/0.4	MeCN ^c	13	77	10:1
3	0.4/0.4	CH ₂ Cl ₂ ^b	59	24	>20:1
4	0.4/0.4	CH ₂ Cl ₂ ^d	<5	83	>20:1
5	0.26/0.26	CH ₂ Cl ₂ ^d	<5	67	>20:1
6	0.26/0.22	CH ₂ Cl ₂ ^d	6	48	>20:1
7	0.22/0.26	CH ₂ Cl ₂ ^d	2	58	>20:1
8	0.22/0.22	CH ₂ Cl ₂ ^d	<5	68	>20:1
9	0.26/0	CH ₂ Cl ₂ ^d	80	0	–
10	0/0.26	CH ₂ Cl ₂ ^d	87	0	–

^a Determined by ¹H NMR analysis using 1,3,5-trimethoxybenzene as internal standard.

^b Anhydrous solvent

^c Water (1.8 μL, 0.10 mmol) added by microliter syringe

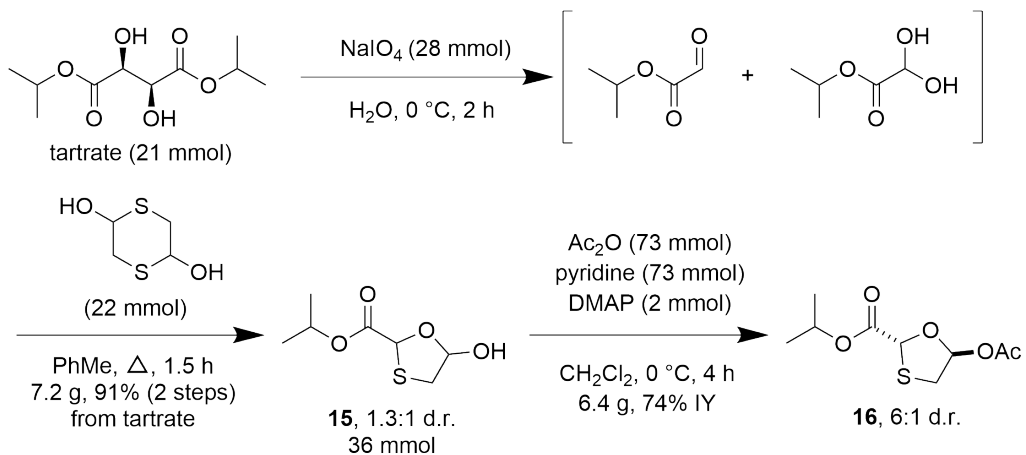
^d CH₂Cl₂ pre-saturated with water (0.2 mmol).

Table 2.3: Optimization of Vorbrüggen glycosylation with *N*-acetyl cytosine and achiral ester.

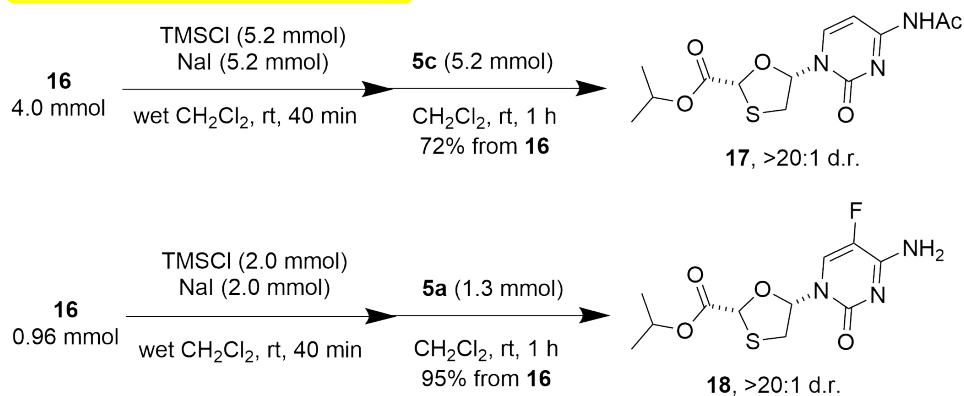
out intermediate purification. The results of the reaction optimization with **3** were validated using **16** and similar trends were observed (Table 2.3). Scale-up of the optimized Vorbrüggen reaction proceeded without issue, and glycosylated products **17** and **18** were isolated in 72% and 95% yield on 4 mmol and 1 mmol scale, respectively. Intriguingly, a single isomer of the intermediate iodide was observed by ¹H NMR (see Experimental Section, compound **24**), supporting the mechanistic rationale depicted in Figure 2-6.

The precedented NaBH₄/K₂HPO₄/NaOH reduction used for removal of the methyl ester protecting group did not translate well to reduction of esters **17** and **18**. We observed ester hydrolysis with no conversion to the primary alcohol (Figure 2-8). Instead, we found that **18** is cleanly reduced to (±)-FTC with 1.1 equiv LiBH₄. Higher stoichiometry of the reductant led to undesired product formation. Ethyl ester derivative **20** was also accessed and was used to explore reduction to (±)-FTC on

Telescoped sequence to glycosyl donor from tartrate



Nal-Promoted Vorbrüggen Reaction



Reduction to (±)-FTC/3TC

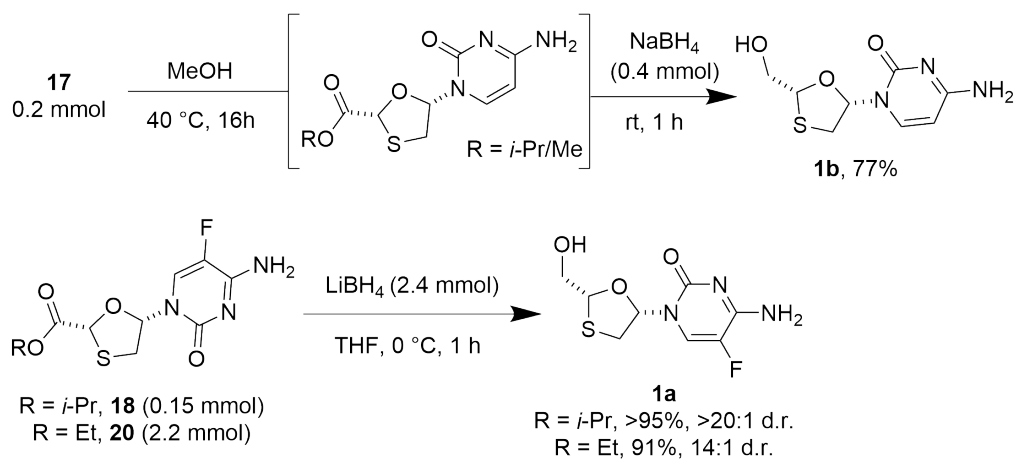


Figure 2-7: Complete route to penultimate FTC/3TC intermediates

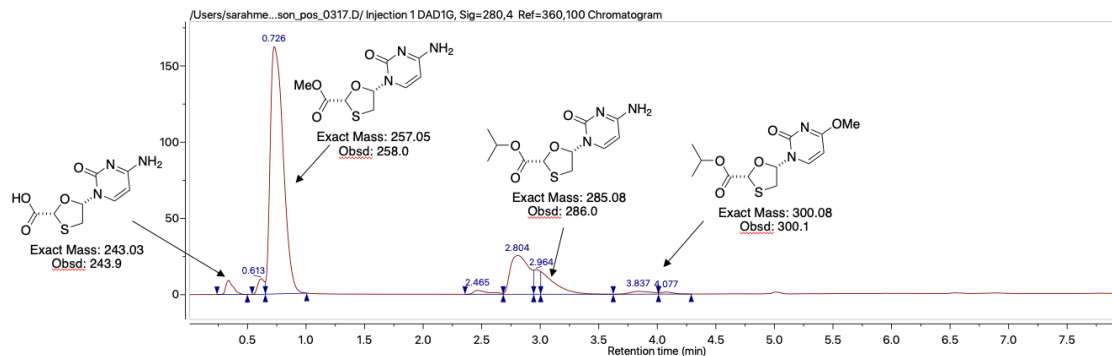
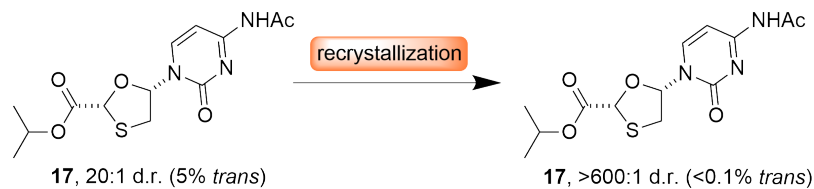


Figure 2-8: Reaction mixture analyzed by LCMS after 16 h acyl cleavage of **17**, prior to reduction to **1b**.

2 mmol scale. For *N*-acetyl derivative **17**, hydrolysis of the amide was required to achieve clean reduction to **1b** with NaBH₄ (Figure 2-8). To overcome the challenge of isolating the polar nucleoside product from the reaction mixture, the reduction was quenched with sodium sulfate decahydrate (Glauber's salt), followed by filtration through Celite. The resulting filtrate was concentrated to yield the desired API.

Although the isolation of 5-fluorocytosine glycosylation product **18** by precipitation is precedented,³ purification of *N*-acetyl cytosine product **17** is not known. Therefore, we saw value in the development of recrystallization conditions for the isolation of **17** (Table 2.4). Gentle heating of the crude reaction mixture in a 1:2 mixture of ethyl acetate and hexanes, followed by cooling to room temperature and filtration provided a 53% yield of the desired *cis* product with >600:1 d.r..



solvent composition*	soluble at rt?	soluble with heating?	crystallization observed?
MeCN/hex 1:1	Yes	Yes	No
IPA/hex 1:1	No	Yes	No
IPA/hex 2:1	No	Yes	No
IPA/hex 1:2	No	Yes	at -20 °C
EA/hex 1:1	No	Yes	at -20 °C
EA/hex 1:2	No	Yes	at 22 °C

*MeCN = acetonitrile, IPA = isopropanol, EA = ethyl acetate, hex = hexanes.

17 (10 mg, 0.03 mmol) was added to a vial and solvent (1 mL) was added.

The resulting mixture was heated with a heat gun until dissolution was observed and monitored for 24 h at room temperature, then moved to -20 °C for 24 h.

Table 2.4: Screening of recrystallization conditions for glycosylation product **17**.

2.3 Conclusion

In conclusion, we have detailed the development of an improved synthetic route to (\pm)-FTC/3TC starting from a commercially available and inexpensive tartrate ester and employing a TMSCl–NaI–H₂O promoted Vorbrüggen glycosylation. The diastereoselectivity of the glycosylation step is crucial for the preparation of material suitable to access emtricitabine (FTC) and lamivudine (3TC) via chiral resolution.

2.4 Experimental Section

2.4.1 General Methods

Reagents were used as supplied commercially without further purification. Solvents were dried and sparged with Argon using a solvent purification system prior to use unless otherwise noted. Reactions were run under Argon atmosphere unless otherwise noted. 5-Fluorocytosine was used as supplied commercially by Oakwood Products. (2*R*)-5-hydroxy-1,3-oxathiolane-2-carboxylic acid (1*R*,2*S*,5*R*)-5-methyl-2-

(1-methylethyl)cyclohexyl ester was purchased from Combi-Blocks. For all procedures described herein, “room temperature” refers to a temperature range of 20–24 °C. For reactions that required heating, an oil bath was used as the heat source. Thin-layer chromatography (TLC) was performed using 0.2 mm coated glass silica gel plates and visualized using either ultraviolet light or staining with KMnO_4 solution. Purification by column chromatography over silica gel was performed on a Biotage Selekt flash chromatography system using Isco RediSep Rf Gold silica gel columns. All NMR spectra were collected on Bruker instruments. Spectra reported with field strength 400 MHz were collected using a two-channel Bruker Avance-III HD Nanobay spectrometer operating at 400.09 MHz. Spectra reported with field strength 500 MHz were collected using a three-channel Bruker Avance Neo spectrometer operating at 500.34 MHz. Both spectrometers were equipped with a 5 mm liquid-nitrogen cooled Prodigy broad band observe (BBO) cryoprobe. Chemical shifts (δ) are reported in units of ppm, relative to the residual solvent peak, which was adjusted to match reported values. Individual peaks are assigned multiplicity with the definitions: s = singlet, d = doublet, t = triplet, q = quartet, hept = heptet, m = multiplet. Reported NMR data follow the general format: Nuclei NMR (resonance frequency, reference solvent) chemical shift (multiplicity, coupling constants, integration). High-resolution mass spectrometry data was recorded using a JEOL AccuTOF 4G LC-plus equipped with a Direct Analysis in Real Time (DART) source. Infrared (IR) resonances were observed using an Agilent Cary 630 FTIR spectrometer. IR samples were prepared as solutions in dichloromethane then loaded onto a diamond surface.

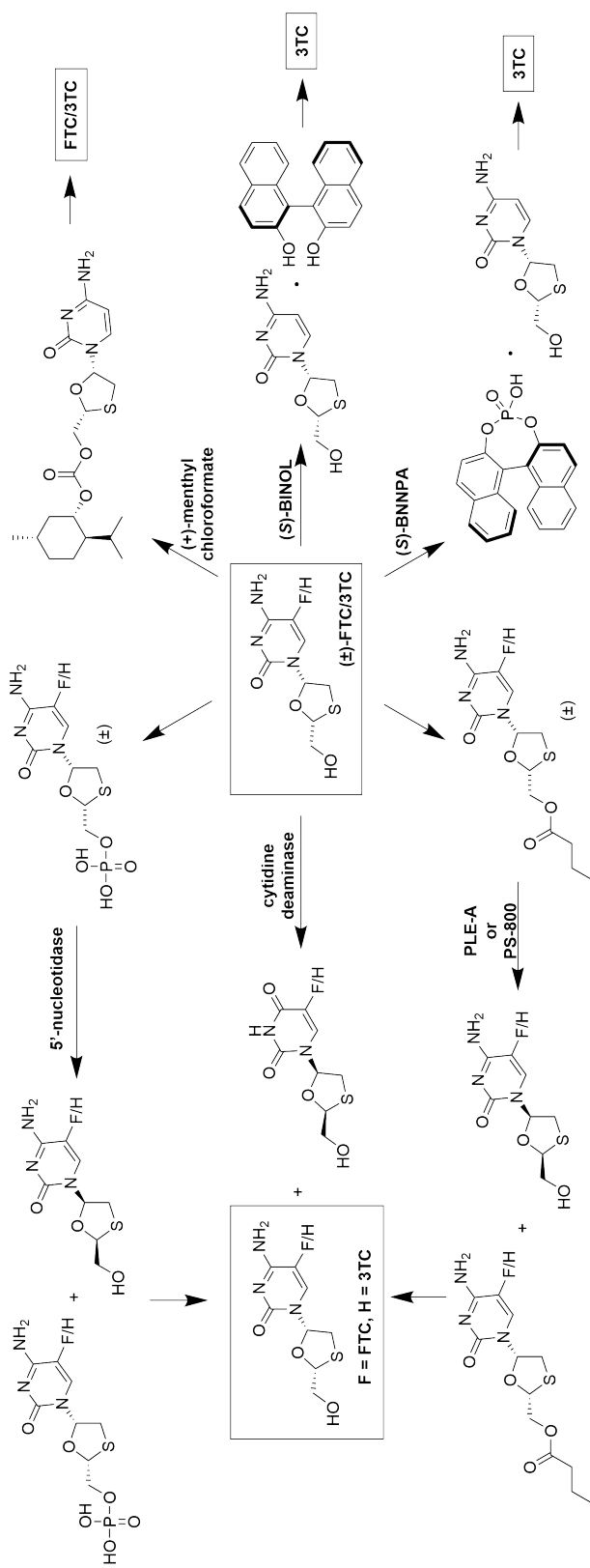
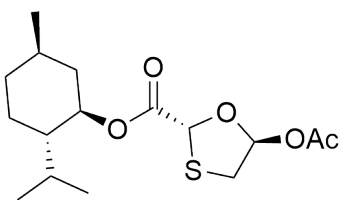
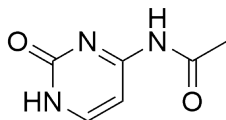


Figure 2-9: Precedented strategies for resolution of 3TC and FTC from (\pm)-FTC/3TC. 7-16

2.4.2 Synthesis of Starting Materials



(1*R*,2*S*,5*R*)-2-Isopropyl-5-methylcyclohexyl (2*R*,5*R*)-5-acetoxy-1,3-oxathiolane-2-carboxylate, (3).¹⁷ By modification of a reported procedure, (2*R*)-5-hydroxy-1,3-oxathiolane-2-carboxylic acid (1*R*,2*S*,5*R*)-5-methyl-2-(1-methylethyl)cyclohexyl ester (8.65 g, 30.0 mmol, Combi-Blocks) was dissolved in CH₂Cl₂ (200 mL) and acetic anhydride (5.7 mL, 60 mmol) was added. The solution was cooled in an ice-water bath, then pyridine (4.8 mL, 60 mmol) was added dropwise with stirring. 4-dimethylaminopyridine (730 mg, 6.0 mmol) was added in one portion. The reaction mixture was warmed to room temperature and stirred for 4 h. Reaction progress was monitored by TLC (EtOAc/hexanes). The reaction mixture was cooled in an ice-water bath, then quenched by addition of water and transferred to a separatory funnel. The organic layer was washed twice with 1 M HCl (aq), then twice with 1 M NaHCO₃ (aq). The organic layer was dried over Na₂SO₄ and concentrated under reduced pressure to yield an orange oil. The crude residue was purified by column chromatography (7–60% EtOAc/hexanes, R_f = 0.62 in 30% EtOAc/hexanes). The resulting material was dissolved in 400 mL *n*-hexane with 2 mL triethylamine. The solution was heated to boiling, then filtered hot by gravity filtration. The filtrate was collected in an Erlenmeyer flask and cooled to room temperature, then cooled at –20 °C for 72 h. The crystals were collected by filtration using a medium porosity sintered glass funnel, washing with hexanes. The filtrate was collected and filtered a second time to collect a second crop (3.82 g, 39%, white needles).



***N*-Acetyl cytosine, (19).**²⁴ A mixture of cytosine (2.22 g, 20.0 mmol), acetic anhydride (9.5 mL, 100 mmol), and pyridine (11.3 mL, 140 mmol) was heated to reflux (125 °C) and stirred for 1.5 h. The mixture was cooled to room temperature. EtOAc (10 mL) was added and the mixture was stirred for 30 min. The white solid was filtered and washed with EtOAc then dried under vacuum to yield a grey-pink amorphous solid (2.98g, 97%).

2.4.3 NMR Assay for Glycosyl Iodide Formation Promoted by TMSCl–NaI

Conversion to glycosyl iodide **4** was observed by ^1H NMR analysis of the anomeric proton. The anomeric proton of **3** appears as a doublet: (^1H NMR, CDCl_3) δ 6.78 (d, $^3\text{J} = 4.2$ Hz). The anomeric proton for glycosyl iodide **4** appears as a doublet: (^1H NMR, CDCl_3) δ 7.21 ppm (d, $^3\text{J} = 4.2$ Hz). Conversion was calculated as follows: Conversion = 100%·(area for **4**)/(area for **3** + **4**).

Chlorotrimethylsilane + sodium iodide in MeCN or CH_2Cl_2 In a dry 1-dram vial, **3** (66 mg, 0.20 mmol) was dissolved in MeCN or CH_2Cl_2 (0.5 mL, 0.4 M). Sodium iodide (45 mg, 0.30 mmol) was added, and the reaction was capped. With stirring, chlorotrimethylsilane (38 μL , 0.30 mmol) was added and stirred at room temperature for 30 min. The reaction mixture was diluted with CH_2Cl_2 , then filtered through cotton. An aliquot of the filtered sample was concentrated under reduced pressure. The residue was diluted in CDCl_3 and analyze by ^1H NMR. Conversion (MeCN): 64%. Conversion (CH_2Cl_2): 25%.

Chlorotrimethylsilane + sodium iodide in MeCN- d_3 , two-step analysis. In a dry 1-dram vial, **3** (16.5 mg, 0.05 mmol) was dissolved in MeCN- d_3 (1 mL). Chlorotrimethylsilane (9.5 μL , 0.075 mmol) was added. The mixture was stirred for 30 min, then transferred to an NMR tube and analyzed by ^1H NMR relative to **3** in MeCN- d_3 . No conversion was observed. The NMR sample was recovered and NaI (22 mg, 0.15 mmol) was added. After stirring for 2 h at room temperature, the mixture was analyzed by ^1H NMR without filtration. Conversion: 87%.

2.4.4 General Procedure for Optimization of TMSCl--NaI-Promoted Glycosylation

TMSCl–NaI Glycosylation Leading to 6, 7, 8, 17, and 18. 5-Fluorocytosine (33.6 mg, 0.260 mmol) was added to an oven-dried 20-mL vial. CH₂Cl₂ (5 mL) was added, followed by *N,O*-bis(trimethylsilyl)acetamide (180 μ L, 0.70 mmol). The mixture was capped tightly with a septum screwcap and heated to 47 °C in a heat block until a clear solution was obtained, indicating formation of **5a**. The solution was then cooled to room temperature. To prepare wet CH₂Cl₂, anhydrous CH₂Cl₂ (10 mL) and DI water (10 mL) were added to a separatory funnel. The biphasic mixture was shaken vigorously, then allowed to separate. The organic layer was collected (wet CH₂Cl₂). Concurrently, NaI (60 mg, 0.40 mmol) was weighed into a separate oven-dried 20-mL vial. Wet CH₂Cl₂ (2 mL) was directly added to the vial containing NaI which was then capped with a septum screwcap. Chlorotrimethylsilane (51 μ L, 0.40 mmol) was added and the heterogeneous mixture was stirred vigorously for 5 min, followed by addition of **3** (66 mg, 0.20 mmol) in one portion. This mixture was stirred vigorously for 40 min leading to the formation of **4**. The prepared silylated nucleobase solution was added rapidly by syringe to the stirring solution of **4** and the resulting mixture was stirred at room temperature for 30 min. The reaction mixture was transferred to a separatory funnel, diluting with CH₂Cl₂ (20 mL). The organic layer was washed with a 5:1 mixture of 1 N Na₂S₂O₃ / saturated NaHCO₃. The aqueous layer was extracted with CH₂Cl₂ (20 mL). The combined organic layers were washed with brine. The organic layer was dried over Na₂SO₄. 1,3,5-Trimethoxybenzene (TMB) was added and the solution was swirled vigorously to dissolve. An aliquot was removed and concentrated under reduced pressure, then analyzed by ¹H NMR in CDCl₃ with a relaxation delay of 25 s. Yield and conversion was determined by integration of the sp² ¹H signal on the 5-fluorocytosine ring of **6** (**6a** δ 8.53 ppm, **6b** δ 7.51 ppm) and the anomeric proton of **3** (δ 6.80 ppm) versus the sp² proton signal of TMB (δ 6.11 ppm). If the sp² protons of **6** were obscured by the N–H ¹H NMR signal, the anomeric proton was used instead (**6a** δ 6.44 ppm, **6b** δ 6.69 ppm).

Modifications to General Procedure: When anhydrous solvent was used (Table 2.1, entries 1–4), the vial was capped with a septum screwcap after addition of NaI, then flame-dried under vacuum. The indicated solvent was then added followed by the indicated amount of water or silanol using a microliter syringe. When MeCN was used for preparation of **5a** or **5c**, the mixture was heated to 87 °C. For screening results in Table 2.3: **16** (47 mg, 0.20 mmol) was used and was added as a solution in CH₂Cl₂ (1 mL). For screening with **19** to prepare **5c**, the following amount of material was used: **19** (40 mg, 0.26 mmol) and *N,O*-bis(trimethylsilyl)acetamide (98 μL, 0.40 mmol) in CH₂Cl₂ (5 mL).

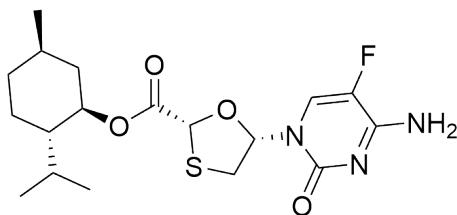
Isolated Yields for Representative Examples of TMSCl–NaI Glycosylation Screening (Table 2.1)

Entry 6: (1*R*,2*S*,5*R*)-2-isopropyl-5-methylcyclohexyl (2*R*,5*S*)-5-(4-amino-5-fluoro-2-oxopyrimidin-1(2*H*)-yl)-1,3-oxathiolane-2-carboxylate, (**6**).¹⁷ From **3** (66 mg, 0.20 mmol) as described in the General Procedure. Purified by column chromatography (3–10% MeOH/CH₂Cl₂, R_f = 0.06 in 3% MeOH/CH₂Cl₂) to yield a crystalline white solid (65 mg, 81%, >20:1 d.r.).

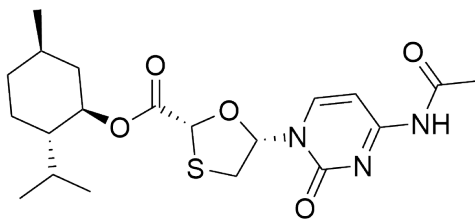
Entry 10: (1*R*,2*S*,5*R*)-2-isopropyl-5-methylcyclohexyl (2*R*,5*S*)-5-(4-amino-5-fluoro-2-oxopyrimidin-1(2*H*)-yl)-1,3-oxathiolane-2-carboxylate, (**6**).¹⁷ From **3** (66 mg, 0.20 mmol) using chlorotrimethylsilane (31 μL, 0.24 mmol) and NaI (36 mg, 0.24 mmol). Purified by column chromatography (3–10% MeOH/CH₂Cl₂, R_f = 0.06 in 3% MeOH/CH₂Cl₂) to yield a crystalline white solid (60 mg, 71%, >20:1 d.r.).

(1*R*,2*S*,5*R*)-2-isopropyl-5-methylcyclohexyl (2*R*,5*S*)-5-(4-acetamido-2-oxopyrimidin-1(2*H*)-yl)-1,3-oxathiolane-2-carboxylate, (**7**).¹⁷ From **3** (66 mg, 0.20 mmol), **19** (40 mg, 0.26 mmol), *N,O*-bis(trimethylsilyl)acetamide (160 μL, 0.65 mmol) isolated by column chromatography (2–12% MeOH/CH₂Cl₂, R_f = 0.20 in 3% MeOH/CH₂Cl₂) as a white solid (69 mg, 81%).

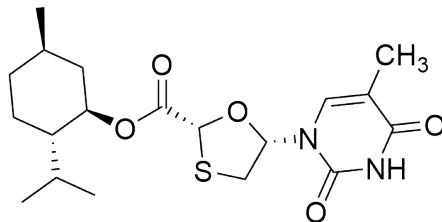
2.4.5 Synthesis of Nucleoside Analogs on 1.0 mmol Scale



(1*R*,2*S*,5*R*)-2-isopropyl-5-methylcyclohexyl-(2*R*,5*S*)-5-(4-amino-5-fluoro-2-oxopyrimidin-1(2*H*)-yl)-1,3-oxathiolane-2-carboxylate, (6).¹⁷ 5-fluorocytosine (168 mg, 1.30 mmol) was weighed into a flame-dried 100-mL round-bottom flask. CH₂Cl₂ (25 mL) was added, followed by *N,O*-bis(trimethylsilyl)acetamide (905 μ L, 3.70 mmol). The mixture was sonicated to disperse the solids, then heated to reflux temperature (47 °C in an oil bath) until dissolution was observed, about 1 h. The solution was cooled to room temperature (**5a**). Separately, NaI (300 mg, 2.00 mmol) was added into a flame-dried 100-mL round-bottom flask. Wet CH₂Cl₂ (10 mL) was added, followed by chlorotrimethylsilane (254 μ L, 2.00 mmol). The mixture was stirred for 5 min, followed by the addition of **3** (330 mg, 1.00 mmol). The mixture was stirred vigorously for 1 h and 40 min (formation of **4**). The solution of **5a** was added rapidly to the stirring solution of **4** and the resulting mixture was stirred for 30 min at room temperature. The reaction mixture was transferred to a separatory funnel, diluting with CH₂Cl₂ (100 mL). The mixture was washed with a 5:1 mixture of 1 N Na₂S₂O₃ and saturated Na₂HCO₃. After separation of the layers, the aqueous layer was back-extracted with CH₂Cl₂. The organic layers were combined and washed with brine, then dried over Na₂SO₄ and filtered through a sintered glass funnel. The filtrate was concentrated and purified by column chromatography (2–20% MeOH/CH₂Cl₂, R_f = 0.06 in 3% MeOH/CH₂Cl₂) by dry-loading onto silica gel to yield a white solid (361 mg, 90%, >20:1 d.r.). Specific Rotation $[\alpha]_D^{20} = -131$ (*c* 0.66, CHCl₃).

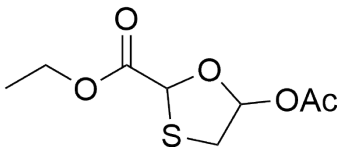


(1*R*,2*S*,5*R*)-2-isopropyl-5-methylcyclohexyl (2*R*,5*S*)-5-(4-acetamido-2-oxopyrimidin-1(2*H*)-yl)-1,3-oxathiolane-2-carboxylate, (7).¹⁷ From **3** (330 mg, 1.00 mmol), chlorotri-methylsilane (254 μ L, 2.00 mmol), and NaI (300 mg, 2.00 mmol) in wet CH_2Cl_2 (10 mL); combined with **19** (199 mg, 1.30 mmol), and *N,O*-bis-(trimethylsilyl)acetamide (905 μ L, 3.70 mmol) in CH_2Cl_2 (25 mL). Purified by column chromatography (2–20% MeOH/ CH_2Cl_2 , $R_f = 0.20$ in 3% MeOH/ CH_2Cl_2) after dry-loading onto silica gel to yield a white solid (403 mg, 95%, >20:1 d.r.). Specific Rotation $[\alpha]_D^{20} = -106$ (c 0.36, CHCl_3).

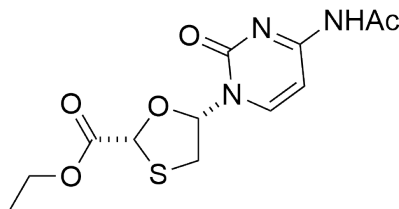


(1*R*,2*S*,5*R*)-2-isopropyl-5-methylcyclohexyl-(2*R*,5*S*)-5-(5-methyl-2,4-dioxo-3,4-dihydropyrimidin-1(2*H*)-yl)-1,3-oxathiolane-2-carboxylate, (8). From **3** (300 mg, 1.00 mmol), chlorotrimethylsilane (254 μ L, 2.00 mmol), and NaI (300 mg, 2.00 mmol) in wet CH_2Cl_2 (10 mL); combined with thymine (164 mg, 1.30 mmol) and *N,O*-bis(trimethylsilyl)acetamide (905 μ L, 3.70 mmol) in CH_2Cl_2 (25 mL). The product was purified by column chromatography (2–20% MeOH/ CH_2Cl_2 , $R_f = 0.26$ in 3% MeOH/ CH_2Cl_2) to yield a colorless foam (248 mg, 63%, >20:1 d.r.). ^1H NMR (400 MHz, CDCl_3) δ 9.26 (s, NH), 8.10 (d, $J = 1.4$ Hz, 1H), 6.45 (dd, $J = 7.7, 4.7$ Hz, 1H), 5.41 (s, 1H), 4.77 (td, $J = 11.0, 4.4$ Hz, 1H), 3.37 (dd, $J = 11.8, 4.8$ Hz, 1H), 3.14 (dd, $J = 11.9, 7.8$ Hz, 1H), 2.08–2.03 (m, 1H), 1.97 (d, $J = 1.3$ Hz, 3H), 1.95–1.89 (m, 1H), 1.85–1.76 (m, 1H), 1.70 (dt, $J = 12.7, 2.8$ Hz, 2H), 1.55–1.48 (s, 1H), 1.47–1.39 (m, 1H), 1.03 (q, $J = 11.6$ Hz, 2H), 0.93–0.89 (m, 6H), 0.77 (d, $J = 6.9$ Hz, 3H). $^{13}\text{C}\{^1\text{H}\}$ NMR (101 MHz, CDCl_3) δ 167.0, 163.7, 150.4, 136.0, 111.6, 89.0, 77.6, 47.3, 40.9, 35.0, 34.2, 31.6, 26.2, 23.4, 22.1, 20.9, 16.3, 12.8. HRMS (DART/AccuTOF) m/z : $[\text{M}+\text{H}]^+$ Calcd for $\text{C}_{19}\text{H}_{29}\text{N}_2\text{O}_5\text{S}$ 397.1792; Found 397.1809. IR (cm^{-1}) 1733, 1700. Specific Rotation $[\alpha]_D^{20} = -55.1$ (c 0.66, CHCl_3).

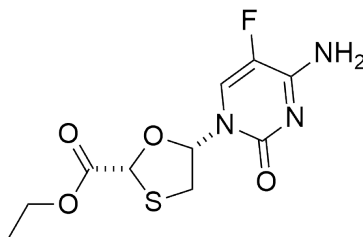
2.4.6 Synthesis of Derivatives for Mechanistic Investigation



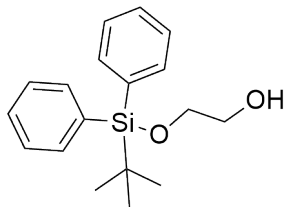
Ethyl 5-acetoxy-1,3-oxathiolane-2-carboxylate, (9). Ethyl glyoxylate (50% solution in toluene, 1.5 mL, 7.5 mmol) was added to a 20-mL vial equipped with a magnetic stirrer. 1,4-dithiane-2,5-diol (460 mg, 3.00 mmol) was added. The heterogeneous mixture was heated to reflux until a clear solution was obtained. The crude residue was directly purified by flash column chromatography (45% EtOAc/hexanes). The resulting clear oil was diluted in CH₂Cl₂ (40 mL). Acetic anhydride (1.1 mL, 12 mmol) and 4-dimethylaminopyridine (150 mg, 1.2 mmol) were added, and the solution was cooled in an ice-water bath. Pyridine (970 μ L, 12 mmol) was added. The mixture was warmed to room temperature and stirred for 4 h, then quenched by addition of water. The reaction mixture was diluted with CH₂Cl₂ and transferred to a separatory funnel. The organic layer was washed with saturated NaHCO₃ (aq) and washed with 1 M HCl (aq), then washed with brine and dried over MgSO₄. The crude mixture was purified by flash column chromatography (7–60% EtOAc/hexanes, R_f = 0.49 in 30% EtOAc/hexanes) to yield a clear oil (852 mg, 65%, 2 steps). *trans*-**9**: ¹H NMR (500 MHz, CDCl₃) δ 6.74 (d, J = 4.1 Hz, 1H), 5.59 (s, 1H), 4.34–4.07 (m, 2H), 3.39 (dd, J = 11.8, 4.1 Hz, 1H), 3.13 (d, J = 11.7 Hz, 1H), 2.06 (s, 3H), 1.24–1.29 (t, J = 7.1 Hz, 3H). ¹³C{¹H} NMR (126 MHz, CDCl₃) δ 169.6, 169.0, 99.8, 79.8, 62.0, 37.2, 21.1, 14.05. *cis*-**9**: ¹H NMR (500 MHz, CDCl₃) δ 6.61 (m, 1H), 5.62 (s, 1H), 4.34–4.07 (m, 2H), 3.25 (dd, J = 11.4, 4.1 Hz, 1H), 3.18 (dd, J = 11.3, 1.2 Hz, 1H), 2.06 (s, 3H), 1.24–1.29 (t, J = 7.1 Hz, 3H). ¹³C{¹H} NMR (126 MHz, CDCl₃) δ 170.1, 169.2, 99.8, 99.3, 80.3, 61.9, 37.7, 21.2, 14.11. HRMS (DART/AccuTOF) m/z: [M+NH₄]⁺ Calcd for C₈H₁₆NO₅S 238.0749; Found 238.0747. IR (cm⁻¹) 1741.



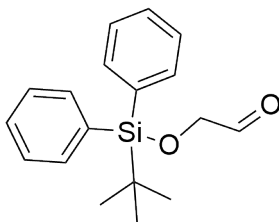
Ethyl 5-(4-acetamido-2-oxopyrimidin-1(2H)-yl)-1,3-oxathiolane-2-carboxylate, (11). Iodine (457 mg, 1.80 mmol) was suspended in CH₂Cl₂ (20 mL) and triethylsilane (575 μL, 3.60 mmol) was added. The solution was mixed until a light pink color was obtained. The resulting solution was cooled in an ice-water bath and a solution of **9** (330 mg, 1.50 mmol) in CH₂Cl₂ (10 mL) was added dropwise. The reaction became yellow-orange in color. CH₂Cl₂ (5 mL) was used to complete the transfer. The reaction was stirred for 1 h. Concurrently, *N,O*-bis(trimethylsilyl)acetamide (744 μL, 3.00 mmol) was added to a suspension of **19** (306 mg, 2.00 mmol) in anhydrous CH₂Cl₂ (15 mL). The mixture was warmed to 40 °C until a clear solution was observed. The mixture was cooled to room temperature, then transferred into the stirring solution of **5c**, using addition CH₂Cl₂ (5 mL) for rinsing. The reaction was warmed to room temperature and stirred for 1 h. The reaction was diluted with CH₂Cl₂, and quenched with saturated NaHCO₃ (aq). The emulsion was washed with 1 N Na₂S₂O₃, then with brine. The aqueous layer was back-extracted with 20% methanol in CH₂Cl₂ (2 x 20 mL). The organic layer was dried with MgSO₄, then concentrated under reduced pressure. The product was isolated by column chromatography (0–15% MeOH/CH₂Cl₂, R_f = 0.29 in 3% MeOH/CH₂Cl₂) by dry-loading onto silica gel to yield an amorphous solid (305 mg, 65%). ¹H NMR (400 MHz, CDCl₃) δ 10.15 (s, 1H), 8.66 (d, J = 7.6 Hz, 1H), 7.49 (d, J = 7.5 Hz, 1H), 6.43 (t, J = 5.3 Hz, 1H), 5.55 (s, 1H), 4.30 (q, J = 7.1 Hz, 2H), 3.67 (dd, J = 12.3, 4.8 Hz, 1H), 3.20 (dd, J = 12.3, 5.9 Hz, 1H), 2.29 (s, 3H), 1.34 (t, J = 7.1 Hz, 3H). ¹³C{¹H} NMR (101 MHz, CDCl₃) δ 171.2, 169.4, 163.3, 155.0, 145.3, 96.9, 90.6, 79.5, 62.5, 37.1, 24.9, 14.0. HRMS (DART/AccuTOF) m/z: [M+H]⁺ Calcd for C₁₂H₁₆N₃O₅S 314.0819; Found 314.0821. IR (cm⁻¹) 1741.



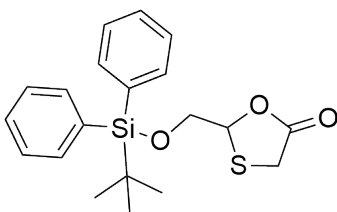
Ethyl (2*R*,5*S*)-5-(4-amino-5-fluoro-2-oxopyrimidin-1(2*H*)-yl)-1,3-oxathiolane-2-carboxylate, (20). Following the same general procedure as for **11** from **9** (220 mg, 1.00 mmol), iodine (300 mg, 1.20 mmol) and triethylsilane (480 μ L, 3.00 mmol), combined with 5-fluorocytosine (168 mg, 1.30 mmol) and *N,O*-bis(trimethylsilyl)acetamide (1.04 mL, 4.20 mmol). Solid formation was observed during aqueous workup, complicating the separation of layers. Purification by column chromatography (0–10% MeOH/EtOAc, $R_f = 0.11$ in 3% MeOH/ CH_2Cl_2) after dry-loading onto silica gel yielded the title compound as a brown solid (129 mg, 45%). ^1H NMR (400 MHz, DMSO) δ 8.19 (d, $J = 7.2$ Hz, 2H), 7.92 (s, 1H), 7.68 (s, 1H), 6.29 (td, $J = 4.9, 2.5$ Hz, 2H), 5.71 (s, 2H), 4.23 (q, $J = 7.1$ Hz, 4H), 4.09 (q, $J = 5.2$ Hz, 1H), 3.54 (dd, $J = 12.1, 5.0$ Hz, 2H), 3.22 (dd, $J = 12.1, 6.3$ Hz, 2H), 1.24 (t, $J = 7.1$ Hz, 6H). $^{13}\text{C}\{^1\text{H}\}$ NMR (101 MHz, DMSO) δ 169.8, 157.8, 157.6, 153.1, 137.3, 134.9, 125.3, 125.0, 89.2, 77.7, 62.0, 35.3, 13.9. HRMS (DART/AccuTOF) m/z : $[\text{M}+\text{H}]^+$ Calcd for $\text{C}_{10}\text{H}_{13}\text{N}_3\text{O}_4\text{SF}$ 290.0605; Found 290.0638. IR (cm^{-1}) 1741, 1625, 1178.



2-((*Tert*-butyldiphenylsilyl)oxy)ethan-1-ol, (21).^{25,26} Sodium hydride, 60% in mineral oil (4.0 g, 100 mmol) was added to a flame-dried 300 mL round-bottom flask equipped with a magnetic stirrer. Hexanes (100 mL) was added and the slurry was swirled gently, then the solvent was removed by cannula. This washing process was repeated once more, then vacuum was pulled on the flask to remove excess hexanes. THF (160 mL) was added, and the mixture was cooled to 0 °C. Ethylene glycol (6.21 g, 100 mmol) was dissolved in THF (10 mL), then added to the stirring suspension of sodium hydride. The resulting mixture was stirred for 45 min. *Tert*-butyldimethylsilyl chloride (26 mL, 100 mmol) was added slowly over 5 min. The mixture was warmed to room temperature and stirred for 2.5 h. The reaction mixture was diluted with diethyl ether (150 mL) and transferred to a separatory funnel and washed twice with a saturated NaHCO₃ (2 x 300 mL), followed by brine (150 mL). The organic layer was dried over Na₂SO₄ and filtered. The solvent was removed under reduced pressure. The resulting residue was purified by column chromatography (2–20% EtOAc/hexanes, R_f = 0.53 in 30% EtOAc/hexanes), resulting in the target compound as a clear oil. (13.6 g, 53%).

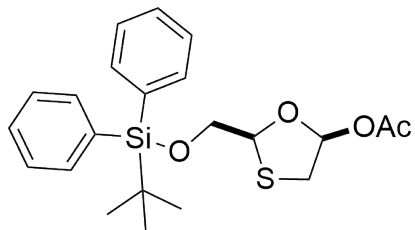


2-((*Tert*-butyldiphenylsilyl)oxy)acetaldehyde, (22).²⁵ A solution of oxalyl chloride (472 μL , 5.50 mmol) in 20 mL CH_2Cl_2 was stirred at $-78\text{ }^\circ\text{C}$. DMSO (781 μL , 11.0 mmol) was added, followed by **21** (1.5 g, 5.0 mmol) as a solution in CH_2Cl_2 (3 mL). The mixture was stirred for 15 min, then triethylamine (3.5 mL) was added. The reaction was warmed to room temperature. The solvent was removed under reduced pressure to afford a white solid, which was triturated with a 1:4 mixture of EtOAc/hexanes and filtered through a plug of silica gel, washing with the same solvent (100 mL). The solvent was removed under reduced pressure to yield an oil which was telescoped to the next step (1.36 g with 83% purity, 75% yield).



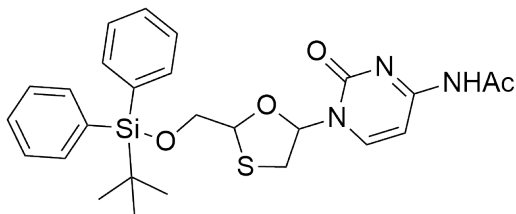
2-(((*Tert*-butyldiphenylsilyl)oxy)methyl)-1,3-oxathiolan-5-one, (23).²⁷

22 (708 mg with 66% purity, 1.57 mmol) was dissolved in toluene (20 mL) in a flame-dried 100-mL round-bottom flask. Thioglycolic acid (130 μL , 1.90 mmol) was added, and the mixture was refluxed for 4 h. The solvent was removed under reduced pressure, and the residue was purified by column chromatography (3–30% EtOAc/hexanes, $R_f = 0.74$ in 30% EtOAc/hexanes) to yield a white solid (483 mg, 83% yield).



2-(((*Tert*-butyldiphenylsilyl)oxy)methyl)-1,3-oxathiolan-5-yl acetate, (12).²⁸

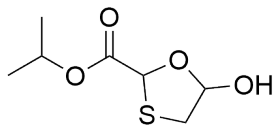
23 (670 mg, 1.8 mmol) was dissolved in CH₂Cl₂ (25 mL) in a 250-mL round-bottom flask. The solution was cooled to -78 °C and DIBAL-H was added (2.0 mL of 1 M solution in toluene, 2.0 mmol) over 10 min. The resulting mixture was stirred for 1 h at -78 °C. Reaction monitoring by TLC (30% EtOAc/hexanes) showed low conversion of **23**, thus additional DIBAL-H (2.0 mL of 1 M solution in toluene, 2.0 mmol) was added and the mixture was stirred at -78 °C for an additional 2.5 h. The reaction was quenched with 5% H₂O/MeOH (10 mL), warmed to room temperature, and stirred for 30 min resulting in a clear solution. Saturated potassium sodium tartrate solution (50 mL) was added, resulting in a slurry. This was stirred at room temperature until separation of layers was observed, about 30 min. The biphasic mixture was transferred to a separatory funnel and washed with water, then washed with brine and dried over MgSO₄. The solvent was removed under reduced pressure. The crude residue was suspended in CH₂Cl₂. Acetic anhydride (260 μL, 2.7 mmol) was added and the mixture was cooled to 0 °C. *N,N*-dimethylaminopyridine (66 mg, 0.54 mmol) was added, followed by pyridine (290 μL, 3.6 mmol). The mixture was stirred for 1.5 h until full conversion was observed by TLC. The reaction was quenched with saturated NaHCO₃ and extracted with CH₂Cl₂. The organic layer was dried with MgSO₄ and concentrated under reduced pressure. The resulting crude residue was purified by column chromatography (3–30% EtOAc/hexanes, R_f = 0.71 in 30% EtOAc/hexanes) to yield the title compound as a clear oil (231 mg, 31% yield, 1.6:1 d.r.).



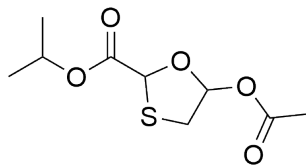
***N*-(1-(2-(((*Tert*-butyldiphenylsilyl)oxy)methyl)-1,3-oxathiolan-5-yl)-2-oxo-1,2-dihydropyrimidin-4-yl)acetamide, (**14**).¹²**

In a 2-dram vial, *N,O*-bis(trimethylsilyl)acetamide (34 μL , 0.14 mmol) was added to a suspension of **19** (14 mg, 0.088 mmol) in CH_2Cl_2 (2 mL). The mixture was warmed to 40 $^\circ\text{C}$ in a heat block until a clear solution was observed (**5c**). The solution was cooled to room temperature. Concurrently, iodine (21 mg, 0.082 mmol) was dissolved in CH_2Cl_2 (2 mL) and triethylsilane (26 μL , 0.16 mmol) was added. The solution was mixed until a light pink color was achieved. After 15 min, the resulting mixture was cooled to 0 $^\circ\text{C}$ and a solution of **11** (28.4 mg, 0.0680 mmol) in CH_2Cl_2 (1 mL) was added dropwise with stirring. The reaction became yellow in color. The reaction was then stirred for 10 min. The cooled solution of **5c** was added rapidly using additional CH_2Cl_2 (5 mL) for rinsing. The reaction was warmed to room temperature and stirred for 1 h. The reaction was quenched with a few drops of saturated NaHCO_3 . The emulsion was washed with 1 N $\text{Na}_2\text{S}_2\text{O}_3$, then with brine. The aqueous layer was back-extracted with CH_2Cl_2 . The organic layers were dried with Na_2SO_4 and concentrated under reduced pressure. The crude residue was purified by flash column chromatography (5–25% MeOH/ CH_2Cl_2 , $R_f = 0.25$ in 3% MeOH/ CH_2Cl_2) to yield the product as a clear oil (21 mg, 59%, 2.5:1 d.r.).

2.4.7 Synthesis of (\pm)-FTC/3TC

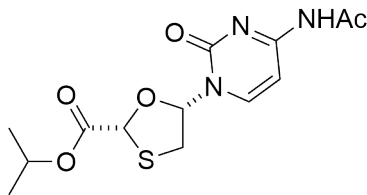


Isopropyl-5-hydroxy-1,3-oxathiolane-2-carboxylate, (15). Diisopropyl-L-tartrate (5.05 g, 20.8 mmol) was dissolved in water (10 mL) in a 100-mL round-bottom flask. The solution was cooled in an ice/water bath. A solution of sodium periodate (5.9 g, 28 mmol) in water (40 mL) was added dropwise with vigorous stirring over 20 min. After completion of addition, the resulting suspension was stirred at 0 °C for 2 h. The reaction mixture was warmed to room temperature and extracted with EtOAc (5 x 30 mL). The combined extracts were dried over Na₂SO₄ and concentrated. The resulting crude residue was dissolved in toluene (5 mL) and transferred to a 100-mL round-bottom flask. 1,4-Dithian-2,5-diol (3.4 g, 22 mmol) was added and the flask was equipped with a reflux condenser. The mixture was heated to reflux for 1 h until the solution turned from yellow to colorless. The mixture was cooled for 5 min, then concentrated under reduced pressure with heating at 45 °C (7.2 g, 91%, 1.1:1 d.r.). The crude material was carried forward to the next step without purification. For characterization, the crude material was purified by column chromatography (10–70% EtOAc/hexanes, R_f = 0.31 in 30% EtOAc/hexanes) to yield the title compound as a colorless oil. ¹H NMR (400 MHz, CDCl₃) δ 6.01 (d, J = 3.9 Hz, 1H), 5.94–5.88 (m, 1H), 5.54 (d, J = 5.6 Hz, 1H), 5.15–5.00 (m, J = 6.3, 5.8 Hz, 1H), 3.28 (dd, J = 11.2, 4.4 Hz, 1H), 3.14 (dd, J = 11.1, 2.1 Hz, 1H), 1.28 (q, J = 5.3 Hz, 6H). ¹³C{¹H} NMR (101 MHz, CDCl₃) δ 172.0, 169.5, 103.0, 101.3, 80.0, 77.80, 70.7, 69.7, 40.1, 38.3, 21.7, 21.7, 21.5, 21.4. HRMS (DART/AccuTOF) m/z: [M+H]⁺ Calcd for C₇H₁₃O₄S 193.0529; Found 193.0534. IR (cm⁻¹) 3023, 1737.



Isopropyl-5-acetoxy-1,3-oxathiolane-2-carboxylate, (16).

15 (7.00 g, 36.4 mmol) was dissolved in CH_2Cl_2 in a 250-mL round-bottom flask. The resulting solution was cooled in an ice-water bath. Acetic anhydride (6.9 mL, 73 mmol) was added, followed by pyridine (5.9 mL, 73 mmol) and 4-dimethylaminopyridine (220 mg, 1.8 mmol). The mixture was warmed to room temperature and stirred for 4 h. The reaction mixture was diluted with CH_2Cl_2 and transferred to a separatory funnel. The organic layer was washed with water, saturated NaHCO_3 , 1 M HCl (aq), then brine. The organic layer was dried with MgSO_4 then concentrated under reduced pressure. The resulting residue was purified by column chromatography (7–60% EtOAc/hexanes, $R_f = 0.54$ in 30% EtOAc/hexanes) to yield the title compound as a clear oil (6.35 g, 9:1 d.r. with 94% purity, 74%). *trans*-**16**: ^1H NMR (400 MHz, CDCl_3) δ 6.78 (d, $J = 4.1$ Hz, 1H), 5.60 (s, 1H), 5.07 (hept, $J = 6.3$ Hz, 1H), 3.43 (dd, $J = 11.7, 4.1$ Hz, 1H), 3.15 (d, $J = 11.7$ Hz, 1H), 2.10 (s, 3H), 1.27 (d, $J = 6.3$ Hz, 6H). $^{13}\text{C}\{^1\text{H}\}$ NMR (101 MHz, CDCl_3) δ 169.4, 168.3, 99.7, 79.8, 69.5, 37.0, 21.5, 21.3, 20.9. *cis*-**16**: ^1H NMR (400 MHz, CDCl_3) δ 6.64 (d, $J = 4.0$ Hz, 1H), 5.62 (s, 1H), 5.07 (hept, $J = 6.3$ Hz, 1H), 3.28 (dd, $J = 11.3, 4.0$ Hz, 1H), 3.21 (dd, $J = 11.2, 1.2$ Hz, 1H), 2.11 (s, 3H), 1.27 (d, $J = 6.3$ Hz, 6H). $^{13}\text{C}\{^1\text{H}\}$ NMR (101 MHz, CDCl_3) δ 169.9, 168.5, 99.1, 80.2, 69.4, 37.5, 21.5, 21.4, 21.0. HRMS (DART/AccuTOF) m/z : $[\text{M}+\text{NH}_4]^+$ Calcd for $\text{C}_9\text{H}_{18}\text{NO}_5\text{S}$ 252.0900; Found 252.0901. IR (cm^{-1}) 1748.

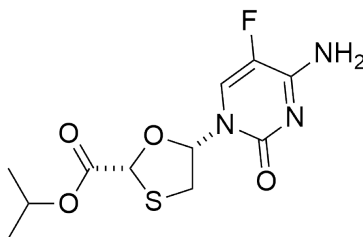


Isopropyl-(*RS,SR*)-5-(4-acetamido-2-oxopyrimidin-1(2H)-yl)-1,3-oxathiolane-2-carboxylate, by recrystallization (17**).**

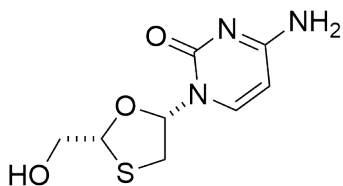
19 (800 mg, 5.2 mmol) was weighed into an oven-dried 200 mL roundbottom flask. CH₂Cl₂ (100 mL) was added. *N,O*-bis-(trimethylsilyl)acetamide (2.0 mL, 8.0 mmol) was added and the mixture was heated to reflux in an oil bath until complete dissolution was observed, approximately 30 min. Concurrently, NaI (780 mg, 5.2 mmol) was added to a 250-mL round-bottom flask followed by wet CH₂Cl₂ (25 mL, water content 0.1 M). With stirring, chlorotrimethylsilane (660 μL, 5.2 mmol) was added, and heterogeneous mixture was stirred at room temperature vigorously for 5 min. **16** (936 mg, 4.00 mmol) was dissolved in dichloromethane (4 mL), then add to the TMSCl–NaI mixture, using additional CH₂Cl₂ (12 mL) to complete the transfer. The resulting mixture was stirred for 15 min at room temperature, resulting in a dark brown solution. The solution of **5c** was added by cannulation, using CH₂Cl₂ (10 mL) to complete the transfer. The resulting mixture was stirred at room temperature for 40 min. The reaction was quenched by addition of saturated NaHCO₃ (10 mL) with rapid stirring. The slurry was filtered through a pad of Celite, washing thoroughly with CH₂Cl₂ to yield an orange-yellow filtrate. The filtrate was transferred to a separatory funnel and washed with a 1:1 mixture of 1 N Na₂S₂O₃ and saturated NaHCO₃, then with brine. The organic layer was dried with MgSO₄ and filtered, then concentrated under reduced pressure. ¹H NMR analysis showed full conversion of **16** to **17** with 20:1 d.r. The crude product was dissolved in a minimal amount of EtOAc and held at –20 °C overnight to yield a precipitate which was collected by vacuum filtration over a sintered glass funnel with fine porosity (697 mg, 53%, >150:1 d.r.). ¹H NMR (500 MHz, CDCl₃) δ 9.45 (s, 1H), 8.70 (d, J = 7.5 Hz, 1H), 7.47 (d, J = 7.6 Hz, 1H), 6.42 (dd, J = 5.8, 4.8 Hz, 1H), 5.51 (s, 1H), 5.13 (hept, J = 6.2 Hz, 1H), 3.66 (dd, J = 12.3, 4.8 Hz, 1H), 3.19 (dd, J = 12.3, 5.9 Hz, 1H), 2.27 (s, 3H), 1.31 (dd, J = 8.0, 6.2 Hz, 6H). ¹³C{¹H} NMR

(126 MHz, CDCl₃) δ 170.7, 169.1, 163.1, 155.1, 145.6, 96.8, 90.9, 79.87, 70.7, 37.2, 25.1, 21.8, 21.6. HRMS (DART/AccuTOF) m/z : [M+H]⁺ Calcd for C₁₃H₁₈N₃O₅S 328.0962; Found 328.0967. IR (cm⁻¹) 1659, 1614, 1562.

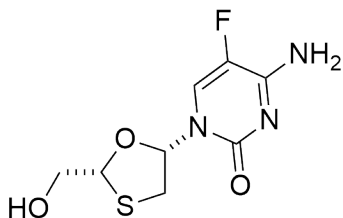
Isopropyl-(RS,SR)-5-(4-acetamido-2-oxopyrimidin-1(2H)-yl)-1,3-oxathiolane-2-carboxylate (17). As above, isolation by column chromatography. Using **19** (800 mg, 5.2 mmol), *N,O*-bis(trimethylsilyl)acetamide (2.0 mL, 8.0 mmol), and CH₂Cl₂ (100 mL) to prepare **5c**. Using chlorotrimethylsilane (660 μ L, 5.2 mmol), NaI (780 mg, 5.2 mmol), and wet CH₂Cl₂ (25 mL), followed by **16** (936 mg, 4.0 mmol) in a solution of CH₂Cl₂ (4 mL), using additional CH₂Cl₂ (12 mL) to complete the transfer, resulting in a dark brown solution. The solution of **5c** was transferred by cannulation, using CH₂Cl₂ (12 mL) to complete the transfer. The reaction was quenched by aqueous workup, transferring the unquenched reaction mixture to a separatory funnel, then washing with a 1:1 mixture of saturated Na₂S₂O₃ and saturated NaHCO₃. A pink solid was observed in the aqueous layer which interfered with the separation (presumably excess **19**). The crude residue was purified by column chromatography (0–7% MeOH/EtOAc, R_f = 0.29 in 3% MeOH/CH₂Cl₂) resulting in a pearly white foam (1.05 g, 72%, >20:1 d.r.).



Isopropyl-(*RS,SR*)-5-(4-amino-5-fluoro-2-oxopyrimidin-1(2H)-yl)-1,3-oxathiolane-2-carboxylate, (18). Using 5-fluorocytosine (168 mg, 1.30 mmol) and *N,O*-bis(trimethylsilyl)acetamide (1.1 mL, 3.4 mmol) in CH₂Cl₂ (25 mL) to prepare **5a**. Using **16** (243 mg, 92% purity, 0.960 mmol), chlorotrimethylsilane (254 μL, 2.00 mmol), and NaI (300 mg, 2.0 mmol), in wet CH₂Cl₂ (10 mL). Formation of the intermediate iodide was observed by ¹H NMR (see section for NMR Spectra, compound **24**). The reaction was quenched by aqueous workup, transferring the unquenched reaction mixture to a separatory funnel, then washing with a 1:1 mixture of saturated Na₂S₂O₃ / saturated NaHCO₃ and extracting with CH₂Cl₂. The product was isolated by column chromatography (0–20% MeOH/CH₂Cl₂, R_f = 0.14 in 3% MeOH/CH₂Cl₂) by dry-loading onto silica gel, yielding the title compound as a white solid (288 mg, >95%). ¹H NMR (400 MHz, CDCl₃ plus MeOD) δ 8.39 (d, J = 6.6 Hz, 1H), 6.32 (ddd, J = 6.7, 4.8, 1.8 Hz, 1H), 5.38 (s, 1H), 5.06 (hept, J = 6.3 Hz, 1H), 3.46 (dd, J = 12.1, 4.7 Hz, 1H), 3.20 (s, 2H), 3.06 (dd, J = 12.1, 6.6 Hz, 1H), 1.25 (t, J = 5.9 Hz, 6H). ¹³C{¹H} NMR (101 MHz, CDCl₃ plus MeOD) δ 169.5, 154.3, 153.9, 138.0, 135.5, 125.9, 125.6, 90.4, 78.7, 70.6, 49.6, 49.4, 49.2, 48.9, 48.7, 36.2, 21.6, 21.3. HRMS (DART/AccuTOF) m/z: [M+H]⁺ Calcd for C₁₁H₁₅N₃O₄FS 304.0762; Found 304.0766. IR (cm⁻¹) 1737, 1681, 1610.



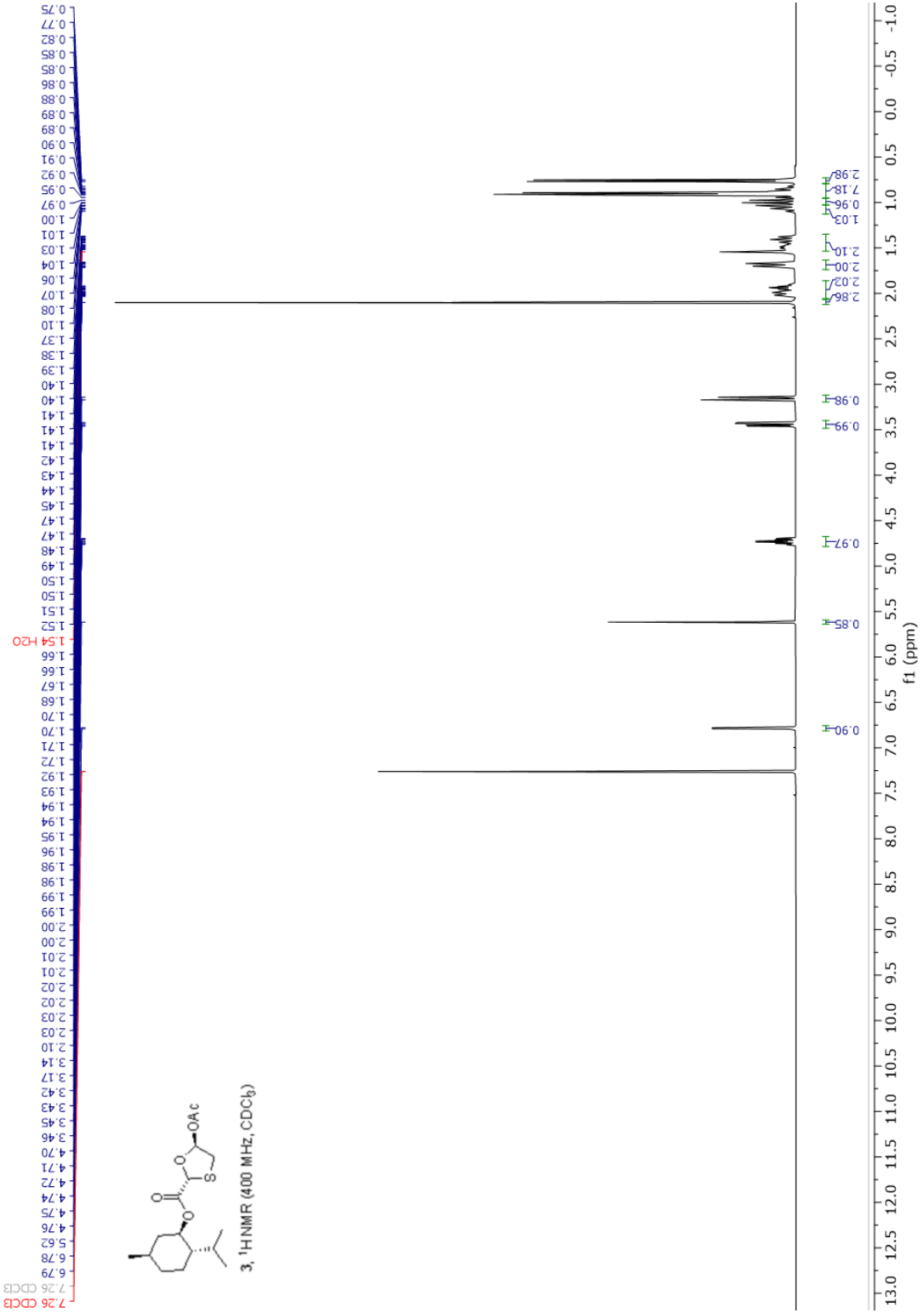
4-amino-1-((*RS,SR*)-2-(hydroxymethyl)-1,3-oxathiolan-5-yl)pyrimidin-2(1H)-one, (1b).¹⁷ **17** (67 mg, 0.20 mmol) was dissolved in methanol (5 mL) in a 20-mL vial and was heated in a heat block to 40 °C for 16 h until cleavage of the acetyl group was observed by HPLC. Sodium borohydride (15 mg, 0.40 mmol) was added and the solution was stirred for 1 h. Glauber's salt (sodium sulfate decahydrate) was added. The mixture was filtered through Celite, washing with methanol. Quantitative NMR analysis with 1,3,5-trimethoxybenzene showed an assay yield of 77% (see section for NMR Spectra). The NMR sample was recovered, dissolved in water, and transferred to a separatory funnel. The aqueous layer was extracted with diethyl ether (3 x 10 mL). The aqueous layer was concentrated to yield a white solid (80 mg, with ca. 44% purity, 77%).

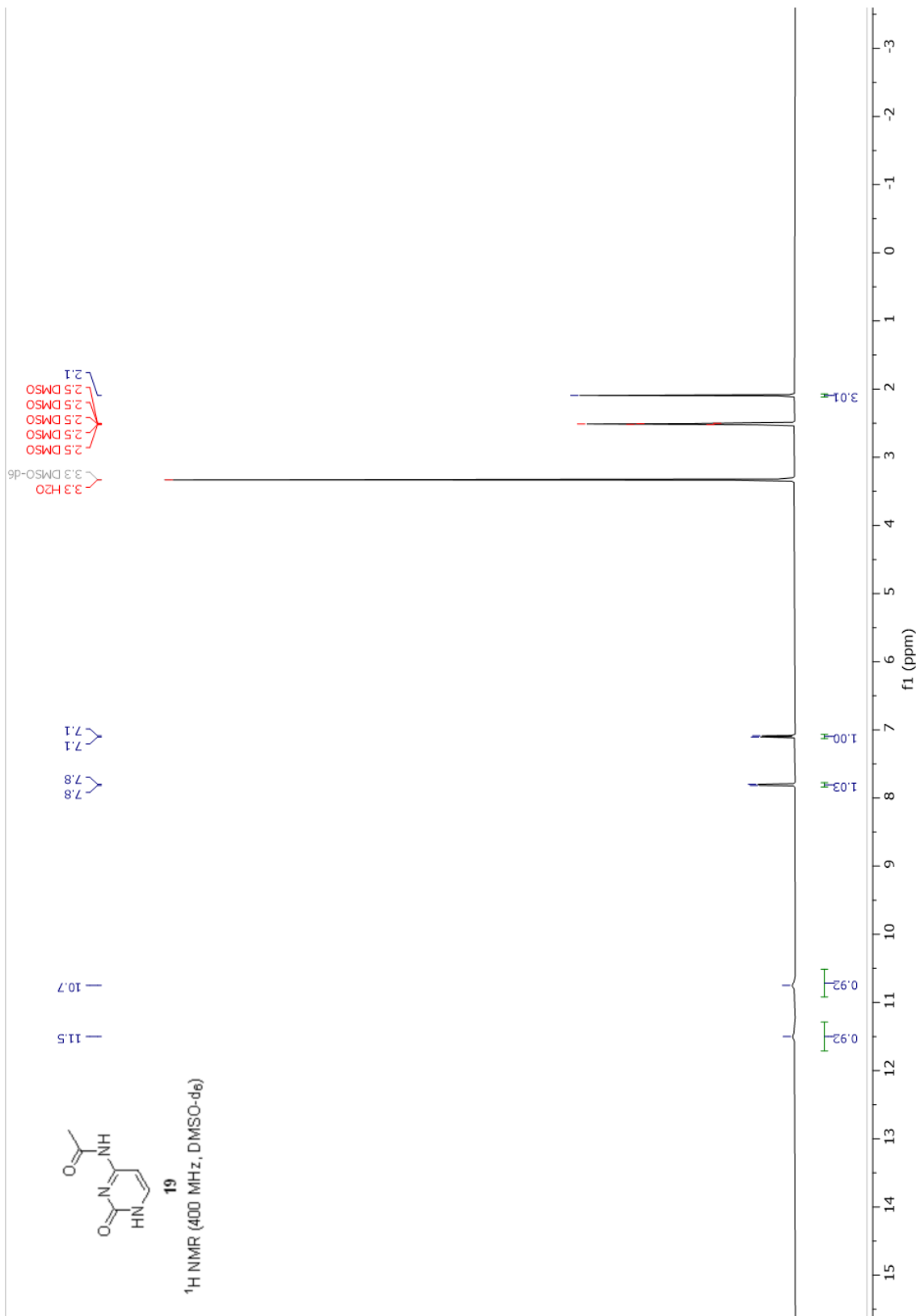


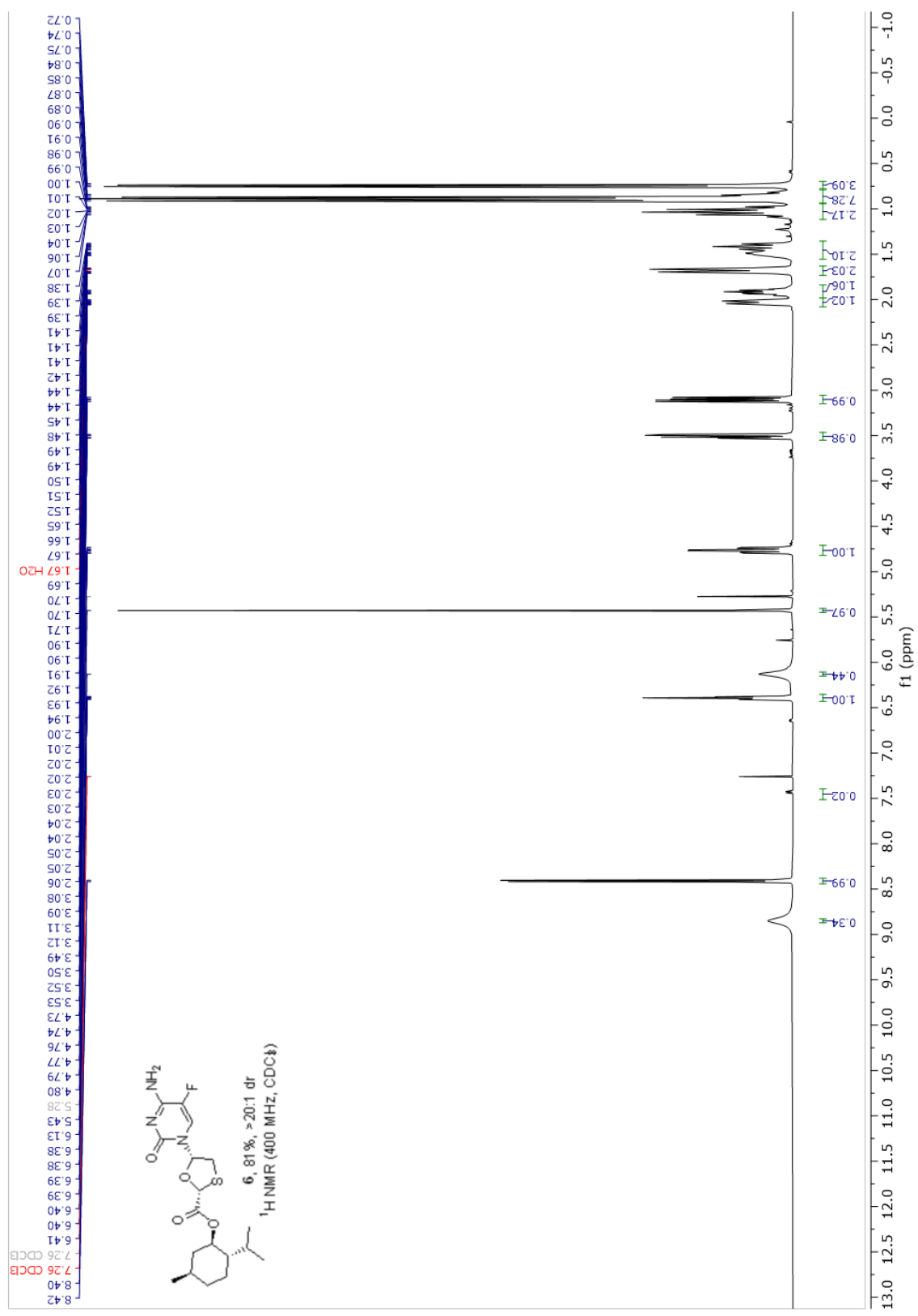
4-amino-5-fluoro-1-((*RS,SR*)-2-(hydroxymethyl)-1,3-oxathiolan-5-yl)pyrimidin-2(1H)-one, (1a).¹⁷ **18** (44 mg, 0.15 mmol) was suspended in THF (5 mL) in a 25 mL round-bottom flask. The suspension was sonicated to disperse the material, which is sparingly soluble. Lithium borohydride (83 μ L of 2.0 M solution in THF, 0.17 mmol) was added to the suspension at 0 °C. The solution was warmed to room temperature and stirred until complete conversion was observed by TLC (5% MeOH/CH₂Cl₂), 1 h. The solution was quenched by addition of MeOH (0.5 mL), followed by addition of silica gel (1 g). The slurry was stirred for 10 min, then transferred to a sintered glass funnel containing a 1 g pad of silica gel. The pad of silica was washed with 20% MeOH/CH₂Cl₂ (25 mL) and the filtrate was evaporated to dryness to yield a white solid (43 mg, >95%, >20:1 d.r.).

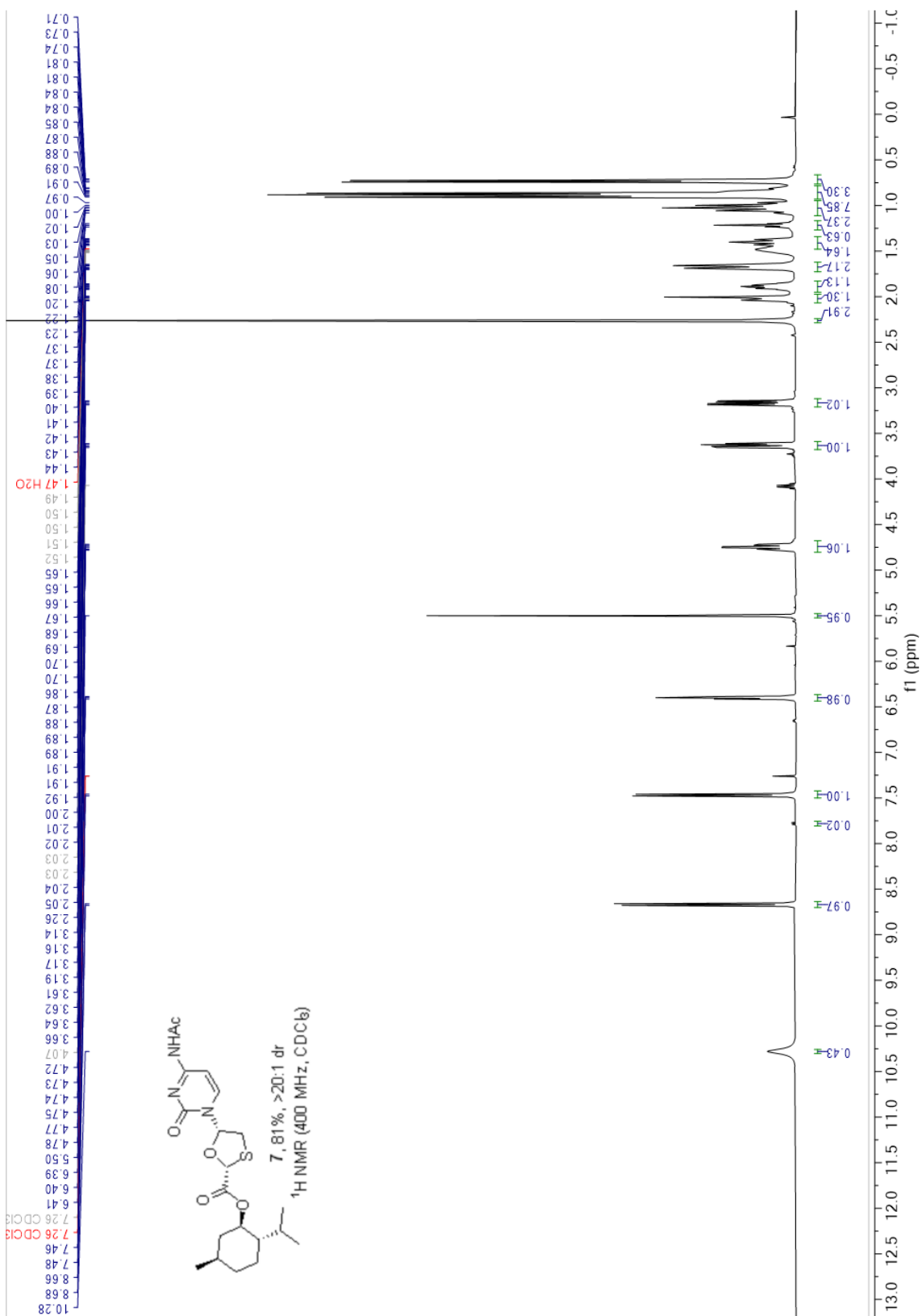
4-amino-5-fluoro-1-((*RS,SR*)-2-(hydroxymethyl)-1,3-oxathiolan-5-yl)pyrimidin-2(1H)-one, (1a).¹⁷ **20** (638 mg, 2.21 mmol) was suspended in 30 mL anhydrous THF in an oven-dried 100-mL round-bottom flask. The suspension was sonicated to disperse material, which is sparingly soluble. Lithium borohydride solution (1.22 mL 2 M in THF, 2.43 mmol) was added dropwise to the suspension at 0 °C. The solution was warmed to room temperature and stirred for 30 min. The reaction was quenched with MeOH (2 mL) followed by slow addition of silica gel (4 g). Gas evolution was observed on addition of silica gel. The slurry was stirred for 30 min, then transferred to a short column and eluted with CH₂Cl₂/MeOH (496 mg, 91%, 14:1 d.r.).

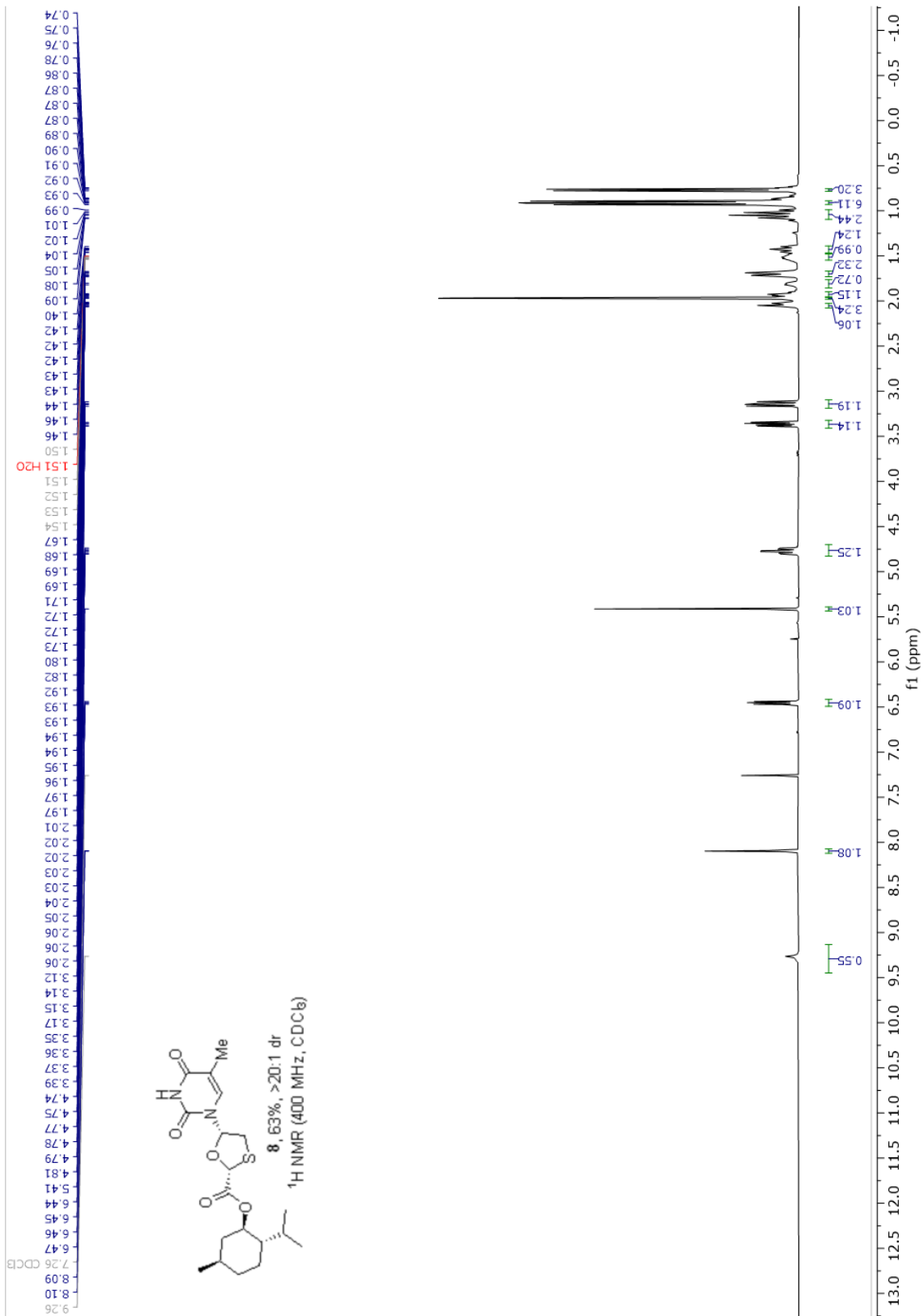
2.5 ^1H and $^{13}\text{C}\{^1\text{H}\}$ NMR Spectra

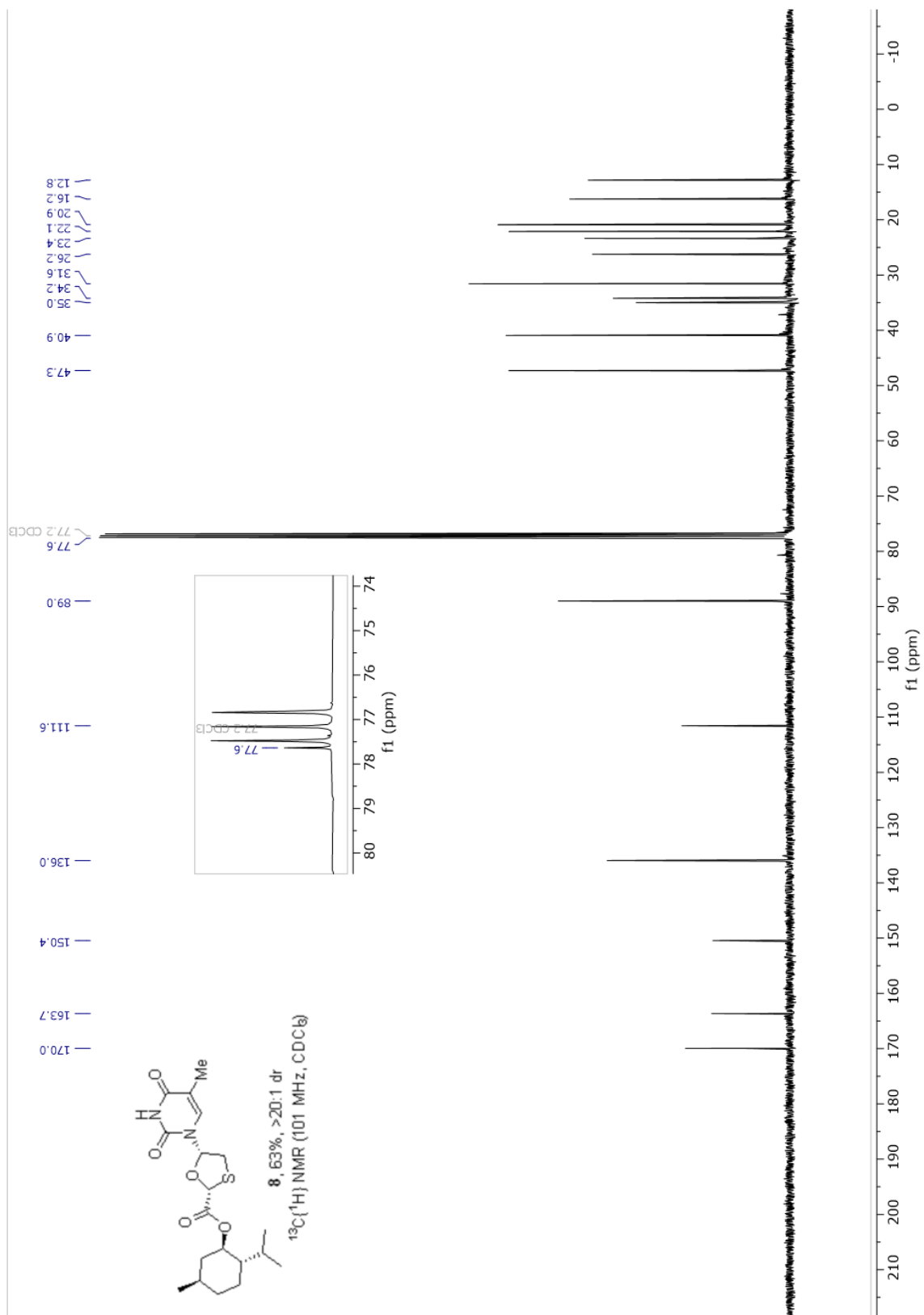


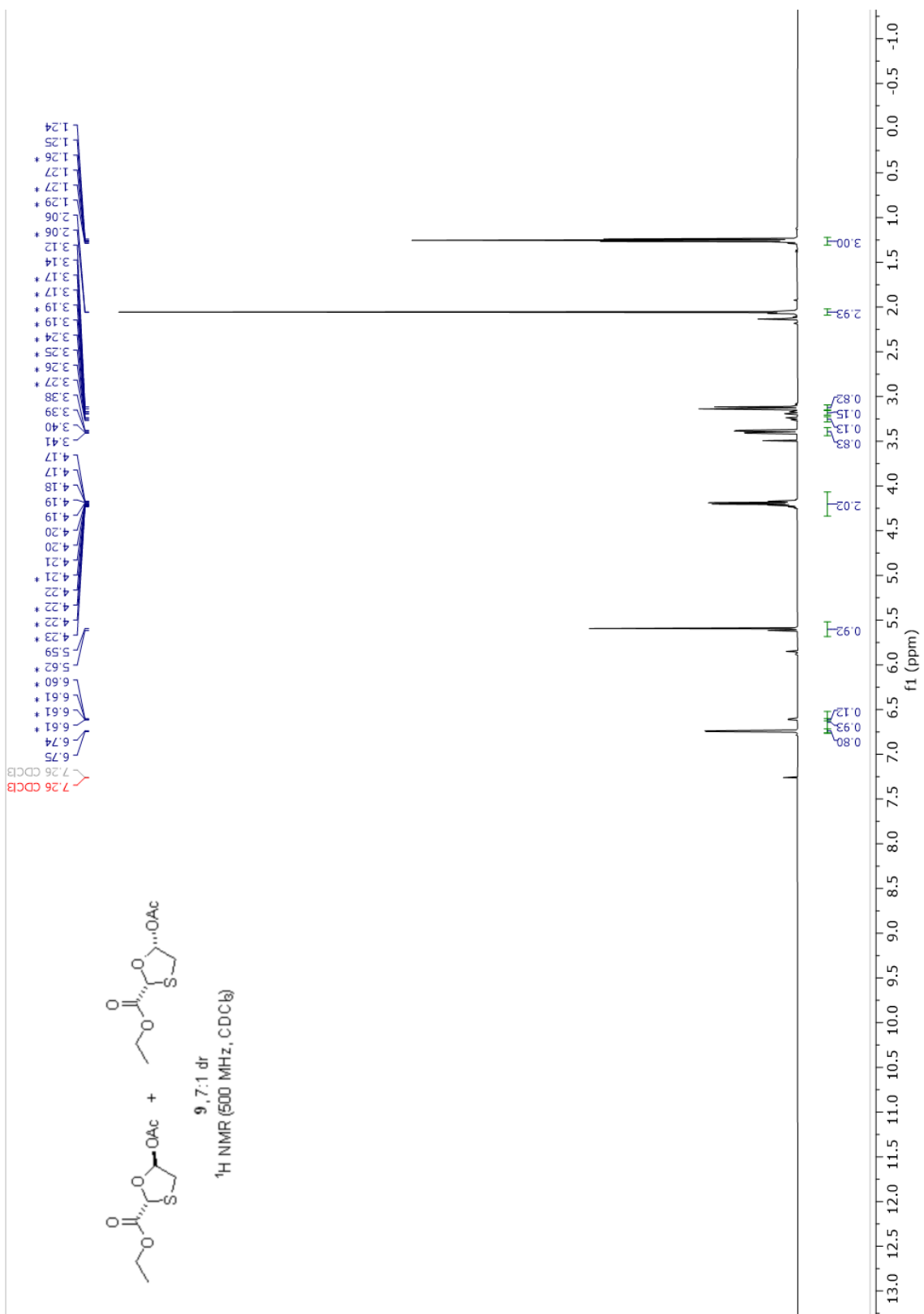


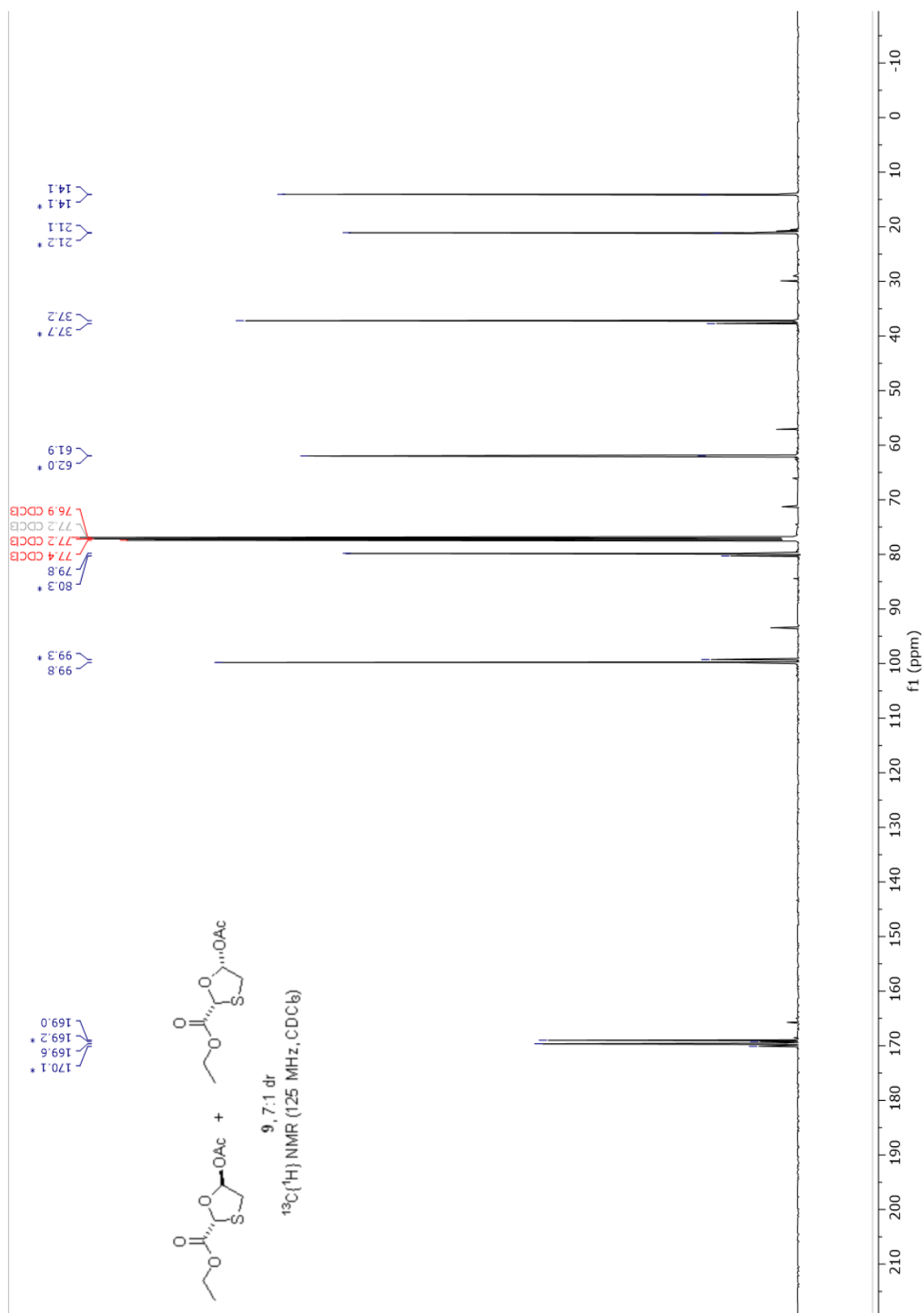


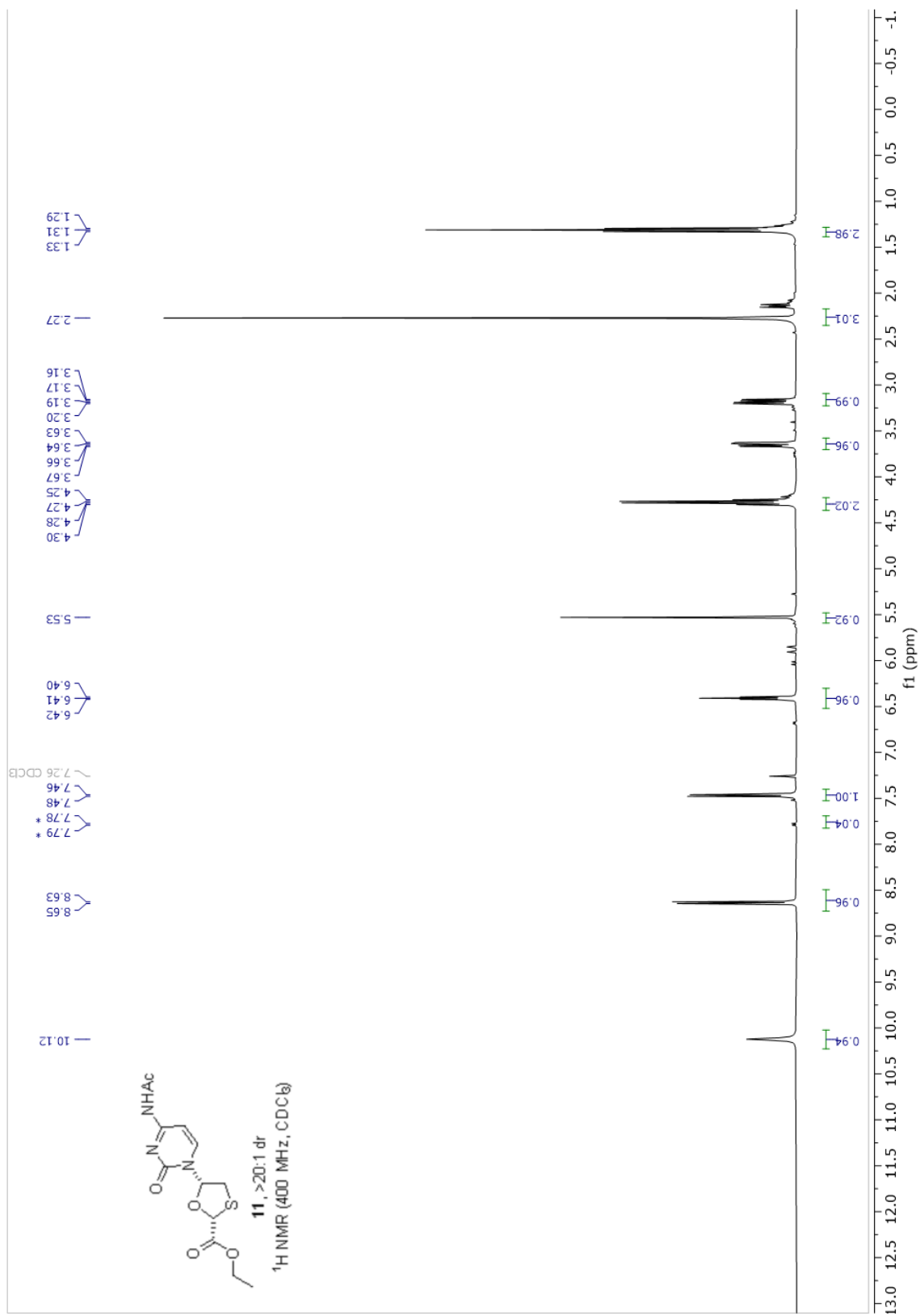


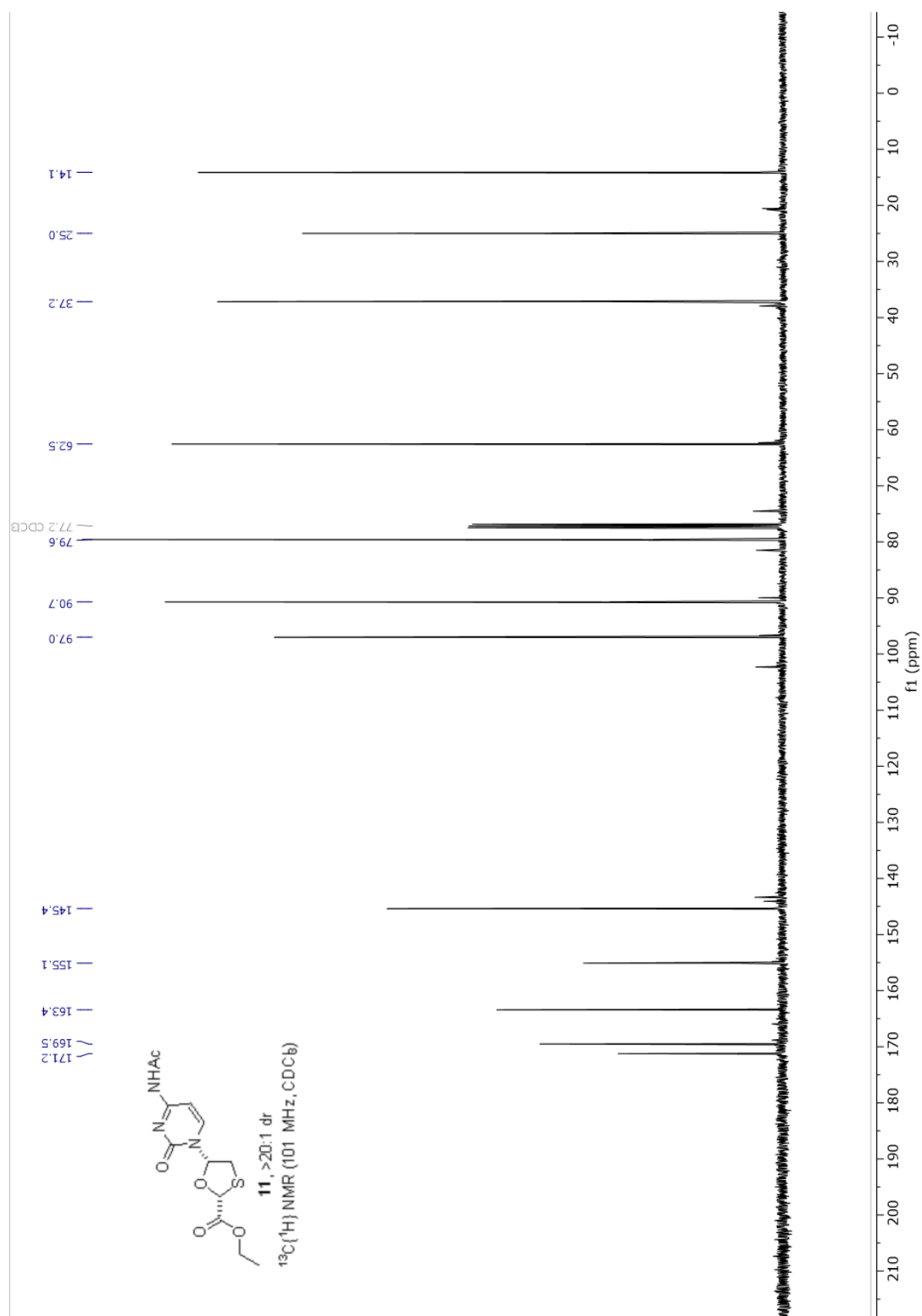


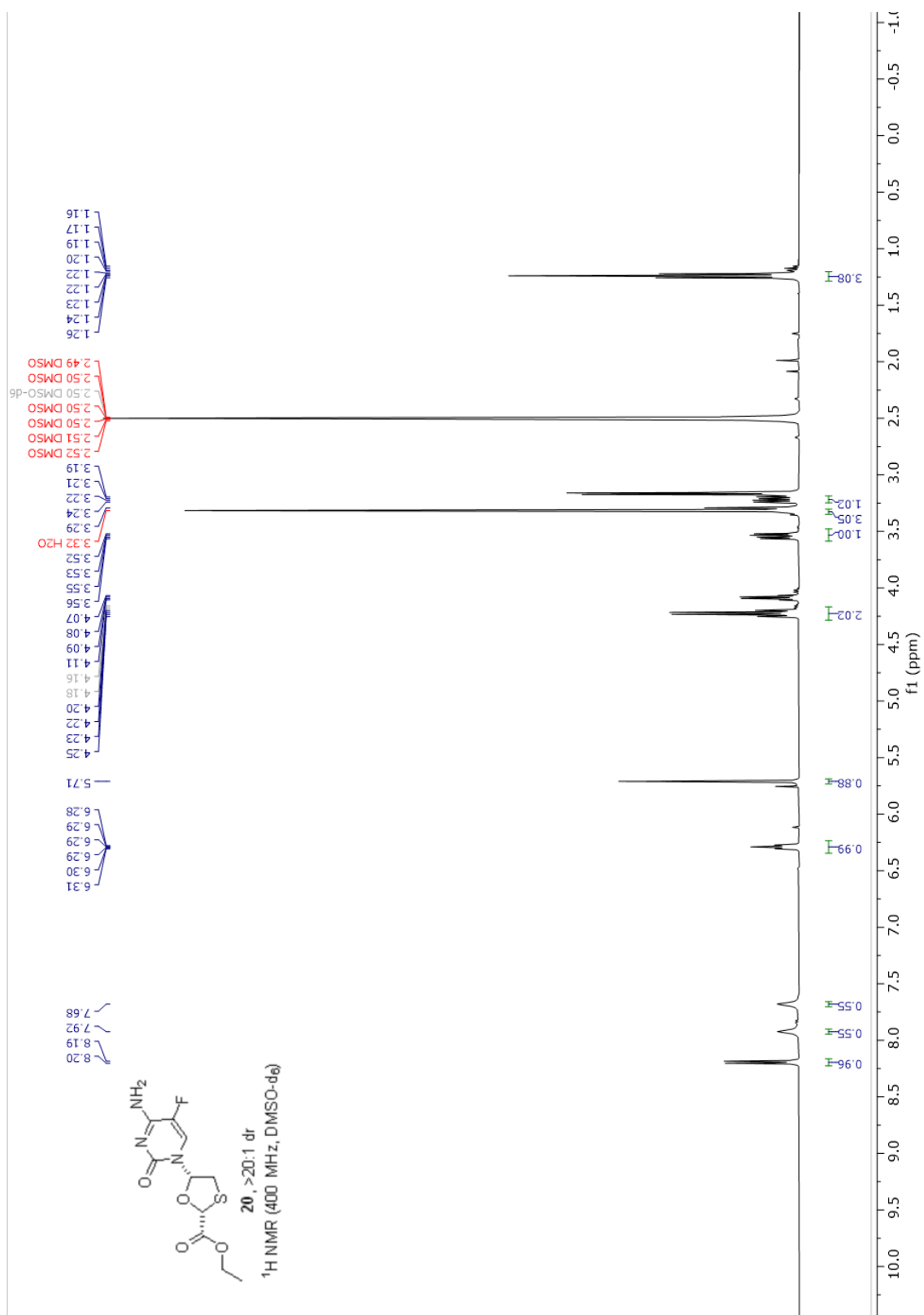


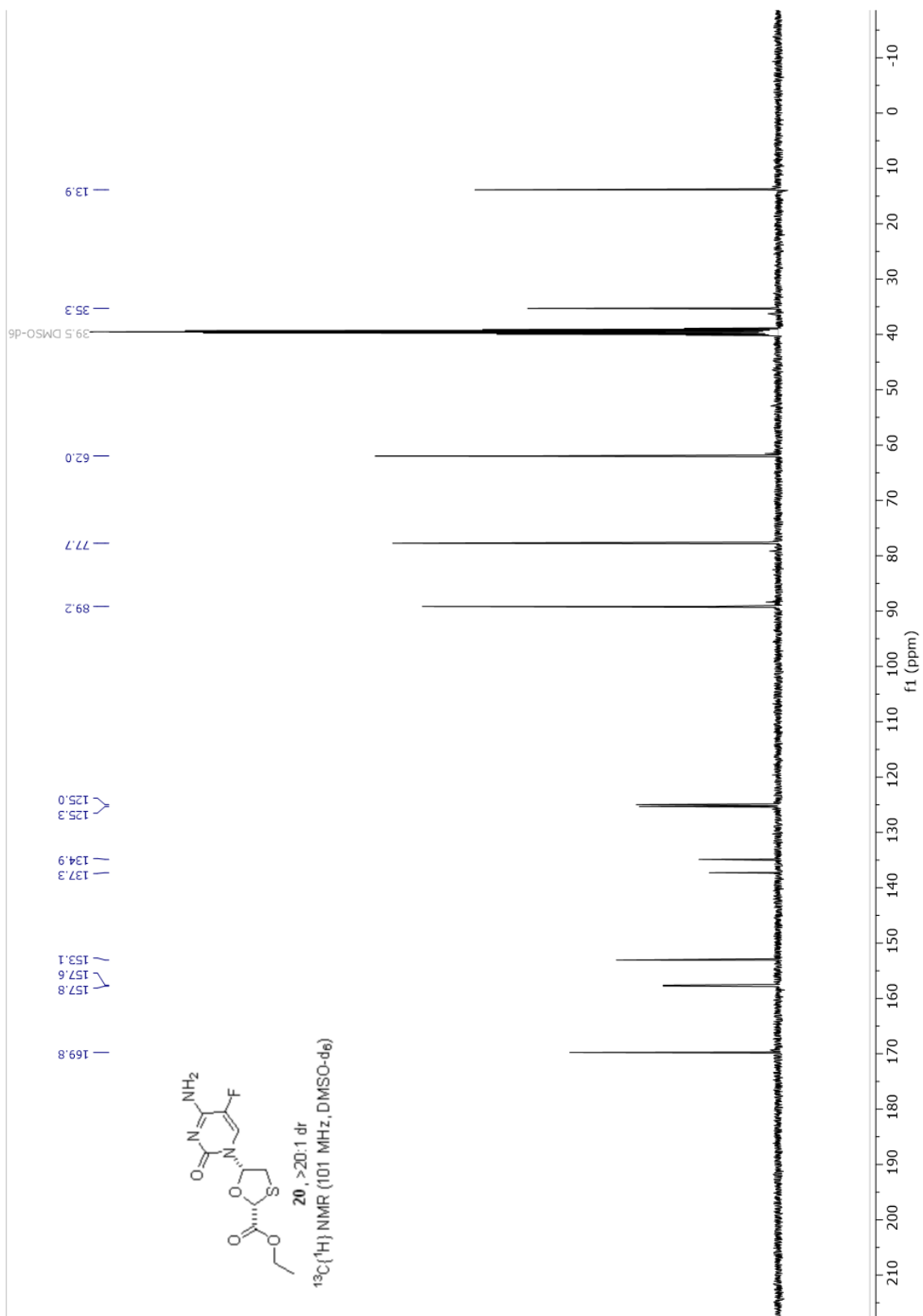


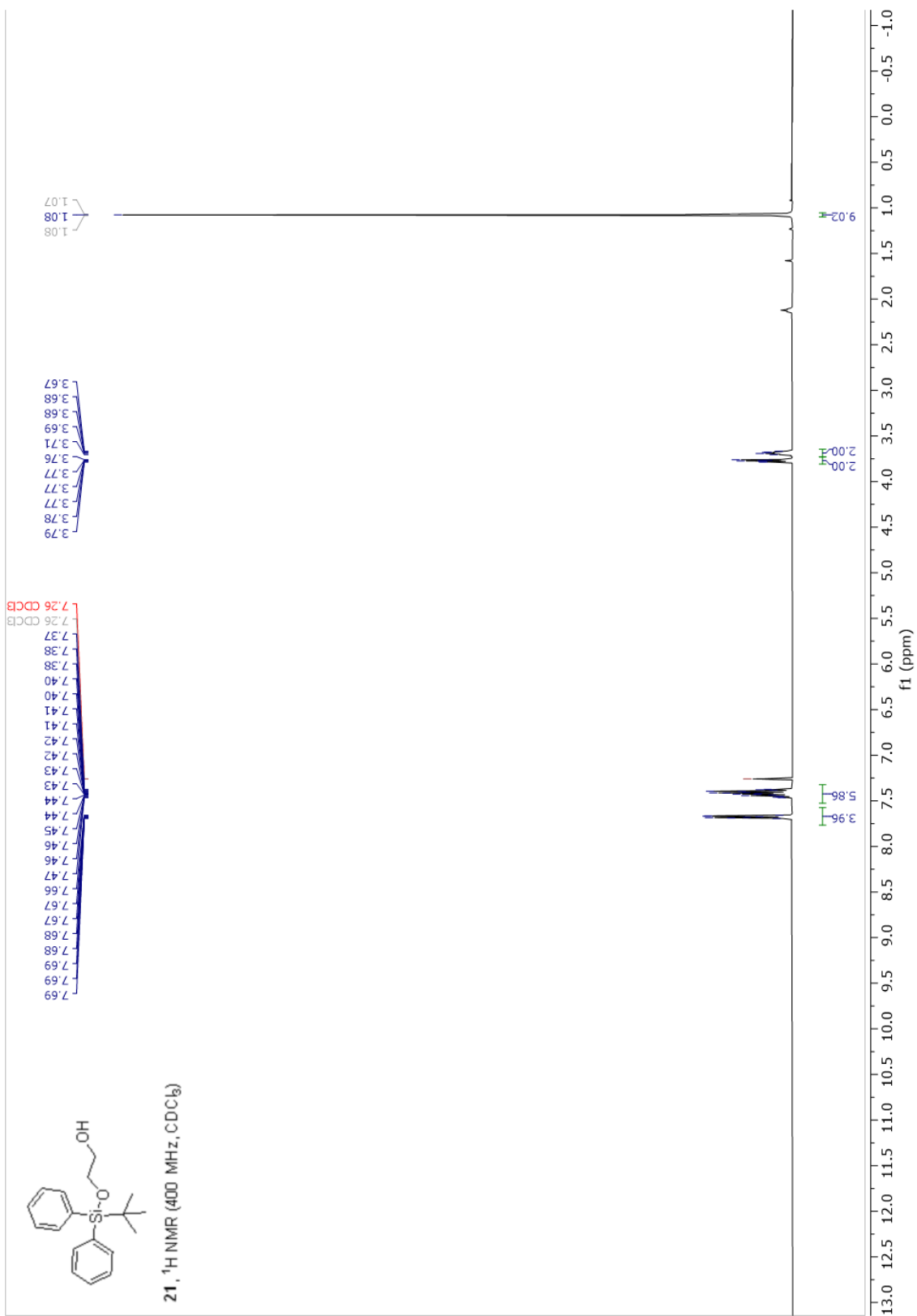


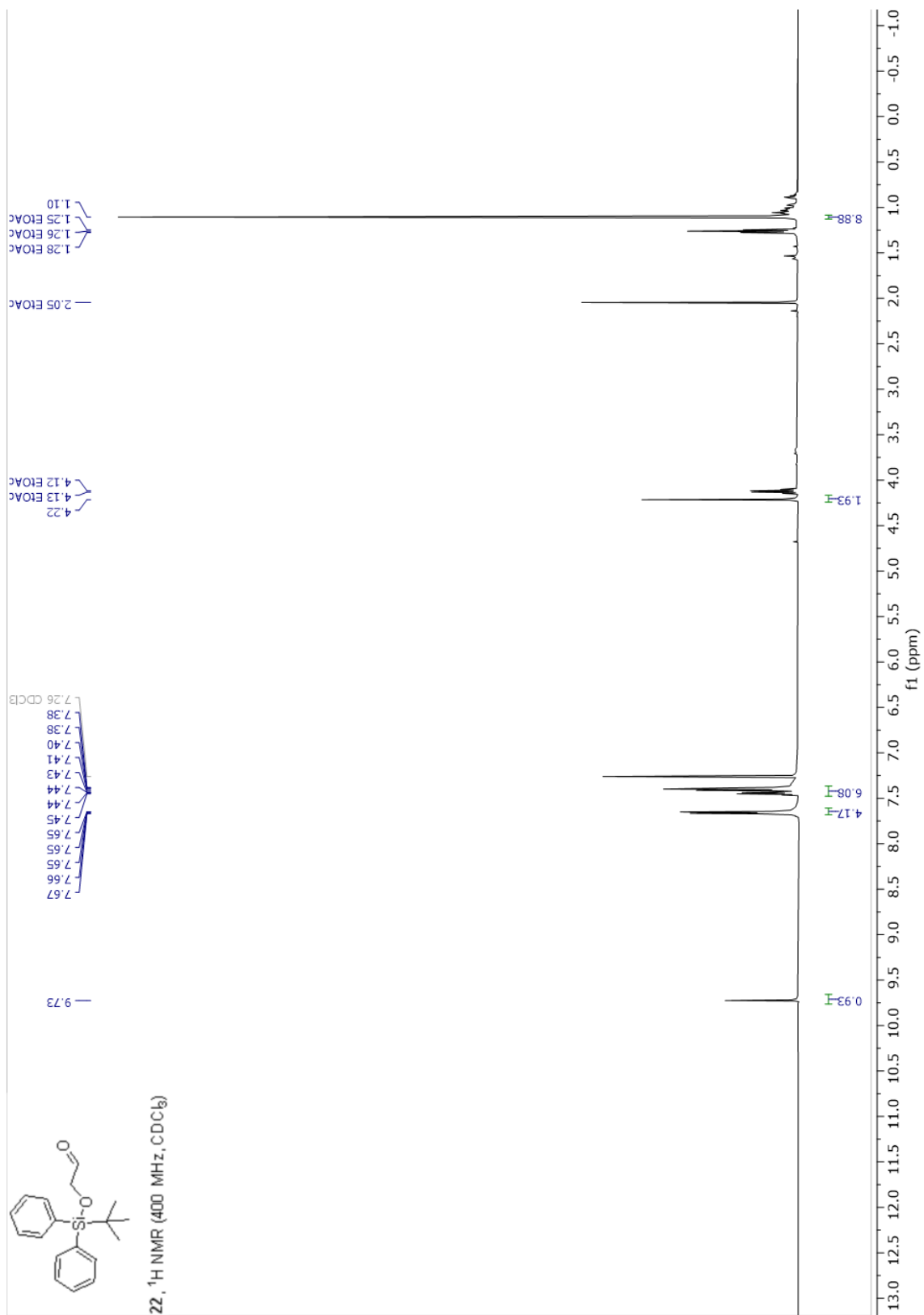


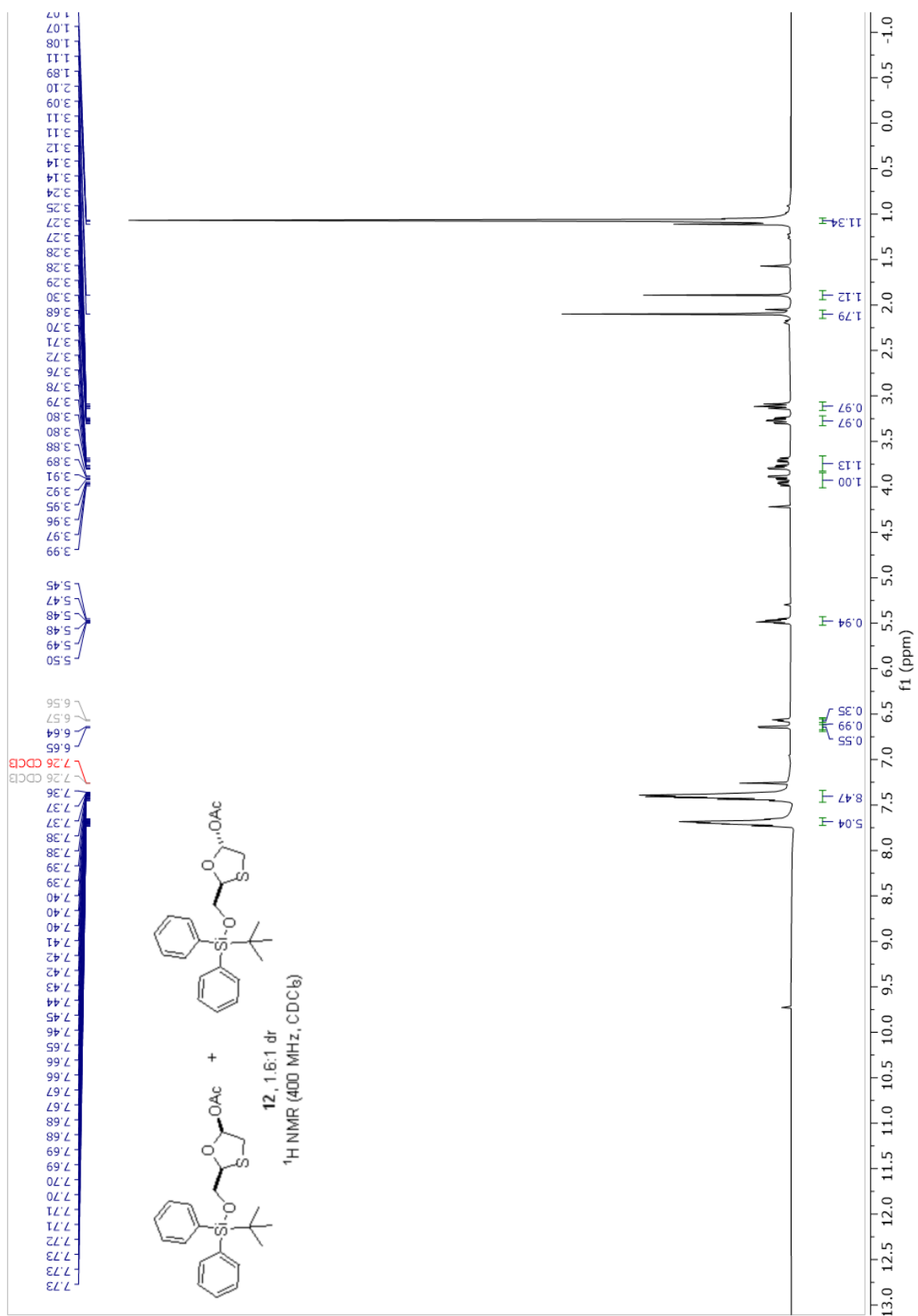


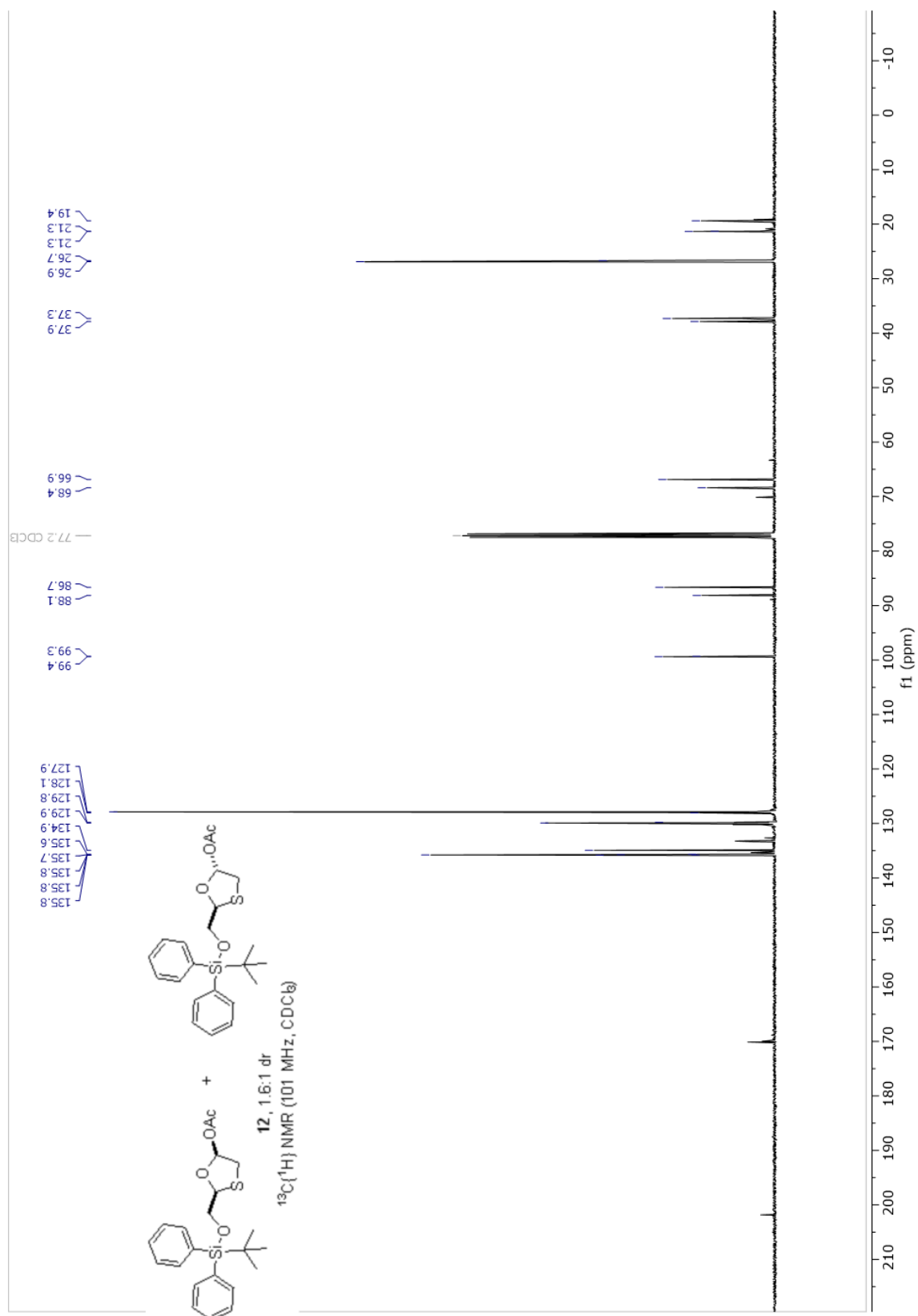


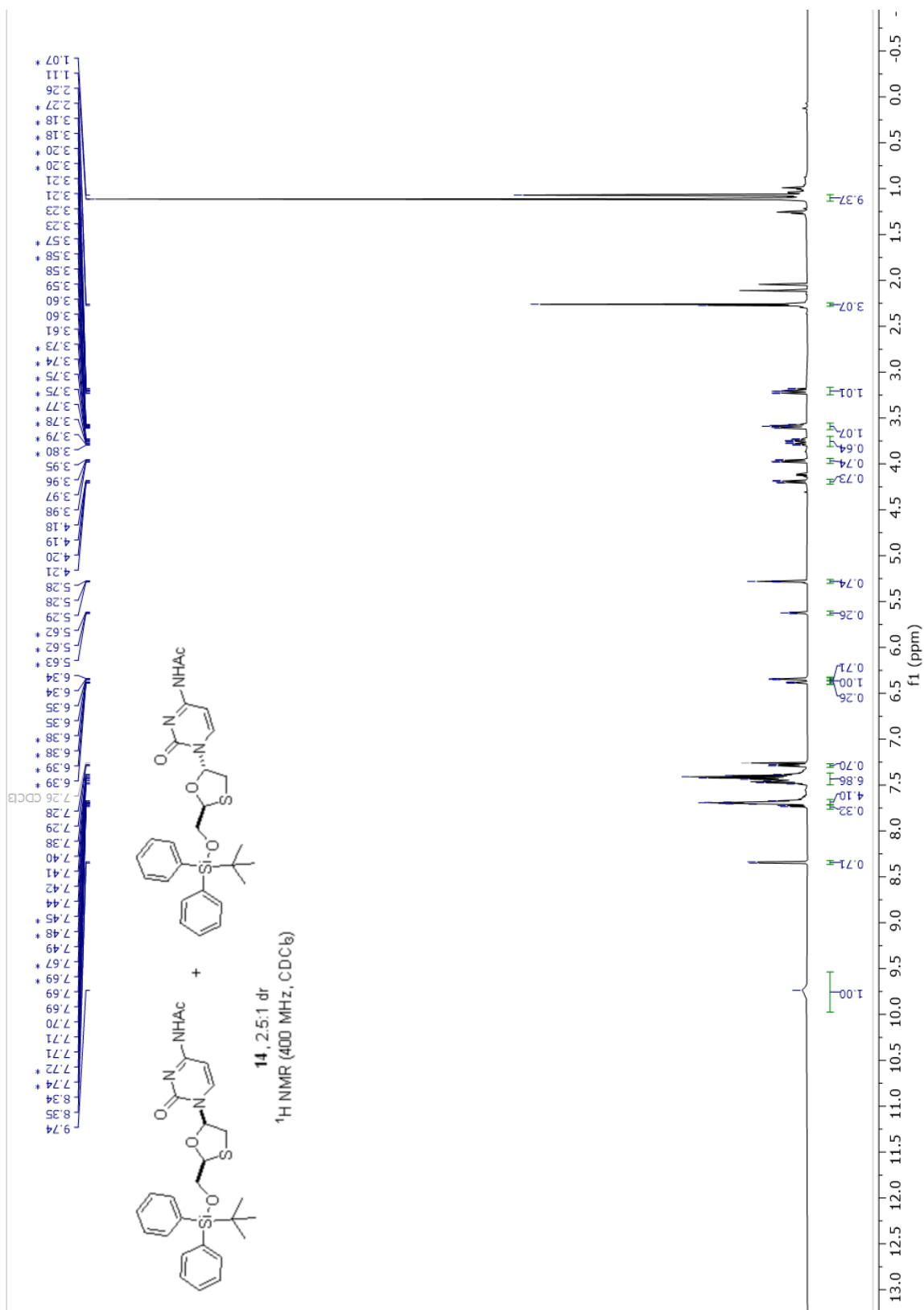


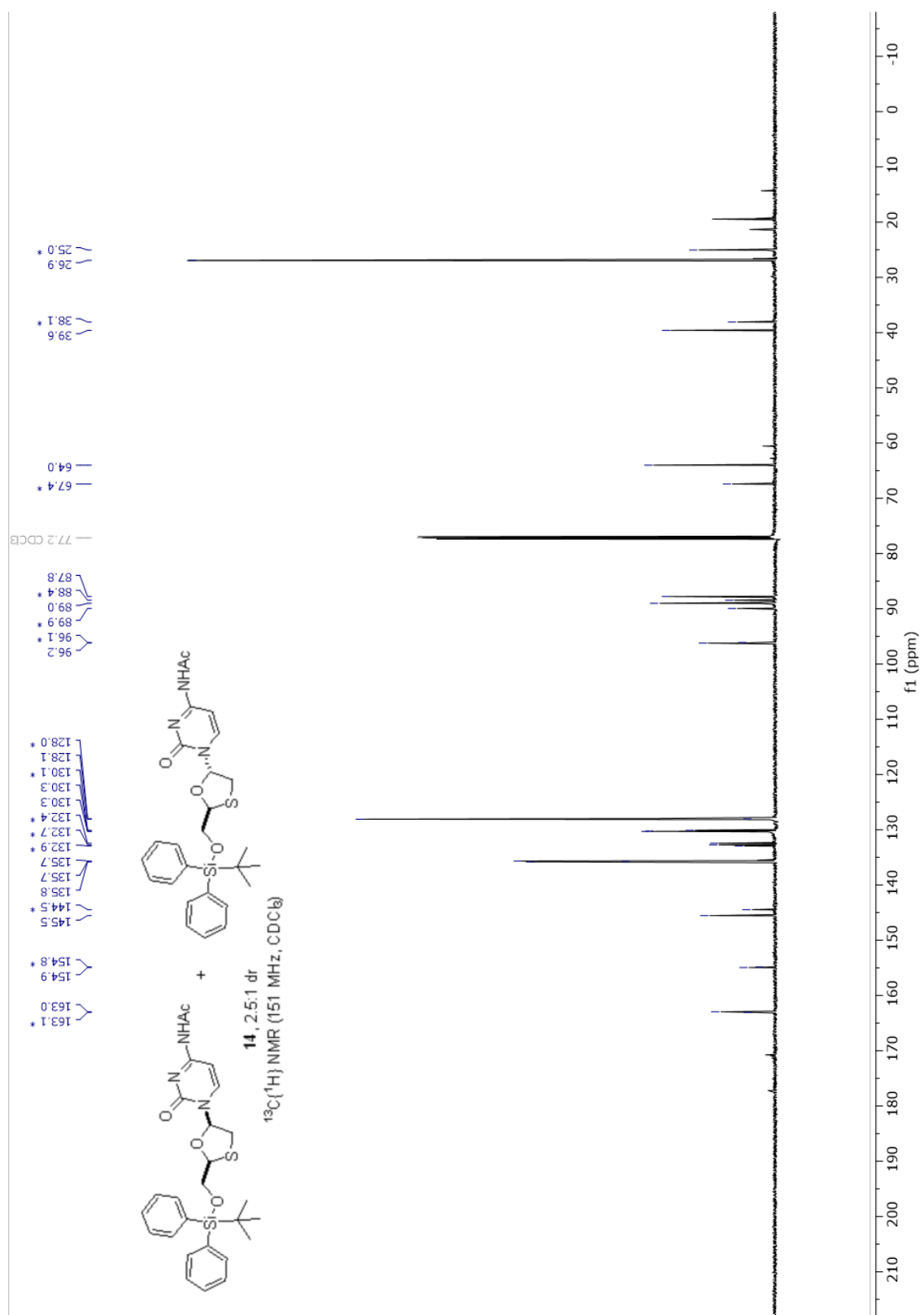


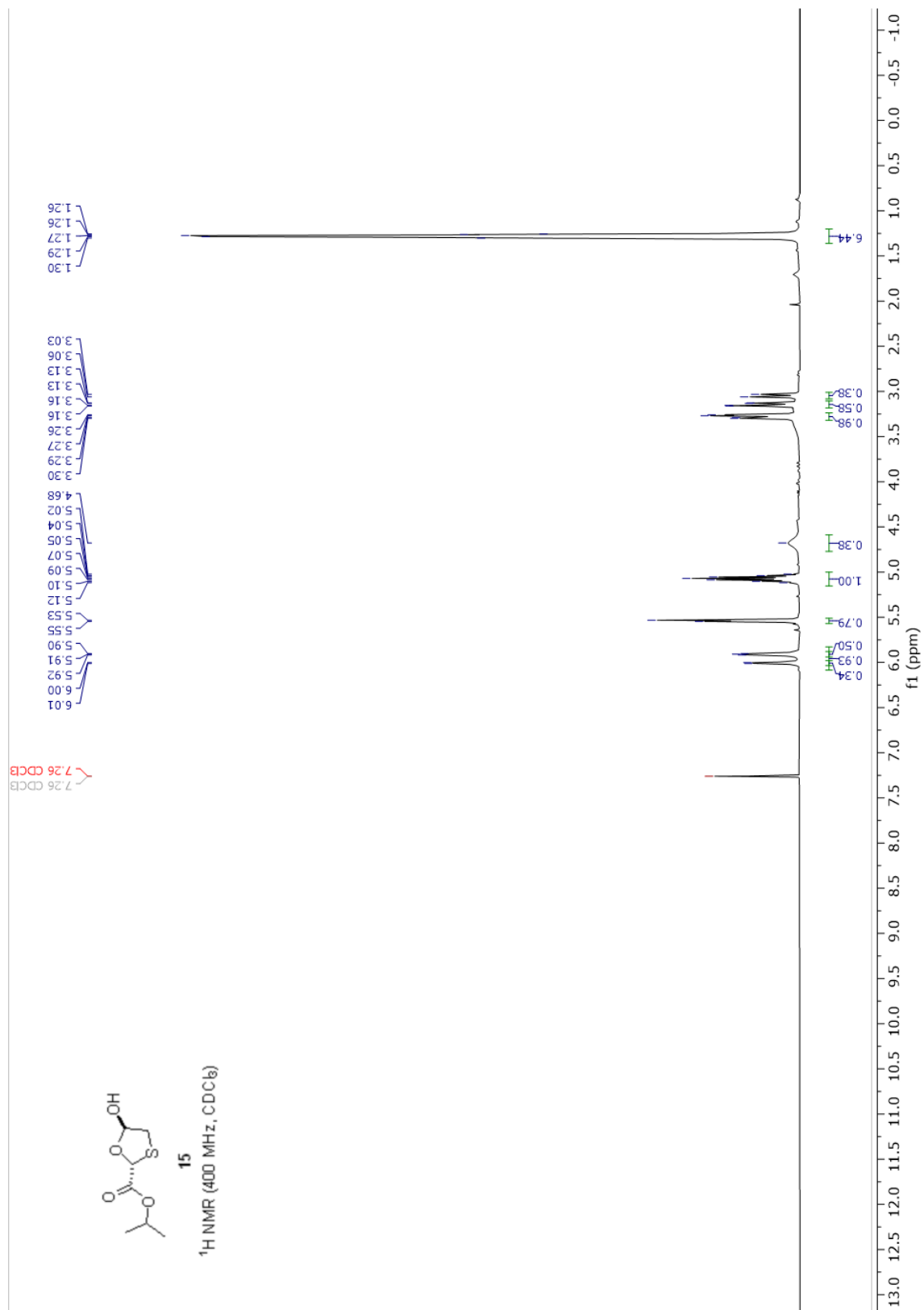


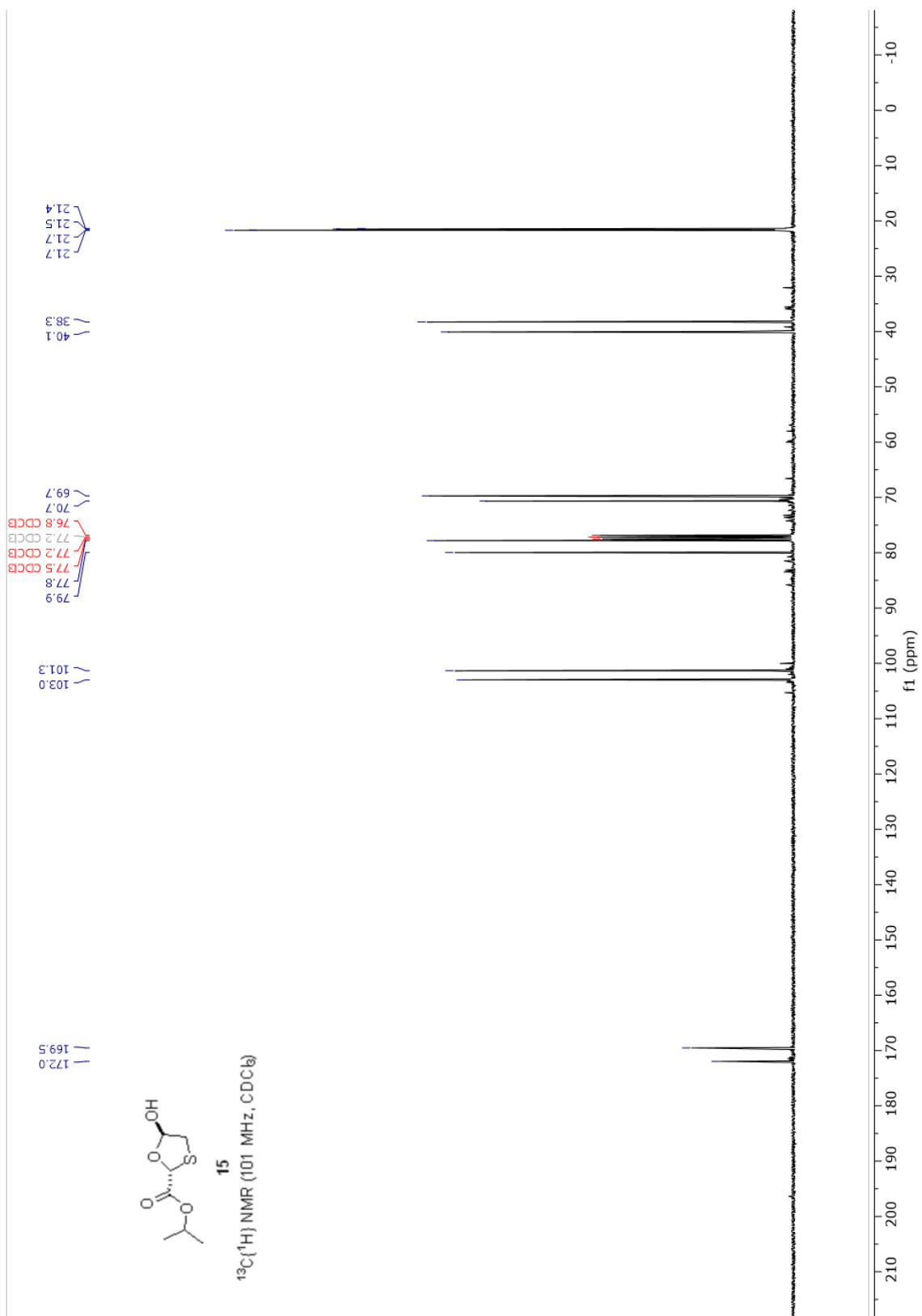


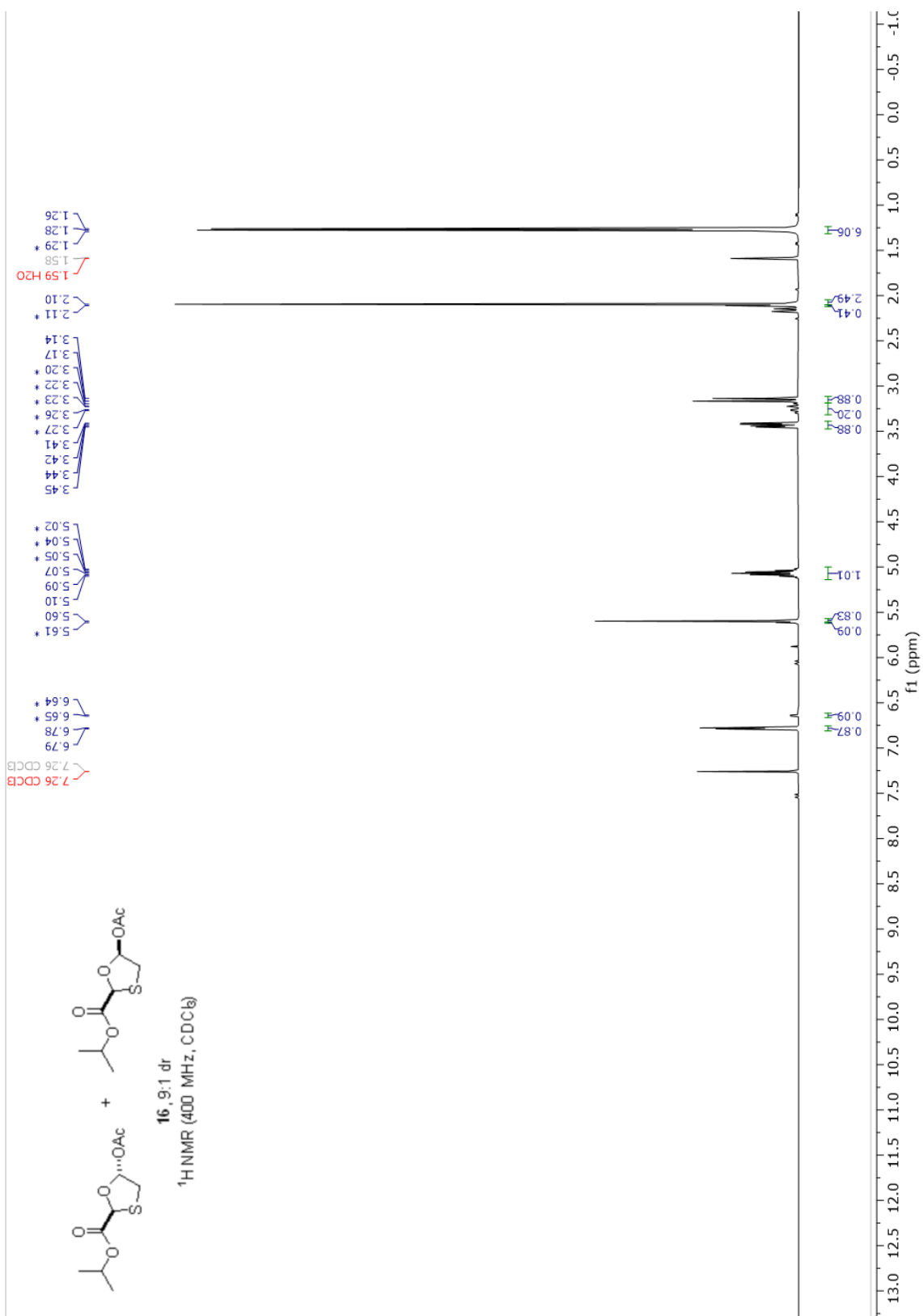


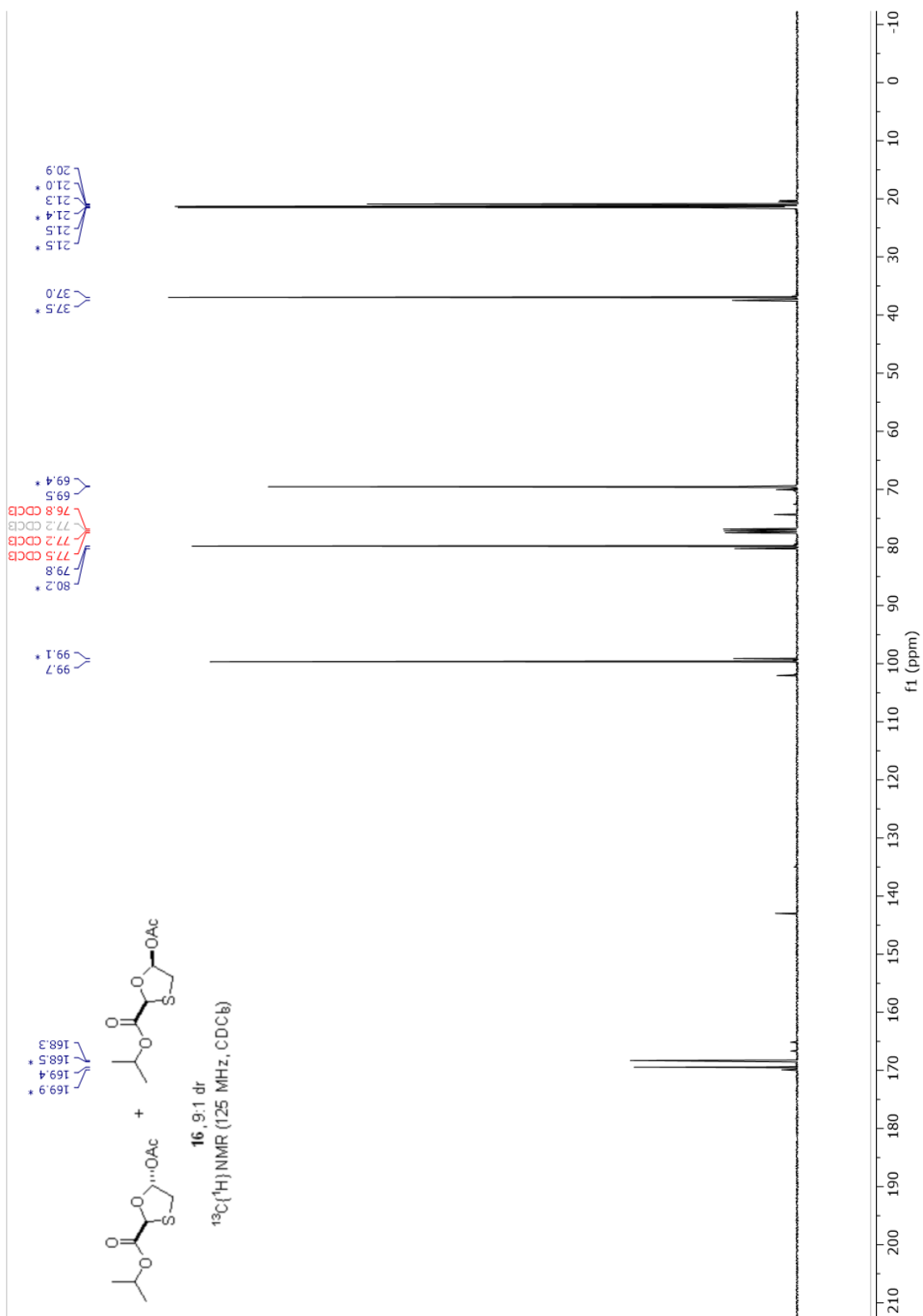


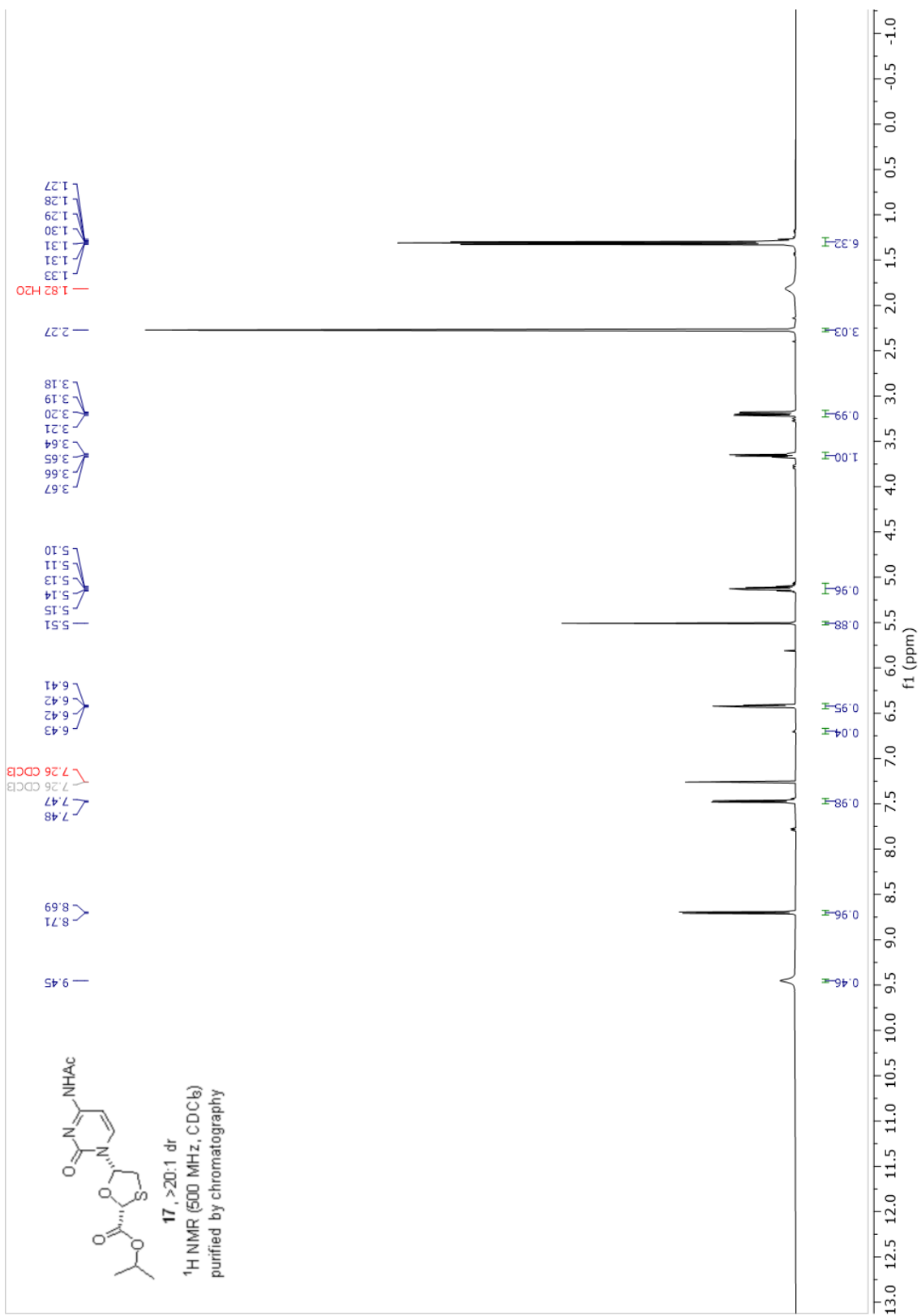


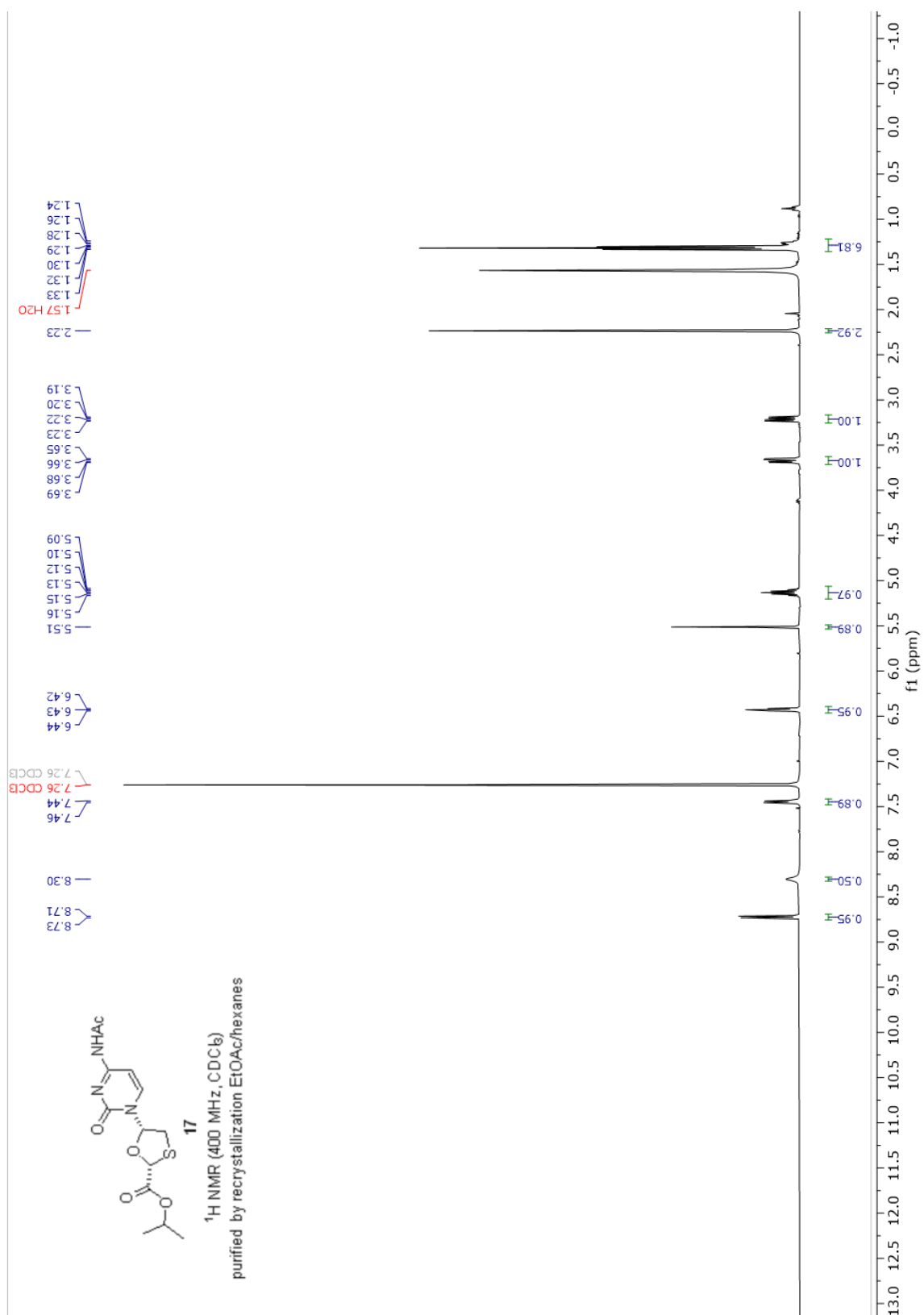


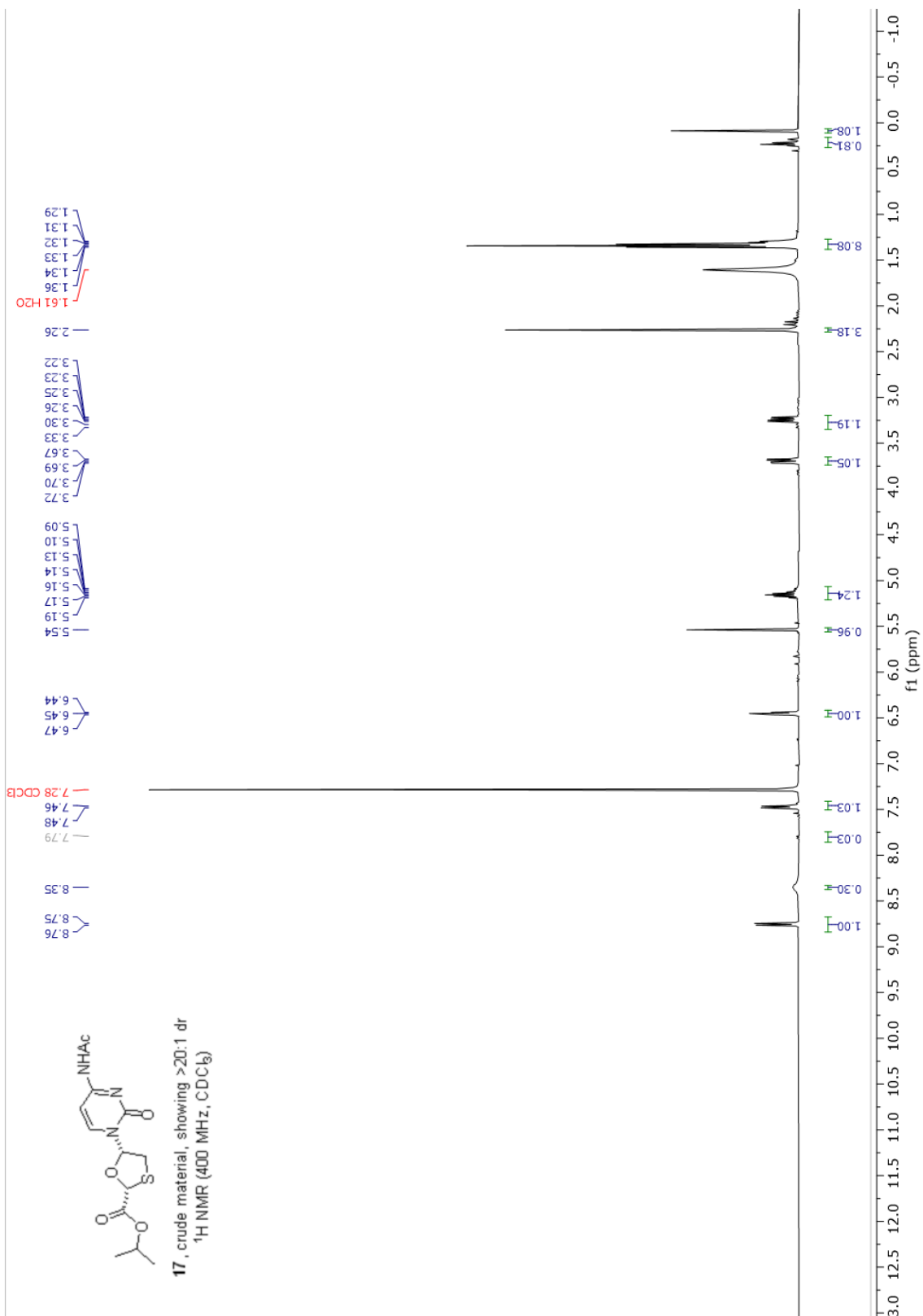


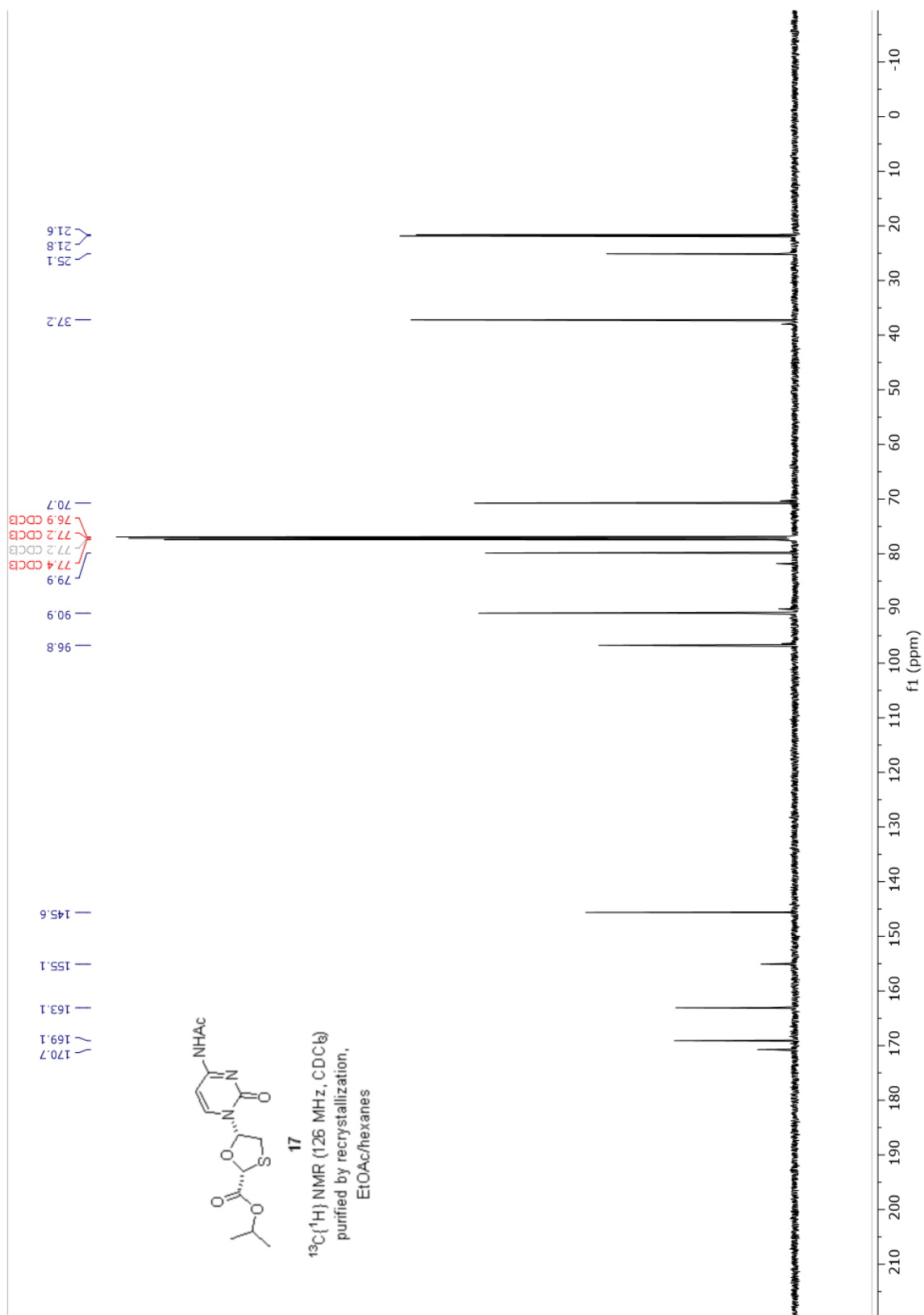


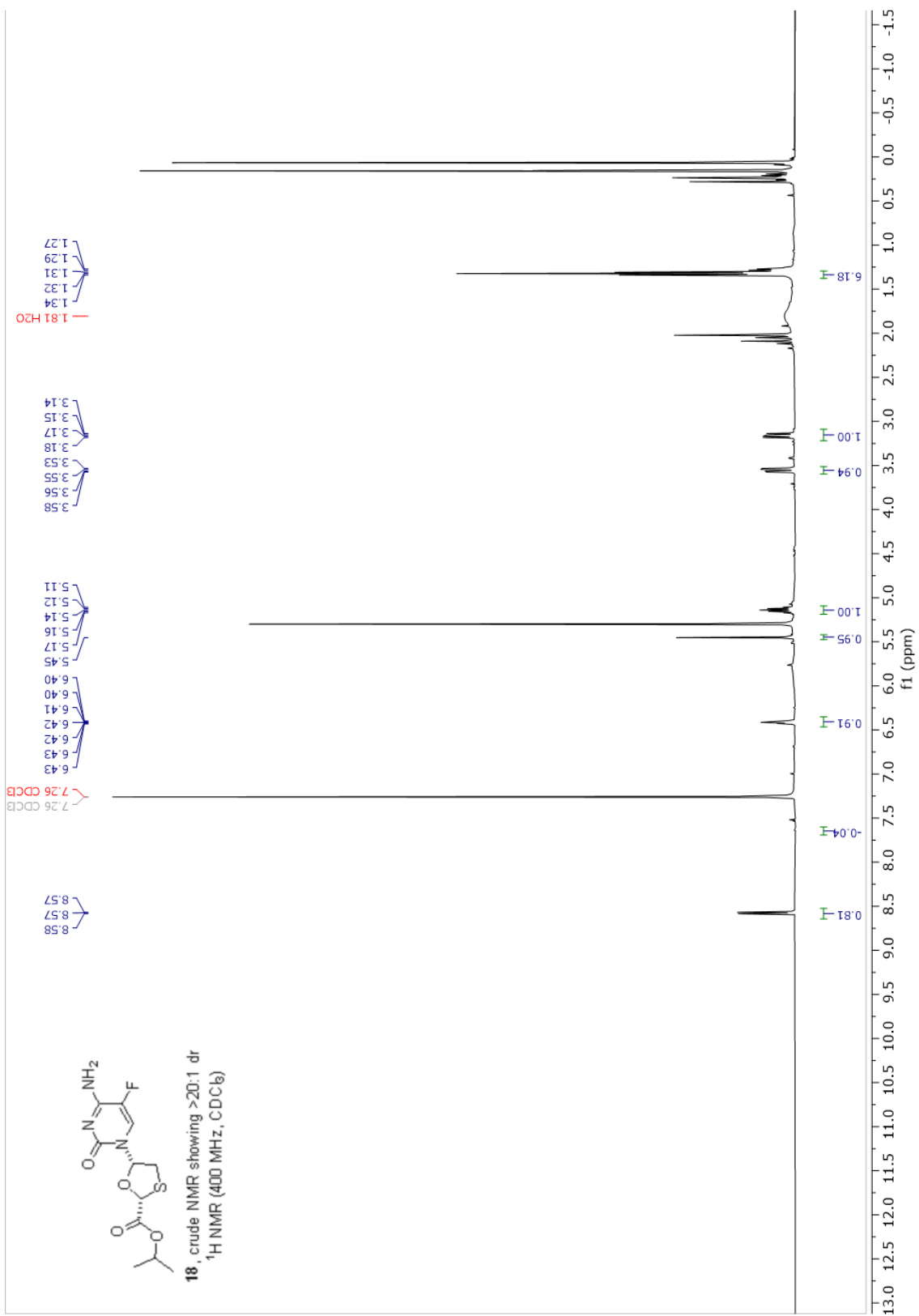


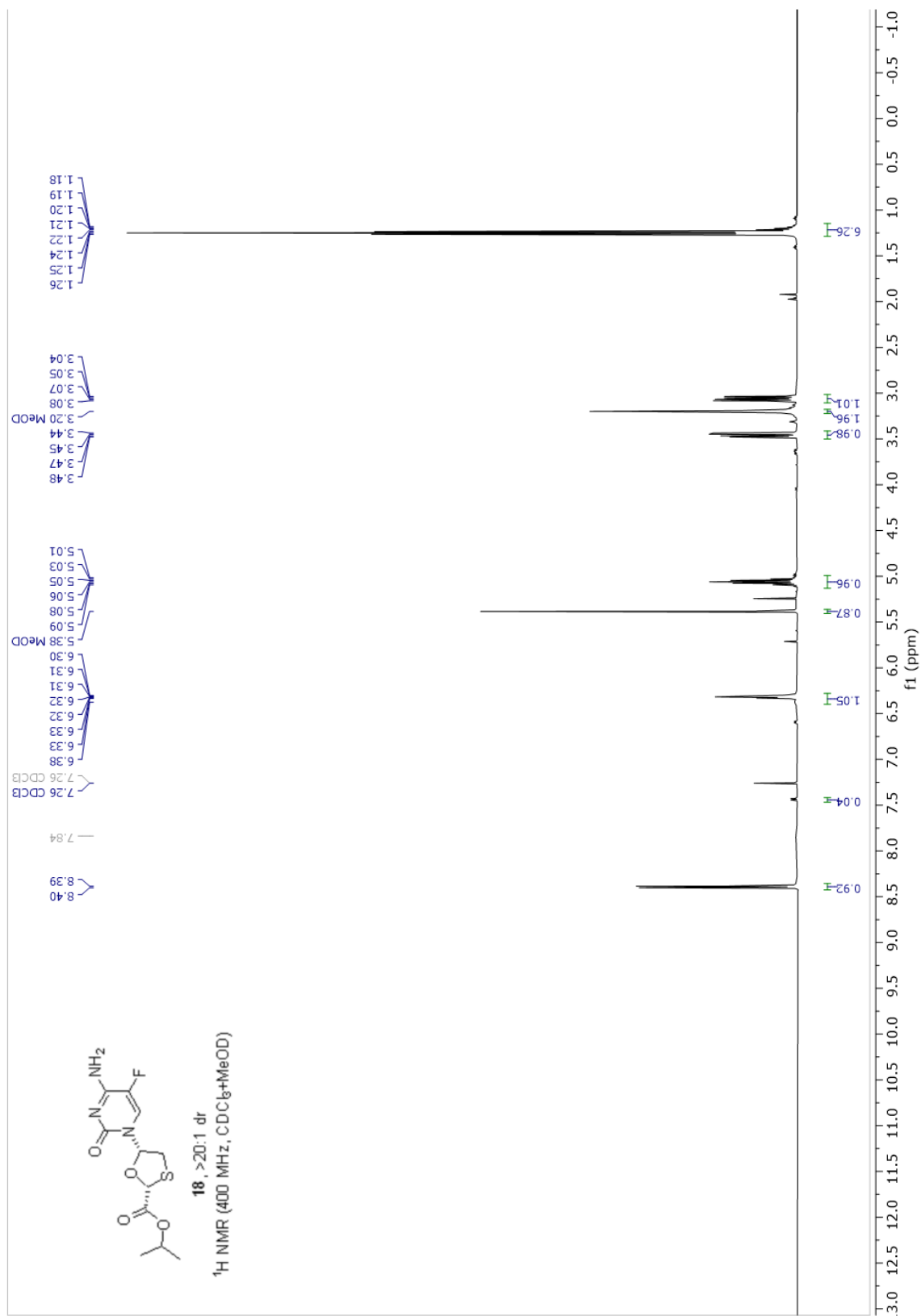


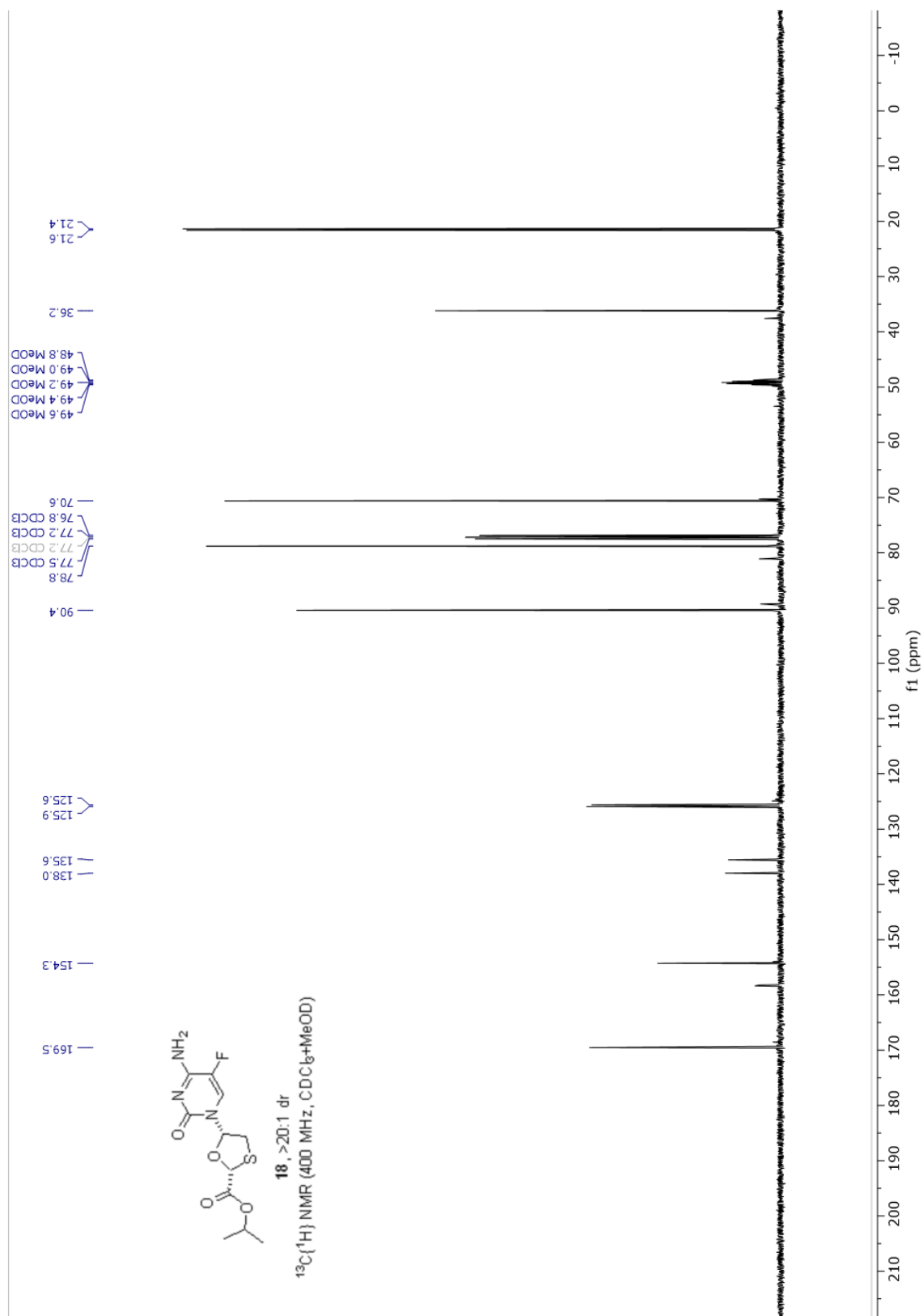


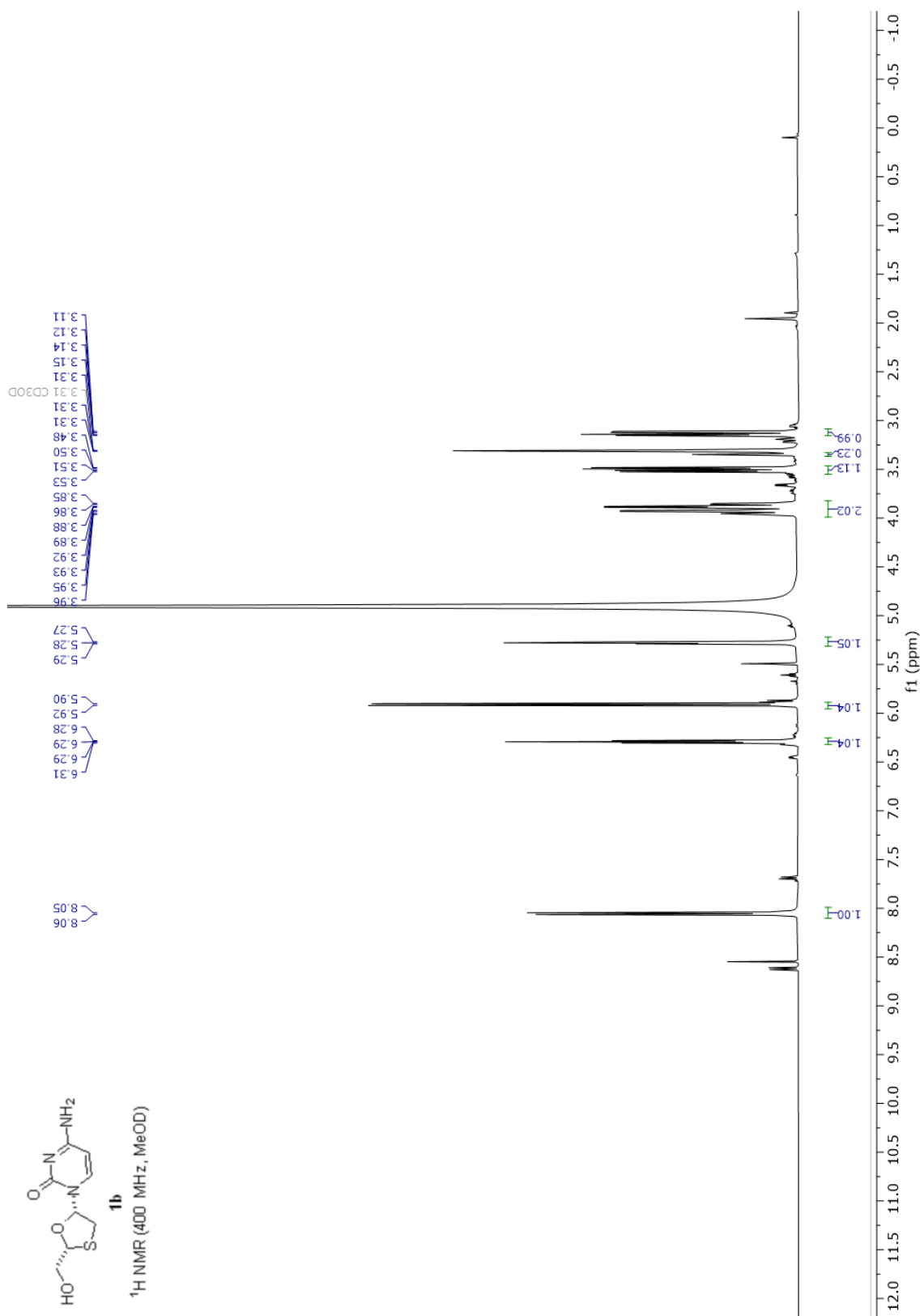


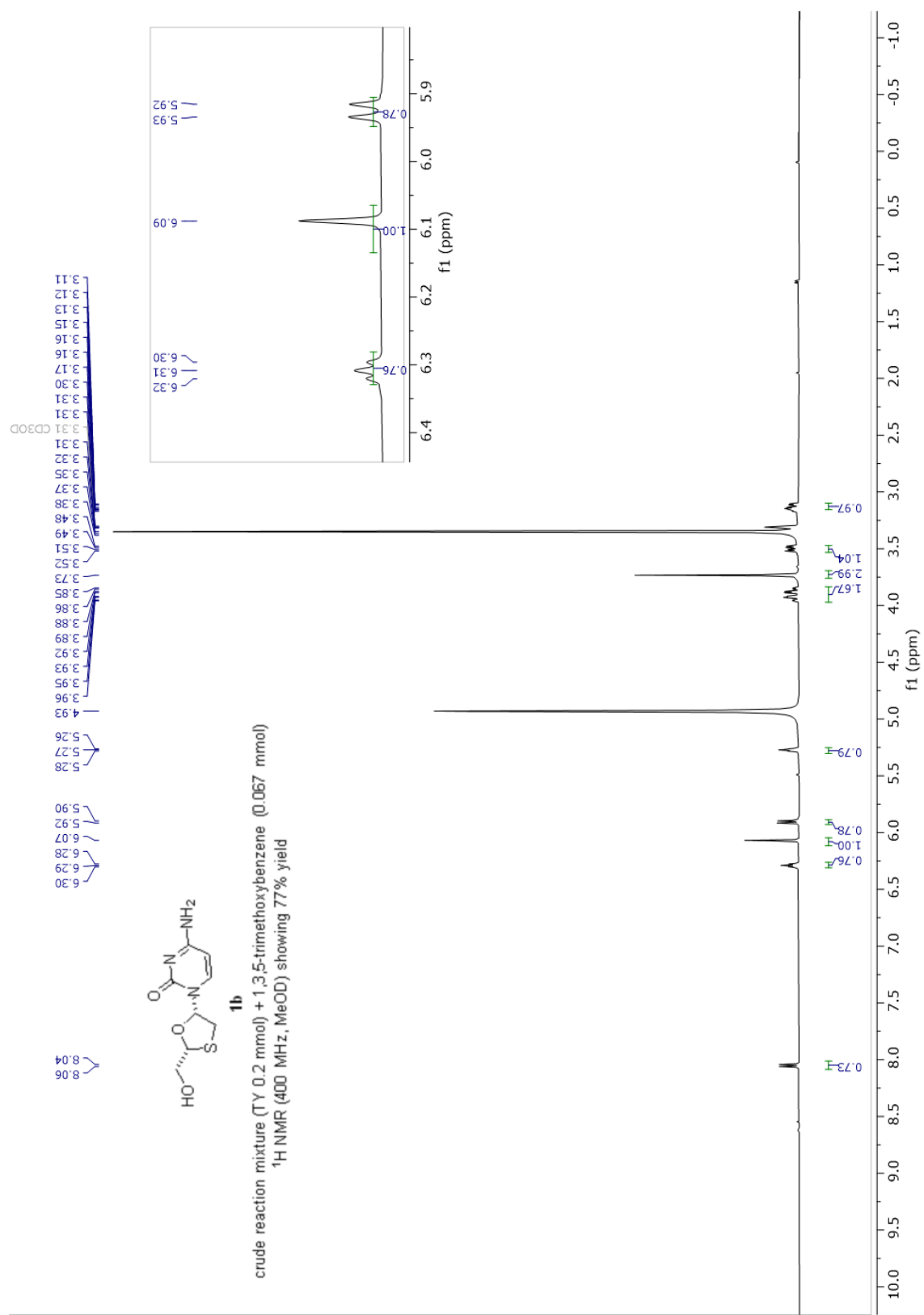


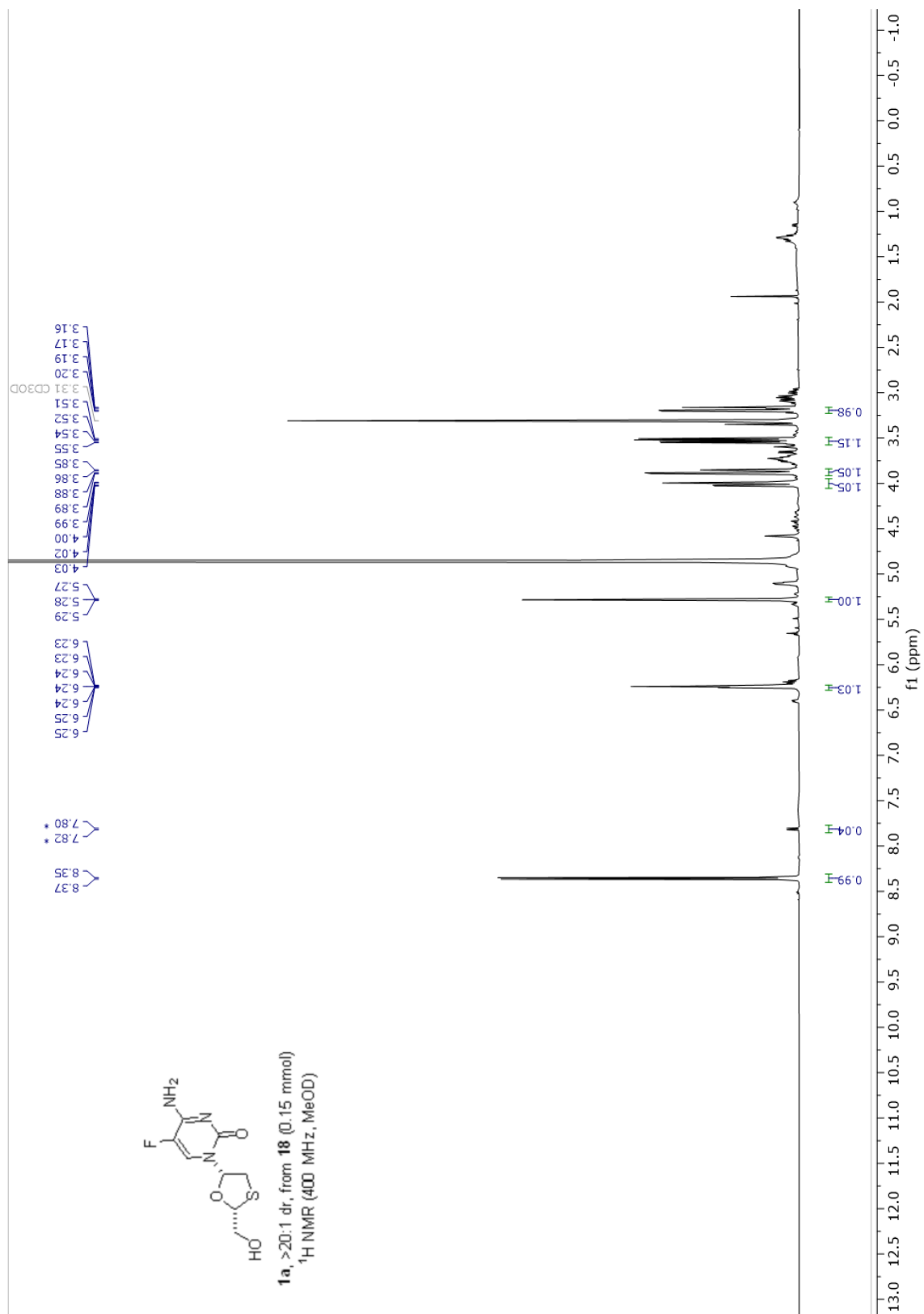


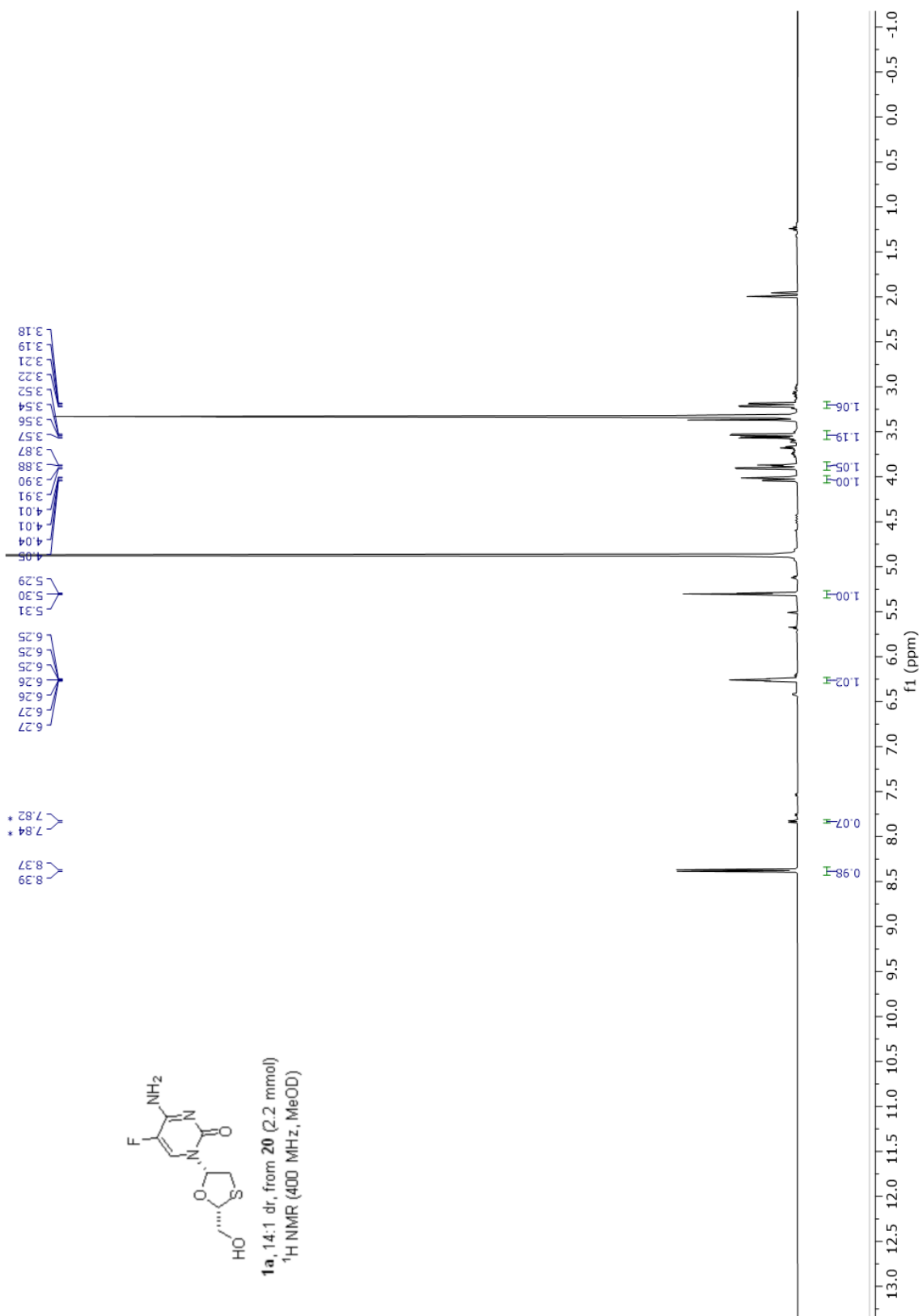


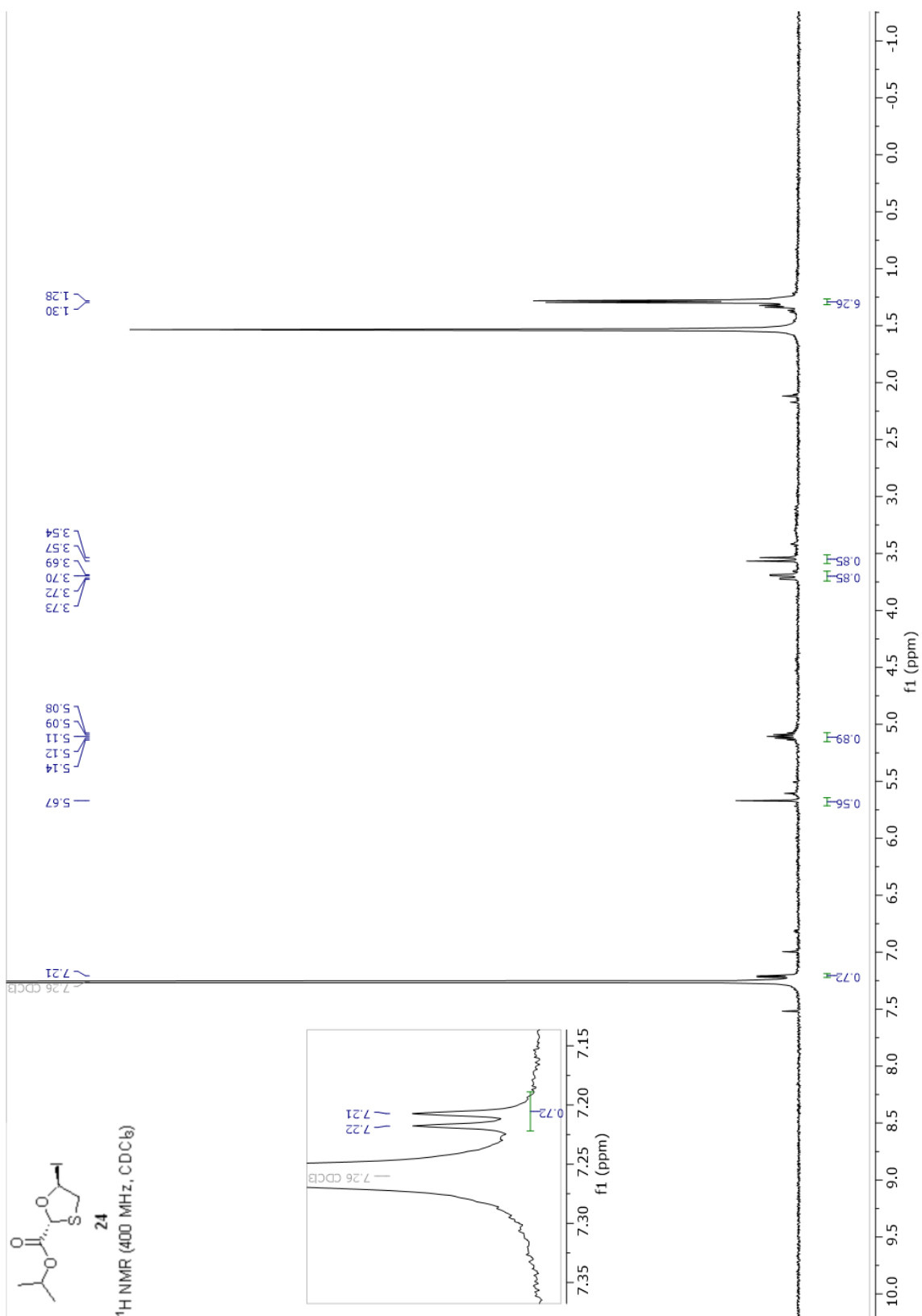












2.6 References

- [1] Liotta, D. C.; Painter, G. R. *Acc. Chem. Res.* **2016**, *49*, 2091–2098.
- [2] Akhtar, R.; Yousaf, M.; Zahoor, A. F.; Naqvi, S. A. R.; Abbas, N. *Phosphorus Sulfur* **2017**, *192*, 989–1001.
- [3] Goodyear, M. D.; Hill, M. L.; West, J. P.; Whitehead, A. J. *Tetrahedron Lett.* **2005**, *46*, 8535–8538.
- [4] Snead, D. R.; McQuade, D. T.; Ahmad, S.; Krack, R.; Stringham, R. W.; Burns, J. M.; Abdiaj, I.; Gopalsamuthiram, V.; Nelson, R. C.; Gupton, B. F. *Org. Proc. Res. Dev.* **2020**, *24*, 1194–1198.
- [5] Milton, J.; Brand, S.; Jones, M. F.; Rayner, C. M. *Tetrahedron Asymmetry* **1995**, *6*, 1903–1906.
- [6] Cousins, R. P. C.; Mahmoudian, M.; Youds, P. M. *Tetrahedron Asymmetry* **1995**, *6*, 393–396.
- [7] Hoong, L. K.; Strange, L. E.; Liotta, D. C.; Koszalka, G. W.; Burns, C. L.; Schinazi, R. F. *J. Org. Chem.* **1992**, *57*, 5563–5565.
- [8] Mahmoudian, M.; Baines, B. S.; Drake, C. S.; Hale, R. S.; Jones, P.; Piercey, J. E.; Montgomery, D. S.; Purvis, I. J.; Storer, R.; Dawson, M. J.; Lawrence, G. C. *Enzyme and Microb. Technol.* **1993**, *15*, 749–755.
- [9] Humber, D. C.; Jones, M. F.; Payne, J. J.; Ramsay, M. V. J.; Zacharie, B.; Jin, H.; Siddiqui, A.; Evans, C. A.; Tse, H. L. A.; Mansour, T. S. *Tetrahedron Lett.* **1992**, *33*, 4625–4628.
- [10] Shen, B.; Bedore, M. W.; Sniady, A.; Jamison, T. F. *ChemComm.* **2012**, *48*, 7444–7446.
- [11] Jin, H.; Siddiqui, M. A.; Evans, C. A.; Tse, H. L. A.; Mansour, T. S.; Goodyear, M. D.; Ravenscroft, P.; Beels, C. D. *J. Org. Chem.* **1995**, *60*, 2621–2623.
- [12] Jeong, L. S.; Schinazi, R. F.; Beach, J. W.; Kim, H. O.; Nampalli, S.; Shanmuganathan, K.; Alves, A. J.; McMillan, A.; Chu, C. K.; Mathis, R. *J. Med. Chem.* **1993**, *36*, 181–195.
- [13] Li, J.-Z.; Gao, L.-X.; Ding, M.-X. *Synth. Commun.* **2002**, *32*, 2355–2359.
- [14] Reddy, B. P.; Reddy, K. R.; Reddy, R. R.; Reddy, D. M.; Srinivas, A. S. Optical Resolution of Substituted 1,3-Oxathiolane Nucleosides. US 0245497 A1, 2011.
- [15] Coates, J. A. V.; Mutton, I. M.; Penn, C. R.; Storer, R.; Williamson, C. 1,3-Oxathiolane Nucleoside Analogs. WO 017159 A1, 1991.

- [16] Liotta, D. C.; Schinazi, R. F.; Choi, W.-B. Antiviral Activity and Resolution of 2-Hydroxymethyl-5-(5-fluorocytosine-1-yl)-1,3-oxathiolane. WO 014743 A2, 1992.
- [17] Caso, M. F.; D'Alonzo, D.; D'Errico, S.; Palumbo, G.; Guaragna, A. *Org. Lett.* **2015**, *17*, 2626–2629.
- [18] Morita, T.; Okamoto, Y.; Sakurai, H. *J. Chem. Soc., Chem. Commun.* **1978**, 874–875.
- [19] Goodyear, M. D.; Dwyer, P. O.; Hill, M. L.; Whitehead, A. J.; Hornby, R.; Hallett, P. Process for the Diastereoselective Synthesis of Nucleoside Analogues. US 6051709 A, 2000.
- [20] Hu, L.; Schaufelberger, F.; Zhang, Y.; Ramström, O. *ChemComm.* **2013**, *49*, 10376–10378.
- [21] Mukaiyama, T.; Hirano, N.; Nishida, M.; Uchiro, H. *Chem. Lett.* **1996**, *25*, 99–100.
- [22] Mata, G.; Luedtke, N. W. *J. Org. Chem.* **2012**, *77*, 9006–9017.
- [23] During our investigations, the commercially available ethyl glyoxylate (50% solution in toluene) was discontinued. The glyoxylate ester was prepared instead by diol cleavage of readily available diisopropyl tartrate.
- [24] Liu, T.; Tang, J.; Liang, J.; Chen, Y.; Wang, X.; Shen, J.; Zhao, D.; Xiong, B.; Cen, J.-D.; Chen, Y.-L. *Tetrahedron* **2019**, *75*, 1203–1213.
- [25] Gannedi, V.; Ali, A.; Singh, P. P.; Vishwakarma, R. A. *J. Org. Chem.* **2020**, *85*, 7757–7771.
- [26] Harbeson, S. L.; Masse, C. E. Hydroxyethylamino Sulfonamide Derivatives. WO 2010047819 A1, 2010.
- [27] Föger, F. Pharmaceutical Formulations for the Oral Delivery of Peptide or Protein Drugs. PCT/EP 073196, 2016.
- [28] Singh, G. P.; Srivastava, D.; Satya, S. A.; Saini, M. B.; Jadhav, H. S.; Warriar, A. M.; Dumre, N. B. Process for the Manufacture of Cis(-)-Lamivudine. US 0257396 A1, 2011.

Chapter 3

Diastereoselectivity is in the Details: Minor Changes Yield Major Improvements to the Synthesis of Bedaquiline

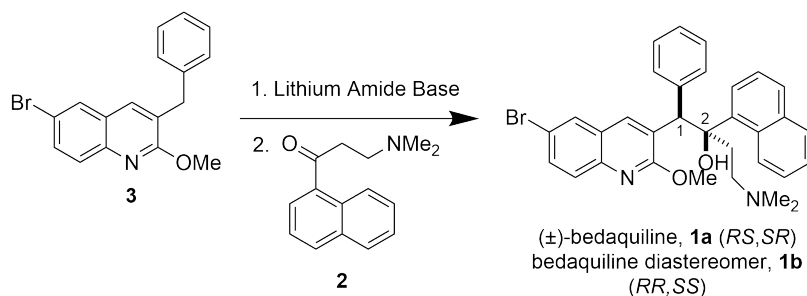
This chapter describes results of a collaboration with the Medicines for All Institute (M4All), including the following contributing institutions: Massachusetts Institute of Technology (MIT, Jamison Group), Johannes Gutenberg University Mainz (JGU Mainz, Opatz Group), Virginia Commonwealth University (VCU, M4All). Individual contributions are described in the Abstract.

3.1 Introduction

Tuberculosis (TB) is the result of infection by the bacillus *Mycobacterium tuberculosis* and is a leading cause of death worldwide despite the fact that it is typically curable.^{1,2} Moreover, nearly one quarter of the global population has a latent TB infection.² The COVID-19 pandemic has hindered diagnosis and treatment of TB, leading to an increase in TB deaths in 2020, reversing several years of progress.² That the proportion of new cases of TB due to multi-drug-resistant TB (MDR-TB) has been

increasing with time further exacerbates this global health crisis. Reducing global TB burden requires a multifaceted approach, as many societal factors such as the prevalence of poverty and general access to healthcare in a country strongly influence its TB infection and mortality rate. The high price of a full TB drug regimen, particularly for MDR-TB, remains a major factor limiting access to care.³

Bedaquiline (BDQ, fumarate adduct sold under the trade name Sirturo[®]), Figure 3-1) is an effective treatment for MDR-TB that received FDA approval in 2012 as the first TB drug with a novel mode of action approved in over forty years.⁴ BDQ inhibits mycobacterial ATP synthase, which differentiates it from first-line therapeutic drugs that disrupt the cell membrane or protein synthesis, to which *M. tuberculosis* commonly develops resistance.⁵ A key structural feature of BDQ is its two vicinal tertiary stereocenters (Figure 3-1). Of the four possible stereoisomers, BDQ represents the (1*R*,2*S*)- or *RS*-enantiomer. According to publicly-available information in patent applications and the scientific literature, the industrially-relevant construction of these stereocenters is accomplished via a 1,2-addition reaction between quinoline fragment **3** and naphthyl ketone **2**.^{4,6-8} This reaction is facilitated by an initial deprotonation of **3** with an amide base, typically lithium diisopropylamide (LDA). A series of crystallization and chiral resolution steps are then applied to access the *RS*-enantiomer as the penultimate intermediate to the API, which is administered as the fumarate salt.⁸ A prerequisite to improving global access to life-saving medications like BDQ is the development of an efficient manufacturing process. Despite significant industrial interest in this reaction, patented procedures remain low-yielding and unselective for the desired diastereomer **1a** (Table 3.1). Chiral amine bases or additives can improve selectivity, but their implementation on scale may be hampered by reagent costs.^{9,10} Alternative disconnections and enantioselective routes to BDQ have also been reported, but feature low yields and/or high reagent costs that restrict their industrial application.^{11,12} Thus, as a first step towards delivery of an improved synthesis of BDQ, we sought to understand key variables influencing the yield and diastereoselectivity of the critical coupling reaction used in the industrial process. We focused on increasing the yield of **1a**, rather than altering the synthesis entirely, to



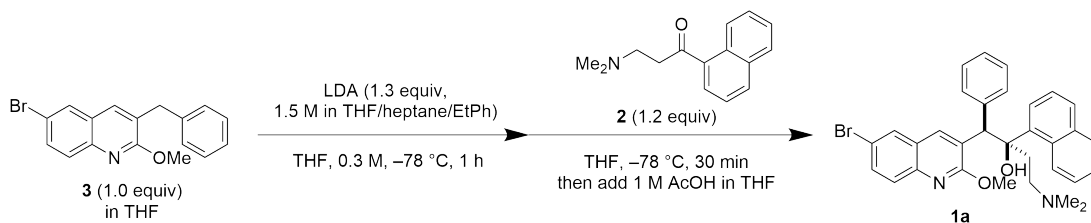
Source	Lithium Amide Base	Additive	IY 1a ^a
Janssen 2006 ⁶	lithium diisopropylamide	None	32%
SIPI 2017 ⁷	lithium diisopropylamide	None	34%
Mylan 2020 ⁸	lithium diisopropylamide	None	23%
Mylan 2020 ⁸	lithium pyrrolidide	None	14%
This work	lithium morpholide	LiBr	61%
	lithium <i>N</i>-methylpiperazide	LiBr	60%
	lithium pyrrolidide	LiBr	56–58%

^a IY = isolated yield, adjusted for purity where reported

Table 3.1: Selected examples of synthesis of **1** reported in process patent applications and improvements described herein.

different operators using the same reagents and seemingly following the same procedure. This situation is familiar to most chemists and supports the recent focus of the broader scientific community,^{15,16} as well as organic chemists in particular,¹⁷ on the importance of reproducibility for high-quality and impactful research. Similarly, we found that our observations were due to incomplete understanding of the key variables that affect reaction outcome.

Following literature precedent, the standard protocol is to prepare **1** by first adding LDA to a stirring solution of **3** at $-78\text{ }^{\circ}\text{C}$, followed by addition of **2** as a room-temperature solution in THF, and finally quenching with an aqueous solution of ammonium chloride (Table 3.2, entry 1). Close examination of the experimental procedure found that the largest variance in yield resulted from unintentional warming of the reaction during normal experimental operations such as reagent addition, removal of an aliquot for analysis, or reaction quenching. To probe the detrimental effect of higher reaction temperatures on the yield of **1**, we warmed the reaction to $-40\text{ }^{\circ}\text{C}$ or $-20\text{ }^{\circ}\text{C}$ after addition of **2** and observed no product formation in either case (Section 3.4.4), compared to 35% yield when the reaction was performed at $-78\text{ }^{\circ}\text{C}$.



Entry	Deviation from Scheme	AY (%) ^a 1 (d.r.) ^b	AY (%) ^a 1a
1	rapid quench NH_4Cl (aq)	35 (0.9: 1.0)	17
2	none (quench AcOH)	53 (1.0:1.0)	26
3	Add 3 to LDA	45 (1.0 : 1.0)	22
4	LDA (0.9 equiv), quench NH_4Cl	32 (1.0 : 1.0)	16
5	CeCl_3 (1.0 equiv) + LDA, then add 3	42 (1.2:1.0)	23
6	remove aliquot for analysis	0	0

^a AY = Assay yield determined by ^1H NMR using benzyl benzoate as internal standard

^b AY **1a** : AY **1b**

Table 3.2: Initial assessment of lithiation/1,2-addition reaction parameters indicating the importance of reagent addition and temperature control. See experimental method in Section 3.4.3

Additionally, warming to room temperature and re-cooling to $-78\text{ }^{\circ}\text{C}$ resulted in 0% yield of **1**.

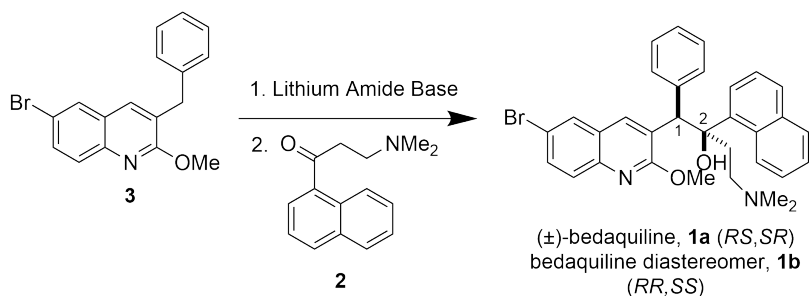
We hypothesized that careful control of reaction temperature during reagent addition and quench would lead to more reproducible results across our research sites. Reversing the order of addition by cannulating the cold reaction mixture containing the lithium salt of **3** after LDA addition into a pre-cooled solution of ketone **2** was effective for the synthesis, but this option was not investigated further as it increased operational complexity without significant improvement in yield of **1**. To avoid increase in reaction temperature during the quench, rapid addition of pre-cooled AcOH solution instead of room temperature NH_4Cl (aq) was explored (Table 3.2, entry 2). This improved yield (53% of **1** vs. 35% with NH_4Cl); however, this method of quenching was problematic for isolation due to formation of insoluble precipitates, presumably the acetate salt of **1**. Altering order of addition in the first step by adding a solution of **3** to LDA led to lower yield (45% of **1**, Table 3.2, entry 3). Due to the enolizable nature of ketone **2**, we explored use of substoichiometric LDA (0.9 equiv), to avoid enolization of **2** by excess LDA remaining after step **1** (Table 3.2, entry 4). Contrary to our hypothesis, lower yield of **1** was obtained (32%). Cerium trichloride

was added to the reaction based on precedent for improvement of 1,2-additions to enolizable ketones (Table 3.2, entry 5). While a slightly higher d.r. was observed (1.2:1.0), the yield was not improved. Importantly, when an aliquot of the reaction mixture was removed for analysis and quenched off-line, no yield of **1** was observed (Table 3.2, entry 6).

We found that variations in reagent quality, most notably LDA, also led to challenges with reproducibility. As has been widely reported, variations in commercial LDA solutions can lead to confounding and irreproducible results.^{14,18} Across our three research sites (MIT, JGU-Mainz, VCU), a variety of commercial LDA solutions were used with varying success, which we attributed in part to differences in the purchased reagents. Freshly prepared LDA, formed by addition of *n*-BuLi to a solution of diisopropylamine in THF, was therefore key to achieving reproducible results, as was thorough drying of all reactants and regular titration of the *n*-BuLi solution.¹⁹ These changes were crucial to achieving high conversion of **3** and clean, reproducible 1,2-addition using a low excess of electrophile **2**.

Preparation of ketone **2** from the commercially supplied HCl salt required attention in our early optimization efforts (Section 3.4.2). Synthesis of the free base by treatment of the HCl salt with aqueous NaOH or NaHCO₃ led to formation of elimination product **6** if extended reaction times were used, or if the sample was heated during solvent removal (Figure 3-2).

With more awareness of these reproducibility challenges, we implemented a “unified procedure” (Section 3.4.5) that represented our baseline of reactivity from which to optimize. This procedure minimized variability across our research sites by specifying techniques for material transfer and moisture and temperature control. Once this procedure was cemented, we achieved improved reproducibility across operators at three institutions (MIT, JGU-Mainz, VCU; 19–25% yield of **1a**, 41–52% yield of **1**) (Table 3.3).



Entry	Operator, Institution*	Scale of 3	AY (%) ^a 1a	AY (%) 1 (d.r.) ^b
1	A, MIT	200 mg	20	41 (1.0 : 1.1)
2	B, JGU Mainz	50 mg	25	52 (1.0 : 1.1)
3	C, VCU	200 mg	19	46 (1.0 : 1.3)

* JGU = Johannes Gutenberg University Mainz, Department of Chemistry, Opatz Group

* VCU = Virginia Commonwealth University, M4All

^a Assay yield determined by ¹H NMR using internal standard

^b AY **1a** : AY **1b**

Table 3.3: Results of “unified procedure” by different operators at different institutions involved with this collaboration: MIT (Jamison Group), JGU Mainz (Opatz Group), VCU (M4All). Experimental method described in Section 3.4.5.

3.2.1 Mechanistic Investigation of the Lithiation/1,2-Addition

An early focus on reproducibility informed our understanding of the reaction mechanism and ultimately, our optimization of the reaction conditions. We investigated the mechanism of this lithiation/1,2-addition sequence with the goal of understanding how step 1 and step 2 individually contribute to yield of **1** in this two-step sequence. In a series of experiments described below, we demonstrate that conversion of **3** and selectivity for the desired deprotonation event in step 1 is low, and that the 1,2-addition step is reversible. Importantly, we identified that the temperature and nature of the lithium amide base are key factors in determining the reaction outcome (Figure 3-2).

Initially we sought to rationalize the low (20–50%) yield of this two-step sequence using LDA as base. Performing step 1 followed by workup and ¹H NMR analysis of the crude reaction mixture, we observed low recovery of **3** (81%), corresponding to undesired reactivity of **3** with LDA (Figure 3-3). We identified the debrominated species **5** as an undesired product, suggesting that lithium-halogen exchange occurs

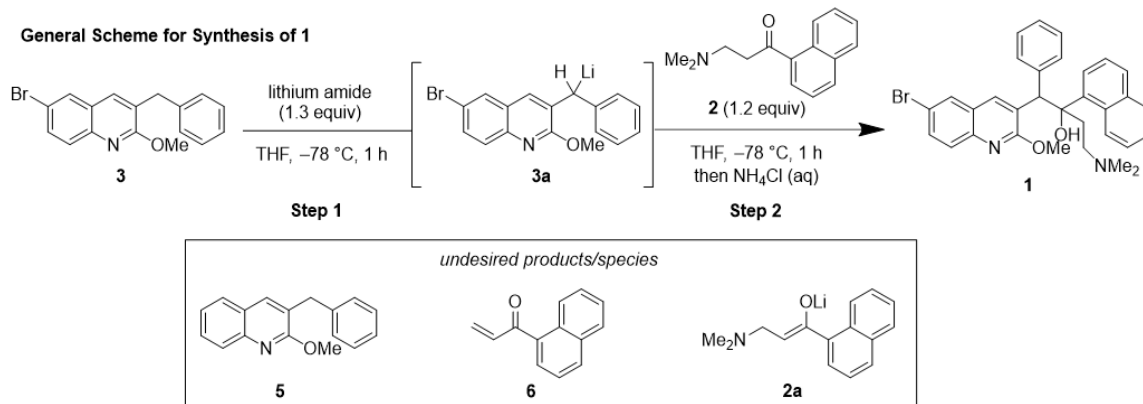


Figure 3-2: General reaction scheme for synthesis of **1** used in mechanistic investigations; undesired products or species observed or formed under reaction conditions.

competitively with benzylic deprotonation.

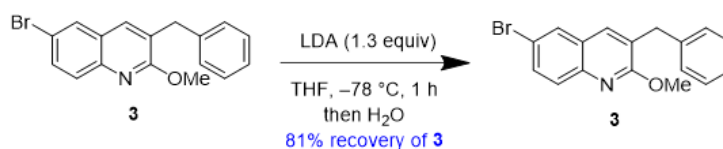


Figure 3-3: Investigation of recovery of **3** after deprotonation with LDA and aqueous workup. See experimental procedure in Section 3.4.6.

We then directly assayed deprotonation by observing a mixture of **3** and LDA by ¹H NMR at -78 °C and identified resonances corresponding to intermediate **3a** (Figure 3-4 and Figure 3-5). Formation of **3a** occurred within minutes, albeit with low conversion of **3** (see Section 3.4.9); we were surprised to observe unreacted LDA in the presence of **3** after 15 minutes. In a second trial (see Section 3.4.10), the spectrometer was cooled to -61 °C and only 7% **3a** was observed within 10 min with 32% consumption of **3** (Figure 3-7). After warming to room temperature inside of the spectrometer over 40 min, consumption of **3** increased to 58%, while formation of **3a** only increased to 11%, suggesting undesired reactivity of **3** with LDA. We rationalized that the deprotonation of **3** by LDA is incomplete due to the steric bulk of LDA.

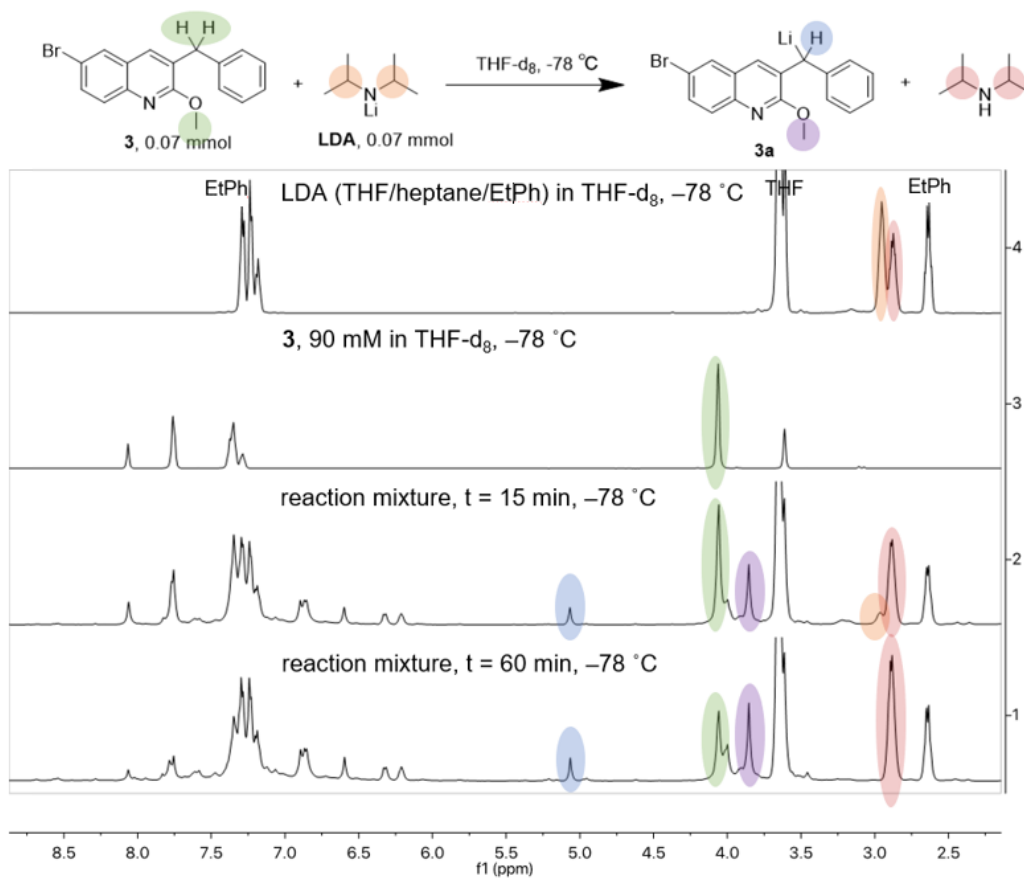


Figure 3-4: ^1H NMR spectra showing observation of **3a** at $-78\text{ }^\circ\text{C}$ and corresponding peak assignments.

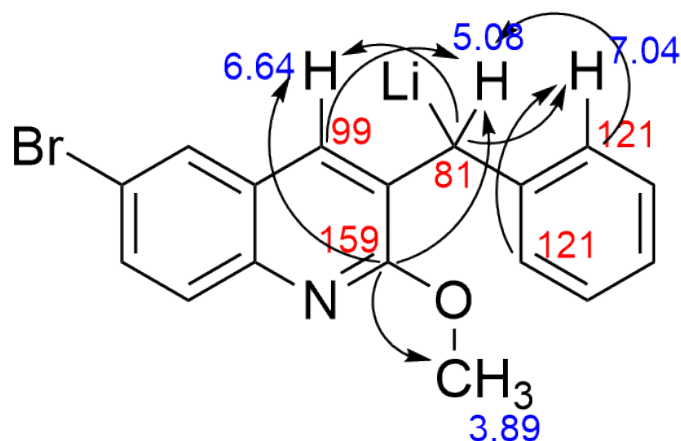


Figure 3-5: ^1H - ^{13}C HMBC correlations with arrows illustrating observed correlations between ^1H (blue) and ^{13}C (red) resonances.

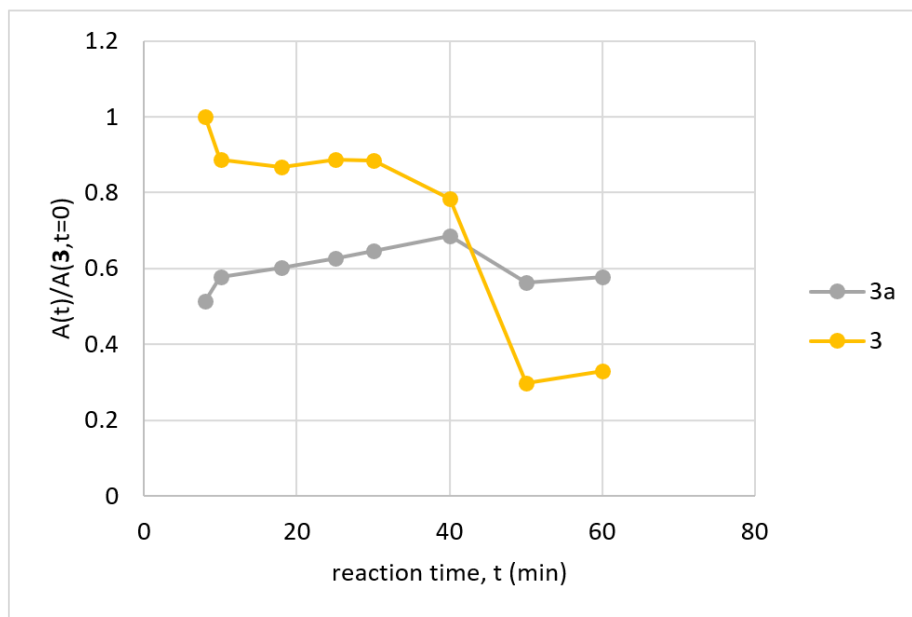


Figure 3-6: Illustration of ^1H NMR assay of time course of lithiation at $-78\text{ }^\circ\text{C}$. Presence of **3** and **3a** measured by integration of ^1H NMR resonance at 8.04 ppm and 5.08 ppm, respectively, and reported as a ratio of absolute signal of these resonances at each timepoint ($A(t)$) vs. absolute signal of compound **3** at $t = 0$. The PhEt signal at 2.63 ppm was used as an internal standard to calibrate the absolute signal observed in each experiment. Note that a relaxation delay of 1 s was used in these ^1H NMR experiments, thus calculated values are approximations and significant error to the calculated values should be assumed.

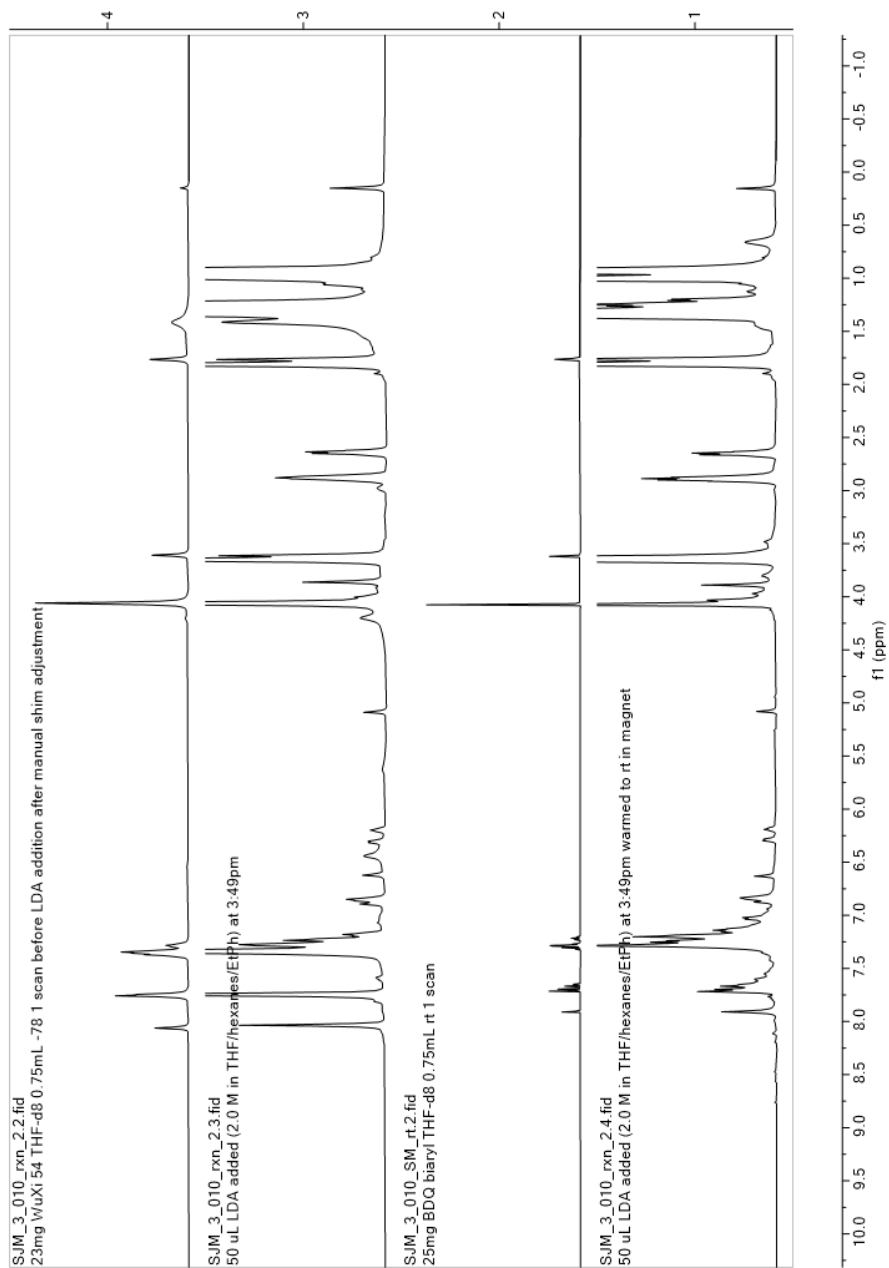


Figure 3-7: ¹H NMR spectra showing observation of **3a** at -61 °C, 10 min postreagent mixing (spectrum 3), and room temperature, 40 min postreagent mixing (spectrum 1), with reference spectra of **3** at -78 °C (spectrum 4) and room temperature (spectrum 2) in THF-d₈. Compound **3** conversion determined by signal at approx. 8–8.2 ppm, corresponding to the C-4 ¹H of quinoline **3**. Formation of **3a** determined by integration of the signal at 5.2 ppm, corresponding to the benzylic position (-CHLi-) of **3a**.

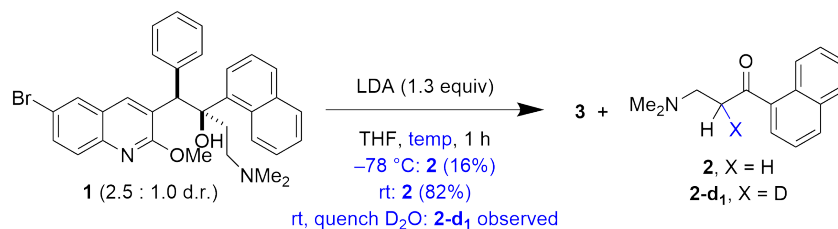


Figure 3-8: Formation of **3** and **2** by treatment of **1** with LDA. For experimental procedure, see Section 3.4.7.

While these observations around step 1 rationalized the yield we observed with our baseline procedure using LDA, we remained perplexed by the detrimental effect of warming during reagent addition and quench for step 2. Initially, we sought to explore the possibility of a reversible sequence by treatment of **1** with LDA (Figure 3-8). We observed formation of starting materials at $-78\text{ }^\circ\text{C}$ (16% of **2**) and at room temperature (82% of **2**), which aligns with observations by Kong and co-workers who demonstrated that **1b** can be recycled into starting materials **2** and **3** under basic conditions.²⁰ Our observations suggest that retroaddition is a major consideration, particularly at higher temperatures. We rationalize the reversibility of this 1,2-addition with the sterically crowded environment and entropic cost of the formation of adjacent tertiary centers in **1**, factors which are exacerbated with temperature increase.

Even with confirmation that reversion of **1** to starting materials can occur at higher temperatures, the observation of 0% yield of **1** after warming and re-cooling the reaction mixture was confounding; in a fully reversible sequence we would expect **1** to re-form upon re-cooling to $-78\text{ }^\circ\text{C}$. A reasonable explanation for this is sequestration of one of the reactants due to undesired reactivity at higher temperatures. After running the reverse reaction at room temperature and quenching with D₂O, we observed formation of deuterated ketone **2-d₁**, suggesting that enolization of ketone **2** occurs under the reaction conditions. We questioned whether **3a** could act not only as a nucleophile but as a base, leading to undesired enolate formation. However, deuterated quinoline **3-d₁** was not observed upon reaction of **3a** with deuterated ketone **2-d₂** at $-78\text{ }^\circ\text{C}$ (Figure 3-9). Therefore, we suspected that deprotonation of ke-

tone **2** occurs primarily by reaction with the lithium amide base or secondary amine, rather than with **3a**. This enolization sequesters **2** from the reaction mixture, limiting formation of **1**.

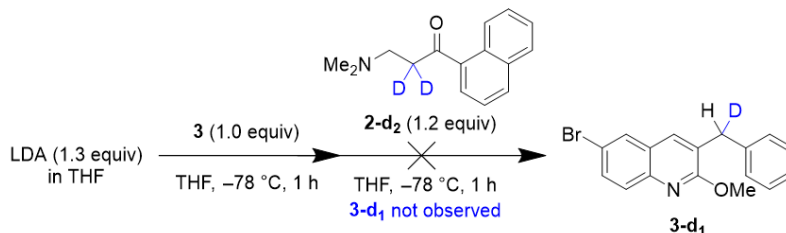


Figure 3-9: Reaction of **3a** with **2-d₂**.

These mechanistic experiments in combination with our early optimization efforts concluded that the reaction of LDA with **3** is unselective and low yielding, and furthermore that the reversibility of step 2 is problematic at higher temperatures. A recent patent reported the use of lithium pyrrolidide as base to minimize formation of impurity **5**, but with a reduced yield of **1a** (14%).⁸ We assayed a mixture of lithium pyrrolidide with **3** by ¹H NMR to determine if altering the nature of the lithium amide base in step 1 could improve conversion of **3** and selectivity for formation of **3a**. We observed 91% formation of **3a**, relative to 22% with LDA under the same conditions (Figure 3-10). This observation suggested that a secondary amine with lower hindrance and higher basicity could provide an opportunity for drastic improvements to the synthesis of bedaquiline (**1**).

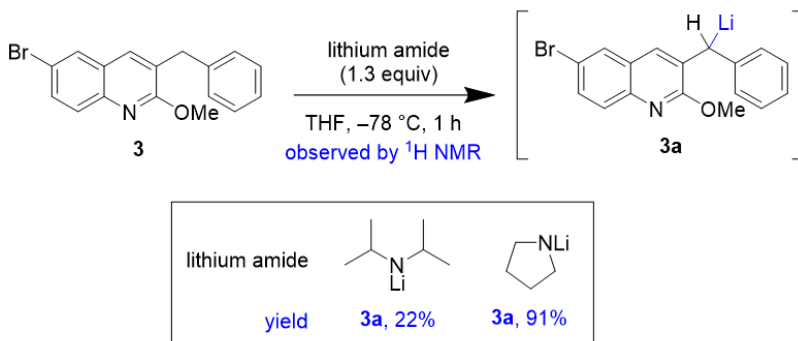


Figure 3-10: Quantification of **3a** formed by addition of **3** to LDA or lithium pyrrolidide. See experimental details in Section 3.4.11.

These mechanistic observations allowed us to further optimize for the synthesis of **1** with improved knowledge of the critical variables influencing its reproducible formation, particularly temperature control and the nature of the lithium amide base.

3.2.2 Optimizing for Maximum Yield of Bedaquiline

The mechanistic investigations described above suggest that altering the nature of the lithium amide base could lead to improved yield of key intermediate **3a**. To investigate whether this observation represented a general trend, we evaluated a series of secondary amine bases which are used in combination with *n*-BuLi to generate lithium amides with varying steric bulk and solubility profiles (Figure 3-11).²¹⁻²⁸ We observed a compelling trend: less sterically hindered bases produce fewer undesired products and likewise, higher recovery of **3** and higher yield of **1**. Bases with high steric bulk such as dicyclohexylamine and 2,2,6,6,-tetramethylpiperidine gave lower overall yields with evidence of debromination, presumably through lithium-halogen exchange with **3**. α -Branched secondary amine bases such as diisopropylamine and 2-methylpyrrolidine generally gave lower yields of 1,2-addition product and lower mass balance of **3** relative to cyclic amines such as piperidine, pyrrolidine, and *N* methylpiperazine which have lower hindrance and higher basicity. In this assay, we formed the lithium amide at $-40\text{ }^{\circ}\text{C}$, followed by warming to room temperature and re-cooling to $-78\text{ }^{\circ}\text{C}$ prior to addition of **3**. The rationale for this temperature variation is based upon precedent which reports an influence of temperature on lithium aggregate formation.⁹ With lithium morpholide, the lithium amide solution turned brown in color upon warming to room temperature, and low yields were observed in the subsequent 1,2-addition, suggesting instability of lithium morpholide at higher temperatures. In subsequent assays, formation of the lithium amide at $0\text{ }^{\circ}\text{C}$ for a shorter time and directly cooling to $-78\text{ }^{\circ}\text{C}$ led to improved yield (vide infra).

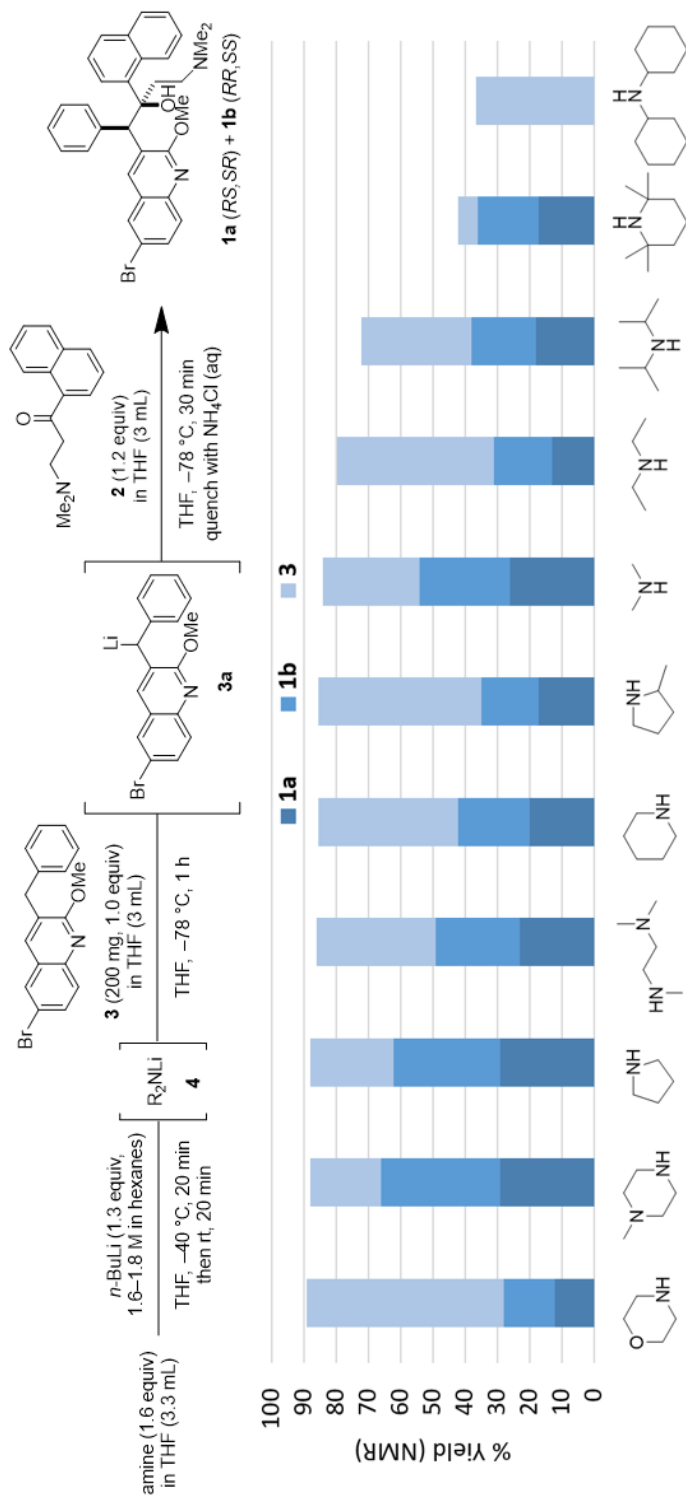


Figure 3-11: Evaluation of lithium amide bases in the lithiation/1,2-addition sequence.

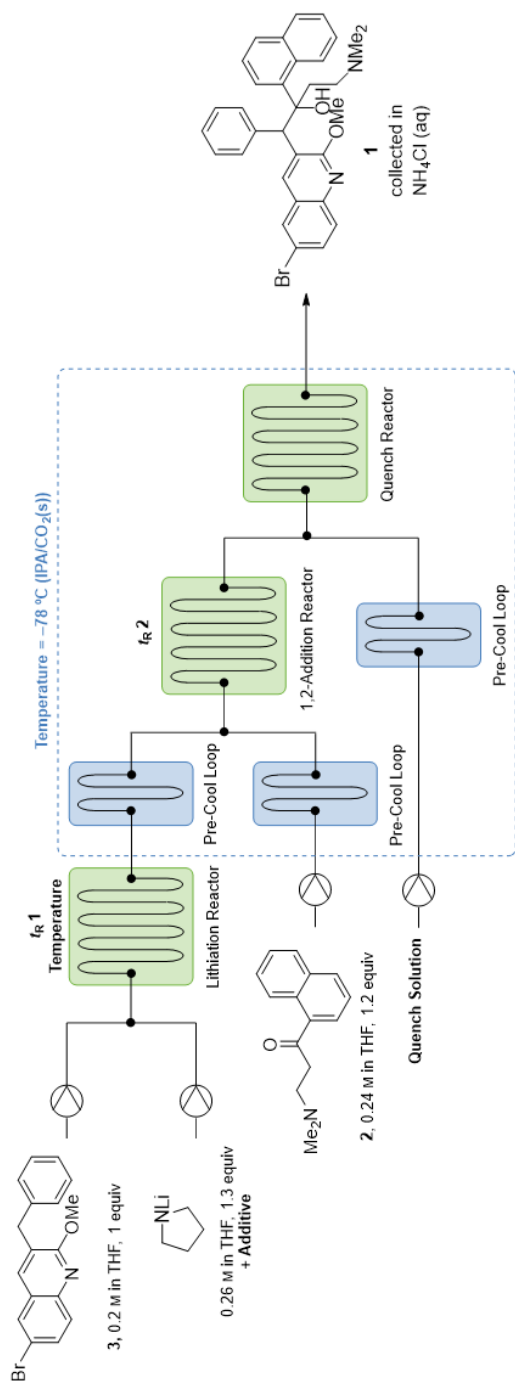
With knowledge that cyclic and less hindered lithium amide bases improve the yield of **1** and limit formation of undesired products, we sought to increase the diastereoselectivity of the 1,2-addition to maximize formation of **1a**. Salt additives are known to affect yield and diastereoselectivity in lithiation reactions by influencing the geometry, equilibrium, or rate of assembly or dissociation of lithium aggregates.²⁸⁻³¹ Adding MgBr₂·OEt₂ resulted in no improvement of the diastereoselectivity (Figure 3-12). When ZnCl₂ was added, no conversion of **3** was observed, which was attributed to the formation of the less nucleophilic Zn-organyl through Li-Zn exchange. Cerium trichloride was evaluated as an additive based on precedent for promoting 1,2-addition of enolizable ketones but the yield of **1a** was not improved,³² which aligns with our earlier observation that **3a** acts only as a nucleophile and not as a base towards ketone **2**.

A significant enhancement in diastereoselectivity was instead observed for the addition of LiBr (Figure 3-12), reversing the d.r. of the reaction from 0.91:1.0 (**1a** : **1b**) to as high as 2.0:1.0, now favouring the desired *RS*-isomer. Similar enhancement was observed when LiBr was premixed with ketone **2** and added in step 2 (see Table 3.10 on page 208). This observation could suggest that LiBr influences the d.r. by chelating the β -amino ketone **2** and thereby impacting the approach of nucleophile **3a**. In order to examine the effect of the counterion, LiCl and LiI were tested, but no significant improvement in diastereoselectivity was observed, possibly due to their lower solubility in THF. 2-MeTHF and 1,2-dimethoxyethane (DME) were investigated as alternative solvents, however THF continued to demonstrate the highest yield and diastereoselectivity.

The stoichiometry of LiBr relative to quinoline **3** was assayed and 2.3 equivalents of LiBr was optimal when LDA was freshly prepared from *i*-Pr₂NH and *n*-BuLi (Table 3.9 on page 207). However, when a commercial solution of LDA was used, only 1.3 equivalents of LiBr was required and further increases in stoichiometry did not have a beneficial effect. This difference is likely due to batch-to-batch variations in salt content of *n*-BuLi and commercial LDA solutions, which is known to have important implications for the rate of lithiation and 1,2-addition reactions.^{14,18}

LiBr used in combination with more basic, less sterically hindered lithium amides drastically improved the yield and diastereoselectivity of the 1,2-addition reaction, increasing the assay yield of **1** to as high as 92% (*N*-methylpiperazine) and improving the d.r. to as high as 2.5:1.0 (**1a** : **1b**), more than doubling the yield of the desired *RS*-isomer (**1a**) as compared to LDA (60%, *N*-methylpiperazine vs. 25%, *i*-Pr₂NH). Across the series of bases, the same trend was observed as in the absence of salt additive; with diisopropylamine, low yield of **1** (37%) was observed, and with the bulky dicyclohexylamine, no product formation was observed at all.

With optimal base and additive choices in hand, we investigated whether enhanced time and temperature control in continuous flow would improve the yield of **1a**.³² We constructed a plug flow reactor to telescope the reaction and quench steps (Table 3.4). Using this setup, a comparable yield of **1** was achieved in a total residence time of 18.3 minutes, albeit at significantly decreased d.r. (Table 3.4, entry 1).



Entry	Additive	Lithiation Temp. (°C)	<i>t_R</i> 1 (min)	<i>t_R</i> 2 (min)	Quench	AY 1a ^a	AY 1 ^a (d.r.) ^b
1	None	-78	10	8.3	0.35 M AcOH in THF	30	74 (0.68 : 1.0)
2	LiBr ^d	-78	10	8.3	0.35 M AcOH in THF	- ^c	- ^c
3	None	22	2.5	8.3	0.35 M AcOH in THF	22	73 (0.43 : 1.0)
4	LiBr ^d , Et ₃ N·HCl ^e	22	2.5	8.3	MeOH	42	72 (1.4 : 1.0)
5	LiBr ^d , Et ₃ N·HCl ^e	22	1	5	MeOH	44	78 (1.3 : 1.0)
6	LiBr ^d	0	1	5	MeOH	42	73 (1.4 : 1.0)
7	LiBr ^d	0	0.4	2	MeOH	33	62 (1.1 : 1.0)

See Table 3.11 for additional details

^a Determined by ¹H NMR with benzyl benzoate as internal standard

^b AY 1a : AY 1b. ^c no data; failure due to clogging at quench

^d 2.3 equiv ^e 0.02 equiv

Table 3.4: Evaluation of a continuous flow process for synthesis of **1**.

We sought to investigate whether the LiBr additive could also improve d.r. in continuous flow. Quench with aqueous ammonium chloride solution in continuous flow was not possible due to freezing of the quench solution at $-78\text{ }^{\circ}\text{C}$. Formation of solids prevented the use of acetic acid as a quenching agent when LiBr was added (Table 3.4, entry 2). Quenching with methanol prevented precipitation and enabled use of the salt additive in flow. LiBr did improve the d.r. of the reaction in flow (Table 3.4, entries 3–4), but the flow reaction remained less selective for the desired diastereomer **1a** than the batch reaction. A LiCl salt additive ($\text{Et}_3\text{N}\cdot\text{HCl}$) was also explored due to precedence from Gupta et al. for rate enhancement in lithium amide deprotonation reactions,¹³ but the additive did not demonstrably affect the reaction (Table 3.4, entries 4–6).

In flow, the lithiation could be performed in as little as one minute at room temperature or $0\text{ }^{\circ}\text{C}$ with rapid cooling before the 1,2-addition at $-78\text{ }^{\circ}\text{C}$ (Table 3.4, entries 4–7); this observation highlights an advantage of flow, as a significant mid-process temperature change is more feasible in flow due to the smaller volumes. Further decrease in residence times led to decreased yield (Table 3.4, entry 7). Ultimately, while comparable yield of **1a** was achieved using a plug flow reactor (Table 3.4, entry 5), the results did not improve upon optimized batch conditions due to the lower diastereoselectivity. While shorter reaction times and higher deprotonation temperatures were also possible in batch (Table 3.10 on page 208), we focused our continued efforts on demonstrating a batch protocol amenable to larger scale processing that did not include the mid-process cooling.

The stability of **3a** when different lithium amide bases are used for deprotonation was assayed by using pyrrolidine, *N*-methylpiperazine, or diisopropylamine and comparing recovery of **3** after aqueous workup. We observed that recovery of **3** is higher at $-78\text{ }^{\circ}\text{C}$ than at room temperature (Figure 3-3).

We translated our optimized batch reaction conditions to a 1 g scale reaction using the most promising amine bases: pyrrolidine, *N*-methylpiperazine and morpholine (Table 3.5, Entry 1–3). The crude reaction mixture consisted of a mixture of isomers of **1** and unreacted starting materials **2** and **3**. For these larger scale reactions, we

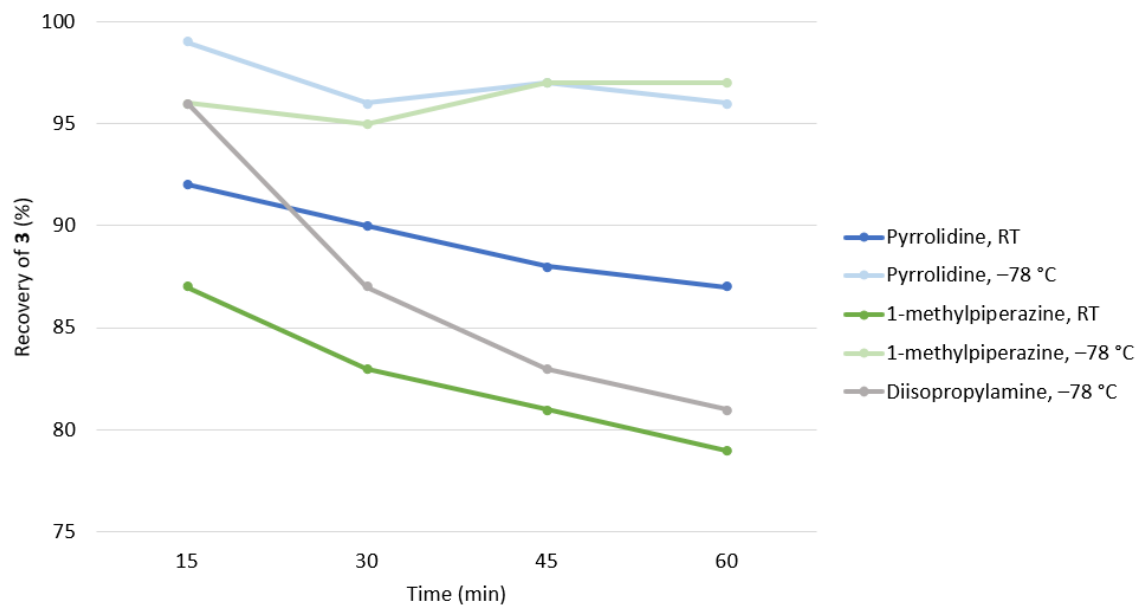
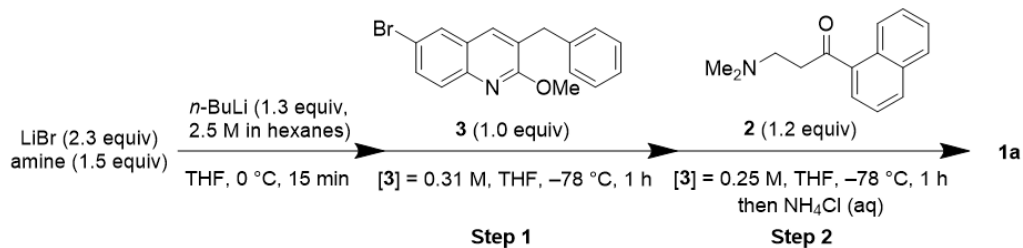


Figure 3-13: Stability of lithiated quinoline **3a** under different conditions as determined by recovery of **3** after water quench. Data points are an average of duplicate runs. RT = room temperature, 22–25 °C.

sought to develop conditions for separation of the desired diastereomer **1a** from the other components of the reaction mixture by crystallization. Recrystallization from toluene resulted in selective crystallization of the undesired diastereomer **1b**. The desired diastereomer **1a** was isolated after recrystallization of the mother liquor from EtOH, resulting in isolation of **1a** in up to 61% yield and >99% purity (1 g scale). A similar procedure was performed on 5 g and 10 g scale (Entries 4–5), yielding similar isolated yield of **1a**. Although the purity of **1a** was lower (88–90%) in the larger scale runs due to retention of **1b**, we anticipate that application of the current industrial purification techniques including seeding can afford the desired diastereomer **1a** in acceptable purity.



Entry	Base	Scale (g of 3)	Assay d.r. ^a of 1	IY 1a (%) ^b	IY 1 (%) ^b
1	morpholine	1	2.4 : 1.0	61	88
2	<i>N</i> -methylpiperazine	1	1.8 : 1.0	60	97
3	pyrrolidine	1	2.4 : 1.0	56	86
4 ^c	pyrrolidine	5	2.0 : 1.0	56	82
5 ^c	pyrrolidine	10	2.1 : 1.0	60	79

IY: Isolated yield

^a AY **1a** : AY **1b**, determined by ¹H NMR of crude reaction mixture.

^b IY **1a** are corrected for purity as determined by ¹H NMR; IY **1b** are uncorrected for purity.

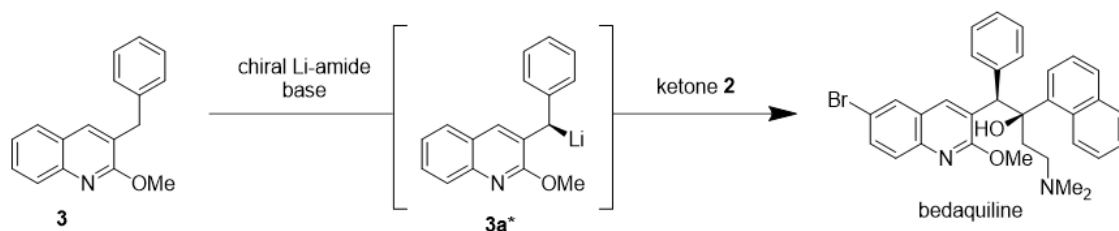
^c *n*-BuLi 1.4 M. Final [3] = 0.30 M, lithium amide formation: 20-25 min, step 2: 30 min.

Table 3.5: Lithiation/1,2-addition for synthesis of **1** on up to 10 g scale.

3.2.3 Enantioselective Synthesis of Bedaquiline by Asymmetric Lithiation-Addition

In the above discussion, we have detailed how the use of less hindered lithium amide bases in combination with additive lithium bromide for synthesis of bedaquiline by a lithiation/1,2-addition sequence results in high yield and increased selectivity for the desired diastereomer (**1a**) of the active pharmaceutical ingredient. Following these considerable improvements to the synthesis of **1a**, we desired to explore the possibility of an enantioselective transformation (Figure 3-14). A review of asymmetric synthesis using chiral lithium amide bases describes only one example of asymmetric benzylic functionalization using a lithium amide base.³³ In the cited example, benzylic tricarbonyl (η^6 -arene)chromium complexes are metalated and reacted with various electrophiles including diphenyl disulfide, alkyl halides, and benzophenone, to prepare a series of chromium complexes with high levels of asymmetric induction.^{33,34} Crucially, the addition of lithium chloride affected the rate of the metalation event, and order of addition and reaction time were shown to influence the enantiomeric

Proposal for Enantioselective Synthesis of Bedaquiline



Cowton, 1996

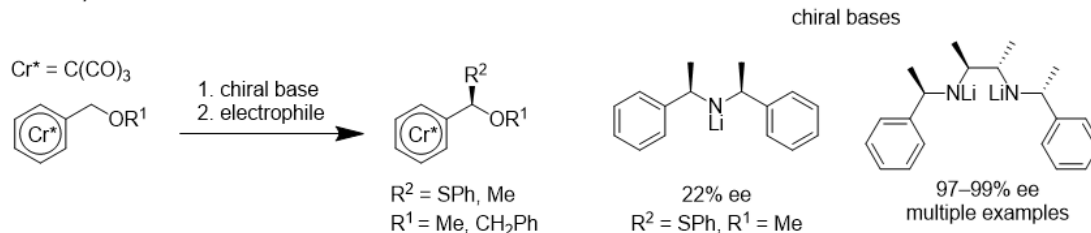


Figure 3-14: Proposal for enantioselective synthesis of bedaquiline by asymmetric lithiation/1,2-addition sequence. Precedent by Cowton, et al. is illustrated.³⁴

excess.³³ In another example by Koga and coworkers for the enantioselective alkylation of ketone enolates using a chiral lithium amide as base, the addition of LiBr (1.1 equiv) increased the enantiomeric excess (e.e.) of the product.³⁵

This precedent encouraged our investigation of chiral lithium amide bases for invoking asymmetric induction for the 1,2-addition event en route to bedaquiline. Naicker, et al. recently disclosed the use of (+)-bis(α -methylbenzyl)amine to achieve improved diastereoselectivity in the 1,2-addition reaction leading to bedaquiline.⁹ However, low yields were observed and racemic product was obtained. Lutz et al. use a similar procedure to achieve enantioselectivity for α -functionalization of ketones.³⁶ In both cases, the addition of LiCl is important for achieving selectivity. When the precedent for asymmetric synthesis using chiral lithium amide bases is considered more broadly, chiral amines containing pendant chelating groups such as norephedrine derivatives are highly effective.³³ Considering this precedent in combination with our success increasing the mass balance and yield of the 1,2-addition reaction using cyclic lithium amide bases, we hypothesized that commercially available pyrrolidine derivatives with a pendant Lewis Basic functional group could be highly effective in achieving the desired enantioselectivity in our lithiation/1,2-addition se-

quence. Encouragingly, enantioenriched derivatives of pyrrolidine could be prepared in a straightforward manner from readily available and inexpensive amino acid Proline, providing an opportunity for a process-relevant synthesis.

An initial assay of chiral secondary amine bases aligned with our previous observation that less hindered secondary amines are higher yielding than sterically encumbered branched or acyclic secondary amines (see Figure 3-15). Promisingly, chiral base **10** yielded 18% e.e. favoring the undesired *S,R*-enantiomer of **1**. The enantiomer of **10** was acquired and further screening was performed to confirm the observation and determine whether we could achieve an e.r. favoring the desired *1R,2S*-enantiomer.

Following our initial observation that the use of (*S*)-(+)-2-(methoxymethyl)pyrrolidine (**10**) for lithium amide formation yields bedaquiline mixture of isomers with 58% yield and 18% e.r. favoring the enantiomer of bedaquiline, we investigated (*R*)-(-)-2-(methoxymethyl)pyrrolidine **12** to see if the desired enantiomer could be prepared selectively. Surprisingly, 0% yield of bedaquiline was observed (Table 3.14, entry 11). To determine whether the hygroscopic LiCl solution could have negatively influenced the reaction outcome, a trial without the salt solution was performed, using only catalytic Et₃N·HCl to ensure enough trace salt was present to catalyze lithium aggregate assembly and dissociation. Improved yield of bedaquiline (25%) was observed, however with worse d.r. (Table 3.14, entry 13). This suggests that moisture control could be an important factor influencing the yield of bedaquiline.

In the synthesis of **1a** described in the preceding section, we found that LiBr had a more significant effect on diastereoselectivity than LiCl. We investigated whether this counterion effect was similar in this context, using (*S*)-(+)-2-(methoxymethyl)pyrrolidine (**10**) and (*R*)-(-)-2-(methoxymethyl)pyrrolidine (**12**). We observed improved d.r. versus LiCl (30:23, LiCl; 44:9, LiBr), however lower yield was observed (53% yield with *S*-enantiomer and 3% yield with *R*-enantiomer of the base). This suggested to us that reagent quality of the *R*-enantiomer was a significant issue. We obtained (*R*)-(-)-2-(methoxymethyl)pyrrolidine from an alternate supplier (Chem-Impex) and tested with the LiCl conditions (Table 3.14, entry 16), but observed 0% yield. Note that with TCI material, a yellow color was observed after addition of *n*-BuLi to chiral

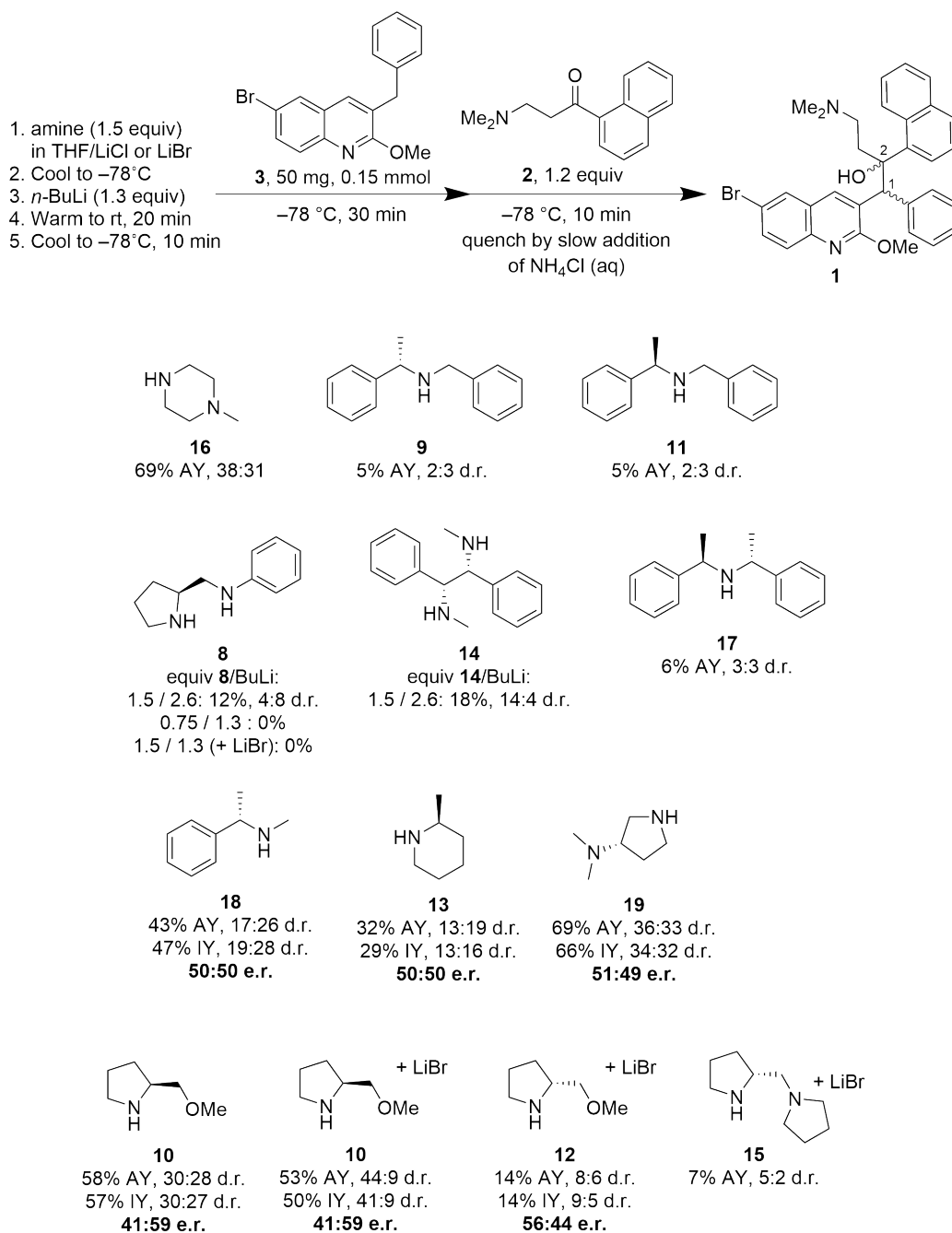


Figure 3-15: Evaluation of chiral lithium amide bases for enantioselective synthesis of bedaquiline. Further experimental details are provided in Table 3.14 on page 211.

amine, however with the Chem-Impex material, no color change was observed, and no reaction was observed. This color could indicate lithium aggregate formation with the chiral base.

The original sample from TCI was redistilled over CaH and the experiment was repeated (Table 3.14, entries 19–20). In these two trials with the redistilled amine, 24% and 11% yield were observed, respectively. These variations suggest that some aspects of reaction setup such as moisture control, temperature, or rate of addition are influencing the yield. Performing this reaction on larger scale could help to control these factors. Also, the results with the same material from different suppliers suggests that reagent quality (presence of nitrogen oxides, for example) could play an important role.

These observations were communicated to collaborators at the Medicines for All Institute at Virginia Commonwealth University. Further investigations of the use of chiral pyrrolidine derivatives for asymmetric synthesis of bedaquiline are underway in their laboratories.

3.3 Conclusion

In summary, we have developed an improved process for the synthesis of racemic bedaquiline **1a** by a higher yielding and more selective lithiation/1,2-addition sequence enabled by use of LiBr as an additive and cyclic lithium amide bases. Initial investigations into an asymmetric route to bedaquiline using chiral lithium amide bases were performed, resulting in synthesis of bedaquiline with 18% e.e. An initial focus on reproducibility of reported methods led to deeper understanding of the reaction mechanism, which guided optimization efforts and led to significant improvement over existing methods. We suggest small changes to the reaction sequence which can be quickly implemented on scale, without the need to qualify new intermediates or vastly change processing parameters. A future direction is further refinement of diastereoselectivity and/or enantioselectivity using chiral amine bases. This work is ongoing in our laboratories.

3.4 Experimental Section

3.4.1 General Experimental Details

General Chemical and Analytical Information

Chemicals were obtained from commercial suppliers and were used without any further purification unless otherwise noted. Organometallic reagents were titrated according to a literature procedure¹⁹ before first use and at least weekly thereafter. LiBr was dried in a vacuum oven overnight at 100 °C and stored in a desiccator before use. Anhydrous THF, 2-MeTHF and toluene were freshly distilled over sodium, purified using a solid-sorbant Solvent Dispensing System from Pure Process Technology, or taken from sealed bottles from Sigma-Aldrich (Darnstadt, Germany). For column chromatography, cyclohexane and ethyl acetate were purchased in technical grade and distilled, or HPLC-grade solvents were used. Deuterated solvents were purchased from Deutero GmbH (Kastellaun, Germany), Cambridge Isotope Labs (Cambridge, MA, USA) or Sigma Aldrich (Darnstadt, Germany). Dry MeOH was purchased from Acros Organics (Breda, Netherlands). All air or moisture sensitive reactions were performed under inert atmosphere (argon or nitrogen) in glassware that was dried using standard Schlenk techniques. Reaction temperatures referred to the temperature of the particular cooling or heating bath unless otherwise indicated. Chromatographic purification was performed using flash column chromatography of the indicated solvent system on silica gel (35–70 μm , Acros Organics) unless otherwise noted. Silica plates (TLC Silica 60 F254, Merck, Darnstadt, Germany) were used for thin-layer chromatography. UV active compounds were detected using UV light ($\lambda = 254 \text{ nm}$ and $\lambda = 365 \text{ nm}$). All NMR spectra were recorded on the following spectrometers: Bruker Avance-III HD (^1H -NMR: 300 MHz, ^{13}C NMR: 75.5 MHz), Bruker Avance-II (^1H -NMR: 400 MHz, ^{13}C NMR: 100.6 MHz). Chemical shifts are referenced to residual solvent signals (chloroform- d_1 : 7.26 ppm and 77.16 ppm for ^1H -NMR and ^{13}C -NMR respectively) and reported in parts per million (ppm) relative to tetramethylsilane (^1H , ^{13}C). Infrared spectra were recorded on a spectrometer (Bruker Tensor

27, Bruker, Ettlingen, Germany) equipped with a diamond ATR unit. Electron spray ionization (ESI) mass spectra were recorded on a 1200-series HPLC-system or a 1260-series Infinity II HPLC-system (Agilent, Santa Clara, CA, USA) with binary pump and integrated diode array detector coupled to a LC/MSD-Trap-XTC-mass spectrometer (Agilent) or a LC/MSD Infinitylab LC/MSD (G6125B LC/MSD). Melting points were determined by using a Krüss-Optronic (Hamburg, Germany) KSP 1 N digital melting point meter.

General Information for Continuous Flow Apparatus

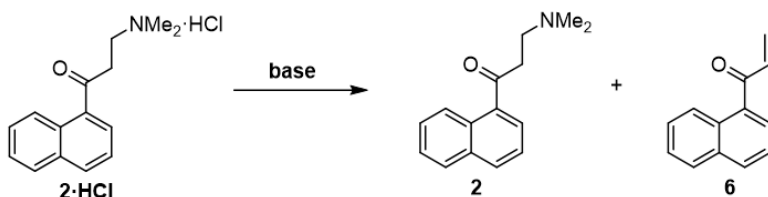
High purity PFA tubing, PEEK mixers and unions, and Super Flangeless nuts and ferrules were purchased from IDEX Scientific (Oak Harbor, WA, USA). Syringe pumps were Harvard (Holliston, MA, USA) PhD Ultra syringe pumps with 8 mL or 20 mL stainless steel Harvard syringes or Syrris Asia (Royston, UK) pumps equipped with 250–500 μL (green) syringes. Solutions for flow reactions were prepared under an argon atmosphere using oven-dried volumetric glassware.

Laboratory Safety Statement

CAUTION: Commercial solutions of reagents such as *n*-butyllithium and lithium diisopropylamide are highly reactive and can be pyrophoric depending on concentrations. Use proper techniques for handling pyrophoric and water-reactive materials and ensure all reagents are fully quenched before work-up. Chemical structures described herein may display bioactive properties. Handle with care.

3.4.2 Synthesis of Starting Materials and Reagents

Compounds **3** and **2·HCl** (the hydrochloride salt of **2**) were obtained from WuXi AppTech. Methods for their synthesis and ¹H NMR spectra of intermediates are included in Section 3.5.1). These materials were used for all reaction development described herein.



3-(Dimethylamino)-1-(naphthalen-1-yl)propan-1-one (**2**)

The free amine **2** was prepared by modification of a reported procedure.³⁷ A 25-mL round-bottom flask was charged with **2·HCl** (502 mg, 1.90 mmol) and DI water (1.5 mL) was added. The mixture was stirred for 5 min until dissolution was observed. An aqueous solution of 25 wt% sodium hydroxide (2 mL) was added, and stirring was continued for 10 min. Additional DI water (4 mL) was added. Oiling out of **2** was observed. CH₂Cl₂ (6 mL) was added and stirring was continued for 5 min. The biphasic mixture was transferred to a separatory funnel. The layers were separated, and the aqueous layer was extracted with CH₂Cl₂ (5 mL). The organic layers were combined and washed with water, then dried over MgSO₄, filtered, and concentrated under reduced pressure. The title compound was isolated as a yellow oil (393 mg, 1.73 mmol, 91%).⁹

Notes:

- As the free amine **2** is prone to undergo elimination to enone **6**, it has to be freshly prepared from its hydrochloride salt **2·HCl**.
- Different approaches for preparing **2** were examined. When salt **2·HCl** is dissolved in water and the amine **2** is liberated by adding NaHCO₃ or NaOH solution, significant amounts of elimination byproduct **6** forms if extended re-

action time is used, or if elevated temperatures (above 25 °C) are used during rotary evaporation.

- Alternatively, the salt **2·HCl** was suspended in DCM and washed with saturated NaHCO₃ solution using a separatory funnel to obtain **2** after solvent removal.

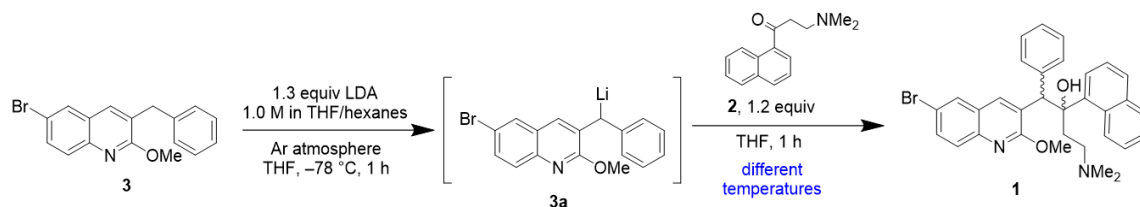
3-(Dimethylamino)-1-(naphthalen-1-yl)propan-1-one-2,2-d₂ (2-d₂)

Deuterium oxide (8 mL) was added to a vial containing **2** (1.74 g, 7.65 mmol). The reaction was vigorously stirred at room temperature for 4 days. The reaction was extracted with CH₂Cl₂ (3 x 10 mL) and brine. The organic phase was dried with Na₂SO₄ and the solvent was removed under reduced pressure. The sample was dried under vacuum during 4 h to remove remaining solvent and water. Ketone **2-d₂** was obtained in 90% yield as a yellow oil.

3.4.3 General Procedure: Early Attempts to Reproduce Precedence for Synthesis of **1**

For results presented in Table 3.2: Quinoline **3** (50.0 mg, 0.15 mmol, 1.0 equiv) was added to a dry 2-dram vial, followed by a dry stir bar. The vial was placed under high vacuum and dried for 2 h at room temperature. THF (500 μ L) was added and the solution was cooled in an IPA/dry ice bath. LDA (130 μ L of 1.5 M solution in THF/heptane/PhEt, 1.3 equiv) was added dropwise, at which point the reaction takes on a dark purple color. The mixture was stirred for 1 h. Ketone **2** (41.0 mg, 0.180 mmol, 1.2 equiv) was weighed into a dry 2-dram vial and placed under high vacuum for 30 min. The ketone was dissolved in THF (1 mL), then added dropwise to the stirring reaction mixture over 3 min. The resulting mixture was stirred for a further 30 min. The reaction mixture was quenched by dropwise addition of quench solution (25 wt% NH_4Cl (aq) or 1 M AcOH in THF, as indicated). After a yellow color was observed, the cooling bath was removed and the mixture was allowed to warm to room temperature. Note: on addition of NH_4Cl (aq) solution, freezing of the aqueous mixture occurs, resulting in a biphasic mixture. The mixture was stirred until a homogenous room temperature solution was obtained. Benzyl benzoate (28.5 μ L, 0.15 mmol) was added and the vial was shaken to dissolve. An aliquot of the organic layer was taken and the solvent was removed from the aliquot under reduced pressure. The residue was suspended in CDCl_3 and analyzed by ^1H NMR with a 30 s relaxation delay to ensure accurate quantification.

3.4.4 Influence of Step 2 (1,2-Addition) Temperature on Yield of **1**



Quinoline **3** (150 mg, 0.46 mmol, 1.0 equiv) was dissolved in anhydrous THF (0.45 mL) and the reaction mixture was cooled to $-78\text{ }^{\circ}\text{C}$. Commercial LDA solution (1 M in THF/hexanes, 0.60 mmol, 0.60 mL, 1.3 equiv) was added dropwise and reaction mixture was stirred under argon atmosphere. After a period of 1 h, a solution of ketone **2** (125 mg, 0.550 mmol, 1.2 equiv) in anhydrous THF (0.45 mL) was added dropwise to the vial containing lithiated quinoline **3a**. After addition of the ketone **2**, the reaction vial was transferred to a temperature-controlled bath (-78 , -40 or $-20\text{ }^{\circ}\text{C}$), and the reaction was stirred for additional 1 h. The resulting mixture was quenched with a saturated aqueous solution of NH_4Cl (1 mL). Mesitylene was added as the NMR internal standard (0.46 mmol, 1.0 equiv) prior to phase separation. The organic phase was dried with anhydrous Na_2SO_4 and concentrated prior to ^1H NMR analysis. At $-78\text{ }^{\circ}\text{C}$ (dry ice/acetone bath), 35% AY of **1** was obtained. At higher temperatures, no bedaquiline (**1**) was observed.

3.4.5 Unified Procedure: Baseline for Reaction Optimization Across Research Sites

The following list describes a general procedure which guided our three research sites (JGU Mainz, VCU, MIT) to align our methods for reaction optimization, mechanistic investigations, and other experimental efforts:

1. Pre-dry three vials or flasks, either by flame-drying or by heating in a 140 °C oven for a minimum of one hour.
2. Charge quinoline **3** (200 mg, 1.0 equiv) into a flask, and put under high vacuum for 1 h. (FLASK A)
3. Charge additive (if necessary) into another flask, and put this under high vacuum for 1 h. (FLASK B)
4. Charge ketone **2** (164 mg, 1.2 equiv) to a third flask. Put this under high vacuum for at least 1 h. (FLASK C)
5. FLASK B. Charge flask with anhydrous THF (1.0 mL, 5 vol) and amine (1.5 equiv, dried over CaH₂ or distilled before use). Cool to -78 °C in a bath of dry ice and acetone or isopropanol. Hold at temperature for 10 min.
6. FLASK B. Add *n*-BuLi (1.6 or 2.5 M in hexanes, titrated prior to use). Upon complete addition, allow reaction mixture to stir for 10 min.
7. FLASK A. Add anhydrous THF (2.0 mL, 10 vol) and mix to dissolve the quinoline **3**.
8. Transfer the contents of FLASK A into FLASK B dropwise over the course of 10 min. Stir for 1 h at -78 °C.
9. FLASK C. Add anhydrous THF (3.0 mL, 15 vol) to dissolve the ketone **2**.
10. Transfer the contents of FLASK C into FLASK B dropwise over the course of 15 min. Stir for 1 h at -78 °C.

11. Add saturated aqueous NH_4Cl (1 mL, approx. 5 equiv) to FLASK B very slowly (approximately one drop every 20 seconds). Remove FLASK B from cooling bath and allow to warm to room temperature when visibly quenched (reaction mixture turns from deep purple to yellow).
12. Separate the organic layers. Extract the aqueous with THF or CH_2Cl_2 (3 x 1 mL). Remove solvent under reduced pressure. (CRUDE). Note: Later it was determined that choice of workup solvent influenced yield due to solubility of **1**.
13. Dissolve CRUDE in desired solvent. Add internal standard for NMR and dilute a small amount of CRUDE in CDCl_3 . Take ^1H NMR spectrum with >15 s relaxation delay.

3.4.6 Assay for Recovery of **3** after Benzylic Deprotonation with Lithium Amide Base

Amine (*i*-Pr₂NH, pyrrolidine or *N*-methylpiperazine, 0.91 mmol, 1.5 equiv) was added to a vial containing anhydrous THF (2 mL) at 0 °C. Then, *n*-BuLi (2.5 M in THF, 0.79 mmol, 1.3 equiv) was added dropwise. The reaction mixture was kept at the same temperature over 20 min, then transferred to a bath at -78 °C or at room temperature. Quinoline **3** (200 mg, 0.61 mmol) was dissolved in anhydrous THF (2 mL) and then added dropwise to the vial containing the lithium amide base. The reaction mixture was stirred under nitrogen atmosphere for the indicated reaction time (15–60 min) before quenching with water (3 mL). Triphenylmethane (0.61 mmol, 1.0 equiv) was added to the sample as the NMR internal standard. The organic phase was separated and dried with anhydrous Na_2SO_4 . The solvent was removed under reduced pressure prior to the ^1H NMR analysis. Each reaction was performed in duplicate and the results averaged. See results in Figure 3-13 on page 175.

3.4.7 Reverse Reaction at $-78\text{ }^{\circ}\text{C}$ and Room Temperature Using LDA

Bedaquiline **1** diastereoisomeric mixture (d.r. **1a/1b** 2.5:1.0), 69% purity, 63.5 mg, 0.230 mmol) was dissolved in anhydrous THF (10 mL) with mild heating. This solution was held at room temperature or transferred to a $-78\text{ }^{\circ}\text{C}$ bath (dry ice/acetone), as indicated. Commercial LDA solution (0.30 mmol, 1.3 equiv) was added dropwise and the mixture was stirred for 1 h under nitrogen atmosphere. The reaction mixture was quenched with saturated aqueous NH_4Cl solution (10 mL). Extraction was performed with CH_2Cl_2 (2 x 10 mL) and the organic phase was dried with anhydrous Na_2SO_4 and concentrated under reduced pressure. Mesitylene (0.23 mmol, 1.0 equiv) was added as an internal standard and the resulting mixture was analyzed by ^1H NMR spectroscopy. At $-78\text{ }^{\circ}\text{C}$: 16% of **2** is observed. At Room Temperature: 82% of **2** is observed.

3.4.8 Reaction of **3a** with **2-d₂**

In an oven-dried vial containing anhydrous THF (2 mL), freshly distilled pyrrolidine or diisopropylamine (0.91 mmol, 1.5 equiv) was added, and the resulting solution was cooled to $0\text{ }^{\circ}\text{C}$. Titrated *n*-BuLi solution (2.45 M in hexanes, 0.79 mmol, 1.3 equiv) was added. After 20 min, the reaction mixture was cooled to $-78\text{ }^{\circ}\text{C}$, and a solution of quinoline **3** (200 mg, 0.61 mmol, 1.0 equiv) in anhydrous THF (2 mL) was added dropwise and stirred under nitrogen atmosphere. After a period of 1 h, a solution of ketone **2-d₂** (0.73 mmol, 1.2 equiv) in anhydrous THF (2 mL) was slowly added to the vial containing **3a**. The reaction was stirred for additional 1 h at the same temperature. The resulting mixture was quenched with AcOH (0.79 mmol, 1.3 equiv), and the solvent removed from the sample prior to ^1H NMR analysis. **3-d₁** was not observed using pyrrolidine or diisopropylamine.

3.4.9 ^1H NMR Characterization of **3a** at $-78\text{ }^\circ\text{C}$

^1H NMR Analysis of commercial LDA Solution (Figure 3-4, spectrum 1).

An oven-dried 5 mm NMR tube was charged with THF- d_8 in a glovebox. The NMR tube was capped and removed from the glovebox and cooled to $-78\text{ }^\circ\text{C}$ in an IPA/dry ice bath. A commercial solution of LDA was added ($50\ \mu\text{L}$ of 1.6 M solution in THF/hexanes/PhEt, 0.070 mmol). This solution was maintained in an IPA/dry ice bath and transferred to a pre-cooled NMR spectrometer for analysis at $-78\text{ }^\circ\text{C}$.

Procedure for ^1H NMR Analysis of **3a in THF- d_8 (Figure 3-4, spectra 2-4).** A solution of **3** (23 mg, 0.070 mmol) in THF- d_8 (0.75 mL) was prepared in a glovebox. The solution was transferred to an oven-dried 5 mm NMR tube and removed from the glovebox. The sample was cooled to $-78\text{ }^\circ\text{C}$ under argon atmosphere and an initial ^1H NMR spectrum at $-78\text{ }^\circ\text{C}$ was recorded. The sample was removed from the spectrometer and returned to an IPA/dry ice bath. A commercial solution of LDA (0.070 mmol, $50\ \mu\text{L}$ of 1.6 M solution in THF/heptane/PhEt, 1.0 equiv) was added and the solution was mixed by vortex with intermittent cooling in the IPA/dry ice bath until a red/black color was observed (about 10 cycles of mixing over 3 min). The resulting mixture was observed by ^1H NMR at $-78\text{ }^\circ\text{C}$ at $t = 8, 10, 18, 25, 30,$ and 40 min. After 40 min, the sample was removed from the spectrometer and mixed by vortexing, taking care to minimize the time the sample was outside of the IPA/dry ice bath. Note: it is assumed that significant warming of the sample occurred during this time. The sample was returned to the spectrometer, and observed by ^1H NMR at $t = 50$ and, 60 min. The signal for PhEt at 2.65 ppm was used as an internal standard to monitor relative conversion of starting material and formation of product over time. Note that in this ^1H NMR experiment a relaxation delay of 1.00 s was used, so quantification of signals is only a rough approximation.

Notes. Upon analysis of the solution of **3a**, ^1H NMR signals at 5.1 ppm and 3.9 ppm were assumed to represent the $-\text{CHLi}-$ and $-\text{OMe}$ resonances for the lithiated quinoline product **3a** (see Figure 3-4 on page 163). The assignment of these resonances was confirmed by $^1\text{H}-^{13}\text{C}$ HMBC (see Figure 3-16 and 3-17 on pages 235

and 236). The spectra taken at different timepoints were analyzed to generate a curve showing conversion of **3** to **3a** over time (see Figure 3-6, page 164). This experiment showed that initial reaction of LDA with **3** is rapid but incomplete. Rapid Additional conversion of **3** was observed on mixing (warming) between $t = 40$ min and $t = 50$ min, however no additional **3a** was observed during the same time period. See supporting figures in Section 3.4.18.

3.4.10 Variable Temperature ^1H NMR Experiment for Reaction Mixture Containing **3a**

A Bruker Avance Neo spectrometer operating at 500.18 MHz was cooled to -61 °C using a liquid nitrogen heat exchanger. Meanwhile, a 5 mm NMR tube equipped with a rubber septum was dried with a heat gun under vacuum, back-filled with argon, brought into a nitrogen-filled glovebox, and charged with a solution of **3** (23 mg, 0.07 mmol) in THF- d_8 (1 g). The sample was removed from the glovebox and cooled in an IPA/dry ice bath under inert atmosphere. A solution of LDA (0.07 mmol, 50 μL of 1.6 M commercial solution in THF/hexanes/PhEt) was added at -78 °C in an IPA/dry ice bath and the resulting solution was mixed by vortexing with intermittent cooling in the IPA/dry ice bath until a red/black color was observed (about 3 min).

Result. The dark red-black sample was analyzed by ^1H NMR at -61 °C and showed approximately 32% conversion of **3** and 7% of lithiated species **3a**. The sample was allowed to warm to room temperature inside the spectrometer, showing 58% conversion of **3** and 11% of lithiated species **3a** after 40 min. This confirmed that consumption of **3** occurs on warming in the presence of LDA, but undesirable reactions occur and formation of **3a** is low.

3.4.11 Quantification of Formation of **3a** by ^1H NMR

In a nitrogen-filled glovebox, a dry 2-dram vial was charged with a solution of **3** (50 mg, 0.15 mmol) and THF- d_8 (550 μL). A second 2-dram vial was charged with a magnetic stirrer and THF- d_8 (550 μL). The vials were capped and removed from the glovebox. To the second vial, mesitylene (21 μL , 0.15 mmol), followed by diisopropyl amine (32 μL , 0.23 mmol) was added, and the solution was cooled to -78 $^\circ\text{C}$. A solution of *n*-BuLi, 2.6 M in hexanes (75 μL , 0.20 mmol) was added dropwise and the mixture was stirred for 10 min. The solution of **3** was added dropwise with stirring, then warmed to room temperature. The resulting dark red-black solution was transferred into an oven-dried and septum-capped 5mm NMR tube under inert atmosphere. The sample was then analyzed by ^1H NMR spectroscopy.

Following the above procedure, the same experiment was performed with pyrrolidine (19 μL , 0.23 mmol). The resulting spectra of reactive intermediate **3a** are shown in Figure 3-19 and Figure 3-18 on page 238.

3.4.12 General Procedure: Screening Secondary Amine Bases

As depicted in Figure 3-11: An oven-dried 20 mL vial was charged with a stir bar, set under argon atmosphere and equipped with a septum cap. THF (3.3 mL) was added followed by pyrrolidine (80 μ L, 0.98 mmol), and the solution was cooled to -40 $^{\circ}$ C with 60:40 ethylene glycol / water in a dry ice bath. *n*-BuLi (0.79 mmol, titrated commercial solution in hexanes) was added dropwise, resulting in a reaction concentration of 0.26 M. The resulting mixture was stirred for 20 min, then moved to room temperature and stirred for an additional 20 min. The solution was moved to an IPA / dry ice bath and cooled to -78 $^{\circ}$ C by stirring for 5 min. Concurrently, quinoline **3** (200 mg, 0.61 mmol) was weighed into an oven-dried 2-dram vial and dried under vacuum for 1 h, then dissolved in THF (3 mL). The solution of **3** was added dropwise to the prepared lithium amide solution resulting in a dark purple solution. The solution was stirred for 1 h. Ketone **2** (170 mg, 0.73 mmol) was weighed into a dry 2-dram vial and dried under vacuum for 1 h. THF (3 mL) was added to dissolve, and the ketone was added dropwise. After addition, the resulting mixture was stirred for an additional 30 min. The reaction mixture was quenched by slow dropwise addition of 2 mL 25 wt% aqueous ammonium chloride solution. The solution was moved to room temperature after a sunflower yellow color is observed. On warming, the solution generally lightens to a sandy brown color. Benzyl benzoate (59 μ L, 0.31 mmol) was added to the biphasic mixture and shaken to dissolve. The organic layer was sampled and the solvent was removed. The resulting residue was dissolved in CDCl₃ and analyzed by ¹H NMR using a 30 s relaxation delay. The yield was calculated by normalizing the signal at 5.4 ppm to 1.02, and reporting the resulting integral for the signals at 5.9 ppm (desired isomer, *RS,SR*, **1a**) and 5.8 ppm (undesired isomer, *RR,SS*, **1b**). See tabulated results in Table 3.6 on page 205.

3.4.13 General Procedure: Screening Salt Additives

As depicted in Figure 3-12a: In an oven-dried Schlenk flask, LiBr (1.3 equiv) was dissolved in THF (0.5 mL) under argon atmosphere and LDA (0.6 M, 1.3 equiv, in THF/hexanes) was added dropwise. The solution was cooled to $-78\text{ }^{\circ}\text{C}$ and a solution of **3** (50 mg, 1.0 equiv) in THF (0.5 mL) was added dropwise. After stirring for 1 h at $-78\text{ }^{\circ}\text{C}$, a solution of ketone **2** (42 mg, 1.2 equiv) in THF (1 mL) was added over 15 min and stirred for 30 min. The reaction was quenched with sat. NH_4Cl solution (1 mL), CH_2Cl_2 and water were added and the organic phase was separated. The aqueous phase was extracted with CH_2Cl_2 (3x), the combined organic phases were dried over sodium sulfate and all volatiles were removed under vacuo. The d.r. was determined by HPLC at 254 nm. Results are summarized in Table 3.7 on page 206.

3.4.14 General Procedure: Screening LiBr Stoichiometry and LiBr + Secondary Amine Bases

As depicted in Figure 3-12b: An oven dried Schlenk flask was charged with the respective amine (1.5 equiv), a solution of LiBr (2.3 equiv) in THF (0.5 mL) under Ar atmosphere. A solution of *n*-BuLi (1.9 M, 1.3 equiv) in hexanes was added slowly at $0\text{ }^{\circ}\text{C}$. The solution was cooled to $-78\text{ }^{\circ}\text{C}$ and a solution of **3** (50 mg, 1.0 equiv) in THF (0.5 mL) was added dropwise. After stirring for 1 h at $-78\text{ }^{\circ}\text{C}$, a solution of ketone **2** (42 mg, 1.2 equiv) in THF (1 mL) was added over 15 min and stirred for 30 min. The reaction was quenched with sat. NH_4Cl solution (1 mL), CH_2Cl_2 and water were added and the organic phase was separated. The aqueous phase was extracted with CH_2Cl_2 (3x), the combined organic phases were dried over sodium sulfate and all volatiles were removed in vacuo. Yield and d.r. are determined by ^1H NMR using 1,4-bis(trimethylsilyl)benzene as internal standard. Results are summarized in Table 3.9 (page 207) and Table 3.8 (page 207).

3.4.15 Reaction Screening in Continuous Flow

General Setup

Plug flow reactors (PFRs) were constructed from 0.03" ID high-purity PFA tubing and connected with IDEX fittings (PEEK nuts, unions, and T-mixers). For cooled reactions, reagent streams were equipped with a 100–200 μL precooling loop before joining other reagents at T-mixers. The precooling loops and PFRs were cooled using ice water or dry ice/isopropanol baths, or placed in room temperature water baths for room temperature reactions.

Solution Preparation

Preparation of quinoline **3** solution (A): To an oven-dried 10-mL volumetric flask with septum cap was added quinoline **3** (0.656 g, 2 mmol). The flask was placed under high vacuum for a minimum for 1 h, then placed under argon. Anhydrous THF was added gradually while the flask was swirled until the solid had dissolved and the homogeneous solution reached 10 mL in volume.

Preparation of Lithium Pyrrolidide solution (B): To an oven dried 10-mL volumetric flask with stir bar and septum cap was added LiBr (0.399 g, 4.6 mmol) and/or $\text{Et}_3\text{N}\cdot\text{HCl}$ (0.006 g, 0.04 mmol) additives (as indicated). The flask was placed under high vacuum for a minimum of 1 h, then placed under argon. Pyrrolidine (0.222 g, 0.256 mL, 3.1 mmol) and anhydrous THF (6 mL) were added with stirring and the flask was placed in an ice water bath. *n*-BuLi (nominally 1.6 M in hexanes, titrated before use, 2.6 mmol) was added dropwise, followed by addition of anhydrous THF until the total volume reached 10 mL (stir bar was briefly lifted out of solution using a magnet to ensure accurate volume measurement). The solution was stirred at 0 °C for 20 min before using.

Preparation of Ketone **2** solution (C): To an oven-dried 10-mL volumetric flask with septum cap was added ketone **2** (0.546 g, 2.4 mmol). The flask was placed under high vacuum for a minimum for 1 h, then placed under argon. Anhydrous THF was added gradually while the flask was swirled until the ketone had dissolved and the

homogeneous solution reached 10 mL in volume.

Experimental Method

For each experiment, the reactors were flushed with anhydrous THF and cooled prior to equilibration. The reaction was allowed to equilibrate for 3 residence times before collection. Samples were collected on at least 0.1 mmol scale in a vial containing 1 M aqueous NH_4Cl solution. After collection, the layers were separated and the aqueous layer was extracted twice with THF (or CH_2Cl_2 , for reactions using a methanol quench, to ensure clean phase separation). Benzyl benzoate was added as an NMR standard and the combined organic layers were dried by rotary evaporation followed by brief exposure to high vacuum. The entire sample was dissolved in CDCl_3 and a portion was taken for ^1H NMR assay yield determination. Additional details (reactor volumes and flow rates) of experiments presented in Table 3.4 (page 173) are included in Table 3.11 (page 209).

3.4.16 General Procedures for Synthesis of **1** on 1–10 g scale

Synthesis of 1-(6-Bromo-2-methoxyquinolin-3-yl)-4-(dimethylamino)-2-(naphthalen-1-yl)-1-phenylbutan-2-ol (**1**) on 1-gram Scale.

A flame-dried Schlenk flask (25 mL) was charged with a solution of LiBr (620 mg, 7.13 mmol, 2.3 equiv) in THF (5 mL) under Ar atmosphere (gentle heating may be required for dissolution). The respective amine (1.5 equiv) was added, the solution was cooled in an ice bath and a solution of *n*-BuLi (1.3 equiv, 2.5 M in hexanes) was added slowly. After stirring for 15 min, the solution was cooled to $-78\text{ }^{\circ}\text{C}$ and quinoline **3** (1.00 g, 3.05 mmol, 1.0 equiv) in THF (5 mL) was added dropwise over 15 min. The mixture was stirred for 1 h at $-78\text{ }^{\circ}\text{C}$. Afterwards, the ketone **2** (832 mg, 3.66 mmol, 1.2 equiv) was dissolved in anhydrous THF (3 mL) under Ar-Atmosphere and added dropwise over 15 min to the deep purple reaction mixture. After 1 h, the reaction mixture was quenched by the slow addition of sat. NH_4Cl solution (aq, 2–3 mL). The cooling bath was removed and the two-phase mixture was transferred to a separation funnel. The mixture was extracted with CH_2Cl_2 (3 x 10 mL) and the organic layers were dried over Na_2SO_4 . All volatiles were removed and the residue was recrystallized in 3–4 mL toluene. The solution was cooled slowly to room temperature and then put in the fridge overnight. After precipitation, the undesired diastereomer is filtered off, washed with 1–2 mL $0\text{ }^{\circ}\text{C}$ toluene. The solvent of the mother liquor is removed, the residue is recrystallized two times from EtOH (3–4 mL) and after filtration, and washing with EtOH and drying in vacuo the desired diastereomer was obtained as a colorless solid in yields up to 61% with a d.r. up to 300 : 1.

Analytical Data of the (*RS,SR*)-Diastereomer 1a:

- $R_f = 0.35$ (*c*-Hex/EtOAc 1:1).
- Melting point: 193.4–193.6 °C.
- ^1H NMR (300 MHz CDCl_3): $\delta = 8.90$ (s, 1H), 8.61 (d, $J = 8.8$ Hz, 1H), 8.36 (s, 1H), 7.97 (d, $J = 2.2$ Hz, 1H), 7.94–7.85 (m, 2H), 7.75–7.58 (m, 4H), 7.52–7.44 (m, 1H), 7.36–7.27 (m, 1H), 7.17–7.09 (m, 2H), 6.94–6.86 (m, 3H), 5.89 (s, 1H), 4.21 (s, 3H), 2.67–2.41 (m, 1H), 2.17–1.88 (m, 9H).
- $^{13}\text{C}\{^1\text{H}\}$ NMR (75 MHz, CDCl_3): $\delta = 161.5, 143.9, 141.8, 140.7, 138.9, 134.8, 132.1, 130.1, 130.0, 129.9, 128.7, 128.3, 128.0, 127.5, 127.3, 127.0, 125.9, 125.4, 125.3, 125.2, 124.6, 117.1, 82.7, 56.5, 54.3, 49.7, 44.8, 33.6$.
- IR: 2980, 2949, 2858, 2823, 2782, 1616, 1598, 1566, 1511, 1081, 753.
- MS (ESI): m/z (%) = 555.2 (100), 557.2 (97) $[\text{M}+\text{H}]^+$.

Representative Procedure for Synthesis of 1-(6-Bromo-2-methoxyquinolin-3-yl)-4-(dimethylamino)-2-(naphthalen-1-yl)-1-phenylbutan-2-ol (1**) on 5 and 10 g scale (5 g scale, 10 V solvent).**

In an oven dry round-bottom flask charged with a stir bar, freshly distilled pyrrolidine (1.90 mL, 22.9 mmol, 1.5 equiv), anhydrous LiBr (610 mg, 35.1 mmol, 2.3 equiv) and anhydrous THF (15 mL, 3 V) were taken under N₂ atmosphere. After LiBr was completely dissolved, the reaction mixture was cooled to 0 °C and titrated *n*-BuLi (19.8 mmol, 1.3 equiv) was added dropwise. After 20 min, the round-bottom flask was transferred to a -78 °C bath (acetone/dry ice) and a solution of quinoline **3** (5.005 g, 15.2 mmol, 1.0 equiv) in anhydrous THF (25 mL, 5 V) was added dropwise over an 1 h period (25 mL/h) into the reaction mixture. Then a solution of ketone **2** (4.150 g, 19.29 mmol, 1.2 equiv) in anhydrous THF (10 mL, 2 V) was added into the reaction mixture over 1 h (10 mL/h) at same temperature. After the whole volume of the ketone **2** solution was added, the reaction was stirred for another 15 min, and then quenched by using 10 mL (2 V) aq. NH₄Cl (dropwise) at -78 °C. The reaction mixture was directly poured into a separating funnel. Water was added (20 mL) and the extraction performed with CH₂Cl₂ (3 x 30 mL). The organic layer was concentrated under reduced pressure and purified by silica gel column chromatography or crystallization. Conditions for column chromatography: Silica gel (10–50% EtOAc/hexanes). Examples are tabulated in Table 3.12 on page 209.

Results from purification by column chromatography: Pure compound **1** was obtained as three fractions after chromatography, one of which contained a mixture of isomers **1a** and **1b**. Total combined yield of **1** (**1a+1b**) (7.77 g, 14.0 mmol, 83–90% purity, 80% yield of **1**). The fraction containing **1a** was isolated (3.97 g, 7.15 mmol, with 90% purity, 42% yield **1a**). The fraction containing **1b** was isolated (1.59 g, 2.86 mmol, with 84% purity, 16% yield **1b**).

Experimental procedure for crystallization: In a round-bottom flask containing the concentrated reaction mixture, 4 V of toluene was added, and the resulting suspension heated to reflux for 10 min until fully dissolved. The solution was cooled to room temperature and left in the fridge at 0–5 °C overnight. The pale-yellow solid was filtered and washed with toluene to get the pure undesired diastereomer, **1b**. The mother liquor were concentrated to dryness and dissolved in 4 V of ethanol and stirred for 3 h at room temperature. The solid was filtered off and washed with cold ethanol to obtain desired diastereomer, **1a**. The final mother liquor contains only unreacted starting materials **2** and **3**. Isolated yields for several representative examples are summarized in Table 3.12 (page 209) and Table 3.13 (page 210).

3.4.17 General Procedure: Enantioselective Synthesis of Bedaquiline Using Chiral Secondary Amine Bases

General Procedure A

- 200 mg scale, *n*-BuLi addition at $-78\text{ }^{\circ}\text{C}$, warm R_2NLi to room temperature for 10 min, re-cool

Lithium chloride was dried overnight in a vacuum oven, then used to prepare a stock solution of LiCl in THF (0.5 M). To a solution of LiCl in THF (0.5 M, 1.6 mL) was added secondary amine or diamine (0.91 mmol, 1.5 equiv). The solution was cooled to $-78\text{ }^{\circ}\text{C}$ and *n*-BuLi (0.79 mmol, 1.3 equiv for amine; 1.6 mmol, 2.6 equiv for diamine; 2.5 M solution in THF titrated prior to use) was added dropwise with stirring. The solution was allowed to warm to room temperature over 10 min then re-cooled to $-78\text{ }^{\circ}\text{C}$ over 10 min. To the cooled reaction mixture was added quinoline **3** (200 mg, 0.61 mmol) in THF (0.8 mL) dropwise over approximately 5 min. The solution was stirred at $-78\text{ }^{\circ}\text{C}$ for a further 10 min. A solution of ketone **2** (166 mg, 0.73 mmol) in THF (0.8 mL) was added slowly over 5 min. The reaction was stirred for a further 10 min then quenched by slow addition of 25 wt% NH_4Cl solution (aq). The aqueous layer was extracted twice with CH_2Cl_2 (2 x 3 mL) and the combined organic layers were dried over NaSO_4 and filtered. Benzyl benzoate was added (58 μL , 0.30 mmol), and a 1 mL aliquot was concentrated and analyzed by ^1H NMR (400 MHz, CDCl_3) using a 30 s relaxation delay. For the highest yielding samples, the NMR sample was recovered and the crude residue was dissolved in a minimal amount of CH_2Cl_2 and purified by column chromatography on silica gel, 12–100% EtOAc/hexanes for separation of the diastereomers. The resulting purified salts subjected to chiral SFC for separation of the enantiomers of **1**.

General Procedure B

- 50 mg scale, *n*-BuLi addition at $-78\text{ }^{\circ}\text{C}$, warm R_2NLi to room temperature for 20 min, re-cool

Lithium chloride was dried overnight in a vacuum oven, then used to prepare a stock solution of LiCl in THF (0.5 M). To a solution of LiCl in THF (0.5 M, 400 μL ; or salt solution as indicated in table) was added secondary amine or diamine (0.91 mmol, 1.5 equiv). The solution was cooled to $-78\text{ }^{\circ}\text{C}$ and *n*-BuLi (0.79 mmol, 1.3 equiv for amine; 1.6 mmol, 2.6 equiv for diamine; 2.5 M solution in THF titrated prior to use) was added dropwise with stirring. The solution was allowed to warm to room temperature over 20 min then re-cooled to $-78\text{ }^{\circ}\text{C}$ over 10 min. To the cooled reaction mixture was added quinoline **3** (200 mg, 0.61 mmol, WuXi) in THF (0.8 mL) dropwise over approximately 5 min. The solution was stirred at $-78\text{ }^{\circ}\text{C}$ for a further 30 min. A solution of ketone **2** (166 mg, 0.73 mmol) in THF (0.8 mL) was added slowly over 5 min. The reaction was stirred for a further 10 min then quenched by slow addition of 25 wt% ammonium chloride solution (aq). The aqueous layer was extracted twice with CH_2Cl_2 (2 x 3 mL) and the combined organic layers were dried over NaSO_4 and filtered. Benzyl benzoate was added (58 μL , 0.30 mmol), and a 1 mL aliquot was concentrated and analyzed by ^1H NMR (400 MHz, CDCl_3) using a 30 s relaxation delay. For the highest yielding samples, the NMR sample was recovered and the crude residue was dissolved in a minimal amount of CH_2Cl_2 and purified by column chromatography on silica gel, 12–100% EtOAc/hexanes for separation of the diastereomers. The resulting purified salts subjected to chiral SFC for separation of the enantiomers of **1**.

General Procedure C

- *n*-BuLi addition at 0 °C, stir 30 min, cool to -78 °C

A dry 2-dram vial was charged with LiBr (30 mg, 0.35 mmol) and THF (400 uL). Amine was added (0.23 mmol, 1.5 equiv) at room temperature and the solution was cooled to 0 °C. *n*-BuLi (0.20 mmol, 1.3 equiv, 2.5 M solution in THF titrated prior to use) was added dropwise with stirring. The solution was stirred at 0 °C for 30 min. The resulting solution was cooled to -78 °C, then to this was added quinoline **3** (50 mg, 0.15 mmol, 1 equiv) in THF (300 uL) dropwise over approximately 2 min. The solution was stirred at -78 °C for a further 30 min. A solution of ketone **2** (41 mg, 0.18 mmol, 1.2 equiv) in THF (300 uL) was added slowly over 5 min. The reaction was stirred for a further 10 min then quenched by slow addition of 25 wt% ammonium chloride solution (aq). Benzyl benzoate (28 μ L, 0.15 mmol) was added. The organic layer was sampled, dried, and analyzed by ¹H NMR (400 MHz, CDCl₃) using a 30 s relaxation delay. For the highest yielding samples, the NMR sample was recovered and the crude residue was dissolved in a minimal amount of CH₂Cl₂ and purified by column chromatography on silica gel, 12–100% EtOAc/hexanes for separation of the diastereomers. The resulting purified salts subjected to chiral SFC for separation of the enantiomers of **1**.

General Procedure for Sample Preparation, Chiral SFC Analysis of Bedaquiline Isomers

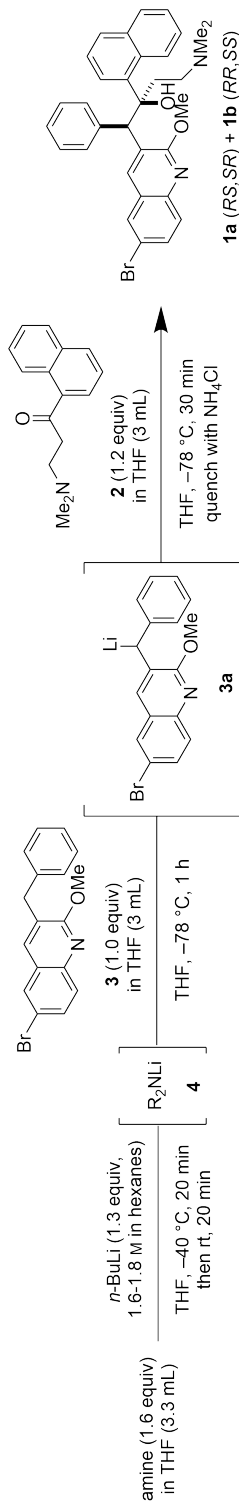
Samples were sent to collaborators at Medicines for All, Virginia Commonwealth University, for enantiomeric ratio analysis. The provided samples were received as known amounts of powder. The samples were dissolved in 6 mL of acetonitrile and sonicated for 15 minutes. BDQ-desired (**1a**) was a clear solution and BDQ-undesired (**1b**) was a clear solution with some remaining particulates. **1b** samples were filtered through 13 mm, 0.45 μm Nylon filters prior to analysis. Enantiomeric ratio was calculated using HPLC Area % values.

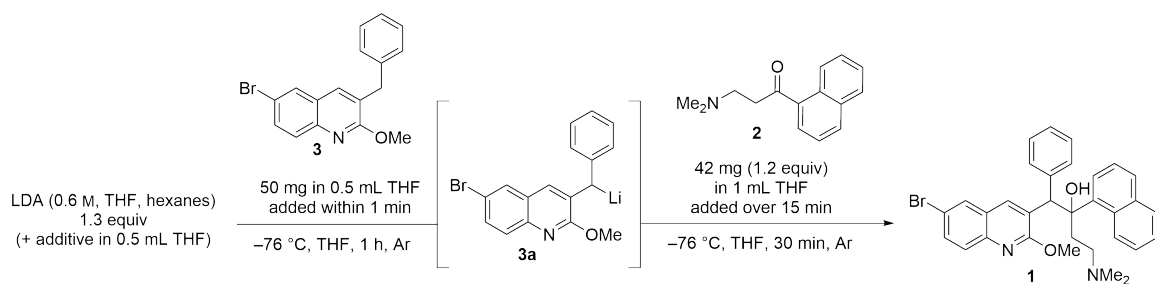
3.4.18 Supplementary Tables

Entry	Amine	Water Content (mol%)	Overall Yield (%) ^a	d.r. (1a:1b)
1	diisopropylamine	7	41	20:21 (0.91 : 1.0)
2	diisopropylamine	0.1	42	20:22 (0.91 : 1.0)
3	pyrrolidine	0.3	55	27:28 (1.0 : 1.0)
4	piperidine	2	42	20:22 (0.91 : 1.0)
5	morpholine	0.4	14	7:7 (1.0 : 1.0)
5b	morpholine, new reagent bottle	–	28	12:16 (0.77 : 1.0)
6	diethylamine	–	32	14:18 (0.77 : 1.0)
7	2,2,6,6-tetramethylpiperidine	–	37	18:19 (0.91 : 1.0)
8	1-methylpiperazine	0.3	65	29:36 (0.83 : 1.2)
9	2-methylpyrrolidine	1	35	17:18 (0.91 : 1.0)
10	<i>N,N'</i> -trimethylethylenediamine	–	48	23:25 (0.91 : 1.0)
11	dicyclohexylamine	–	0	–
12	dimethylamine	2	53	26:27 (1.0 : 1.0)

^a Determined by ¹H NMR using benzyl benzoate as internal standard.

Table 3.6: Tabulated results of secondary amine base screen.





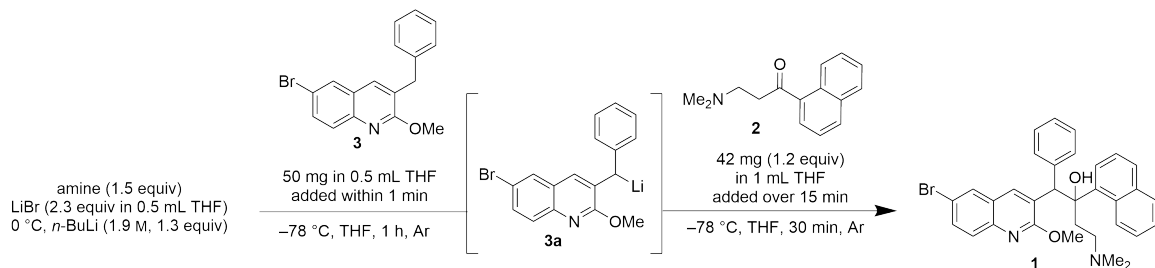
Entry	additive	equiv	d.r. ^a
1	–	–	0.91 : 1.0
2	MgBr ₂ ·OEt ₂	1.3	1.0 : 1.0
3	ZnCl ₂	1.3	– ^b
4	LiBr	1.3	2.0 : 1.0
5	LiCl	1.3	1.2 : 1.0
6	LiI	1.3	1.1 : 1.0
7	LiBr (2-Me-THF)	1.3	– ^c
8	LiBr (DME)	1.3	0.4 : 1.0

^a determined by HPLC (**1a** : **1b**)

^b no conversion (HPLC)

^c product only in traces (HPLC-MS)

Table 3.7: Investigation of the influence of salt additives on diastereoselectivity of the 1,2-addition reaction.



Entry	amine	AY (%) ^a 1a	AY (%) ^a 1 (d.r.) ^b
1 ^c	diisopropylamine	25	37 (2.0 : 1.0)
2 ^c	dicyclohexylamine	0	0
3 ^c	pyrrolidine	53	74 (2.5 : 1.0)
4 ^d	pyrrolidine	57	80 (2.5 : 1.0)
5 ^d	dimethylamine	54	77 (2.4 : 1.0)
6 ^d	<i>N</i> -methylpiperazine	60	92 (1.9 : 1.0)
7 ^d	morpholine	61	87 (2.4 : 1.0)

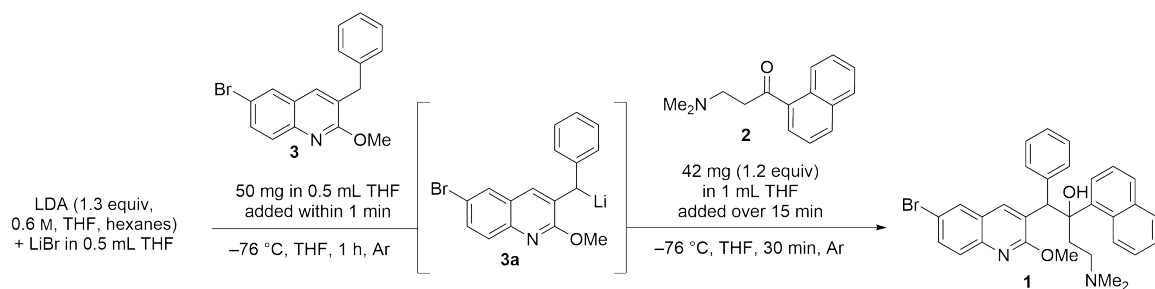
^a Determined by NMR using 1,4-bis(trimethylsilyl)benzene as internal standard.

^b AY 1a : AY 1b

^c 50 mg scale

^d 200 mg scale

Table 3.8: Impact of LiBr on yield and diastereoselectivity of 1,2-addition reaction using different lithium amide bases.



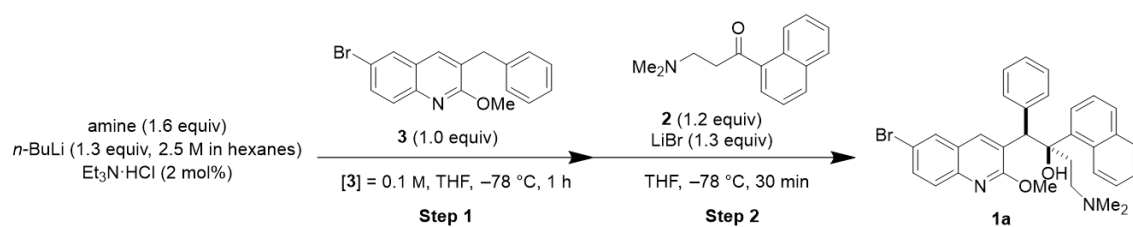
Entry	LiBr (eq)	d.r. (1b/1a)	AY (%) ^b
1 ^a	0.6	1 : 1.1	— ^c
2 ^b	1.1	1 : 1.8	36
3 ^b	1.3	1 : 2.0	42
4 ^b	1.5	1 : 2.0	43
5 ^b	2.0	1 : 1.6	19
6 ^a	2.6	1 : 1.3	— ^c

^a determined by HPLC.

^b Determined by NMR using 1,4-bis-TMS-benzene as internal standard.

^c AY was not determined.

Table 3.9: Assay for stoichiometry of LiBr.



Entry	Amine	Variation	AY 1a (%) ^a	AY 1 (%) ^a (d.r.) ^b
1	pyrrolidine		45	69 (1.9 : 1.0)
2	pyrrolidine	$t_2 = 4$ min	45	68 (2.0 : 1.0)
3	<i>N</i> -methylpiperazine	$t_2 = 4$ min	48	75 (1.8 : 1.0)
4	<i>N</i> -methylpiperazine	$T_1 = 23$ °C $t_1, t_2 = 2$ min	48	74 (1.8 : 1.0)
5	morpholine	$T_1 = 0$ °C $t_1, t_2 = 2$ min	49	76 (1.8 : 1.0)

^a Determined by ¹H NMR

^b AY **1a** : AY **1b**

t = reaction time; T = reaction temperature

Table 3.10: Assay for the influence of reaction time and temperature on yield and diastereoselectivity of lithiation/1,2-addition leading to **1**.

Table 3.4 Entry	Lithiation RV	1,2-Addn RV	Quench RV (mL)	flow A	flow B	flow C	flow quench
1, 2	2	2.5	0.2	0.1	0.1	0.1	0.2
3, 4	1	5	0.5	0.2	0.2	0.2	1
5	0.5	3	0.5	0.2	0.2	0.2	1
6	0.5	3	0.5	0.2	0.2	0.2	0.2
7	0.5	3	0.5	0.5	0.5	0.5	0.5

*flow in mL/min; RV = reactor volume (mL)

Table 3.11: Additional details of flow reaction setup in Table 3.4

Entry	Solvent	V_{total}	[<i>n</i> -BuLi] (M)	Scale of 3 (g)	AY 1 ^a (d.r.) ^b	Isolation	IY (%) ^d
1	10 V	2.45	2.45	5.0	87 (2.2 : 1.0)	chromatog.	79
2	10 V	1.40	1.40	5.0	90 (2.0 : 1.0)	recrys.	80
3	10 V	1.40	1.40	10.0	90 (2.1 : 1.0)	recrys.	77
4	6 V	1.40	1.40	5.0	88 (1.8 : 1.0)	recrys.	73
5	6 V	2.40	2.40	10.0	88 (1.9 : 1.0)	recrys.	75

^a Percent yield determined by ¹H NMR

^b AY **1a** : AY **1b**, triphenylmethane as internal standard

^c Isolated **1** with purity varying from 83 to 92% due to the presence of remaining solvent in the sample

^d Corrected isolated yield of **1** based on sample purity.

Table 3.12: Scale-up of bedaquiline **1** – variation of reaction concentration and use of *n*-BuLi solution with different molarities

Entry	IY 1a [g, mmol, % purity] ^a	IY 1a [%] ^c	IY 1b [g, mmol, % purity] ^a	IY 1b [%] ^c
1 ^d	3.97, 7.15, 90	42	1.59, 2.86, 84	16
2	5.31, 9.56, 90	56	2.12, 3.82, 92	23
3	11.61, 20.9, 88	60	3.21, 5.78, 90	17
4	5.05, 9.09, 91	54	1.75, 3.15, 91	18
5	10.02, 18.0, 87	52	4.28, 7.70, 91	23

^a purity determined by ¹H NMR using triphenylmethane as internal standard

^c Calculated by the product of isolated mass and purity

^d Purified by column chromatography. See further details in descriptive procedure.

Table 3.13: Isolated yields of **1a** and **1b** obtained on 5 g and 10 g scale after purification of corresponding entries 1–5 in Table 3.12.

Entry	Amine	Method	AY 1 (%)	1a : 1b (%)	IY 1a , 1b (%)
1	16	A	69	38 : 31	–
2	17	A	6	3 : 3	–
3	18	B	43	17 : 26	19, 28
4	19	B	69	36 : 33	34, 32
5	8	B ^a	12	4 : 8	–
6	9	B	5	2 : 3	–
7	10	B	58	30 : 23	30, 27
8	11	B	5	2 : 3	–
9	13	B	32	13 : 19	13, 16
10	8	B ^b	0	–	–
11	12 , TCI	B ^c	0	–	–
12	12 , TCI	B ^d	3	1 : 2	–
13	12 , TCI	B ^e	25	10 : 15	9, 15
14	10 , Sigma	B ^d	53	44 : 9	41, 9
15	12 , TCI	C	14	8 : 6	9, 5
16	12 , Chem-Impex	C	0	–	–
17	8	C ^f	0	–	–
18	14	C ^g	0	–	–
19	12 , TCI redistill	C	24	15 : 9	–
20	12 , TCI redistill	C	11	7 : 4	–
21	15	C	7	5 : 2	–

^a *n*-BuLi (0.40 mmol, 2.6 equiv)

^b amine (0.11 mmol, 0.75 equiv); *n*-BuLi (0.20 mmol, 1.3 equiv)

^c commercial LiCl solution (0.5 M in THF, TCI)

^d LiBr (31 mg, 0.35 mmol) in THF (400 μ L)

^e Et₃N·HCl (0.5 mg, 2 mol%) in THF (400 μ L), no LiCl

^f amine (0.23 mmol, 1.5 equiv); *n*-BuLi (0.2 mmol, 1.3 equiv)

^g amine (0.23 mmol, 1.5 equiv); *n*-BuLi (0.4 mmol, 2.6 equiv)

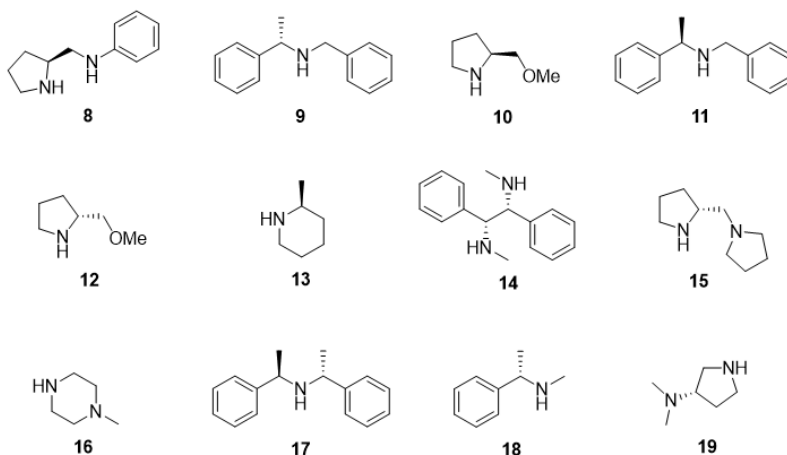
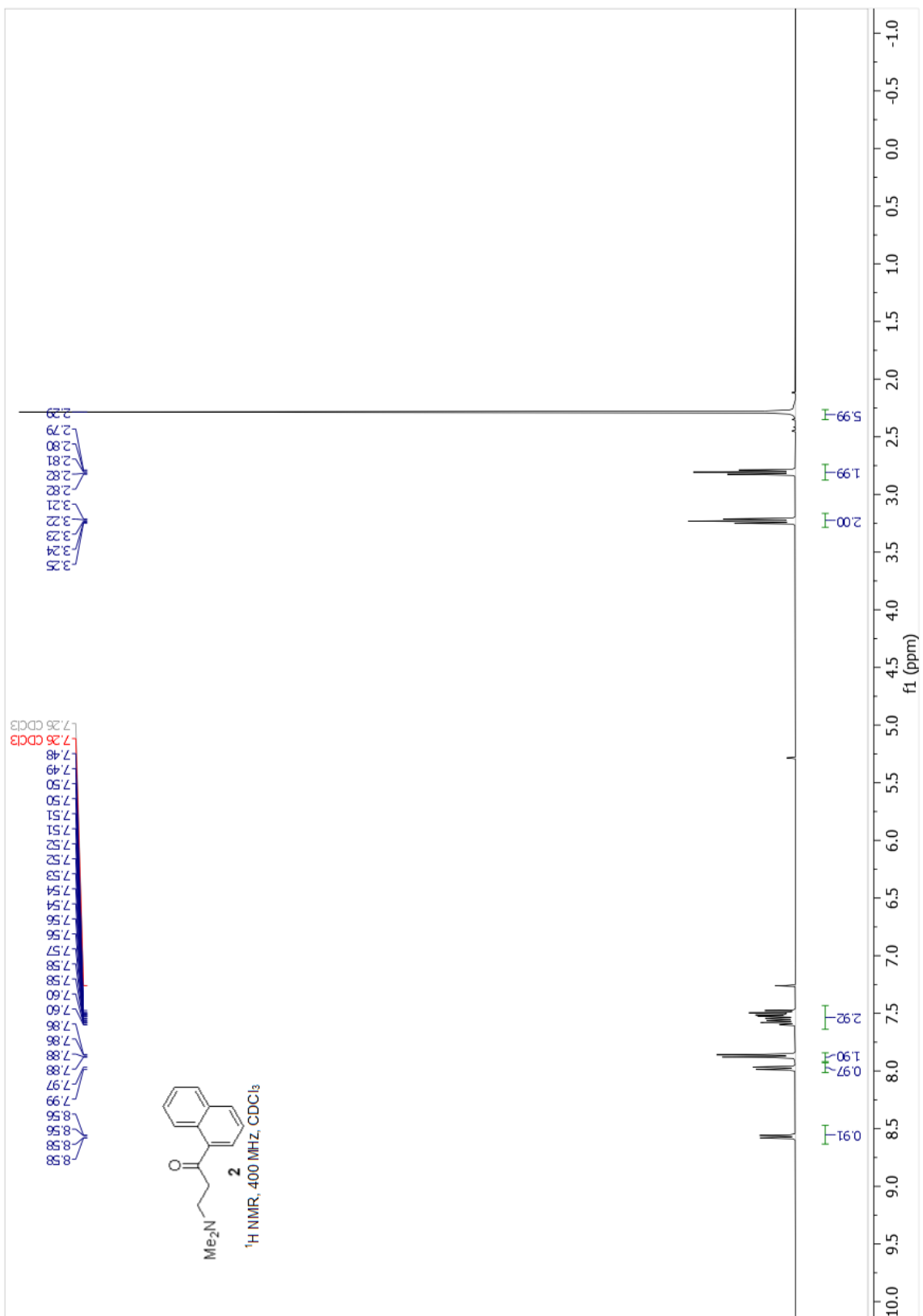
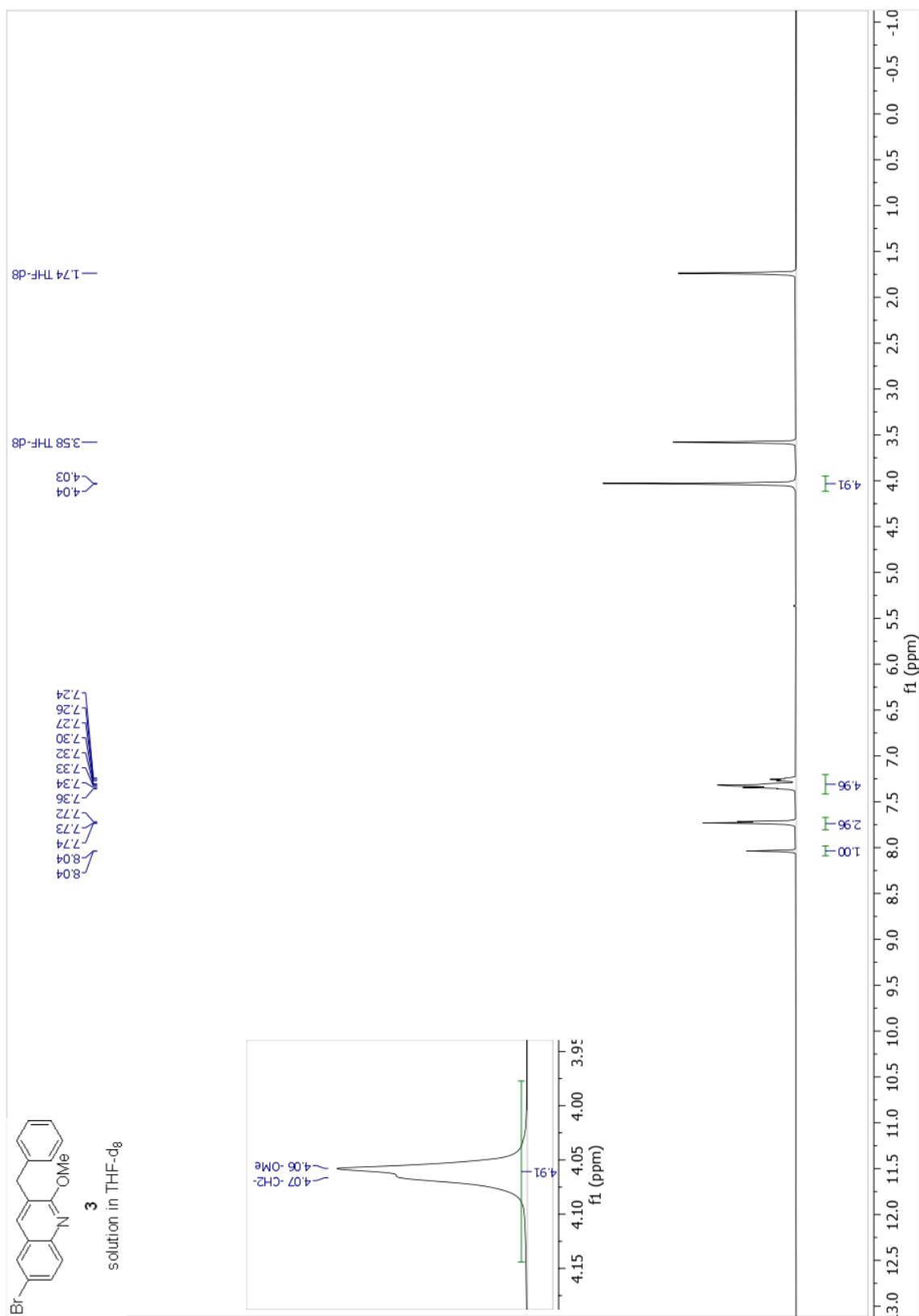
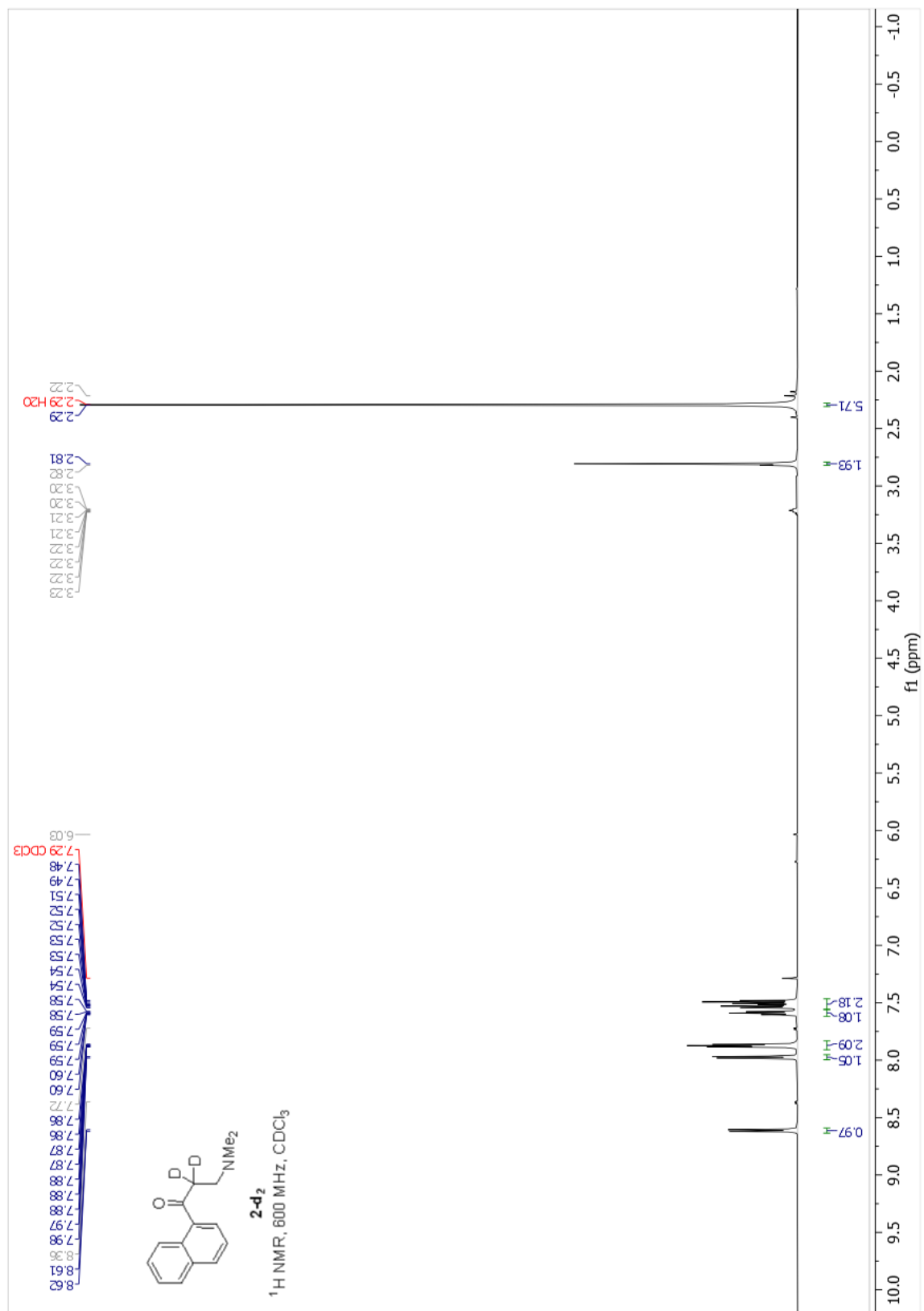


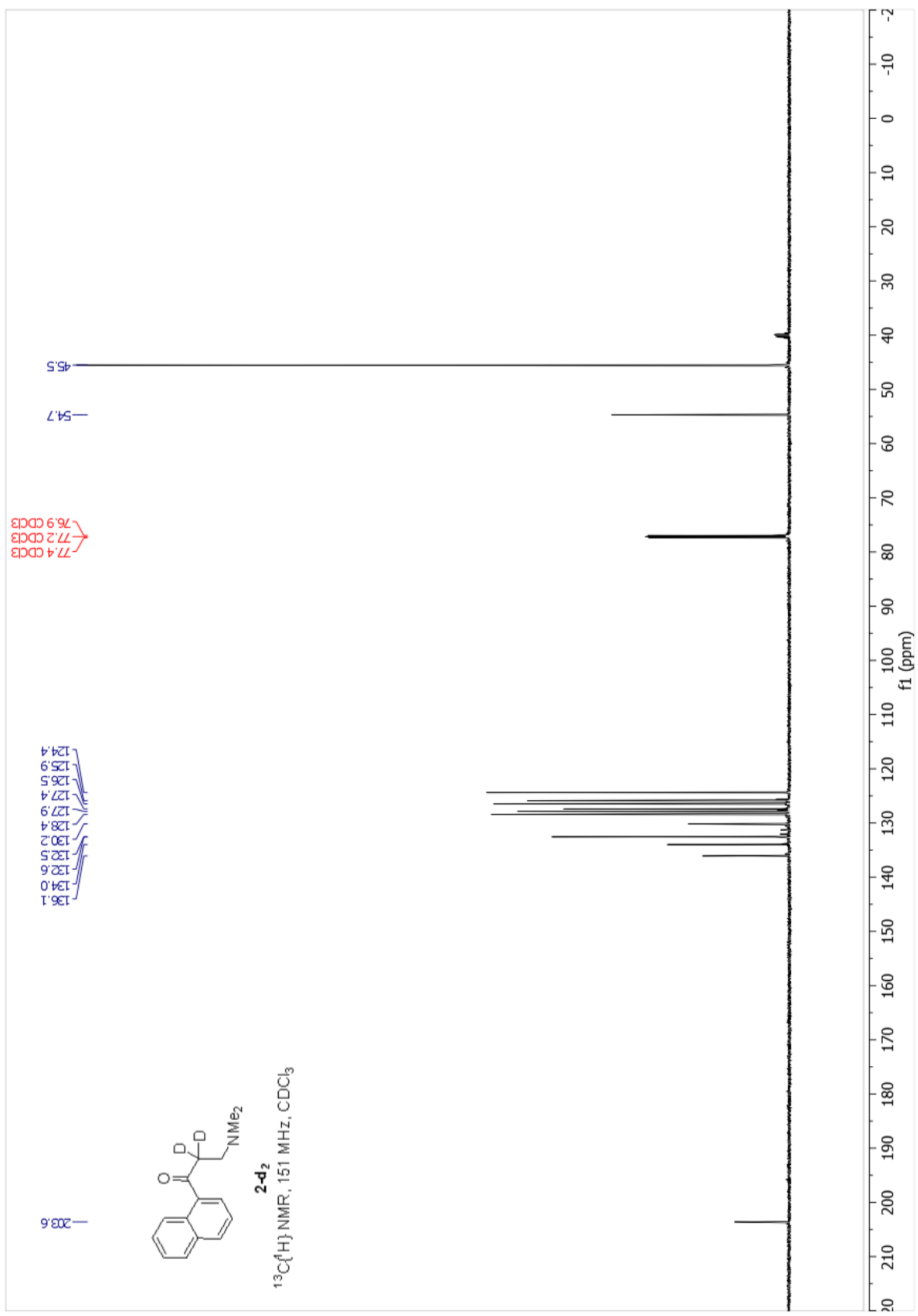
Table 3.14: Assay for enantioselectivity in the synthesis of bedaquiline (**1**) using chiral secondary amine bases. Assay yield determined by ¹H NMR.

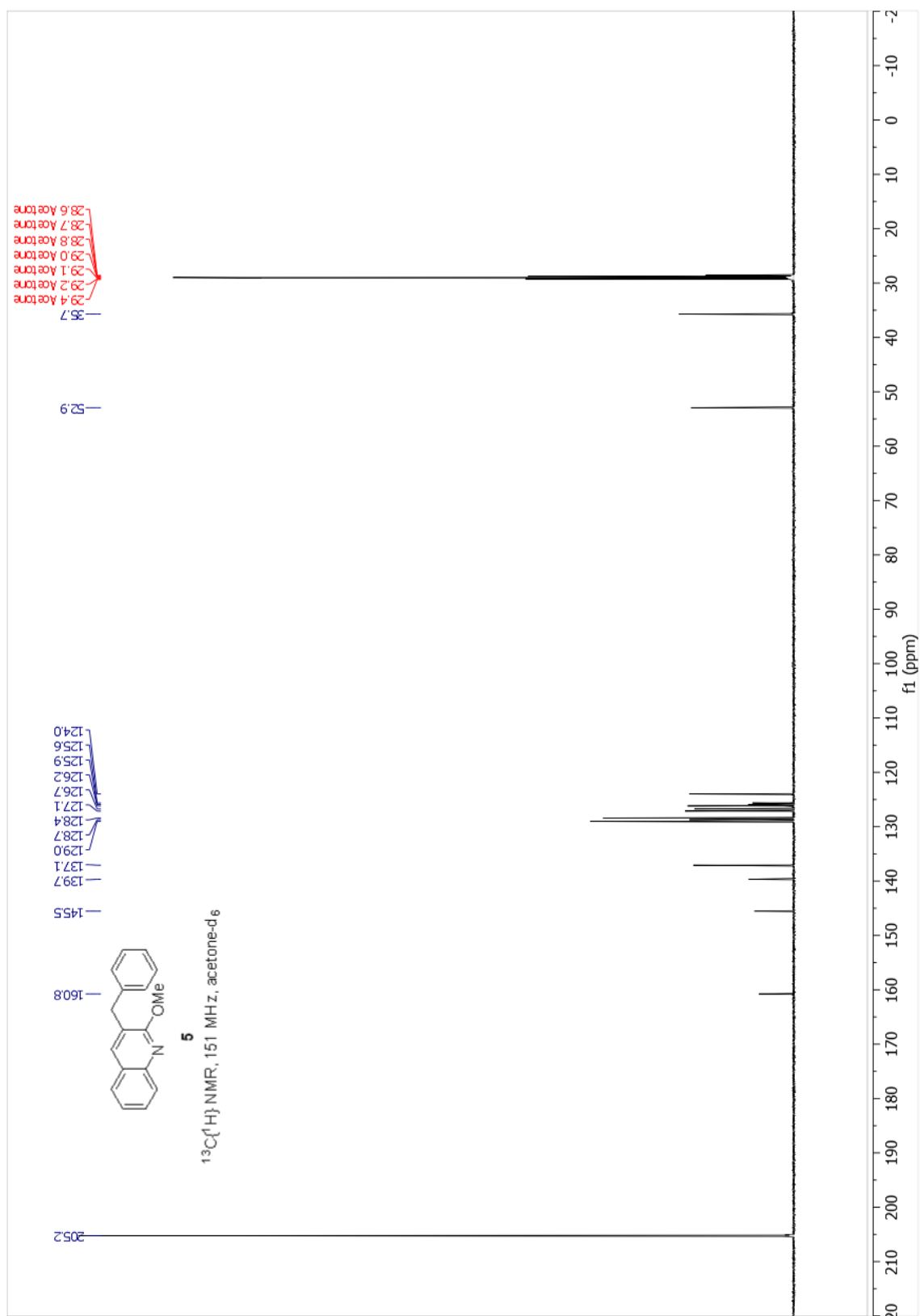
3.5 ^1H and $^{13}\text{C}\{^1\text{H}\}$ NMR Spectra

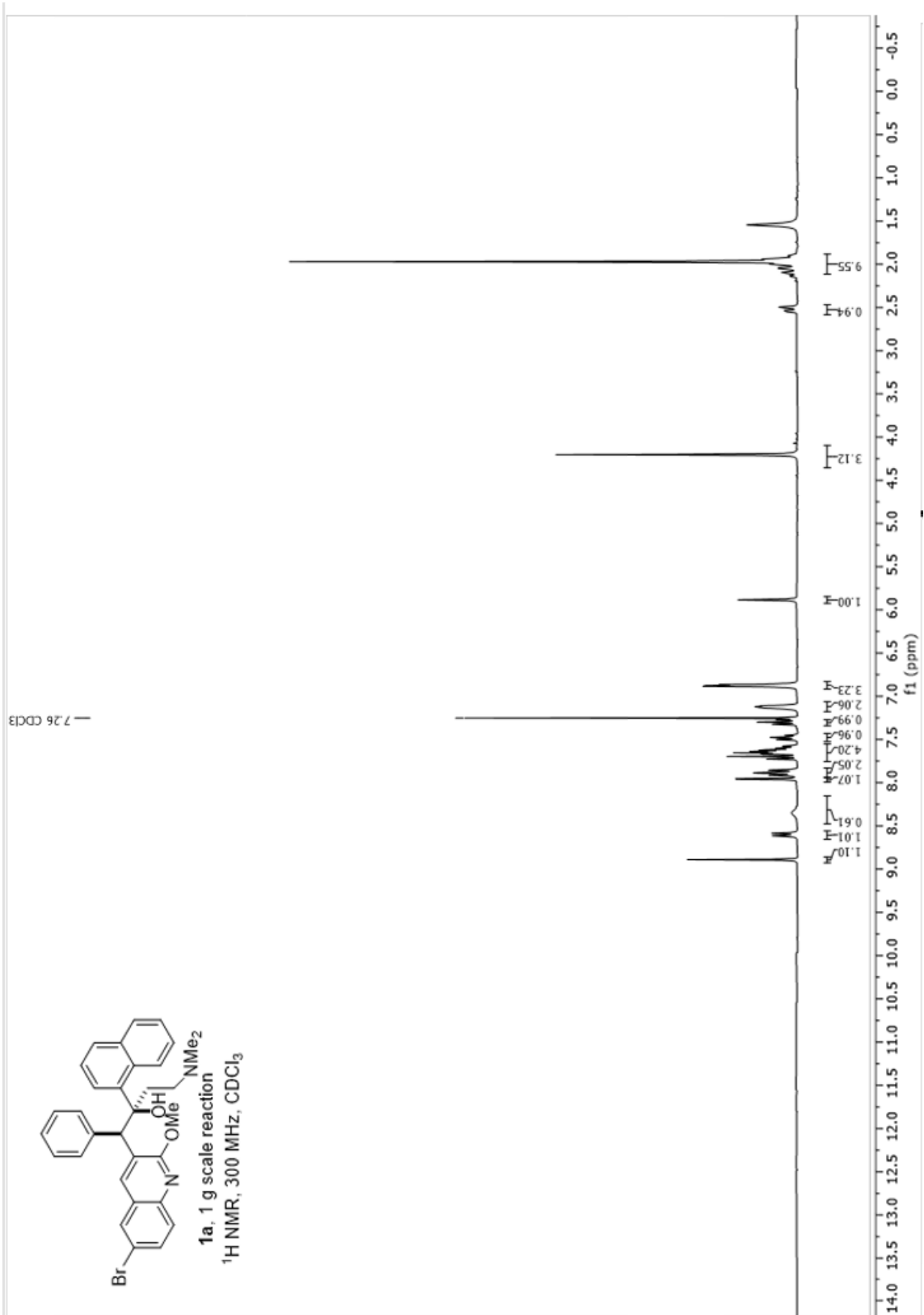


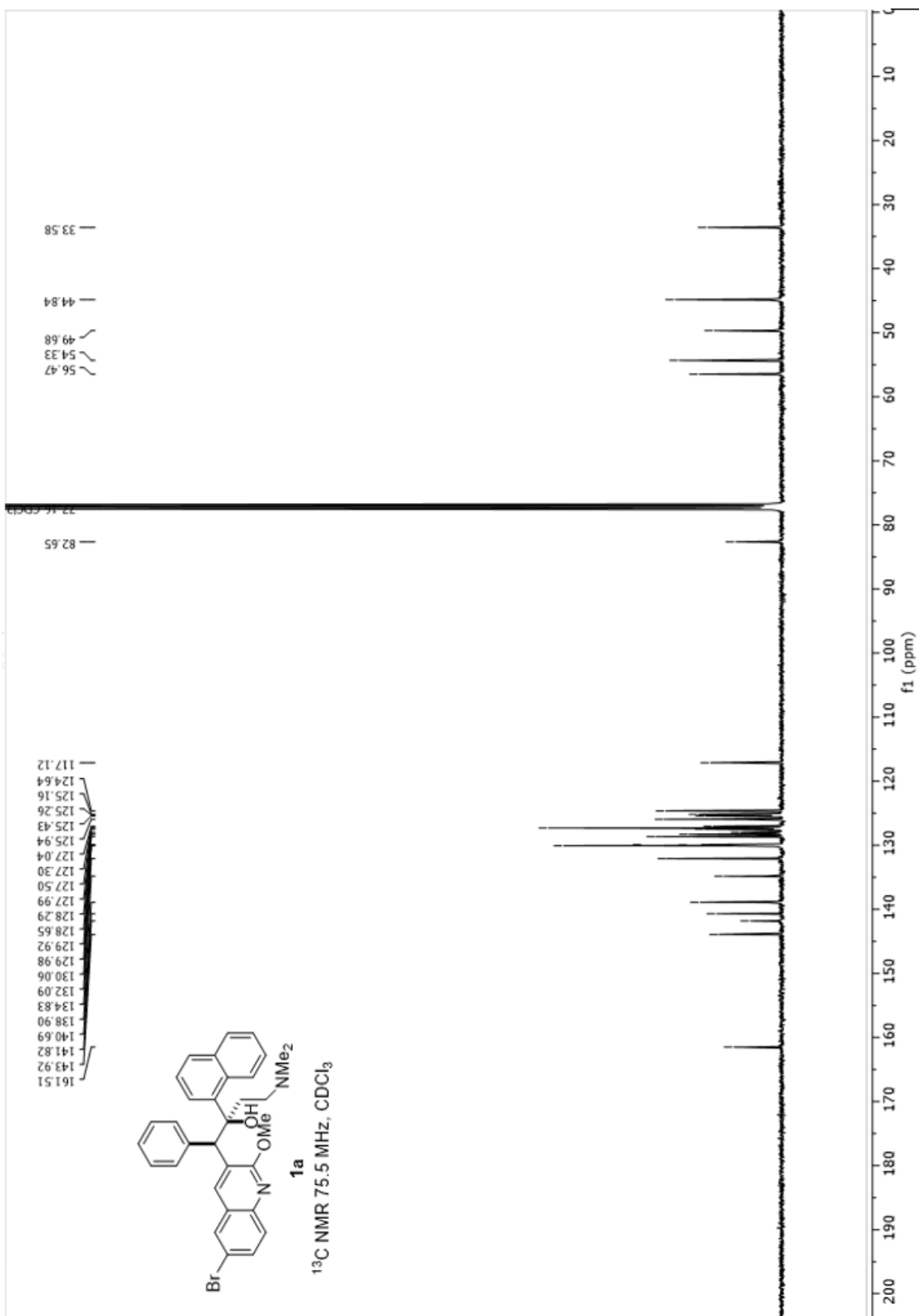


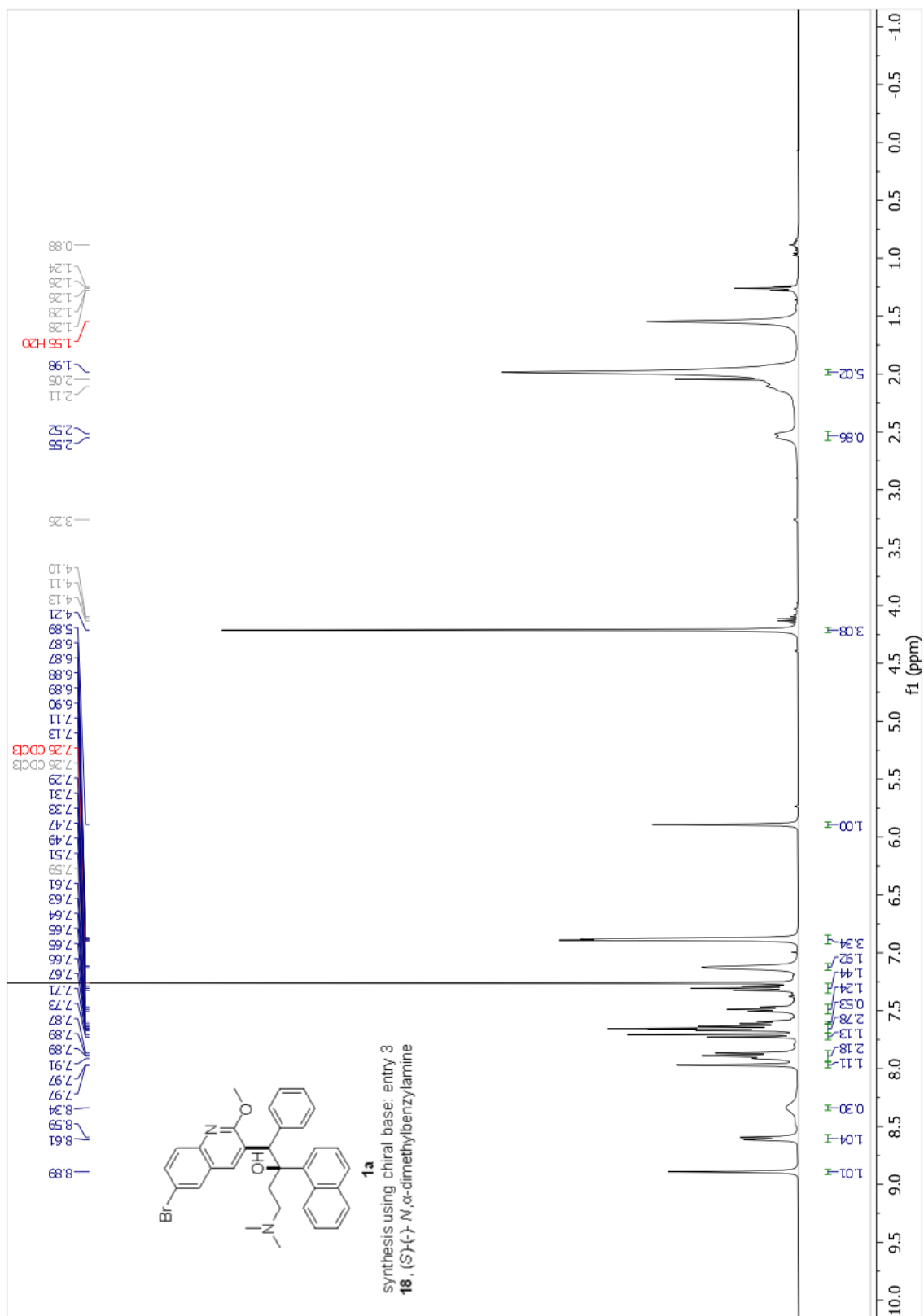


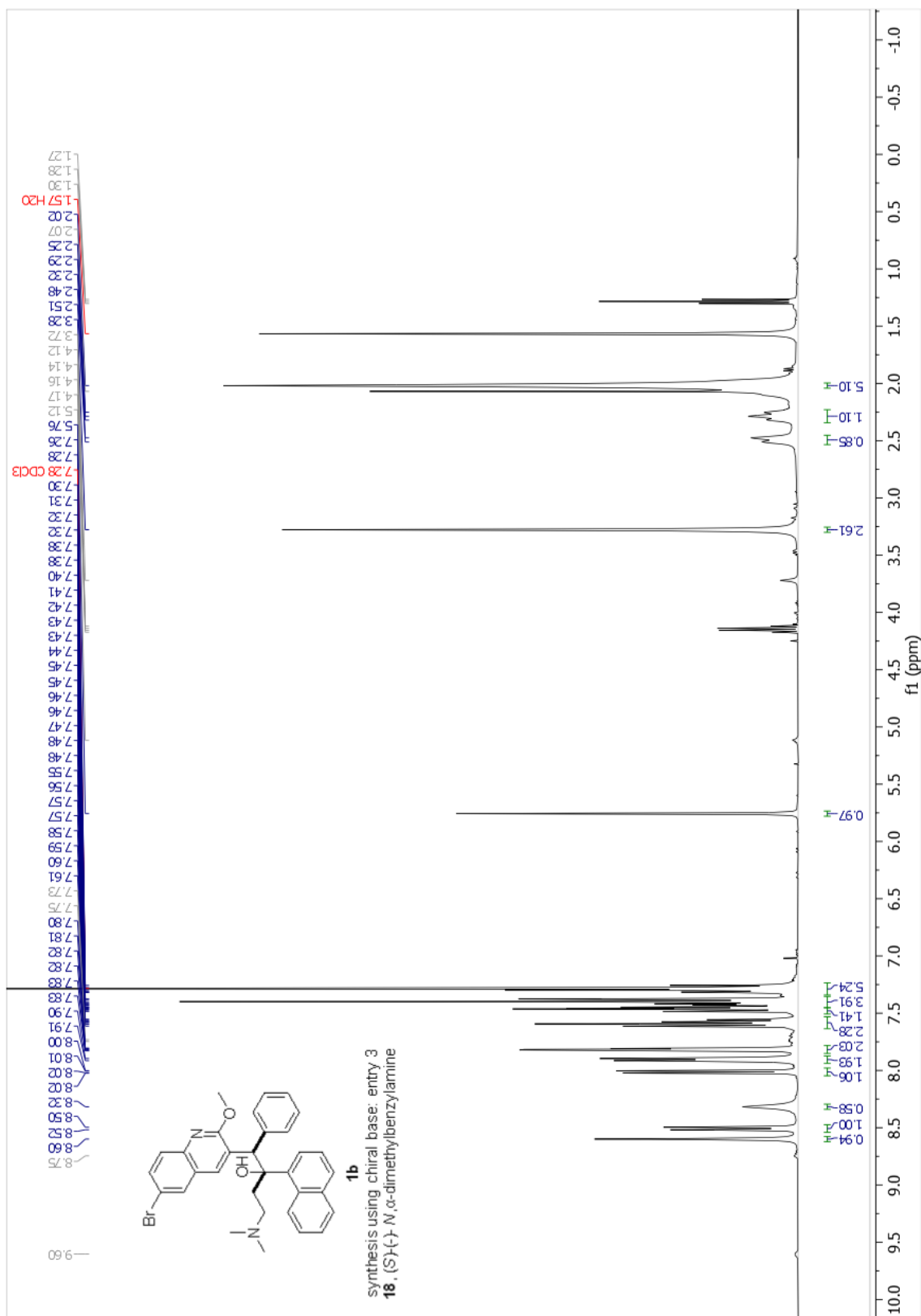


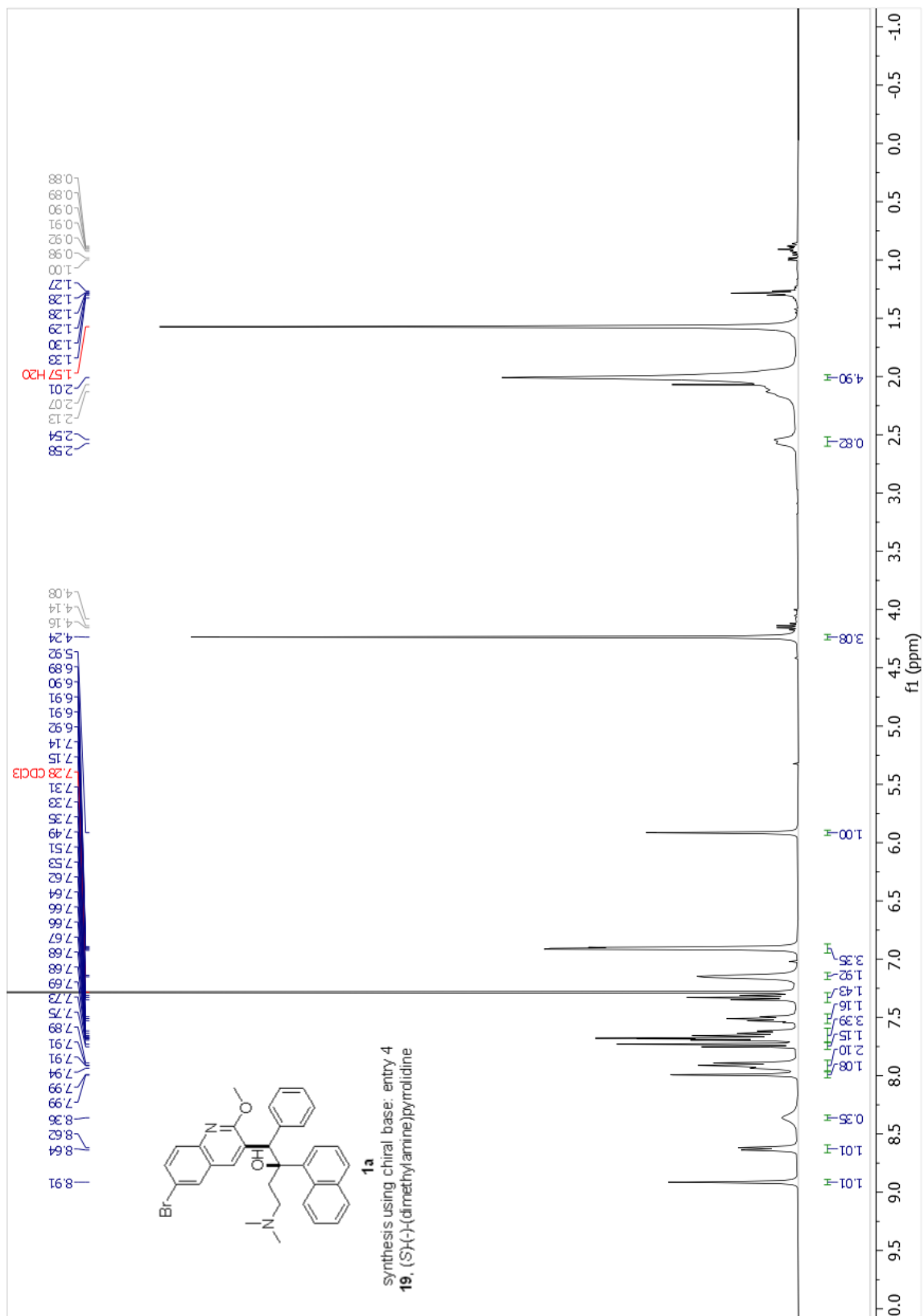


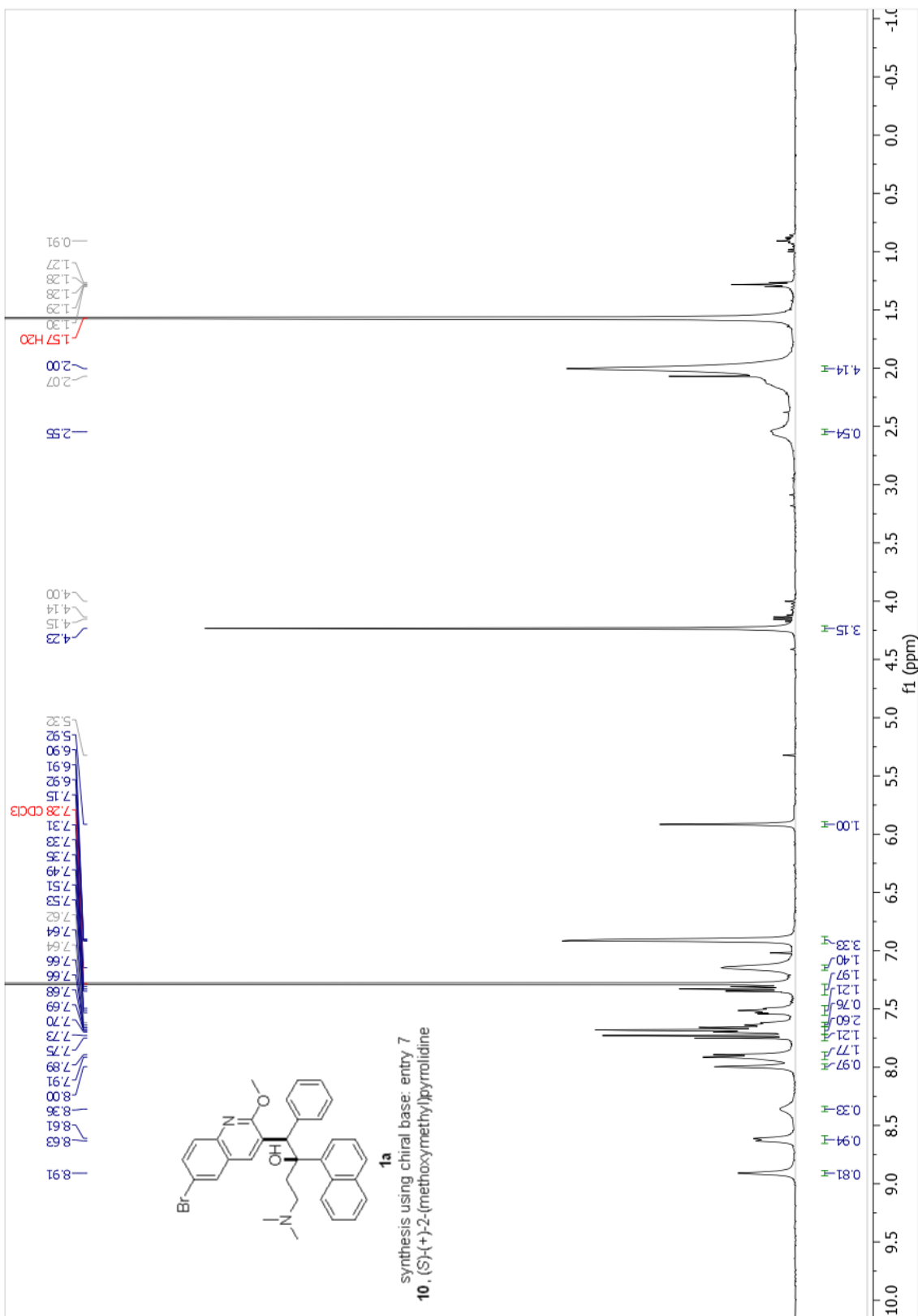


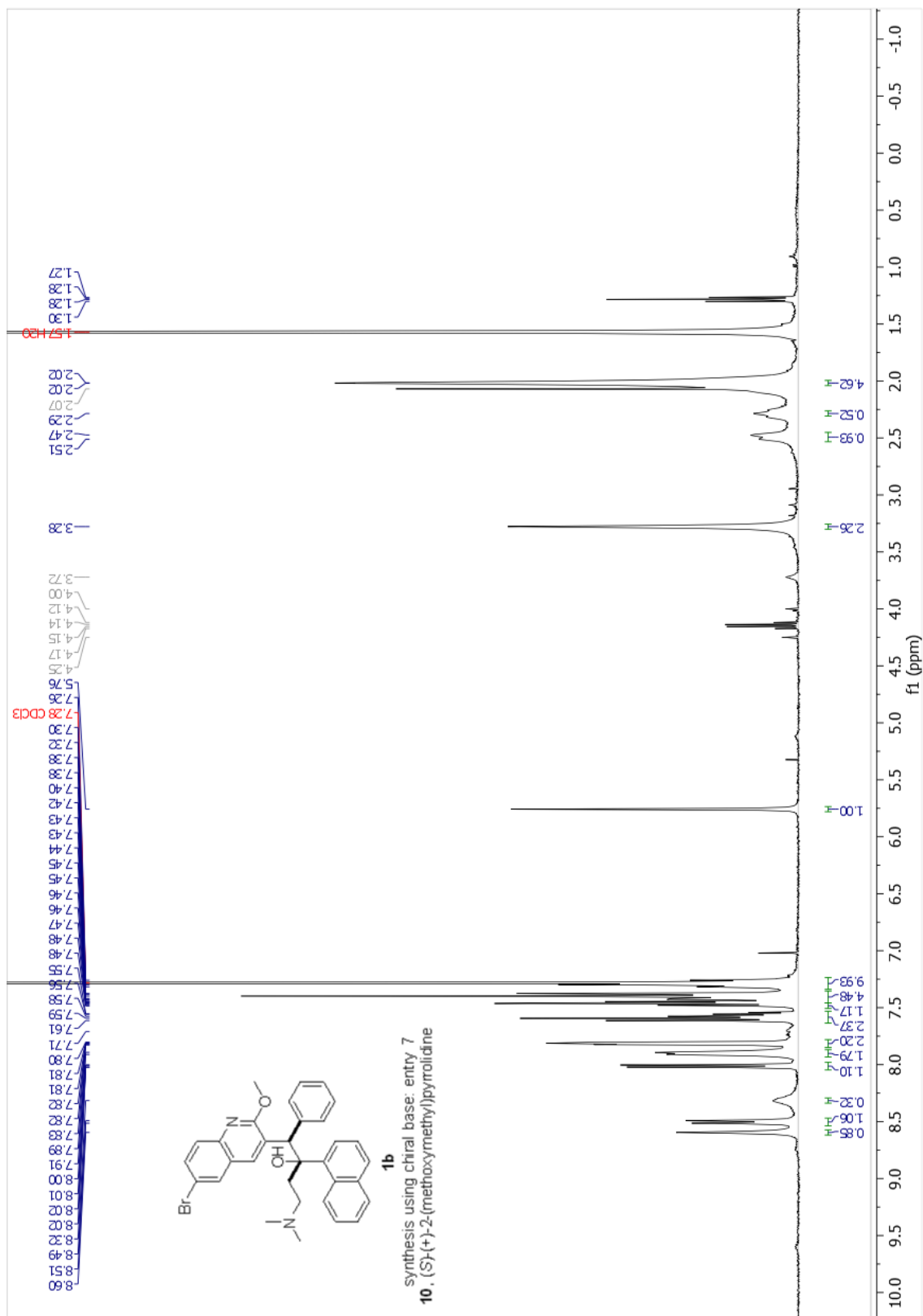


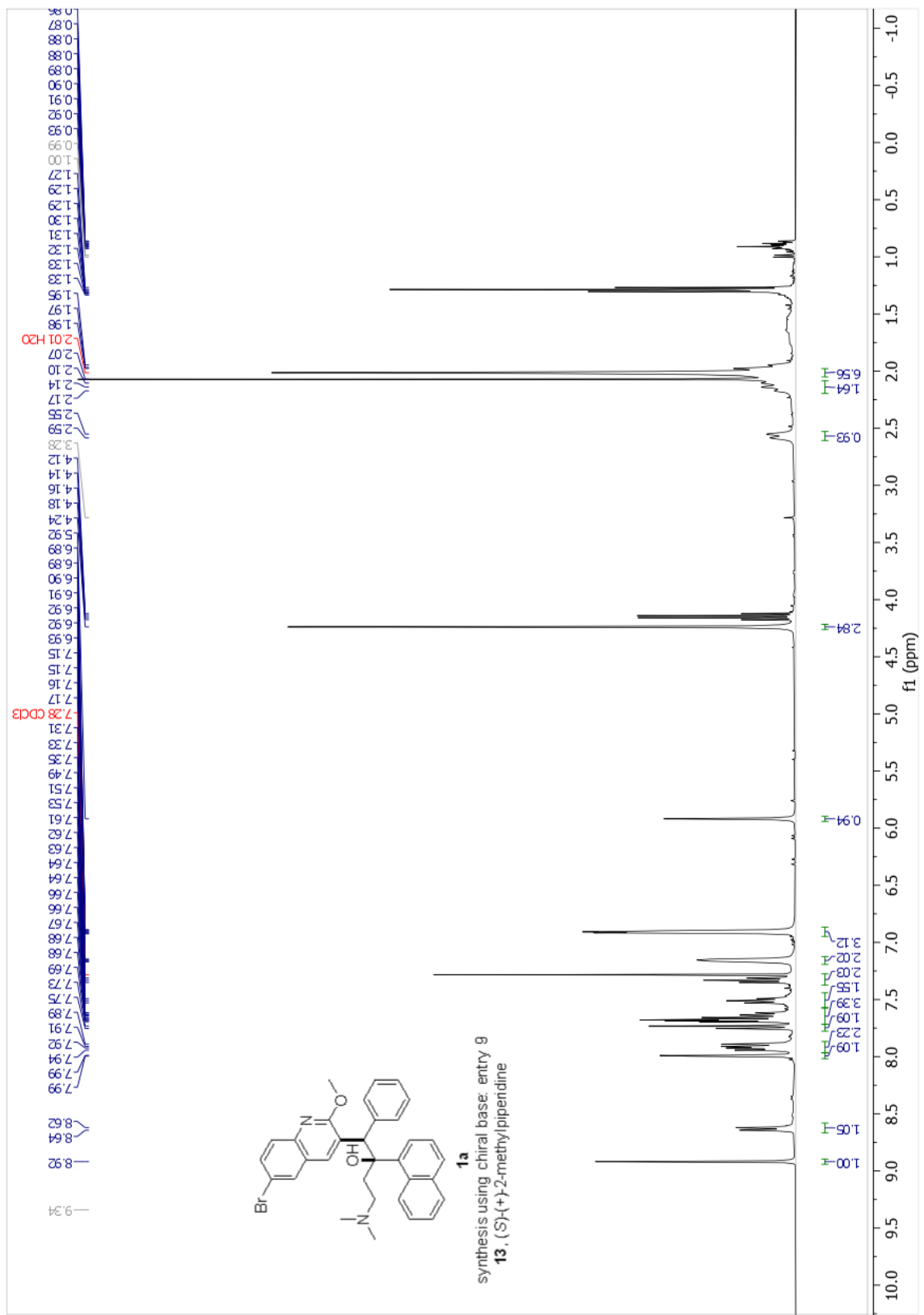


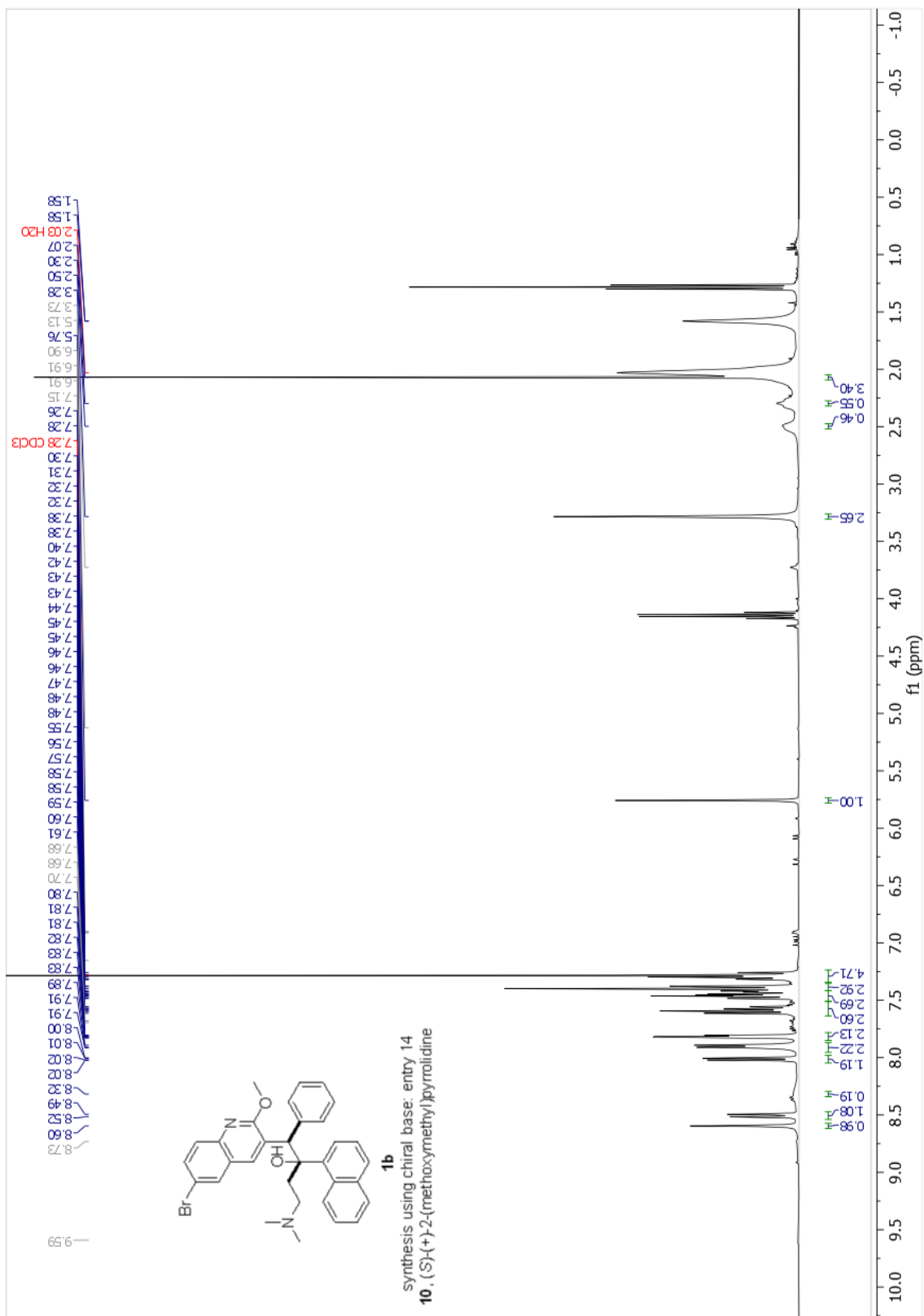


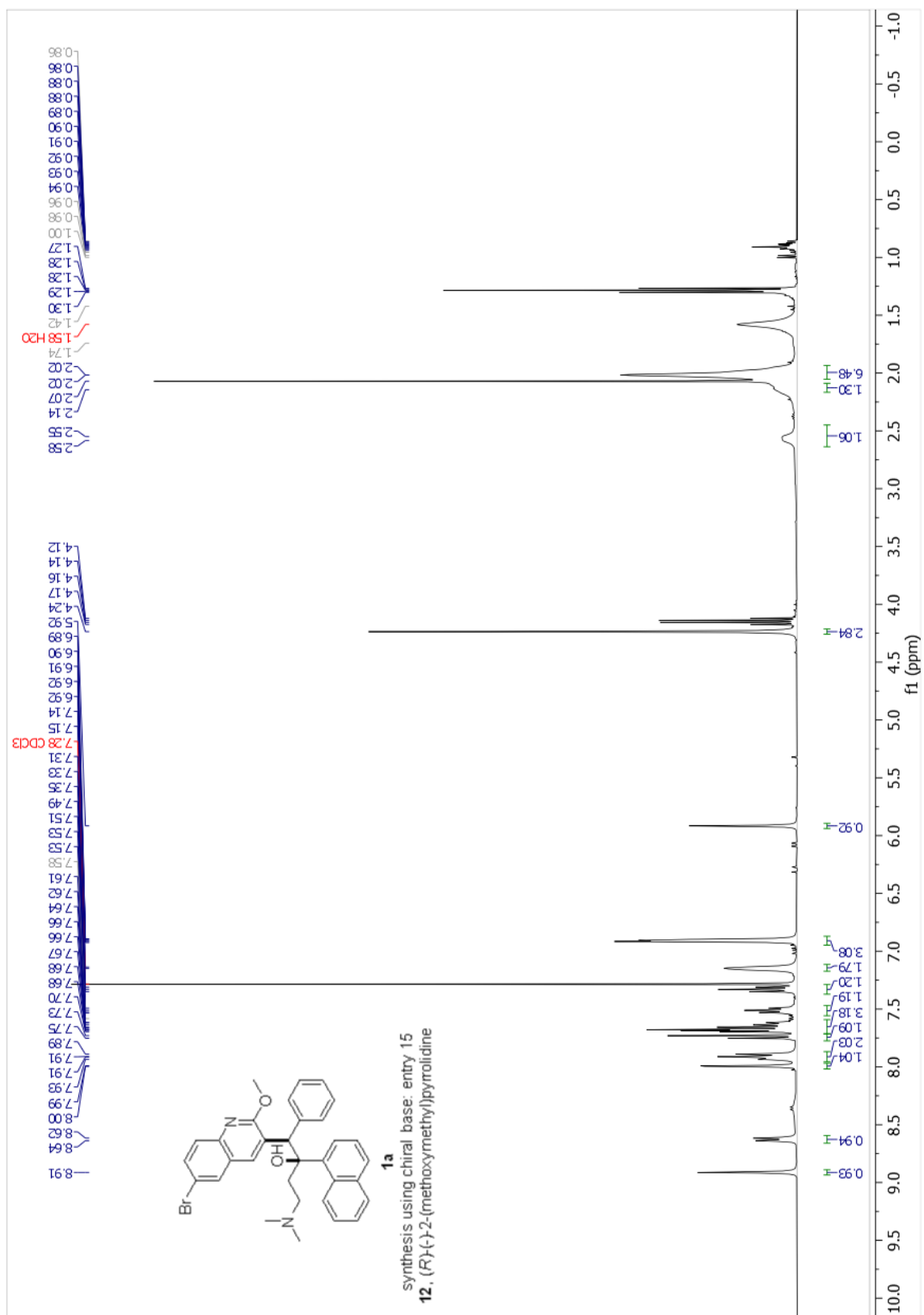


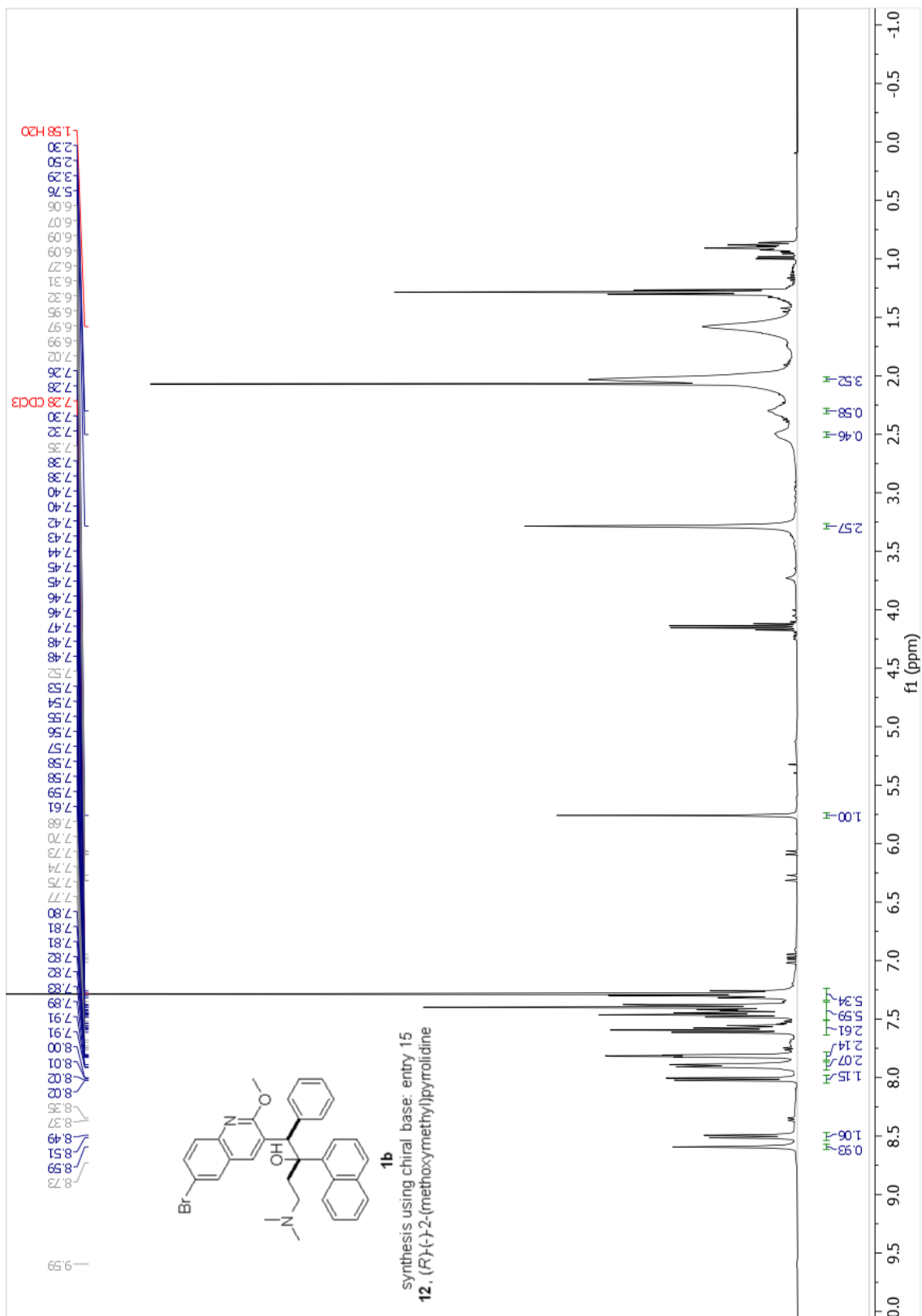












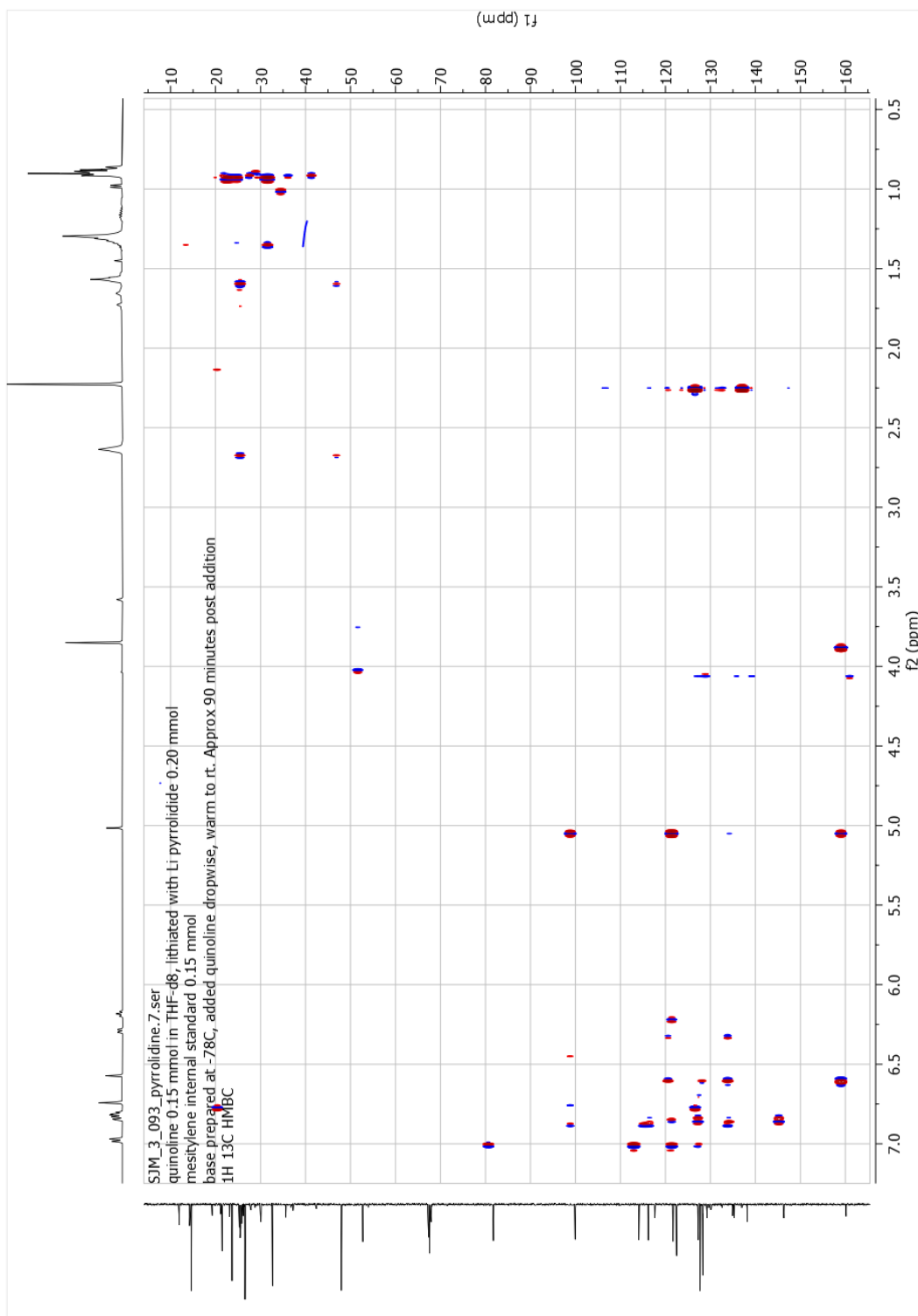


Figure 3-16: ^1H - ^{13}C HSQC of lithium pyrrolidide/**3** reaction mixture in THF- d_8 .

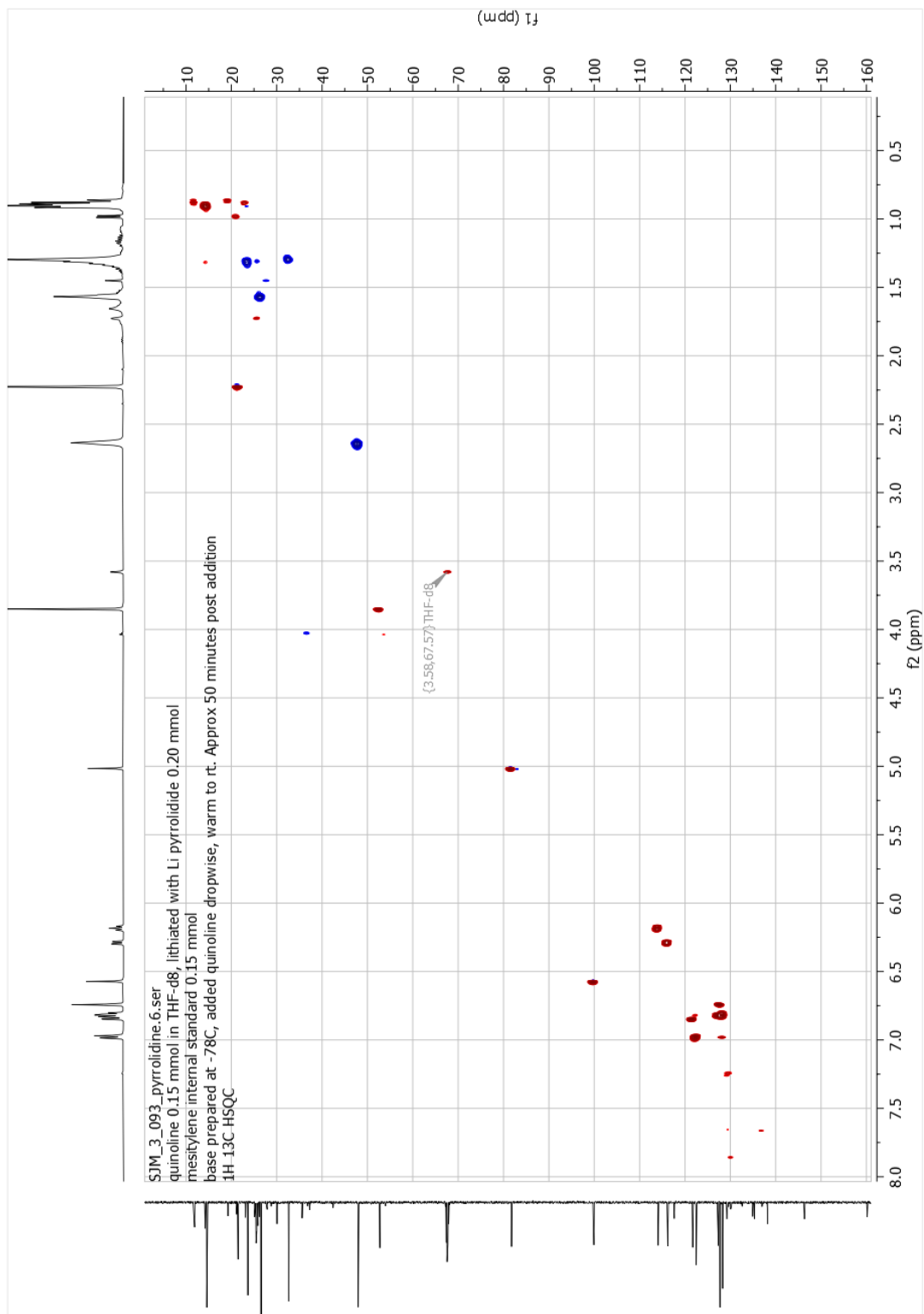


Figure 3-17: ^1H - ^{13}C HMQC of lithium pyrrolidide/**3** reaction mixture in THF- d_8 .

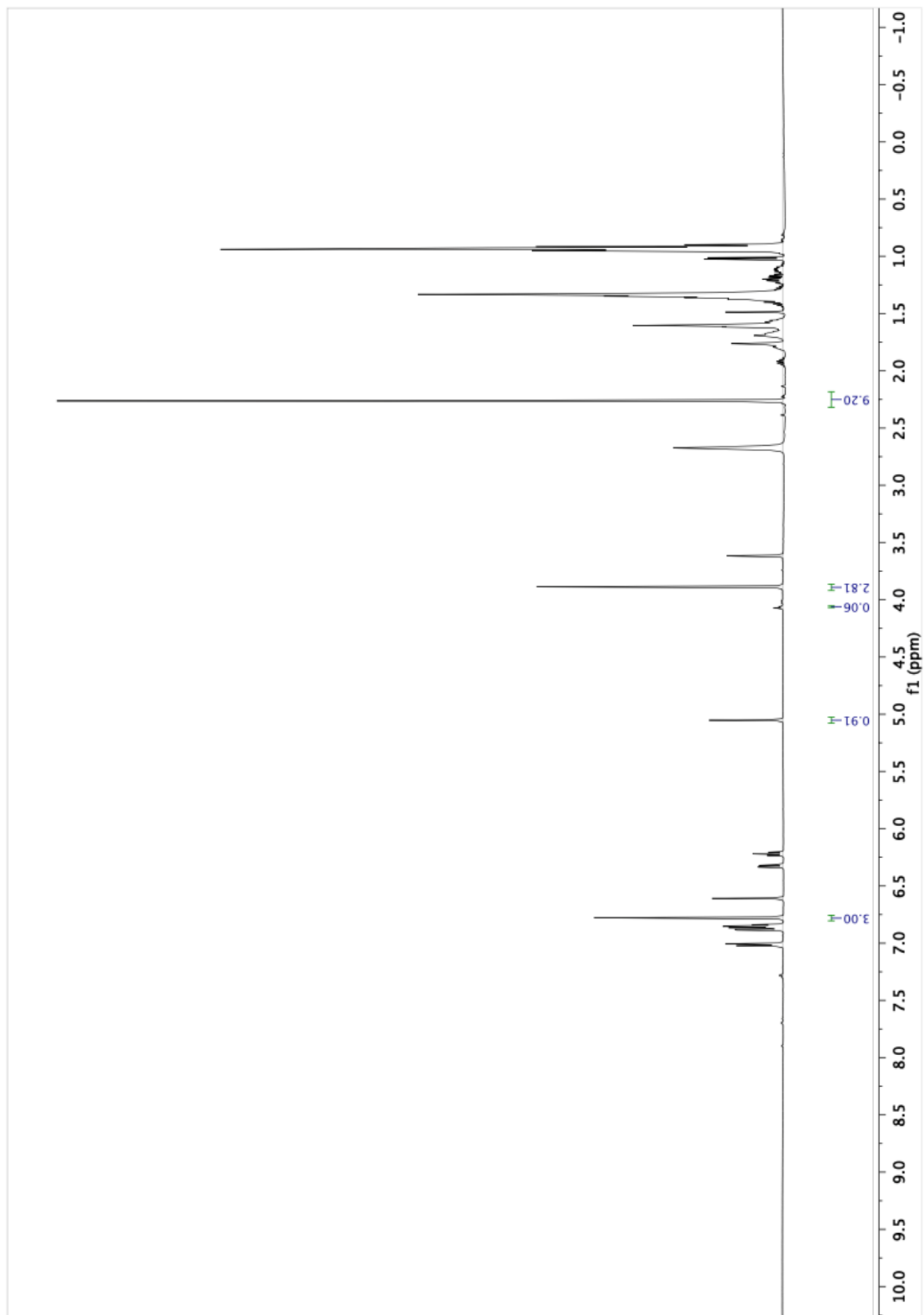


Figure 3-18: ¹H NMR spectrum of lithium pyrrolidide / **3** with mesitylene internal standard showing 91% yield of **3a**.

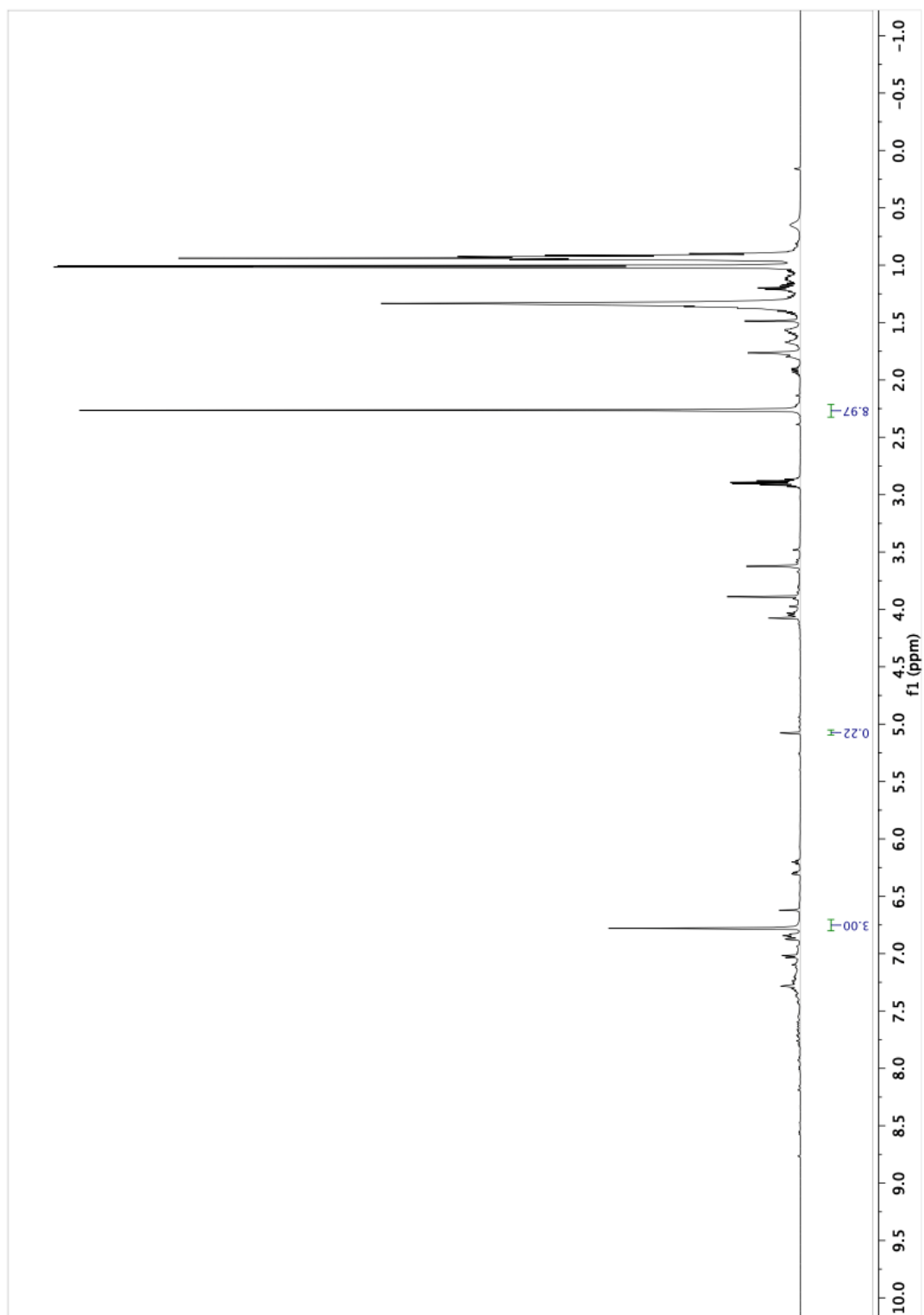
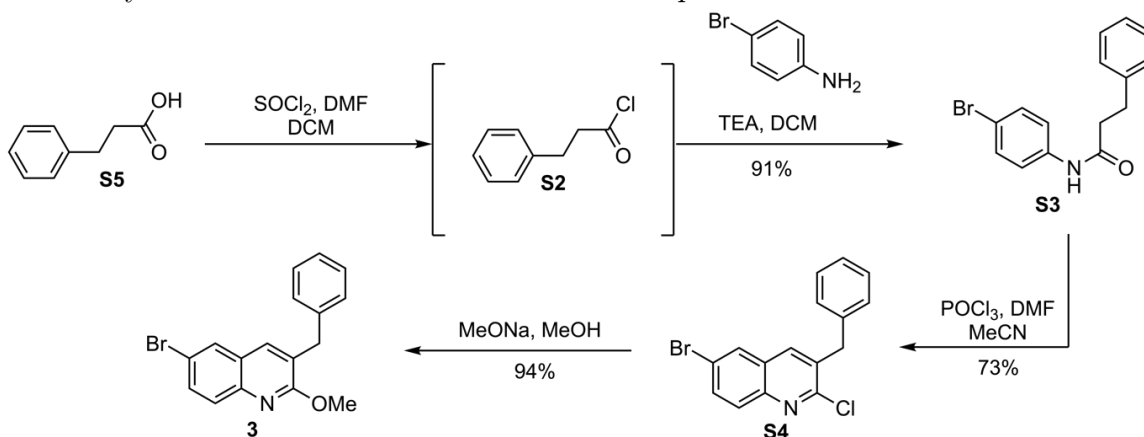


Figure 3-19: ^1H NMR spectrum of lithium diisopropylamide / **3** with mesitylene internal standard showing 22% yield of **3a**.

3.5.1 Synthesis of Materials **3** and **2·HCl** by WuXi AppTech

Synthesis of 3-(dimethylamino)-1-(naphthalen-1-yl)propan-1-one hydrochloride (2·HCl**)**. 1-acetonaphthone (80 g, 470 mmol, 1 equiv), dimethylamine hydrochloride (57.5 g, 705 mmol, 1.5 equiv), and paraformaldehyde (30 g, 1.5 equiv) were dissolved in ethanol (140 mL). Concentrated HCl (12 M, 10 mL, 120 mmol, 0.25 equiv) was added and the solution was warmed to 80 °C and stirred for 30 h. Upon completion, the reaction mixture was concentrated under reduced pressure to remove the majority of the ethanol, then cooled to 4–5 °C for 4 h to precipitate **2·HCl**. The resulting suspension was filtered and the filter cake was washed with ethanol (2 x 50 mL) and dried in vacuo to afford **2·HCl** as a white solid (68 g, 53%, 97% purity). The analytical data were consistent with those reported in the literature.²⁰



Synthesis of 3-benzyl-6-bromo-2-methoxyquinoline (3**)**. In summary: Quinoline **3** was prepared starting from 3-phenylpropanoic acid.²⁰ The acid **S5** was chlorinated to form acyl chloride **S2**, which was directly reacted with 4-bromoaniline to yield compound **S3**. A Vilsmeier-Haack reaction and subsequent condensation then furnished quinoline **S4**. After nucleophilic substitution with sodium methoxide and recrystallization, the desired product **3** was obtained in 62% overall yield from **S5** with 99% purity.

N-(4-Bromophenyl)-3-phenylpropanamide (S3**)**. 3-phenylpropanoic acid (100 g, 666 mmol, 1.0 equiv) and DMF (4.87 g, 66.6 mmol, 5.1 mL, 0.1 equiv) were dissolved in CH_2Cl_2 (1000 mL). SOCl_2 (158 g, 1.33 mol, 96.6 mL, 2.0 equiv) was added dropwise over 1 h at 0 °C. The solution was warmed to 20 °C and stirred for

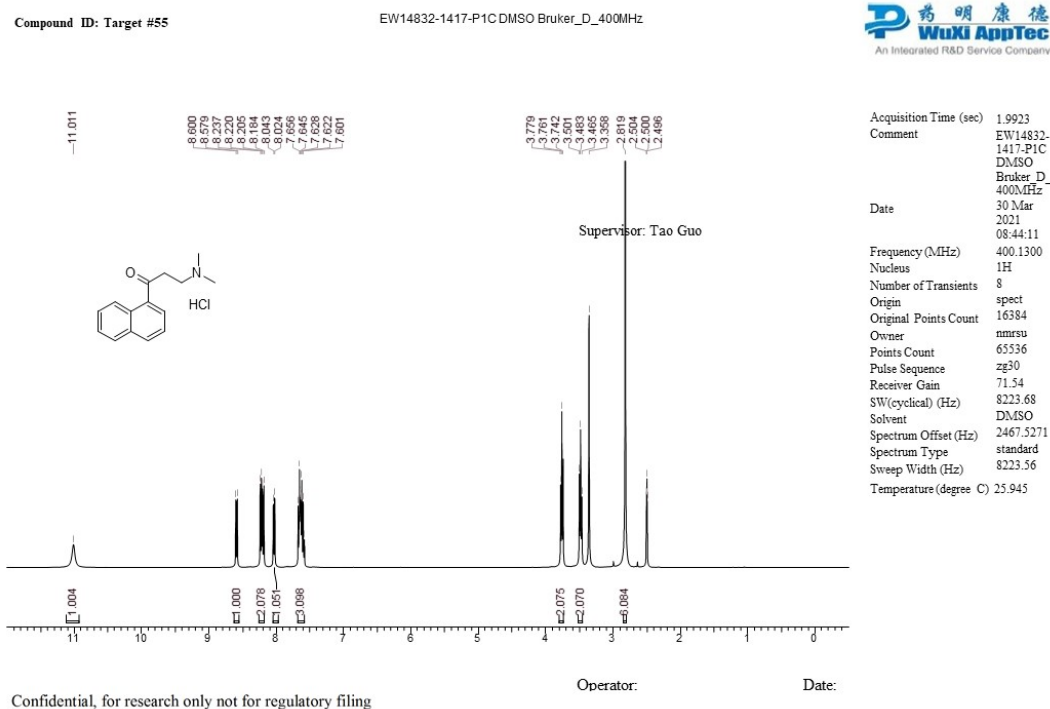
a further 2 h. During stirring, periodic 0.5 mL aliquots were removed and quenched with methanol (1 mL) for monitoring by TLC and ^1H NMR spectroscopy. Upon completion, the reaction was concentrated under reduced pressure to give **S2** (113 g, 100%) as a colorless oil. This material was used directly in the next step without further purification. 4-Bromaniline (121 g, 704 mmol, 1.05 equiv) was dissolved in CH_2Cl_2 (1000 mL) and triethylamine (81 g, 804 mmol, 112 mL, 1.2 equiv) under nitrogen atmosphere. The solution was cooled to 0 °C and 3-phenylpropanoyl chloride (**S2**, 113 g, 670 mmol, 1.0 equiv) was added dropwise over 1 h. The solution was allowed to warm to 20 °C and stirred for an additional 1 h. Ice water (500 mL) was then added to quench and a white solid precipitated upon addition. The resultant suspension was filtered to obtain the filter cake as a white solid. The filtrate was then partitioned and the aqueous phase was extracted with CH_2Cl_2 (2 x 500 mL). The combined organic layers were washed with 1 M aqueous HCl (2 x 500 mL) and saturated aqueous NaCl (2 x 300 mL), then dried over Na_2SO_4 . The mixture was filtered and concentrated under reduced pressure until significant white precipitate formed. The suspension was then filtered to obtain the filter cake as a white solid. The combined filter cakes were dried in vacuo to yield **S3** (185 g, 91%, 100% purity). The analytical data were consistent with those reported in the literature.¹⁰

3-Benzyl-6-bromo-2-chloroquinoline (S4). DMF (48 g, 658 mmol, 51 mL, 4.0 equiv) was cooled to 0 °C under nitrogen atmosphere. POCl_3 (202 g, 1.32 mol, 122 mL, 8.0 equiv) was added dropwise while stirring. After complete addition, the mixture was stirred for 1 h at 20 °C followed by addition of MeCN (150 mL) and **S3** (50 g, 164 mmol, 1.0 equiv). The reaction mixture was heated to 80 °C and stirred for a further 36 h. After completion, the reaction mixture was cooled to room temperature and added slowly to water (2000 mL), resulting in precipitation of **S4**. The suspension was filtered and the filter cake was washed with cold methanol (2 x 50 mL). The filter cake was then dried in vacuo to afford **S4** (41 g, 73%, 98% purity) as an off-white solid. The analytical data were consistent with those reported in the literature.²⁰

3-Benzyl-6-bromo-2-methoxyquinoline (3). To a suspension of **S4** (60 g,

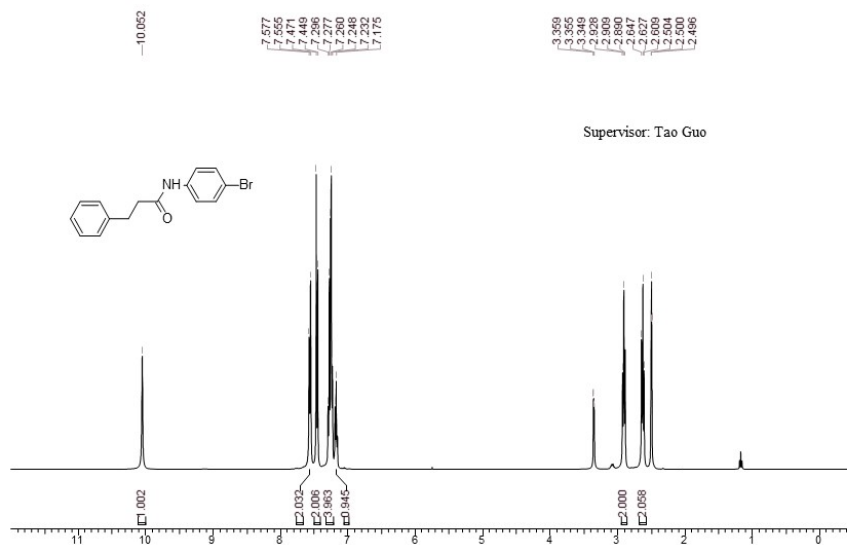
177 mmol, 1.0 equiv) in MeOH (300 mL) was added a solution of sodium methoxide in methanol (5 M, 177 mL, 5 equiv). The reaction mixture was heated to 80 °C and stirred for 8 h under nitrogen atmosphere. The reaction mixture was then cooled to 20 °C and filtered, and the filter cake was washed with cold methanol (2 x 50 mL). The filter cake was added to water (200 mL) and the resulting suspension was stirred for 30 min at 20 °C. The suspension was then filtered and the filter cake was washed with water (100 mL) and dried in vacuo to yield **3** (55 g, 94% yield, 99% purity) as an off-white solid. The analytical data were consistent with those reported in the literature.²⁰

¹H NMR Spectra for WuXi AppTech Products and Intermediates



Compound ID:

EW14832-1233-P1C DMSO Bruker_D_400MHz



Acquisition Time (sec) 1.9923
Comment EW14832-1233-P1C DMSO Bruker_D_400MHz
Date 17 Nov 2020 19:22:47
Frequency (MHz) 400.1300
Nucleus 1H
Number of Transients 8
Origin spect
Original Points Count 16384
Owner nmrsu
Points Count 65536
Pulse Sequence zg30
Receiver Gain 63.78
SW(cyclical) (Hz) 8223.68
Solvent DMSO
Spectrum Offset (Hz) 2468.0474
Spectrum Type standard
Sweep Width (Hz) 8223.56
Temperature (degree C) 25.144

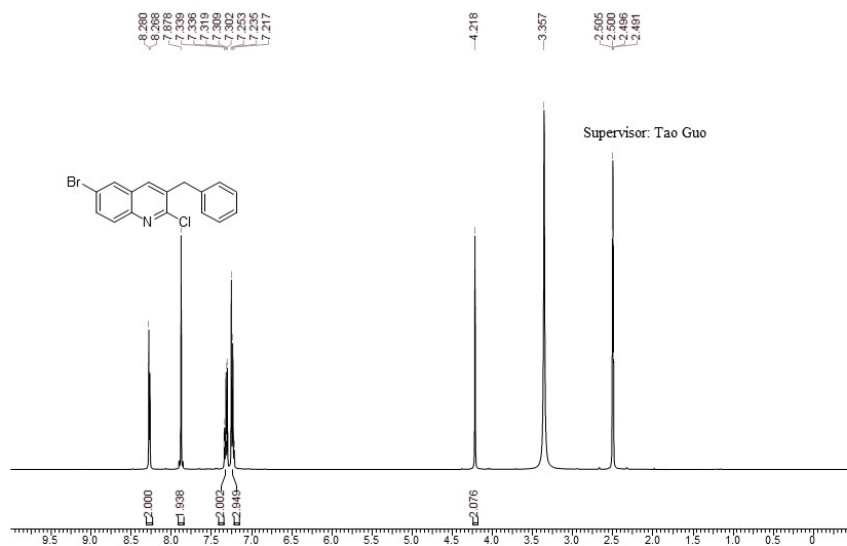
Confidential, for research only not for regulatory filing

Operator:

Date:

Compound ID:

EW14832-1238-P1C DMSO Bruker_F_400MHz



Acquisition Time (sec) 2.0447
Comment EW14832-1238-P1C DMSO Bruker_F_400MHz
Date 20 Nov 2020 13:30:51
Frequency (MHz) 400.1700
Nucleus 1H
Number of Transients 8
Origin spect
Original Points Count 16384
Owner nmrsu
Points Count 65536
Pulse Sequence zg30
Receiver Gain 90.28
SW(cyclical) (Hz) 8012.82
Solvent DMSO
Spectrum Offset (Hz) 2398.0991
Spectrum Type standard
Sweep Width (Hz) 8012.70
Temperature (degree C) 25.191

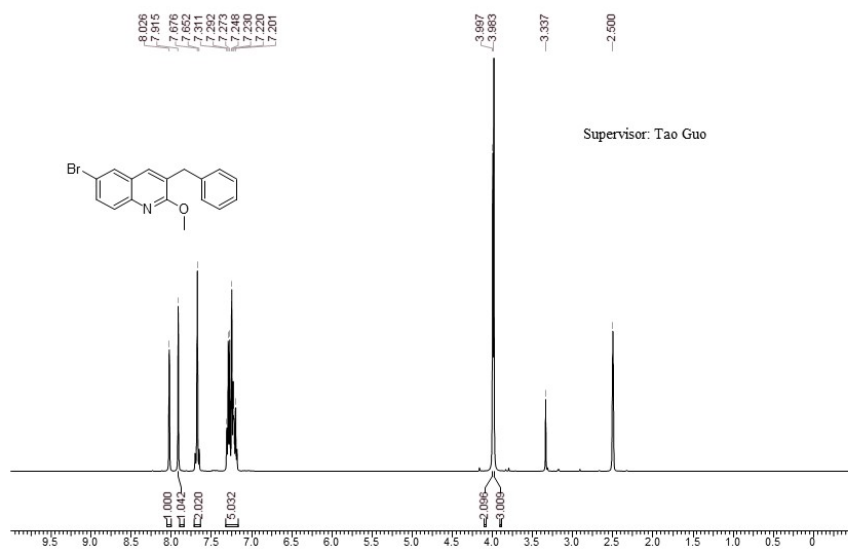
Confidential, for research only not for regulatory filing

Operator:

Date:

Compound ID: Target #54

EW14832-1243-P1C DMSO Bruker_A_400MHz



Acquisition Time (sec) 2.0447
Comment EW14832-1243-P1C DMSO Bruker_A_400MHz
Date 24 Nov 2020 17:44:51
Frequency (MHz) 400.1300
Nucleus 1H
Number of Transients 8
Origin spect
Original Points Count 16384
Owner mmsu
Points Count 65536
Pulse Sequence zg30
Receiver Gain 112.05
SW(cyclical) (Hz) 8012.82
Solvent DMSO
Spectrum Offset (Hz) 2397.5386
Spectrum Type standard
Sweep Width (Hz) 8012.70
Temperature (degree C) 26.523

Supervisor: Tao Guo

Confidential, for research only not for regulatory filing

Operator:

Date:

3.6 References

- [1] Wiens, K. E.; Woyczynski, L. P.; Ledesma, J. R.; Ross, J. M.; Zenteno-Cuevas, R.; Goodridge, A.; Ullah, I.; Mathema, B.; Djoba Siawaya, J. F.; Biehl, M. H.; Ray, S. E.; Bhattacharjee, N. V.; Henry, N. J.; Reiner Jr., R. C.; Kyu, H. H.; Murray, C. J. L.; Hay, S. I. *BMC Med.* **2018**, *16*, 196.
- [2] Global tuberculosis report 2021. Geneva: World Health Organization; 2021. Licence: CC BY-NC-SA 3.0 IGO.
- [3] Médecins Sans Frontières Issue Brief: DR-TB DRUGS UNDER THE MICROSCOPE, 6th edition. October, 2019. https://msfaccess.org/sites/default/files/2019-10/IssueBrief_UTM_6th_Ed_FINAL_web.pdf (accessed 2022-02-28).
- [4] Calvert, M. B.; Furkert, D. P.; Cooper, C. B.; Brimble, M. A. *Bioorg. Med. Chem. Lett.* **2020**, *30*, 127–172.
- [5] Cox, E.; Laessig, K. *N. Engl. J. Med.* **2014**, *37*, 689–691.
- [6] Porstmann, F. R.; Horns, S.; Bader, T. Process for preparing (alpha s, beta r)-6-bromo-alpha-[2-(dimethylamino)ethyl]-2-methoxy-alpha-1-naphthalenyl-beta-phenyl-3-quinolineethanol. WO 125769 A1, 2006.
- [7] Sebastian, S.; Singh, S. K.; Polavarapu, S.; Veera, U. Process for the preparation of bedaquiline fumarate. WO 161743 A1, 2020.
- [8] Zhang, F.; Pan, L.; Zhu, J.; Wang, X.; Zhao, L.; Ren, Z.; Song, Y. Method for separating diastereoisomer a of bedaquiline. WO 015793 A1, 2017.
- [9] Lubanyana, H.; Arvidsson, P. I.; Govender, T.; Kruger, H. G.; Naicker, T. *ACS Omega* **2020**, *25*, 3607–3611.
- [10] Zhao, X.; Huang, Y.; Zheng, Z.; LIN, Y.; Chen, Z. Chiral inducer for synthesizing (1R,2S)-Bedaquiline. CN 106866525A, 2017.
- [11] Saga, Y.; Motoki, R.; Makino, S.; Shimizu, Y.; Kanai, M.; Shibasaki, M. *J. Am. Chem. Soc.* **2010**, *132*, 7905–7907.
- [12] Chandrasekhar, S.; Babu, G. S. K.; Mohapatra, D. K. *Eur. J. Org. Chem.* **2011**, *11*, 2057–2061.
- [13] Gupta, L.; Hoepker, A. C.; Singh, K. J.; Collum, D. B. *J. Org. Chem.* **2009**, *74*, 2231–2233.
- [14] Zhang, W.-Y.; Sun, C.; Hunt, D.; He, M.; Deng, Y.; Zhu, Z.; Chen, C.-L.; Katz, C.; Niu, J.; Hogan, P. C.; Xiao, X.-Y.; Dunwoody, N.; Ronn, M. *Org. Process Res. Dev.* **2016**, *20*, 284–296.
- [15] Begley, C.; Ellis, L. M. *Nature* **2012**, *483*, 531–533.

- [16] Serra-Garcia, M.; Gneezy, U. *Sci. Adv.* **2021**, *7*, eabd1705.
- [17] Bergman, R. G.; Danheiser, R. L. *Angew. Chem. Int. Ed.* **2016**, *55*, 12548–12549.
- [18] Alegra, R. F.; Gupta, L.; Hoepker, A. C.; Liang, J.; Ma, Y.; Singh, K. J.; Collum, D. B. *J. Org. Chem.* **2017**, *82*, 4513–4532.
- [19] Burchat, A. F.; Chong, J. M.; Nielsen, N. *J. Organomet. Chem.* **1997**, *542*, 281–283.
- [20] Kong, D.-L.; Huang, Y.; Ren, L.-Y.; Feng, W.-H. *Chin. Chem. Lett.* **2015**, 790–792.
- [21] Comins, D. L.; Joseph, S. P. Encyclopedia of Reagents for Organic Synthesis: Lithium Morpholide, **2001**, <https://onlinelibrary.wiley.com/doi/10.1002/047084289X.r1130> (accessed 2021-12-14).
- [22] Comins, D. L.; Joseph, S. P. Encyclopedia of Reagents for Organic Synthesis: Lithium *N*-Methylpiperazide, **2001**, <https://onlinelibrary.wiley.com/doi/abs/10.1002/047084289X.r1128> (accessed 2021-12-14).
- [23] Iwema Bakker, W. I.; Lee Wong, P.; Snieckus, V.; Warrington, J. M.; Barriault, L. Encyclopedia of Reagents for Organic Synthesis: Lithium Diisopropylamide, **2001**, <https://onlinelibrary.wiley.com/doi/abs/10.1002/047084289X.r1101.pub2> (accessed 2021-12-14).
- [24] Wicki, M.; Snieckus, V. Encyclopedia of Reagents for Organic Synthesis: Lithium Pyrrolidide, **2001**, <https://onlinelibrary.wiley.com/doi/abs/10.1002/047084289X.r1140> (accessed 2021-12-14).
- [25] Tsukazaki, M.; Snieckus, V.; Coghlan M. J. Encyclopedia of Reagents for Organic Synthesis: Lithium Diethylamide, **2001**, <https://onlinelibrary.wiley.com/doi/abs/10.1002/047084289X.r1096.pub2> (accessed 2021-12-14).
- [26] Campbell, M.; Snieckus, V.; Baxter, E. W. Encyclopedia of Reagents for Organic Synthesis: Lithium 2,2,6,6-Tetramethylpiperidide, **2001**, <https://onlinelibrary.wiley.com/doi/abs/10.1002/047084289X.r1143.pub2> (accessed 2021-12-14).
- [27] Ho, T.-L.; Fieser, M.; Fieser, L. Encyclopedia of Reagents for Organic Synthesis: Lithium dicyclohexylamide, **2006**, <https://onlinelibrary.wiley.com/doi/abs/10.1002/9780471264194.fos06416> (accessed 2021-12-14).

- [28] Ho, T.-L.; Fieser, M.; Fieser, L. Fieser and Fieser's Reagents for Organic Synthesis: Lithium piperidide, **2006**, <https://onlinelibrary.wiley.com/doi/abs/10.1002/9780471264194.fos06554> (accessed 2021-12-14).
- [29] Coumbarides, G.; Eames, J.; Weerasooriya, N. *Can. J. Chem.* **2000**, *78*, 935–941.
- [30] Bunn, B. J.; Simpkins, N. S. *J. Org. Chem.* **1993**, *58*, 533–534.
- [31] Sugasawa, K.; Shindo, M.; Noguchi, H.; Koga, K. *Tetrahedron Lett.* **1996**, *37*, 7377–7380.
- [32] Majewski, M.; Gleave, D. M. *J. Org. Chem.* **1992**, *57*, 3599–3605.
- [33] O'Brien, P. *J. Chem. Soc., Perkin Trans. 1* **1998**, 1439–1458.
- [34] Cowton, E. L. M.; Gibson, S. E.; Schneider, M. J.; Smith, M. H. *ChemComm.* **1996**, 839–840.
- [35] Murakata, M.; Nakajima, M.; Koga, K. *J. Am. Chem. Soc., Chem. Commun.* **1990**, 1657–1658.
- [36] Lutz, V.; Baro, A.; Fischer, P.; Laschat, S. *Eur. J. Org. Chem.* **2010**, *2010*, 1149–1157.
- [37] Porstmann, F. R.; Horns, S.; Bader, T. Process for Preparing (α S, β R)-6-Bromo- α -[2-(Dimethylamino)Ethyl]-2-Methoxy- α -1-Naphthalenyl- β -Phenyl-3-Quinolineethanol, WO 125769 A1, 2006.

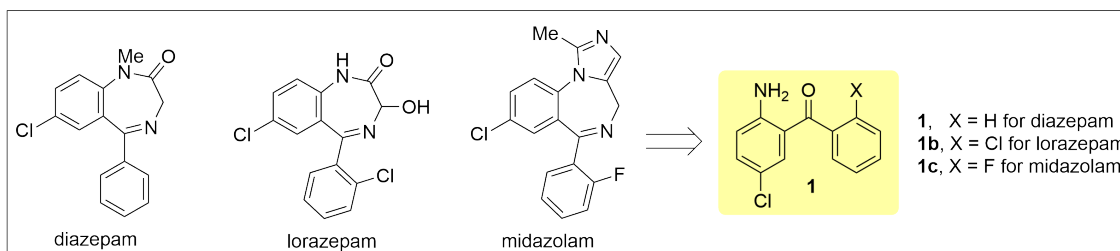
Chapter 4

Synthesis of a Key Precursor to Benzodiazepines by Copper Hydride Reduction of 2,1-Benzo[*c*]isoxazoles

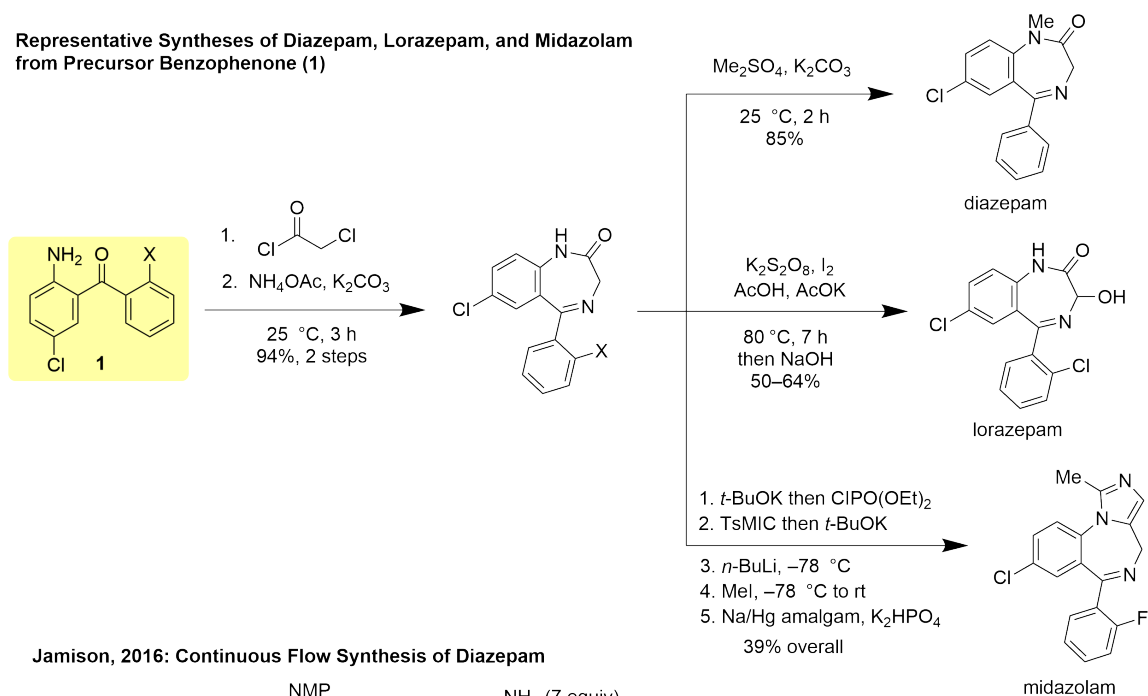
4.1 Introduction

The benzodiazepine class of pharmaceuticals is used to treat anxiety disorders as well as insomnia, seizures, general anesthesia, sedation, muscle relaxation, and other types of panic and agitation.¹ Within this large drug class, three active pharmaceutical ingredients (APIs) on the World Health Organization's List of Essential Medicines² are used most commonly for general anesthesia: midazolam (Versed[®]), lorazepam (Ativan[®]), and diazepam (Valium[®]).¹ These drugs can also be used to sedate patients on assisted ventilation, which became increasingly relevant during the COVID-19 pandemic. Given the high demand for these life-saving molecules, investigation of new synthetic routes which could secure the pharmaceutical supply chain is valuable.

One strategy for delivery of cost-saving solutions in pharmaceutical synthesis is identification of lower-cost alternatives for key starting materials or precursors; techno-economic analysis of pharmaceutical manufacturing processes has shown that an increase in cost of a single key intermediate can have a large impact on the over-



Representative Syntheses of Diazepam, Lorazepam, and Midazolam from Precursor Benzophenone (1)



Jamison, 2016: Continuous Flow Synthesis of Diazepam

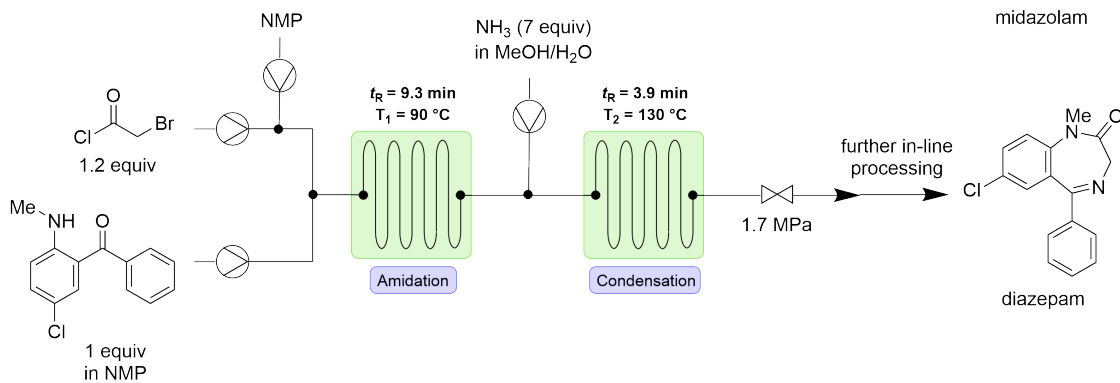


Figure 4-1: Representative syntheses of midazolam, lorazepam, and diazepam from a common benzophenone precursor.

all cost-of-goods, particularly if this precursor is used early in the manufacturing process.^{3,4} Assessment of a number of routes for commercial synthesis of diazepam, midazolam, and lorazepam,⁵⁻¹⁰ including a continuous process developed by our own research group,¹¹ shows that a key precursor is 2-amino-5-chlorobenzophenone or related 2'-chloro or 2'-fluoro derivatives (**1**, **1b**, **1c**). Technoeconomic analysis performed by our collaborators at the Medicines for All Institute (M4All) identified compound **1** as a high-cost starting material used for synthesis of the benzodiazepines, and concluded that investigation of more efficient synthesis of these 2-amino-5-chlorobenzophenones would help to reduce the cost and therefore secure the supply chain for benzodiazepines. Synthesis of **1** in continuous flow could provide further benefits by expanding the existing continuous manufacturing strategy for diazepam (Figure 4-1). Representative syntheses of these benzodiazepines by a divergent strategy is depicted in Figure 4-1. In a typical approach, the 2-amino functionality of **1** is reacted with an α -halo acid chloride. The resulting amide then cyclizes by a substitution-condensation event in the presence of ammonia or an ammonium salt, leading to the core structure of the benzodiazepines. Further elaboration by methylation, oxidation, or imidazole formation leads to diazepam, lorazepam, and midazolam, respectively (Figure 4-1).

The aim of this investigation was to deliver a novel strategy for synthesis of **1** which could reduce the cost to manufacture diazepam, lorazepam, or midazolam. Existing synthetic approaches to **1** include a ZnCl_2 -catalyzed Friedel-Crafts reaction of 4-chloroaniline reported with a maximum of 50% yield.¹² A recent report in the patent literature shows synthesis of **1** by *N,O*-reduction of 2,1-benzo[*c*]isoxazole **2**, which is readily prepared by cyclization of nitrile **3** with nitrobenzene **4** (Figure 4-2).^{13,14} The patented approach for this *N,O*-reduction utilizes iron powder, attractive due to its low cost, yet not amenable to continuous flow synthesis due to the heterogeneous nature of the reductant. β -Amino ketones and β -amino alcohols in general can be accessed from isoxazoles by catalytic hydrogenation using hydrogen and a transition metal catalyst such as palladium.¹⁵ The rising cost of these transition metal catalysts, and the challenge of scale-up of packed bed reactors,¹⁶ encourages the development

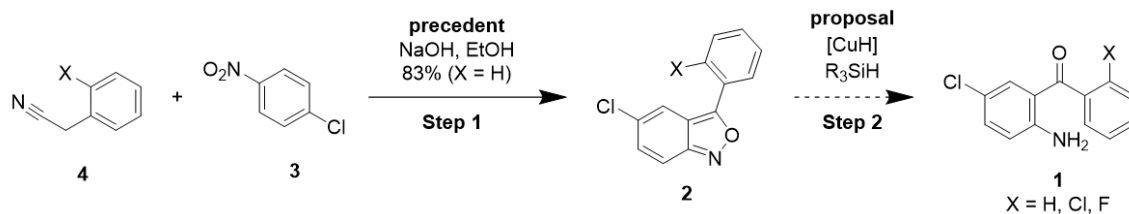


Figure 4-2: Precedented formation of 2,1-benzo[*c*]isoxazole **2** and proposed copper hydride reduction to form target **1**.

of a homogenous catalytic system for this transformation in continuous flow.

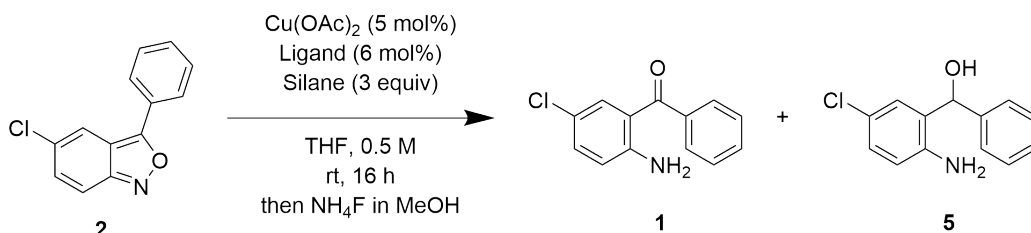
Herein, we describe a new method for synthesis of benzodiazepine precursor **1** from 2,1-benzisoxazole **2** by reduction catalyzed by copper hydride. The chemoselective nature of copper hydride makes it broadly useful for catalytic reductions of organic functional groups.^{17,18} Reaction optimization aimed to design reaction conditions which select for *N,O*-reduction to **1** without undesired overreduction of the carbonyl group.

4.2 Results and Discussion

4.2.1 Feasibility and Side Product Identification

Initial screening efforts showed that reduction of 2,1-benzo[*c*]isoxazole **2** to benzophenone **1** with copper hydride is possible using precedented conditions for copper hydride reduction (Table 4.1, entry 1).¹⁹ Control experiments in the absence of phosphine ligand or in the absence of copper catalyst resulted in <5% yield of **1** (entries 2–3). The identity of the silane had a large impact on the selectivity for *N,O*-reduction relative to 1,2-reduction. Dimethylphenylsilane gave selective *N,O*-reduction and 26% yield of **1** with no observable side products (entry 4), compared to dimethoxymethylsilane which had produced 19% yield of **1** with 51% of **5**, resulting from undesired 1,2-reduction (entry 1). Changing the solvent to toluene – also precedented for use in copper hydride reductions¹⁷ – had little impact on yield or selectivity (entries 5,6 vs. 1,4). Other solvents were not evaluated at this stage (vide infra). Reducing the stoichiometry of the silane or reducing reaction time to 8 h did not prevent the

formation of **5** (entries 7 and 13). Undesired product **5** was identified by exposing a commercial sample of **1** to the reaction conditions (see Section 4.3.2, page 273), leading to formation of **5** in 85% yield. Early identification of **5** focused optimization efforts on achieving conversion of **2** without subsequent 1,2-reduction.



entry*	ligand	silane	deviation	AY 2	AY 1	AY 5
1	<i>rac</i> -BINAP	DMMS		17	19	51
2	no ligand	DMMS		94	4	0
3	no ligand	DMMS	no catalyst	96	0	1
4	<i>rac</i> -BINAP	PhMe ₂ SiH		59	26	0
5	<i>rac</i> -BINAP	DMMS	toluene	12	13	59
6	<i>rac</i> -BINAP	PhMe ₂ SiH	toluene	56	22	0
7	<i>rac</i> -BINAP	DMMS	silane (1.5 equiv)	49	23	24
8	DCyPE	DMMS		0	0	88
9	DPPF	DMMS		47	5	41
10	P(<i>o</i> -tol) ₃	DMMS	ligand 12 mol%	84	9	0
11	DCyPE	DMMS		24	5	72
13	<i>rac</i> -BINAP	DMMS	8 h	64	17	19
14	DCyPE	PhSiH ₃		13	1	71
15	DPPP	PhSiH ₃		54	14	38
16	<i>rac</i> -BINAP	PhSiH ₃	8 h	79	2	19
17	DCyPE	PhMe ₂ SiH		77	16	0
18	DPPP	PhMe ₂ SiH		69	27	2
19	<i>rac</i> -BINAP	PhMe ₂ SiH	8 h	88	11	1
20	<i>rac</i> -BINAP	PhMe ₂ SiH	8 h + <i>t</i> -BuOH	39	52	10
21	<i>rac</i> -BINAP	Et ₃ SiH	8 h	99	1	0
22	<i>rac</i> -BINAP	TMDS	8 h	92	5	4
23	<i>rac</i> -BINAP	PMHS	8 h	83	12	5
24	<i>rac</i> -BINAP	PMHS	8 h + <i>t</i> -BuOH	6	15	79

* entries 1–18 AY (assay yield) determined by HPLC, entries 19–24 determined by ¹H NMR

Table 4.1: Results of initial feasibility screening for Copper Hydride reduction of 2,1-benzo[*c*]isoxazole. Experimental details on page 274.

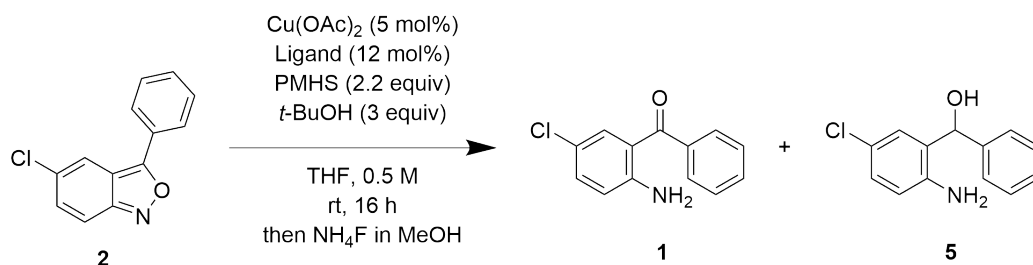
A series of phosphine ligands were evaluated for their utility in stabilizing copper hydride for the desired *N,O*-reduction (Table 4.1, entries 8–11). 1,1'-Bis(diphenylphosphino)ferrocene (DPPF) and 1,2-Bis(dicyclohexylphosphino)ethane (DCyPE) gave

nearly complete overreduction to **5** (entries 8, 9, 11). 1,2-Bis(diphenylphosphino)ethane (DPPE) and 1,3-bis(diphenylphosphino)propane (DPPP) were also evaluated and resulted in product mixtures with >50% yield of undesired product **5** (precise yield not quantifiable). Monodentate ligand tri(*o*-tolyl)phosphine (P(*o*-tol)₃) showed selectivity for *N,O*-reduction without further carbonyl reduction, although with <10% yield after an overnight reaction (entry 10). This encouraging observation aligns with precedent that bidentate phosphine ligands increase the rate of 1,2-reductions.^{20,21} Further evaluation of different ligand–silane combinations using phenylsilane, dimethylphenylsilane, triethylsilane, tetramethyldisiloxane (TMDS), and polymethylhydrosiloxane (PMHS) with bidentate ligands failed to show a combination of high conversion and high selectivity for **1** (entries 14–24). Promisingly, addition of *t*-BuOH improved conversion of **2**, likely by accelerating turnover of the copper catalyst. We proceeded with further evaluation of monodentate phosphine ligands, with knowledge that subsequent evaluation of other reaction parameters could lead to a desirable combination of selectivity and conversion.

4.2.2 Investigation of Monodentate Phosphine Ligands

After observing that monodentate phosphine ligands are capable of promoting copper hydride-catalyzed *N,O*-reduction while avoiding subsequent 1,2-reduction under the same conditions, and that adding *t*-BuOH to the reaction mixture accelerates the reaction, we evaluated a series of monodentate phosphine ligands with varying steric and electronic properties (Table 4.2).

Bulky trialkyl phosphines including tricyclohexylphosphine, tri-*tert*-butyl phosphine, and tri-*n*-octyl phosphine gave highest selectivity for the desired *N,O*-reduction with less than 1% formation of **5** (Table 4.2, entries 2, 3, and 5). When the selectivity for **1** vs **5** is plotted relative to the computed cone angle for the phosphine ligand, a general trend is observed in which ligands with a larger cone angle give less 1,2-reduction and therefore higher selectivity for the desired *N,O*-reduction (see Figure 4-3). A correlation with the electronic properties of the ligand was observed: P(*t*-Bu)₃ and PPh₃ which are slightly stronger σ -donors, gave less 1,2-reduction than



entry	ligand, stoichiometry	AY 2*	AY 1*	AY 5*
1 ^a	<i>rac</i> -BINAP, 6 mol%	39	52	10
2	PCy ₃ , 12 mol%	21	74	1
3	P(<i>t</i> -Bu) ₃ , 12 mol%	53	52	0
4	P(<i>n</i> -Bu) ₃ , 12 mol%	10	56	30
5	P(<i>n</i> -octyl) ₃ , 12 mol%	43	52	1
6	P(OEt) ₃ , 12 mol%	28	28	39
7	P(OPh) ₃ , 12 mol%	10	17	64

* AY = Percent yield determined by ¹H NMR ^a 8 h reaction

Table 4.2: Evaluation of monodentate phosphine ligands for reduction of 2,1-benzo[*c*]isoxazoles. Experimental details described in Section 4.3.4 on page 275.

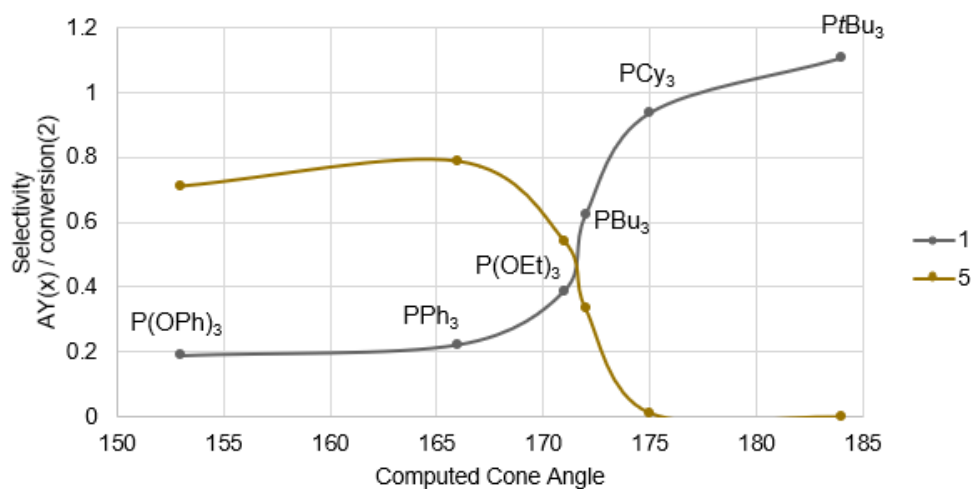


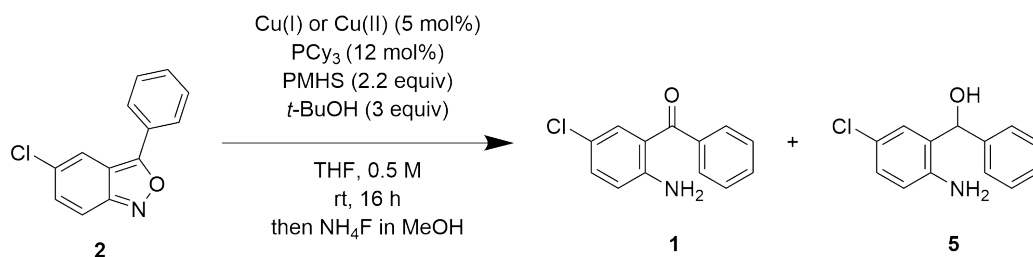
Figure 4-3: Selectivity for formation of **1** vs. computed cone angle of monodentate phosphine ligands. Computed cone angle for [Ni(CO)₃(PR₃)] complexes.²²

P(OEt)₃, a weaker σ -donor. PCy₃ gave 74% yield of **1** with only traces of overreduction to **5**. PCy₃ was selected for further optimization due to the fast rate of reaction (79% conversion with PCy₃ vs. 47% with P(*t*-Bu)₃).

4.2.3 Investigation of Additives, Copper Catalyst Source and Ligand Stoichiometry

While the use of monodentate phosphine ligands provided the desired selectivity for **1** by avoiding 1,2-reduction, a 16 h reaction time was not amenable to an economical continuous flow process; extended reaction time in continuous flow creates increased waste during system equilibration and increased instrument run-time. We sought to evaluate other reaction parameters which could accelerate the desired transformation. We evaluated alternative copper sources, including both copper(I) and copper(II) salts with different counterions (Table 4.3). Copper(II) acetate (anhydrous) remained the pre-catalyst of choice (77% yield of **1**), with copper(II) acetate monohydrate behaving similarly, yielding 70% of **1** in an overnight reaction. The bromide and chloride copper(II) salts and copper(I) chloride were ineffective at producing any **1**. Previous literature suggested that addition of base such as NaO*t*-Bu can help to accelerate the rate of copper hydride reductions,¹⁷ however with our system we noticed that the reaction became heterogeneous on addition of base, and much lower conversion was observed (Table 4.3, entries 2, 3, 5). Due to the problematic nature of heterogeneous reactions in continuous flow, this option was not pursued further.

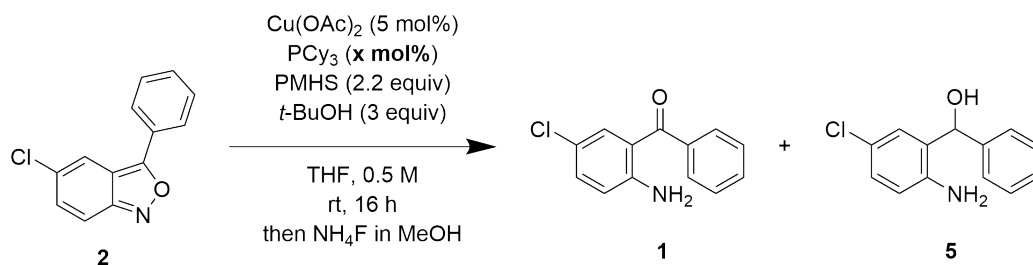
Relative stoichiometry of the copper catalyst and ligand was evaluated (Table 4.4), using 5 mol% Cu(OAc)₂ and tricyclohexylphosphine at 1, 6, and 12 mol%. Although unligated copper didn't lead to overreduction and formation of **5** (entry 3), highest yield of **1** was observed with nearly equimolar ligand and catalyst (entry 2).



entry	catalyst	additive	AY 2*	AY 1*	AY 5*
1	Cu(OAc) ₂		26	77	0
2	Cu(OAc) ₂	NaOt-Bu (1 equiv)	44	15	0
3	Cu(OAc) ₂	NaOMe (1 equiv)	67	18	0
4	Cu(OAc) ₂ ·H ₂ O		30	70	1
5	Cu(OAc) ₂ ·H ₂ O	NaOt-Bu (1 equiv)	70	37	8
6	CuBr ₂		>99	0	0
7	CuCl ₂		>99	0	0
8	CuCl		>99	0	0

* AY = Percent yield determined by ¹H NMR

Table 4.3: Investigation of additives and alternative copper sources. Experimental details described in Section 4.3.6 on page 277.



entry	ligand (mol %)	AY 2*	AY 1*	AY 5*
1	12	63	36	2
2	6	15	83	2
3	1	35	66	2

* AY = Percent yield determined by ¹H NMR as a ratio of signal for **2**, **1**, and **5**

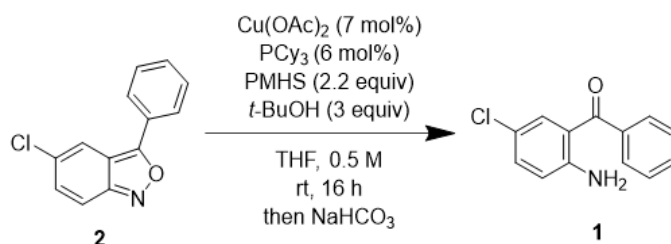
Table 4.4: Assay for stoichiometry of monodentate phosphine ligands relative to copper(II) acetate. Experimental details described in Section 4.3.5 on page 276.

4.2.4 Reaction Optimization: Temperature, Additives, and Silane Stoichiometry

Given our goal of implementing a continuous flow process, shortening the reaction time to minutes rather than hours while increasing conversion and maintaining selectivity for **1** remained the target of our optimization of the *N,O*-reduction leading to **1**. Performing the reaction at higher reaction temperature (40 °C) for shorter reaction times (4 h) did not improve yield of **1** (Table 4.5, entry 2). When less *t*-BuOH was used, increased formation of **5** was observed (Table 4.5, entry 3). As previously observed, addition of base was detrimental (Table 4.5, entry 4). We next tried driving the reaction by increasing the stoichiometry of the silane. While a large excess of silane (14 equiv) led to increased formation of overreduction product **5** (Table 4.5, entry 6), an intermediate level of silane (7 equiv) led to complete conversion of starting material with less overreduction product (Table 4.5, entry 5). Comparable results were obtained with P(*t*-Bu)₃, albeit with lower conversion of **2** (Table 4.5, entries 7, 8).

Up to this point, 0.3 M NH₄F in MeOH was used to quench excess silane after completion of this reaction. The choice of quenching agent was based on literature precedent for its known reactivity and effectiveness.¹⁹ However, due to the dilute concentration of this quenching agent, a large reaction vessel (20-mL vial) was needed to accommodate the large volume of quench solution (10 mL). This large vial size was non-ideal for the 0.5 mmol reaction with a total reaction volume of approximately 2 mL. Thus, the quenching agent was switched to aqueous NaHCO₃, which gave a similar result (Table 4.5, entries 1–2).

While conversion of **2** improved with higher stoichiometry of silane, overreduction to **5** became problematic at high levels of conversion. We probed the nature of the alcohol additive and tested an alternative solvent (toluene) to see if these variables influenced the rate of 1,2-reduction. When *i*-PrOH was used in place of *t*-BuOH, lower conversion of **2** was observed (74% (*i*-PrOH) vs >99% (*t*-BuOH) after 16 h; 66% (*i*-PrOH) vs 98% (*t*-BuOH) after 3 h; Table 4.6, entries 1–3, 5) with little impact

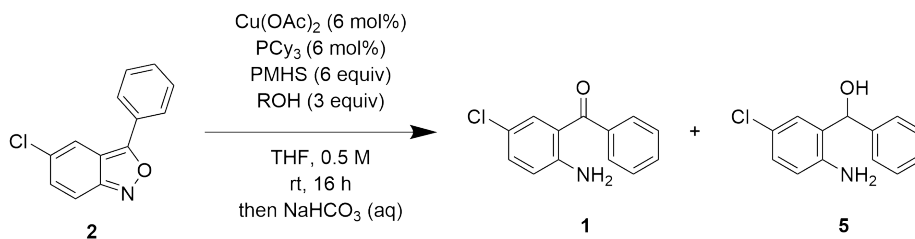


entry	ligand	variation	AY 2 ^a	AY 1 ^a	AY 5 ^a
1, Table 4.3	PCy_3	quench NH_4F , cat. 5 mol%	26	77	2
1	PCy_3	none	24	80	0
2	PCy_3	40 °C, 4 h	38	51	2
3	PCy_3	40 °C, 4 h, $t\text{-BuOH}$ (1 equiv)	45	36	10
4 †, ^b	PCy_3	PMHS (7 equiv)	44	15	66
5 †	PCy_3	PMHS (7 equiv)	0	63	13
6 †	PCy_3	PMHS (14 equiv)	0	29	11
7 †, ^c	$\text{P}(t\text{-Bu})_3$	PMHS (14 equiv)	29	86	0
8 ^{b,c}	$\text{P}(t\text{-Bu})_3$	PMHS (14 equiv)	0	45	49

^a AY = Percent yield by ¹H NMR. † Error in mass balance of internal standard impacts AY

^b NaOt-Bu (1 equiv) ^c $\text{P}(t\text{-Bu})_3$ 10 w/w% solution in hexanes

Table 4.5: Assay for selectivity of **1** with varying reaction temperature and silane stoichiometry. Experimental details described in Section 4.3.7 on page 278.



entry	ROH	Variation	AY 2*	AY 1*	AY 5*
1	$t\text{-BuOH}$	PMHS (4 equiv)	0	86	6
2	$i\text{-PrOH}$	none	26	23	7
3	$t\text{-BuOH}$	3 h	2	83	7
4	$t\text{-BuOH}$	40 °C, 3 h	0	75	13
5	$i\text{-PrOH}$	3 h	34	65	1
6	$t\text{-BuOH}$	1 h	7	90	3
7	$i\text{-PrOH}$	toluene, 1 h	44	56	0

* AY = Percent yield by ¹H NMR

Table 4.6: Investigation of reaction time, temperature and alcohol additive. Experimental details described in Section 4.3.7 on page 278.

on the formation of product **5**. As previously observed, increasing the temperature to 40 °C led to increased formation of **5** (Table 4.6, entry 4). When toluene was used as solvent, no 1,2-reduction was observed in 1 h, although yield of **1** was reduced (56% yield with toluene, 90% yield with THF; Table 4.6, entries 6–7). With conditions in hand that produced high yields (up to 90%, entry 6, Table 4.6) of **1** within 1 h, we transitioned to evaluate this system in continuous flow.

4.2.5 Implementation in Continuous Flow

Operationally, synthesis of **1** in a batch reactor was performed by first pre-mixing the copper catalyst and ligand in a solution of *t*-BuOH and THF, followed by addition of silane. Within minutes, the solution color turns from bright blue (of Cu^{II}) to a red-orange color (of Cu^I), indicating formation of copper hydride. Upon observation of this color change (approximately 10 minutes), starting material **2** is added. We designed a 2-step continuous flow process to mimic this 2-step additions sequence in batch (Figure 4-4).

Using Syrris syringe pumps and standard plug-flow reactors, we first performed a qualitative analysis in which we adjusted residence time while watching for formation of the red color in the first reactor. We determined that approximately a 4 minute reaction time was required in the first reactor for observation of the characteristic red color (see Figure 4-5). The 2-step sequence was then assayed, mimicking the optimized batch conditions (approx. 80% yield **1** in 1 h), albeit with shorter reaction times. A 12% yield of **1** was observed with a total residence time of 16.7 minutes. Extending the reaction times to a total of 24.9 min with an increased catalyst loading of 10 mol% improved the yield to 19%. Maintaining 10% catalyst loading with 12.5 min reaction time gave 13% yield (Table 4.8).

In this initial test of the continuous flow setup, we observed significant gas evolution in the second reactor (Figure 4-6). This led to inconsistent flow, particularly at slower flow rates (Table 4.8, entry 2). Additionally, laminar flow was observed following the T-mixer leading to the second reactor; poor mixing in combination with shorter reaction time could account for the low yield in continuous flow relative to

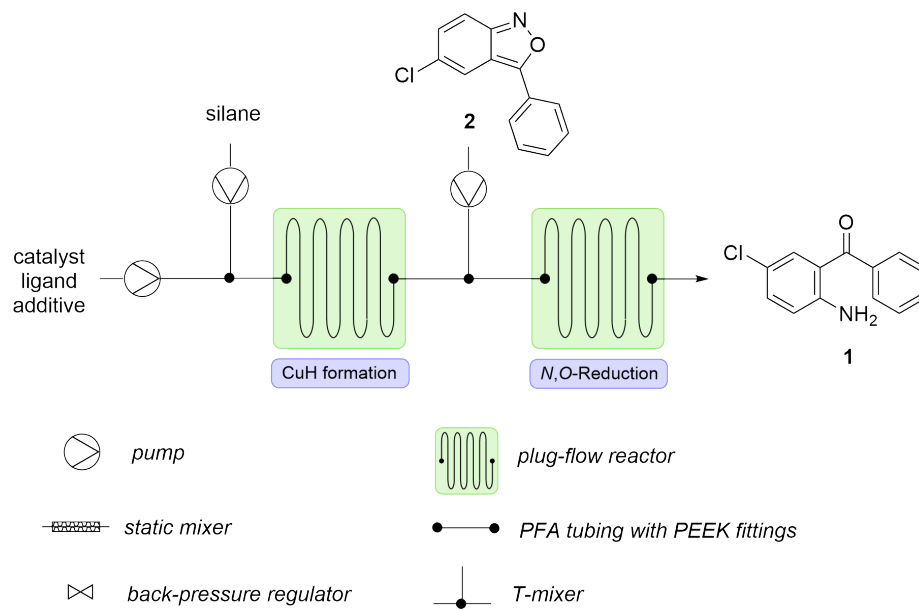


Figure 4-4: General setup for continuous flow reactor.



Figure 4-5: Visual assessment of CuH formation in continuous flow showing color change from blue to red after a 4 min reaction time.

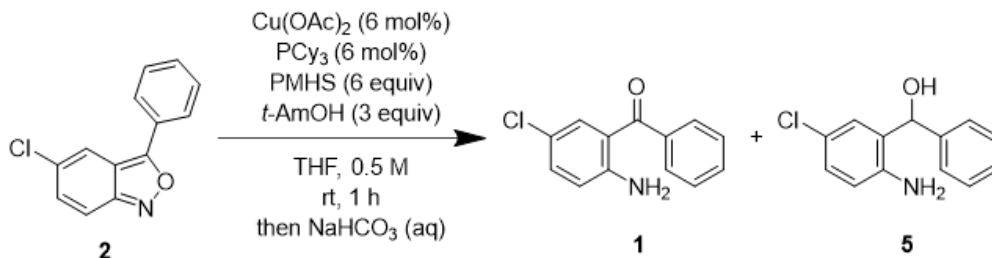


Figure 4-6: Image of gas evolution in continuous flow reactor lacking back pressure regulator.

batch.

Upon observation of the gas evolution in continuous flow, we considered that this phenomenon could lead to pressure buildup in the batch reaction, which is run in a sealed vial, while pressure was dissipated in the continuous flow setup, which lacked a back pressure regulator. Pressurization could account for the difference in yield by altering the solution dynamics of the mixture, or by some action of the dissolved gas. We ran a series of reaction in batch to probe the influence of pressure on the reaction outcome. We found that a reaction vented with a N₂ balloon gave lower yield (64% of **1**) relative to a sealed vessel under the same conditions (88% of **1**), as summarized in Table 4.7. Running the reaction under hydrogen atmosphere in the absence of silane led to no formation of **1**. This observation suggested that pressurizing the continuous flow reactor could help increase the yield of **1**.

The continuous flow setup was altered based on the observations described above. A back pressure regulator was added, allowing the system to operate at 50 psi. Additionally, a static mixer after the T-mixer leading to the second reactor improved mixing. The full setup is depicted in Figure 4-7. In this second trial, improved results were obtained, with 24% yield of **1** obtained within 16.3 minutes (Table 4.9, entry 1).

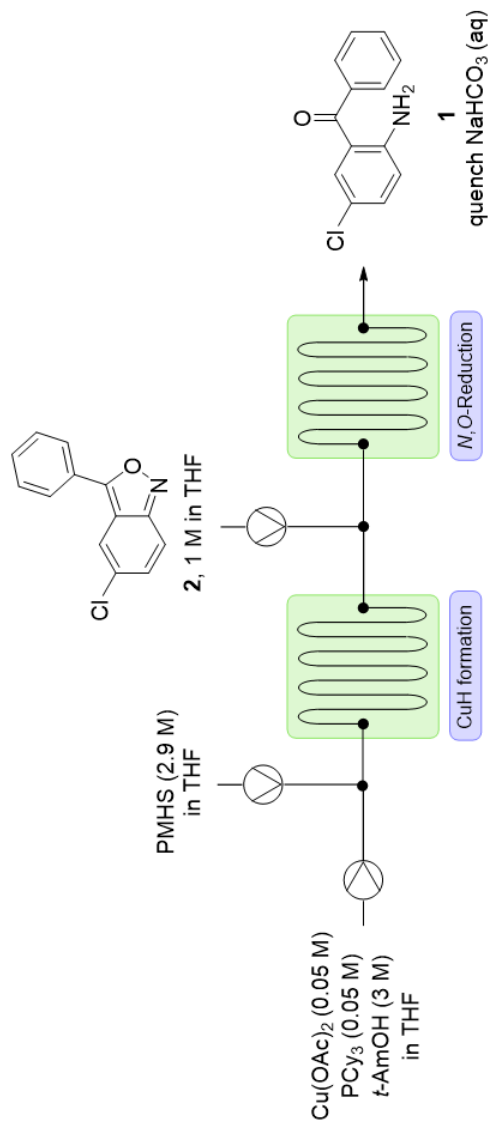


entry	variation	AY 2*	AY 1*	AY 5*
1	sealed 1-dram vial	9	88	3
2	N_2 balloon	27	64	2
3	H_2 balloon, no PMHS	101	0	–

* AY = Percent yield determined by ^1H NMR

Table 4.7: Assessment of pressure buildup during reaction and influence on yield and selectivity. Method described in Section 4.3.7 on page 278.

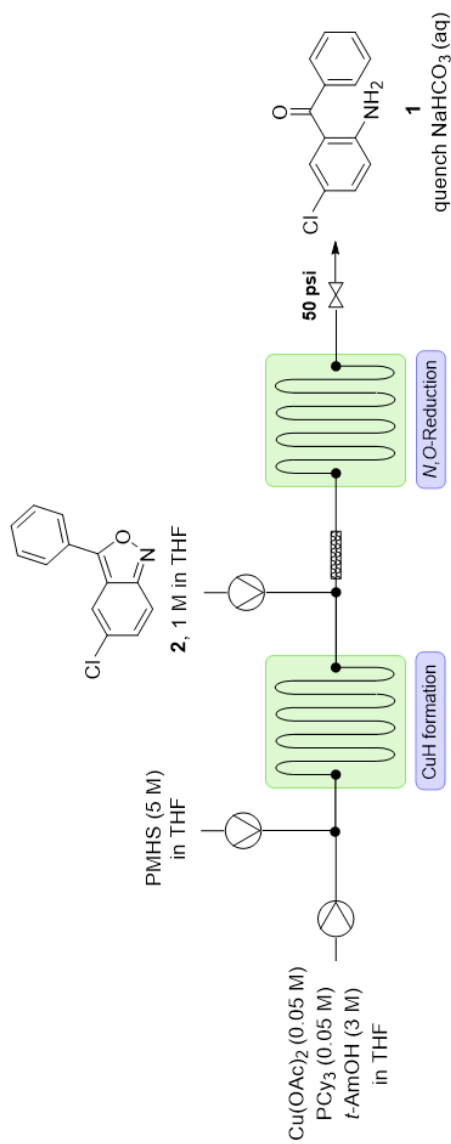
Reducing residence times by half by doubling all flow rates resulted in 17% yield of **1** (Table 4.9, entry 3). Curiously, when a second sample of each of these experiments was collected and work-up was performed using NaOH (aq) instead of NaHCO_3 (aq), higher yields were obtained (37% and 34%, Table 4.9, entries 2 and 4 relative to 24% and 17% with NaHCO_3). Longer reaction time in continuous flow could lead to comparable results to those obtained in batch. However, alternative continuous flow strategies underway in our laboratory were showing potential for similar yields with shorter reaction times and fewer operational challenges. Scale-up and isolation of **1** in the batch process was prioritized.



entry	cat./lig. (mol%)	ROH (equiv)	PMHS (equiv)	time (min) CuH formation	time (min) N,O-Reduction	AY 2*	AY 1*
1	5	3	3.5	4.4	12.3	92	12
2	10	6	3.6	6.1	18.8	81	19
3	10	6	3.5	3.1	9.4	84	13

* AY = Percent yield determined by ^1H NMR

Table 4.8: Initial reaction screening in continuous flow. Experimental details described in Section 4.3.8 on page 279.



entry	cat./lig. (mol%)	ROH (equiv)	PMHS (equiv)	CuH Formation time (min)	<i>N,O</i> -Reduction time (min)	AY 2*	AY 1*
4	5	3	7	4.3	12.0	63	24
5 ^a	5	3	7	4.3	12.0	58	37
6	5	3	7	2.1	6.0	71	17
7 ^a	5	3	7	2.1	6.0	62	34

* AY = Percent yield determined by ¹H NMR ^a quench 1 M NaOH (aq)

Table 4.9: Reaction screening in continuous flow. Experimental details on page 280.

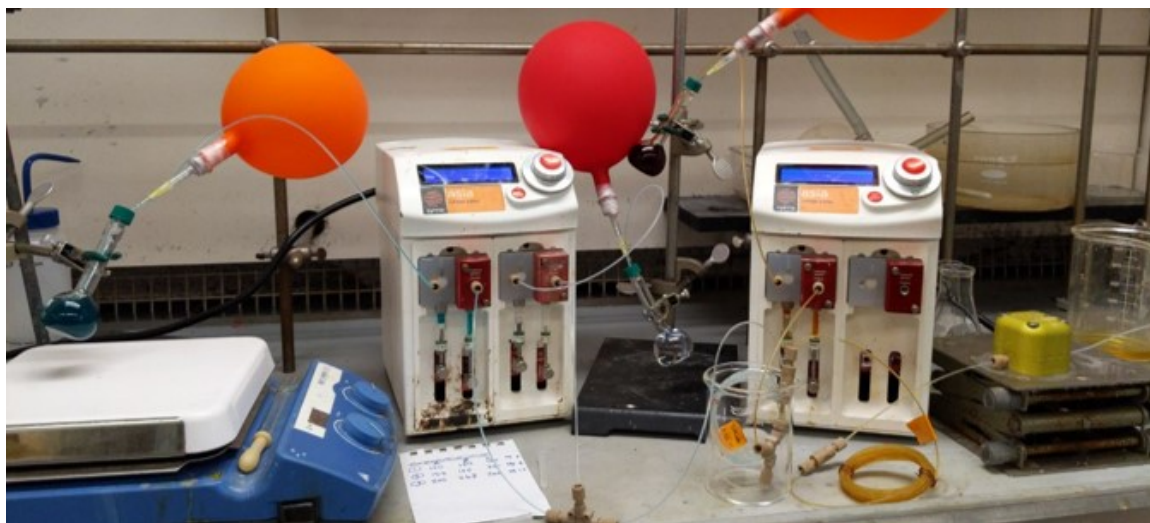


Figure 4-7: Continuous flow setup leading to **1** by copper hydride reduction.

4.2.6 Batch Scale-Up and Purification

We returned to optimization in batch to investigate isolation of the material on larger scale. Under our optimized conditions on 0.5 mmol scale, an excess of silane is used to drive formation of **1** at short reaction times. High yield of **1** (up to 90% assay yield) is obtained, with alcohol **5** or starting material **2** accounting for the mass balance. With the goal of presenting a process-relevant synthesis, a recrystallization strategy for isolation of **1** from the crude reaction mixture was investigated. A solubility screen of **1** showed dissolution in polar organic solvents (methanol, acetone, EtOAc, Et₂O) and insolubility in water or hexanes. After overnight evaporation, crystalline material of **1** was observed from the methanol solution, while only amorphous solid was observed in the other samples (Figure 4-8). Additionally, recrystallization from a hexanes–Et₂O or hexanes–EtOAc mixture was not observed. The product was insoluble in water while showing high solubility in methanol, so recrystallization was attempted from a MeOH–water mixture. Solutions of various solvent composition were assayed and it was determined that a 0.1–1 M solution of **1** is insoluble in approximately 30% aqueous methanol at room temperature, with dissolution on heating. Recrystallization by addition of cosolvent (water) led to amorphous aggregation of water-insoluble **1** without crystal formation. Thus recrystallization by supersaturation was investigated

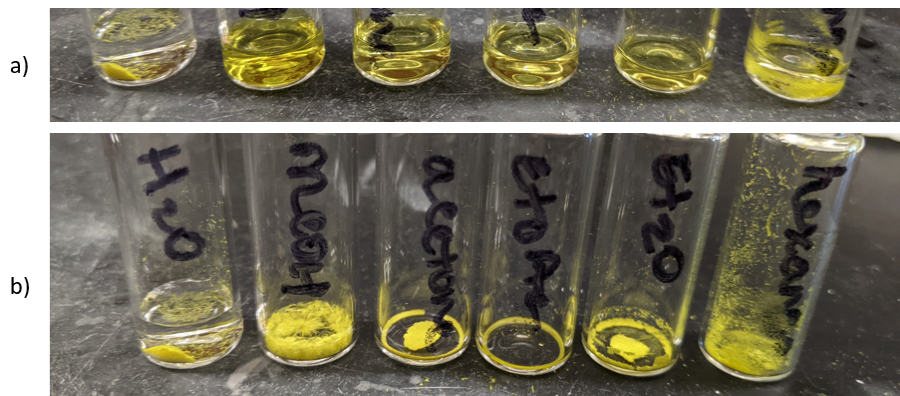


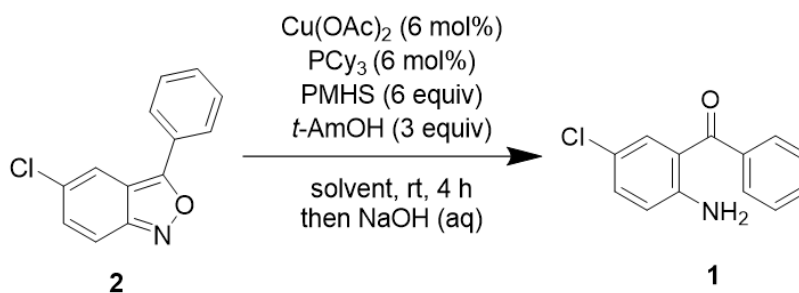
Figure 4-8: (a) Solubility screen of commercial sample of **1** in various solvents, (b) after overnight evaporation of solvent, recrystallization from MeOH is observed. From left to right: water, methanol, acetone, ethyl acetate, diethyl ether, hexanes.

and recrystallization from 0.1 M **1** in 30% water–MeOH was observed.

Purification of **1** from the crude reaction mixture by recrystallization from MeOH–water was performed as follows (see further details in Experimental Section):

- Suspend crude residue in 30% water–methanol
- Heat to reflux (solubilize **1**)
- Hot filtration to remove insoluble PMHS byproduct
- Cool filtrate, collect crystals of **1**

An image of the hot filtration process is shown in Figure 4-9. Concurrently, alternative reaction solvents were evaluated, which is discussed in more detail below. Recrystallization of a crude mixture after reaction in cyclopentylmethyl ether (CPME), from a solution of **1** (approximately 0.3 M **1** in 30% water–methanol) led to 55% yield of **1** with some PMHS byproducts remaining (Figure 4-10). For the reaction performed in toluene (Table 4.10, entry 2), high purity **1** was obtained in 40% yield by recrystallization (approximately 0.1 M **1** in 30% water–methanol) after successful separation of insoluble PMHS byproducts (Figure 4-9, Entry 2 and Figure 4-10). In a subsequent reaction with 2-MeTHF as solvent, lower purity **1** was obtained in 51% yield after quite unsuccessful separation of PMHS byproducts (Figure 4-9, Entry 3



entry	solvent, [M]	purification	purity (%)	IY 1 (%)
1 ^d	CPME, 0.2	recrystallization	–	55 ^a
2 ^d	PhMe, 0.2	recrystallization	–	40 ^a
3	2-MeTHF, 0.3	recrystallization	–	51 ^a
4	PhMe, 0.2	chromatography	–	66 ^a
5 ^d	THF, 0.1	chromatography	–	79 ^a
6	THF, 0.3	chromatography	57	76
7	2-MeTHF, 0.3	chromatography	54	74
8 ^b	THF, 0.3	chromatography	>99	79
9 ^{b,c,d}	THF, 0.3	chromatography	–	84 ^a

^a uncorrected for purity ^b quench with NH_4F in MeOH

^c 3 equiv PMHS ^d 20 h reaction

Table 4.10: Synthesis of **1** using different solvents and purification methods. Experimental details described in Section 4.3.10 on page 4.3.10.

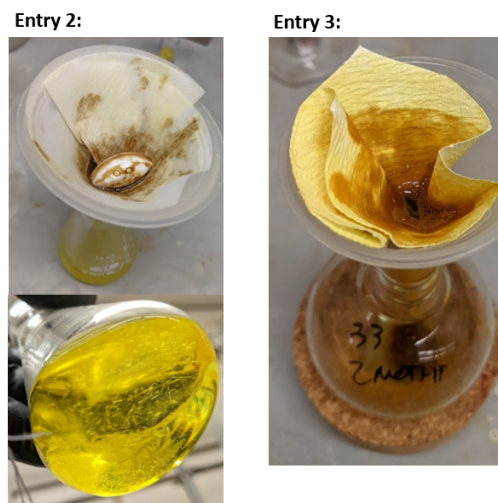


Figure 4-9: Hot filtration of crude reaction mixture dissolved in 30% water–MeOH. (Entry 2) Separation of insoluble brown gel (PMHS byproduct) from crude reaction mixture (Table 4.10, entry 2). (Entry 3) Less successful separation in a subsequent attempt (Table 4.10, entry 3).

and Figure 4-10). Comparison of the ^1H NMR spectra of the recrystallized product from these three trials shows the challenge of reproducibly separating the PMHS byproducts (Figure 4-10).

To comment briefly on the nature of the reaction in alternative solvents, the starting material **2** was less soluble in cyclopentylmethyl ether (CPME) and toluene (PhMe) relative to THF, so these reactions were run at a reduced concentration of 0.2 M (Table 4.10, entries 1–2 and 4). Accordingly, these reactions were more sluggish and thus the system was left to react overnight to achieve high conversion. Analysis of the crude reaction mixture showed higher selectivity for **1** relative to a 4 h reaction in THF, although residual starting material **2** was present after these overnight reactions. Estimation of the yield by ^1H NMR analysis of the crude reaction mixture showed the expected 75–90% yield of **1**, however only 40–55% was obtained after recrystallization. Analysis of different components of the recrystallization process show that **1** is lost to the polymeric PMHS byproduct and to the mother liquor (Figure 4-11). We observe by eye that some yield of **1** is lost during other material transfer operations related to filtration.

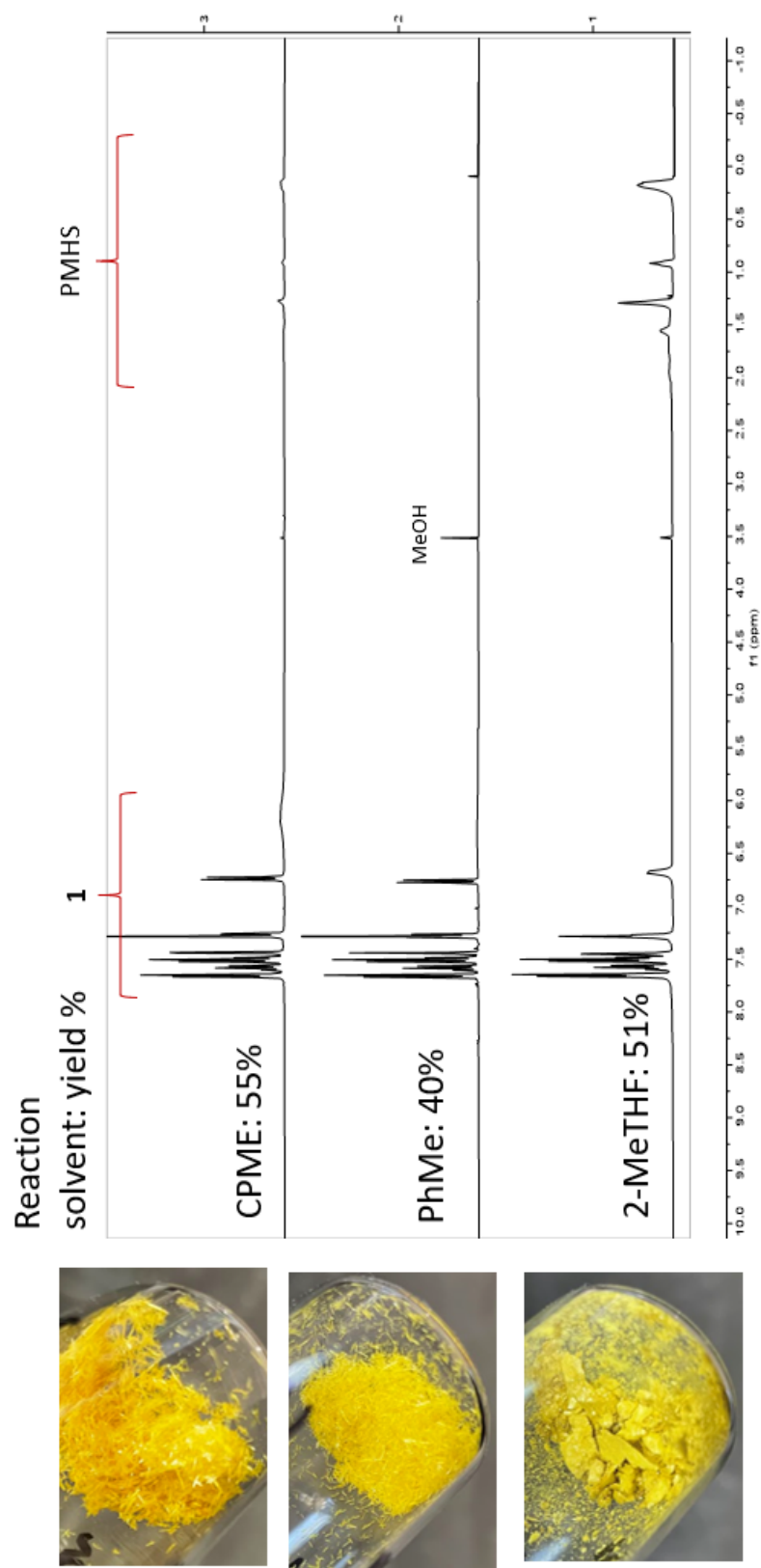


Figure 4-10: ^1H NMR Spectra (400 MHz, CDCl_3) of recrystallized product **1** for 2 mmol scale reactions described in Table 4.10.

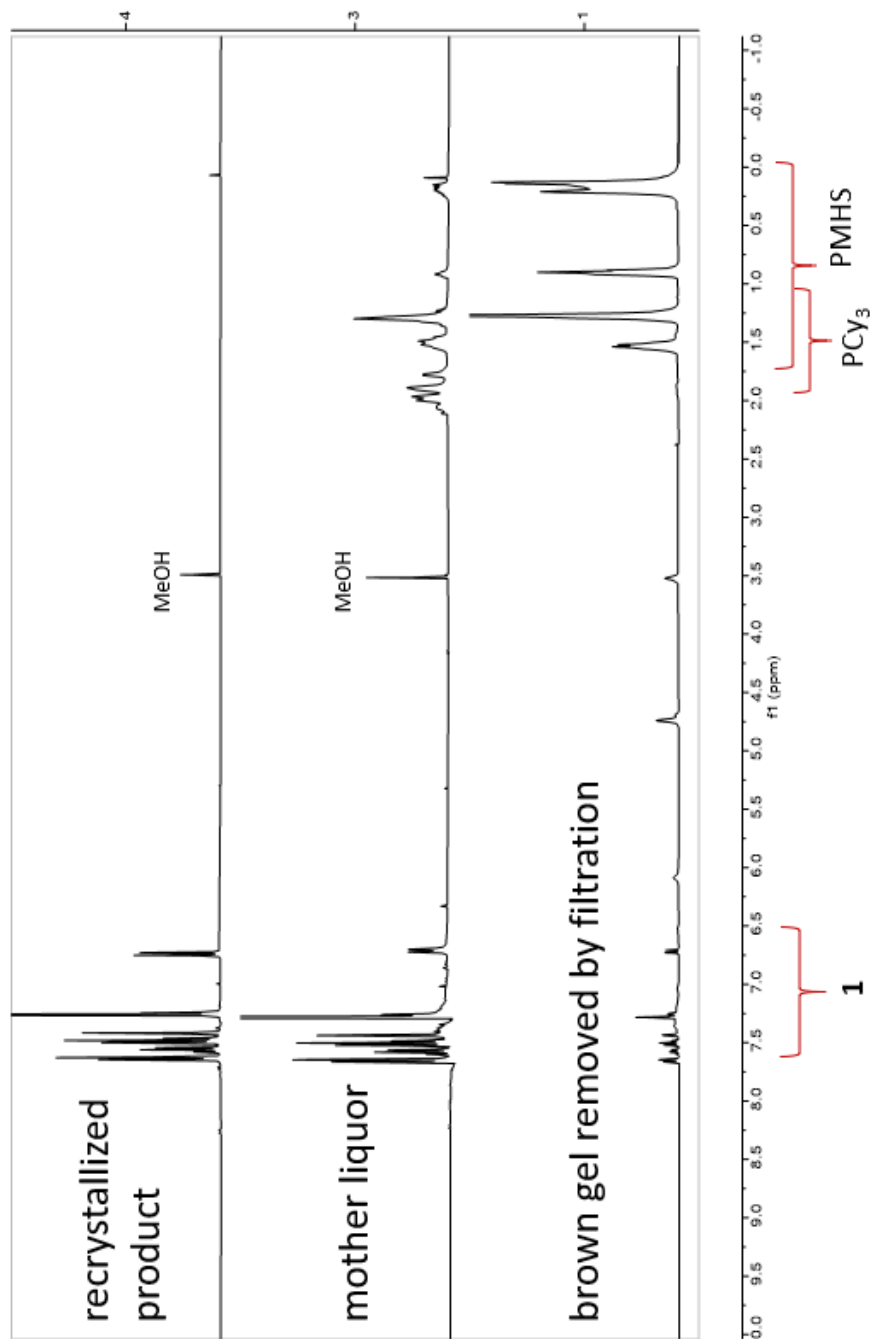


Figure 4-11: ¹H NMR analysis (400 MHz, CDCl₃) of fractions separated during the recrystallization process for purification of **1** (Table 4.10, entry 2).

Due to the cumbersome nature of hot filtration, and material loss during this filtration process, isolation by column chromatography was performed to validate the 75–90% assay yield observed on 0.5 mmol scale. Given that less formation of undesired product **5** was observed in Table 4.10 entries 1 and 2 (by ^1H NMR analysis of crude reaction mixture) versus a reaction at higher concentration in THF, we evaluated the reduction of **2** to **1** on 2 mmol scale in THF at 0.1 M and 0.3 M concentrations. These experiments showed similar yield of **1**, suggesting that reaction concentration has a small impact on formation of **5**. 2-MeTHF behaved similarly to THF and was evaluated at 0.3 M reaction concentration, yielding 74% of **1** in 4 h after chromatographic purification. In general, these isolated yields on 2 mmol scale reflected the previously obtained assay yields on 0.5 mmol scale, and THF remained the optimal solvent among those which were evaluated.

Interestingly, low purity material (54–57% purity) was obtained by column chromatography, presumably due to co-elution of the silane polymer which has a similar solubility profile to **1** (Table 4.10, entries 6, 7). These purification challenge may explain the relatively unpopular use of polymethylhydrosiloxane on process scale, despite its low cost. Encouragingly, altering the quench method to use NH_4F in MeOH instead of aqueous NaOH improved the purity of the isolated material, resulting in isolation of **1** with 99% purity and 79% yield after chromatographic purification. We think that this improvement is due to changed solubility properties of silane polymer with a different quenching method. Further development of the recrystallization procedure using this alternative quenching method is underway in our laboratory.

4.2.7 Conclusion

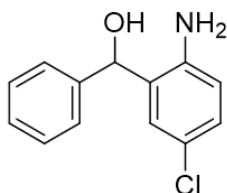
In summary, key benzodiazepine precursor **1** was prepared by a copper hydride-catalyzed reduction of 2,1-benzo[*c*]isoxazole **2**. Use of a bulky monodentate phosphine ligand improved selectivity for *N,O*-reduction over 1,2-reduction and introduction of an alcohol additive improved catalyst turnover, leading to reaction conditions which provide **1** in 79–84% isolated yield after chromatographic purification. Isolation by recrystallization from MeOH/ H_2O yielded **1** in up to 55% yield.

4.3 Experimental Section

4.3.1 General Methods

Reagents were used as supplied commercially without further purification. Solvents were dried and sparged with Argon using a solvent purification system prior to use unless otherwise noted. Reactions were run under Argon atmosphere unless otherwise noted. 5-Chloro-3-phenylbenzo[*c*]isoxazole was obtained from Combi-Blocks. Copper(II) acetate, anhydrous and all phosphine ligands was obtained from Sigma-Aldrich/Millipore Sigma. Polymethylhydrosiloxane (1700-3200 MW polymer, Sigma Aldrich) was used and stoichiometry of silane was calculated as approx. 65.4 μL polymer per 1 mmol of silane using the provided molecular weight range and density. For all procedures described herein, “room temperature” refers to a temperature range of 20–24 °C. Thin-layer chromatography (TLC) was performed using 0.2 mm coated glass silica gel plates and visualized using either ultraviolet light. Purification by column chromatography over silica gel was performed on a Biotage Selekt flash chromatography system using Isco RediSep Rf Gold silica gel columns. All NMR spectra were collected using a two-channel Bruker Avance-III HD Nanobay spectrometer operating at 400.09 MHz equipped with a 5 mm liquid-nitrogen cooled Prodigy broad band observe (BBO) cryoprobe. Chemical shifts (δ) are reported in units of ppm, relative to the residual solvent peak, which was adjusted to match reported values.

4.3.2 General Procedures for Reaction Optimization and Synthesis



Synthesis of (2-amino-5-chlorophenyl)(phenyl)methanol (5). In a nitrogen-filled glovebox, copper(II) acetate (5 mg, 0.03 mmol, 5 mol%) was added to an oven-dried 20 mL vial equipped with a magnetic stirrer. Racemic BINAP (19 mg, 0.030 mmol, 6 mol%) was added. The vial was capped and removed from the glovebox. THF (0.5 mL) was added. The mixture was stirred for 10 minutes. Silane (1.5 mmol) was added and the mixture was stirred for 10 minutes. (2-amino-5-chlorophenyl)(phenyl)methanone (116 mg, 0.500 mmol) was dissolved in THF (0.5 mL) and added. The reaction was stirred overnight. The reaction was vented by inserting a needle through the septum cap. A solution of 0.3 M ammonium fluoride in MeOH (10 mL) was added and the resulting mixture was stirred for 30 minutes at room temperature. TLC analysis of the crude reaction mixture showed full conversion of starting material to a single product ($R_f = 0.1$, 10% EtOAc/hexanes). Silica gel was added to the quenched reaction mixture and the solvent was removed under reduced pressure. The material was purified by column chromatography (5–60% EtOAc/hexanes) to yield the title compound as a white solid (99.5 mg, 0.426 mmol, 85%). ESI-MS m/z $[M-H_2O]^+$ 215.9, 217.9. Analytical data were consistent with reported values.²³

4.3.3 General Procedure for Initial Screening and Feasibility Assessment

Method for Table 4.1 on page 251. In a nitrogen-filled glovebox, copper(II) acetate (4.5 mg, 0.025 mmol, 5 mol%) was added to an oven-dried 20 mL vial equipped with a magnetic stirrer. The indicated ligand (0.03 mmol, 6 mol%) was added. The vial was capped and removed from the glovebox. The indicated solvent (1.0 mL) was added. The mixture was stirred for 10 minutes. The indicated silane (1.5 mmol) was added. A solution of 5-chloro-3-phenylbenzo[*c*]isoxazole (1.0 mL of 0.5 M solution) was added. The reaction was stirred overnight. Each reaction was vented by inserting a needle through the septum, followed by addition of 0.3 M NH₄F solution in MeOH (10 mL). The mixture was stirred for 30 minutes at room temperature.

For HPLC analysis: The reaction mixture was transferred to a 25-mL volumetric flask and diluted to 25 mL with MeOH. Solutions were directly analyzed by reverse-phase HPLC (MeCN/H₂O) after filtration through a 0.2 μm syringe filter.

For ¹H NMR analysis: A solution of ethylene carbonate (¹H NMR standard) was added. A pipette column was flushed with MeOH. The quenched reaction mixture was run through the column, washing with 2 column volumes of MeOH. This results in a bright yellow solution. Note this method results in poor mass balance due to retention of ethylene carbonate on the pipette column. An alternate method was used in ongoing screening.

4.3.4 General Procedure for Investigation of Monodentate Phosphine Ligands

Method for Table 4.2 on page 253. A stock solution of 3 M *t*-BuOH was prepared: *t*-BuOH (5.55 g, 74.9 mmol) was added to a 25-mL volumetric flask and diluted with THF. In a nitrogen-filled glovebox, copper(II) acetate (5 mg, 0.03 mmol, 6 mol%) was added to an oven-dried 20-mL vial equipped with a magnetic stirrer. The indicated monodentate phosphine ligand (0.06 mmol, 12 mol%) was added. The vial was capped and removed from the glovebox. The *t*-BuOH solution (0.5 mL of 3 M solution) was added. The mixture was stirred for 10 minutes. Polymethylhydrosiloxane (70 μ L, 1.1 mmol) was added. A solution of **2** (0.5 mL of 1 M solution in THF) was added. The vial was vented by briefly piercing the septum with a needle. The reaction was stirred for 16 h. A solution of 0.3 M NH₄F in MeOH (10 mL) was added and the mixture was stirred for 30 minutes at room temperature. A pipette column was flushed with MeOH. The reaction mixture was run through the column, washing with 2 column volumes of MeOH. 1,3,5-Trimethoxybenzene was added as an NMR standard. An aliquot was removed and used for ¹H NMR analysis in DMSO-d₆.

4.3.5 General Procedure for Screening Monodentate Phosphine Ligand Stoichiometry

Method for Table 4.4 on page 255. Copper(II) acetate (5 mg, 0.03 mmol) was added to an oven-dried 2-dram vial equipped with a magnetic stirrer. Ligand (12 mol%) was added. *t*-BuOH solution (0.5 mL of 3 M solution in THF) was added. The mixture was stirred for 10 minutes. Polymethylhydrosiloxane (95 μ L, 1.5 mmol) was added. A solution of **2** (1.0 M in THF) was prepared and 0.5 mL of this solution was added to each respective reaction (0.5 mmol). The reaction was stirred for the indicated time. The reaction was quenched by addition of methanol (1 mL) and was stirred for 30 min at room temperature. The reaction was diluted with EtOAc and washed with a saturated solution of sodium bicarbonate (2 mL). 1,3,5-Trimethoxybenzene solution was added (^1H NMR standard). An aliquot was collected and the solvent was removed under reduced pressure. Yield was determined by ^1H NMR analysis in DMSO- d_6 .

4.3.6 General Procedure for Investigation of Additives and Copper Catalyst Source

Method for Table 4.3 on page 255. Copper(II) acetate (5 mg, 0.03 mmol) was added to an oven-dried 20-mL vial equipped with a magnetic stirrer. Ligand (0.06 mmol) was added. *t*-BuOH solution (3 M in THF) was added (0.5 mL, 1.5 mmol). The mixture was stirred for 10 minutes. Polymethylhydrosiloxane (70 μ L, 1.1 mmol) was added. A solution of **2** (1.0 M in THF) was prepared and 0.5 mL of this solution was added to each respective reaction (0.5 mmol). The reaction was stirred for 16 h. The reaction was quenched by addition of 0.3 M NH₄F in MeOH (10 mL). The quenched mixture was vented with a needle and stirred for 30 min at room temperature. 1,3,5-Trimethoxybenzene solution of known concentration was added. Pipette column method described in Section 4.3.4 was used, however columns were clogging so only a small silica plug for the NMR aliquot was performed. The aliquot was dried down for ¹H NMR analysis in DMSO-d₆.

4.3.7 General Procedure for Screening Temperature, Additives, and Silane Stoichiometry

Method for Table 4.5 (page 257), Table 4.6 (page 257), and Table 4.7 (page 261). Copper(II) acetate (5 mg, 0.03 mmol) was added to an oven-dried 2-dram vial equipped with a magnetic stirrer. Ligand (PCy₃ 8 mg, 6 mol%; P(*t*-Bu)₃, 10 w/w% solution in hexanes, 60 μL, 6 mol%) was added and the vial was removed from the glovebox. *t*-BuOH solution (0.5 mL of 3 M solution in THF, 1.5 mmol) was added. NaO*t*-Bu (250 μL of 2 M solution in THF, 0.5 mmol) was added as indicated. The mixture was stirred for 10 minutes. Polymethylhydrosiloxane (variable) was added, the solution was stirred for 10 min. A solution of **2** (1 M in THF) was prepared and 0.5 mL was added to each respective reaction (0.5 mmol). The reaction was stirred overnight at room temperature. The reaction was quenched by addition of methanol (0.5 mL) and was stirred for 10 min at room temperature. A saturated solution of sodium bicarbonate (1 mL) was added and the heterogeneous mixture was stirred for 10 min. The quenched mixture was diluted with Et₂O (2 mL) and water (1 mL) and the layers were separated. Enough water was added to achieve two clear layers. The aqueous layer was removed. The organic layer was washed with brine. 1,3,5-Trimethoxybenzene was added as a ¹H NMR standard. An aliquot was removed and the solvent was evaporated to dryness. The yield was determined by ¹H NMR.

4.3.8 Continuous Flow Trial 1

Reagent stream A (0.05 M Cu(OAc)₂, 0.05 M PCy₃, 3 M *t*-AmOH in THF):

Cu(OAc)₂ (227 mg, 1.25 mmol) and PCy₃ (350 mg, 1.25 mmol) were added to a 25-mL volumetric flask. *t*-Amyl alcohol (8.1 mL, 75 mmol) was added and the mixture was diluted with anhydrous THF. The mixture was sonicated until a homogeneous mixture was obtained.

Reagent stream B (2.9 M polymethylhydrosiloxane in THF):

Polymethylhydrosiloxane (4.7 mL, 72 mmol) was added to a 25-mL volumetric flask and diluted with THF.

Reagent stream C (5-chloro-3-phenylbenzo[*c*]isoxazole 1 M in THF):

2 (5.74 g, 25.0 mmol) was added to a 25 mL volumetric flask and diluted with THF.

Method

A Syrris syringe pump was equipped with green (250, 500 μ L) syringes. The pump was primed with anhydrous THF. Reagent Streams A and B were connected 90° at a T-mixer, leading to a 1 mL reactor (0.03" ID / 1/16" OD HP-PFA tubing). Starting material Reagent Stream C was connected 90° at a T-mixer, leading to a 4 mL reactor (0.04" ID / 1/16" OD HP-PFA tubing). Reagent streams were fixed with N₂ balloons to equilibrate pressure. All pumps were started and the system was equilibrated for 2.5 equilibration times. The reagent stream was collected for a theoretical yield of 0.2 mmol in a vial containing saturated sodium bicarbonate solution (1.0 mL). The organic layer was collected by extraction with Et₂O (2 x 1 mL). 1,3,5-Trimethoxybenzene was added as a ¹H NMR standard and yield was determined by ¹H NMR in DMSO-d₆.

4.3.9 Continuous Flow Trial 2

The continuous flow trials summarized in Table 4.9 were performed following the same general procedure described above with the following differences: For reagent stream B, a 5 M solution of PMHS was used (8.1 mL, 124 mmol, in 25-mL volumetric flask). The system was equilibrated for 3 residence times prior to sample collection.

4.3.10 Representative Procedure for Synthesis of (2-amino-5-chlorophenyl)(phenyl)methanone (1) on 2 mmol Scale

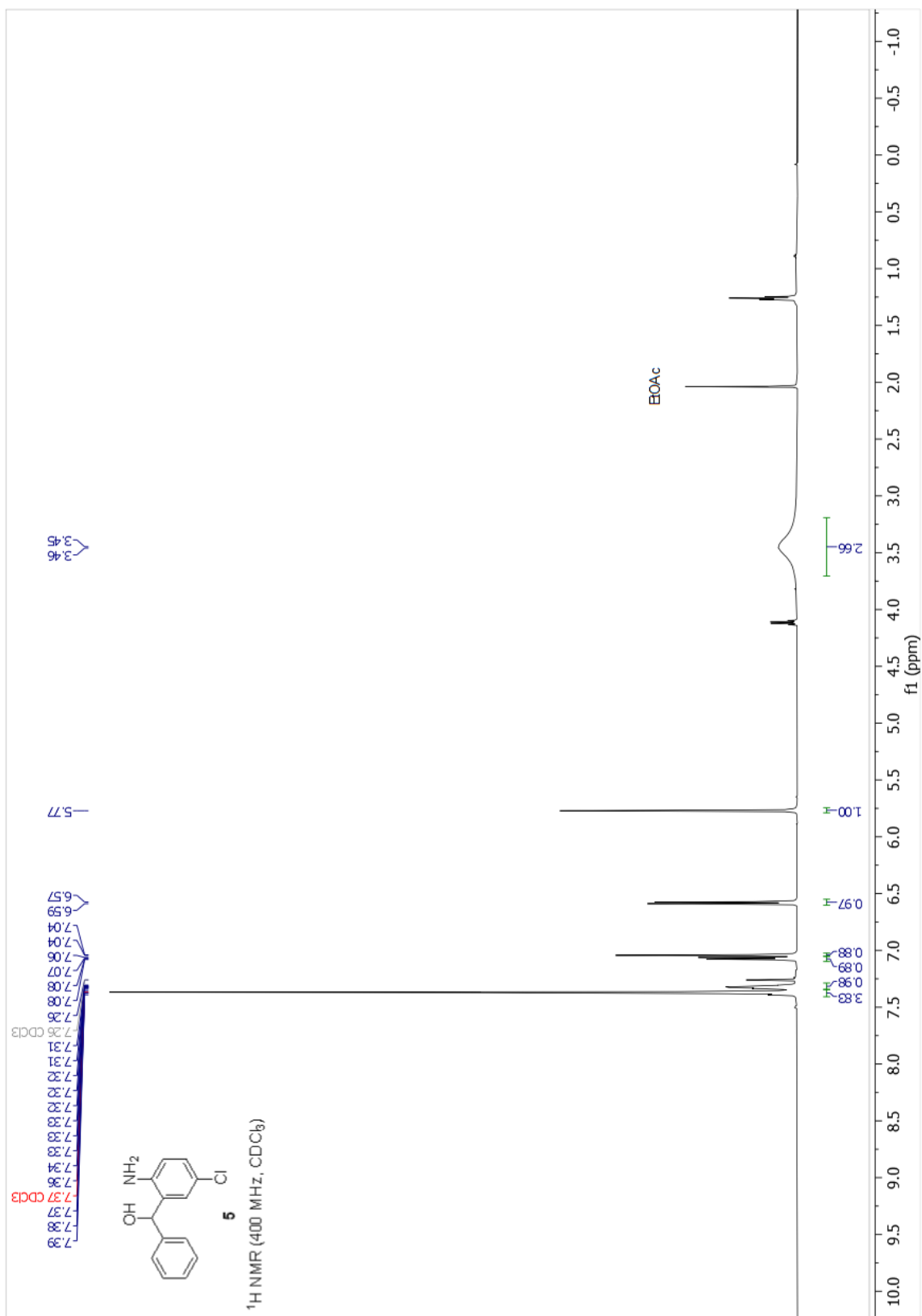
Representative method for results summarized in Table 4.10. In a nitrogen-filled glovebox, copper(II) acetate (22 mg, 0.12 mmol, 6 mol%) was added to an oven-dried 50-mL roundbottom flask equipped with a magnetic stirrer. Tricyclohexylphosphine (34 mg, 0.12 mmol, 6 mol%) was added and the flask was capped with a rubber septum and removed from the glovebox. THF (2 mL) was added followed by *tert*-amyl alcohol (650 μ L, 6 mmol, 3 equiv). Note: *tert*-Amyl alcohol was sparged with Argon for 10 minutes prior to use. The mixture was stirred for 10 minutes. A nitrogen-filled balloon was connected via the rubber septum cap. Polymethylhydrosiloxane (785 μ L of 1700-3200 MW polymer, 12 mmol, 6 equiv) was added. The solution was stirred for 10 min and a red-brown color developed. 5-chloro-3-phenylanthranil **2** (459.3 mg, 2.00 mmol, 1.0 equiv) dissolved in THF (2 mL) was added. Additional THF (1 mL) was used to complete transfer. The final reaction concentration is 0.3 M. The reaction was stirred for 4 h. The reaction was quenched by slow addition of 1 M NH_4F in MeOH (12 mL). The solvent was removed under reduced pressure to yield a yellow solid. The residue was suspended in ethyl acetate and dry-loaded onto silica gel. Purification by column chromatography (5–40% EtOAc/hexanes) yields a bright yellow crystalline solid (367.3 mg, 1.59 mmol with >99% purity, 79%). ^1H NMR (400 MHz, DMSO-d_6) δ 7.78–7.48 (m, 5H), 7.32 (dd, $J = 8.9, 2.6$ Hz, 1H), 7.25–7.06 (m, 3H), 6.90 (d, $J = 9.0$ Hz, 1H). $^{13}\text{C}\{^1\text{H}\}$ NMR (101 MHz, DMSO-d_6) δ 196.8, 150.6, 139.2, 134.0, 132.1, 131.3, 128.5, 128.4, 118.9, 116.98, 116.96. Purified samples were

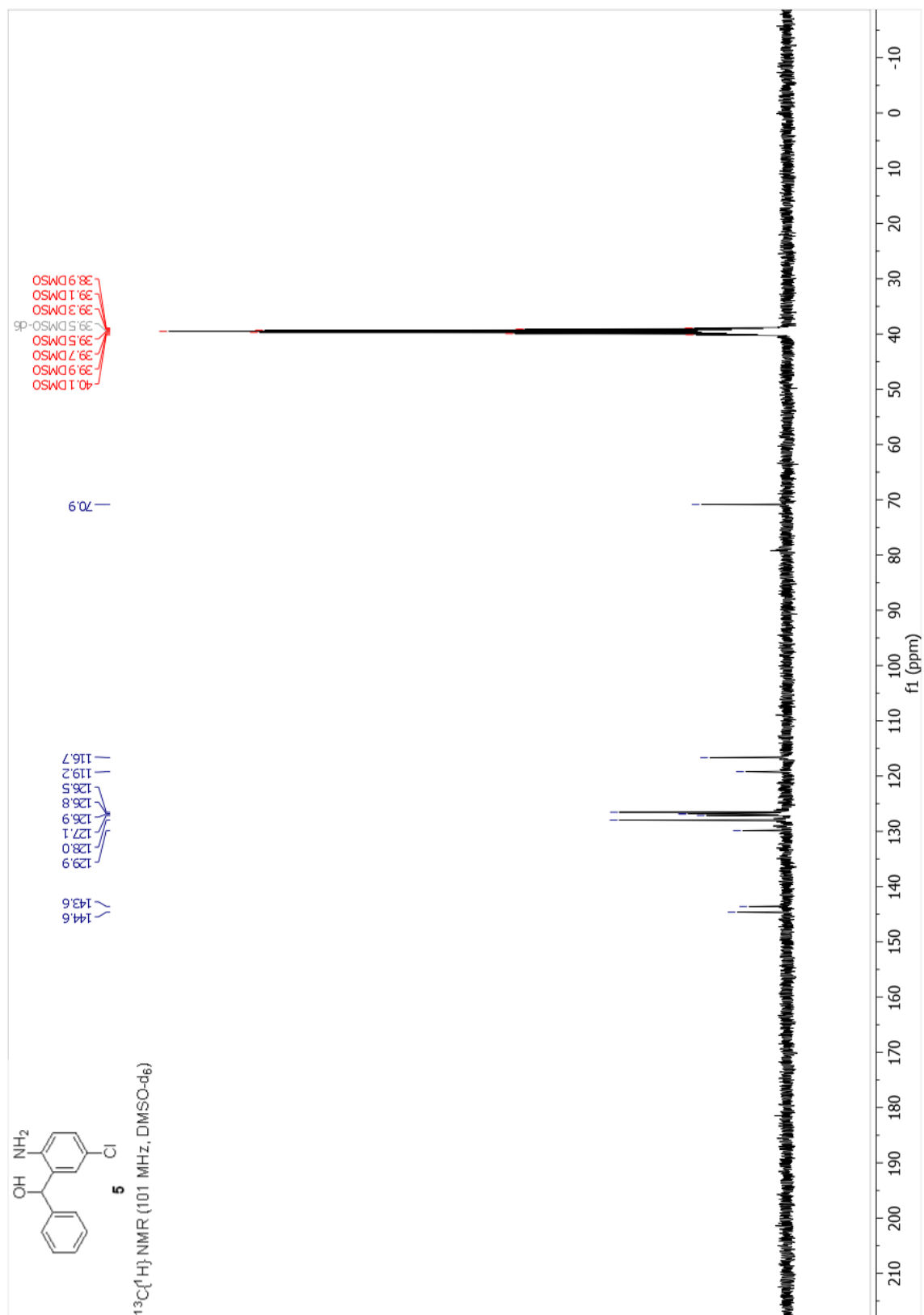
compared to commercial material obtained from Sigma-Aldrich and were consistent with those reported in the literature.²⁴

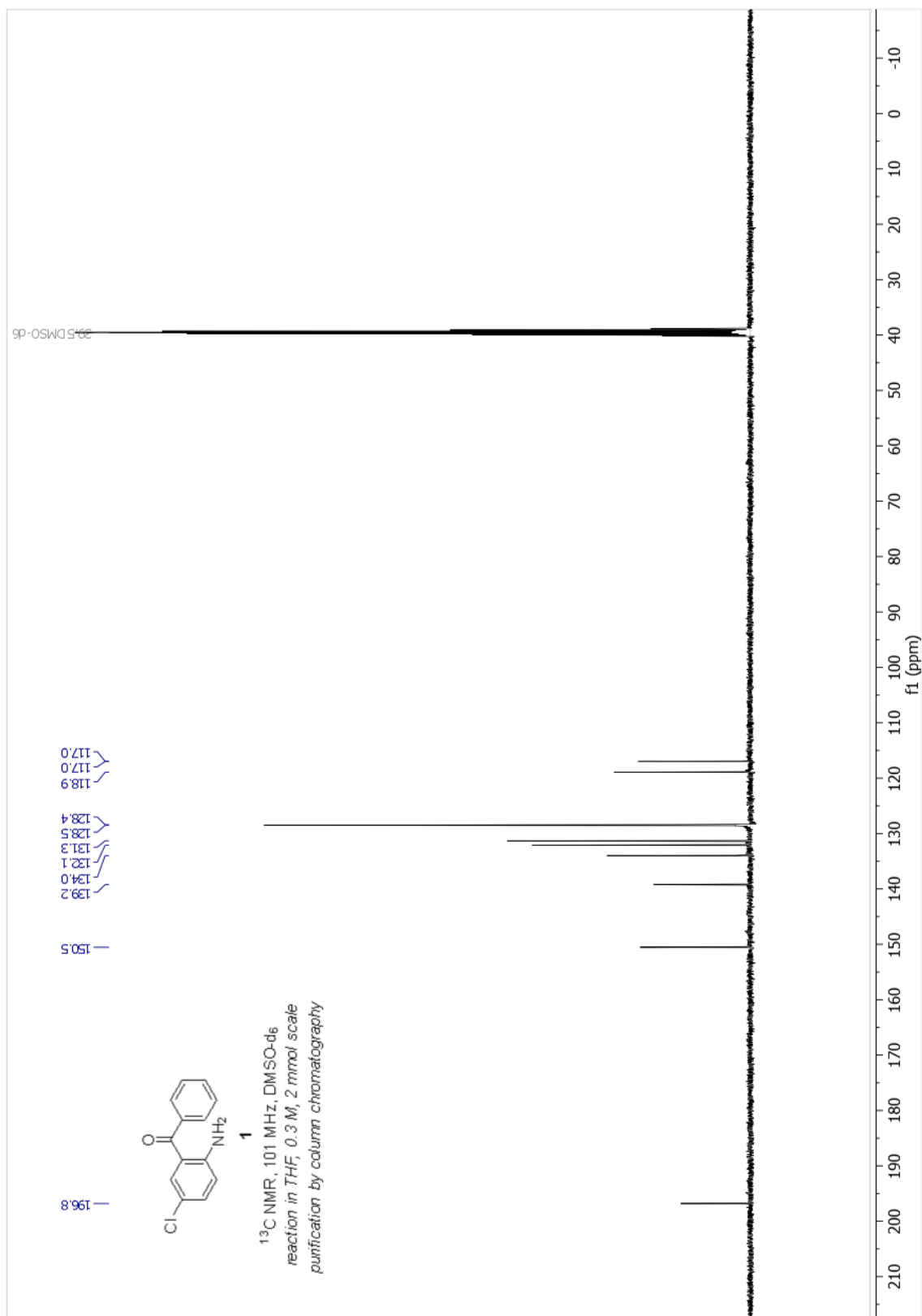
Alternative Work-up Procedure. The septum cap was removed from the reaction vessel and a solution of 0.1 M NaOH (aq) was added dropwise (3 mL) and stirring was continued for 30 min. The reaction mixture was diluted with Et₂O, washed with water, back extracted with Et₂O. The combined organic extracts were dried with MgSO₄, filtered, and the solvent was removed.

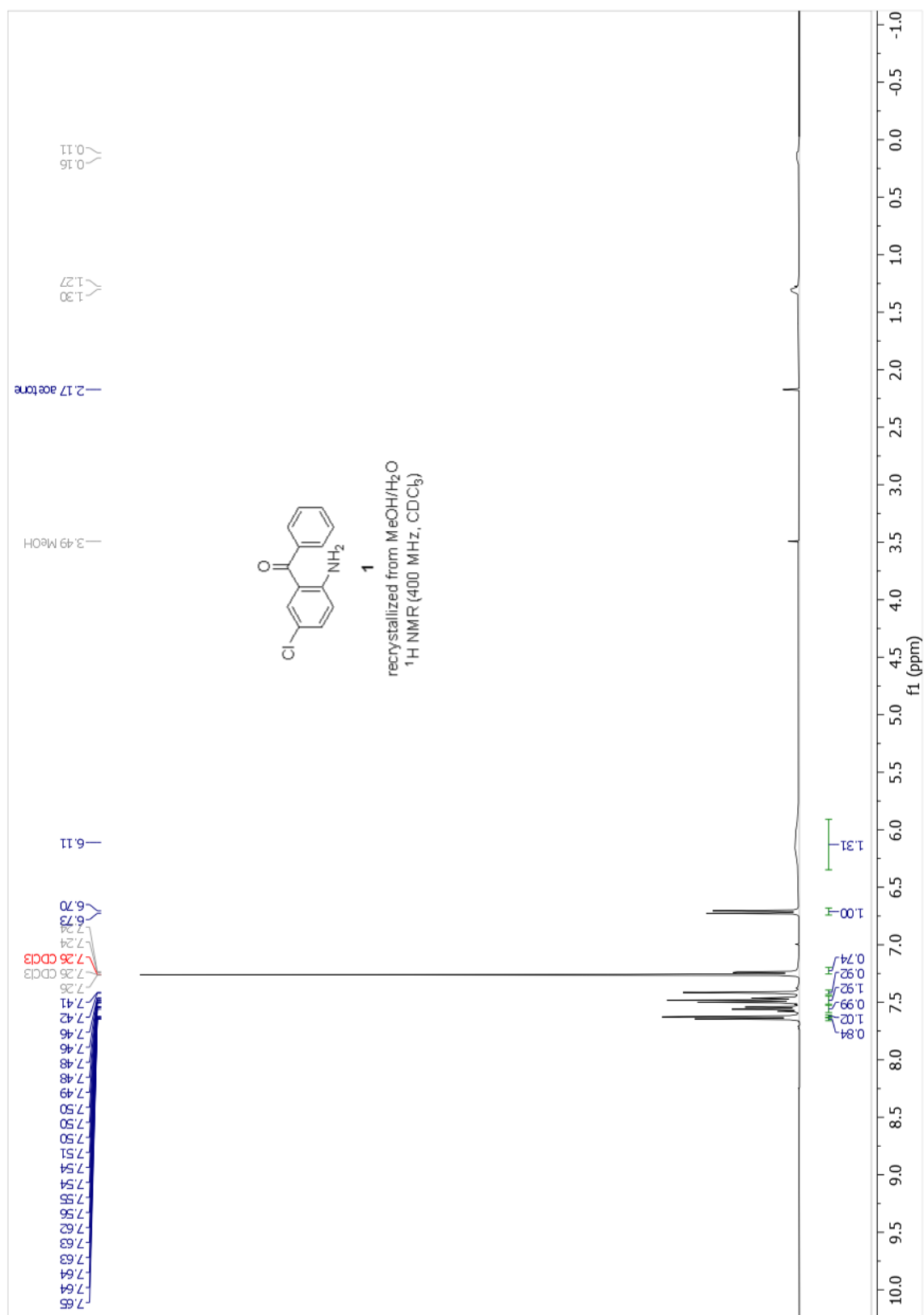
Isolation by Recrystallization. The crude residue was suspended in a solution of 30% aqueous MeOH (6 mL). A reflux condenser was attached and the suspension was heated to reflux (sand bath heated to 85 °C). The mixture was refluxed for 10 minutes. Additional 30% aqueous MeOH was heated in parallel. The reflux condenser was removed, and the hot solution was filtered, washing with hot aqueous methanol solution (5–20 mL). The resulting filtrate was cooled to room temperature, then transferred to the refrigerator overnight. Crystals were collected by vacuum filtration.

4.4 ¹H and ¹³C{¹H} NMR Spectra









4.5 References

- [1] Ogbru, A. G. RxList: Benzodiazepines. **2021**, <https://www.rxlist.com/benzodiazepines/drug-class.htm> (accessed 2022-03-16).
- [2] WHO List of Essential Medicines - 22nd List, **2021**, <https://www.who.int/publications/i/item/WHO-MHP-HPS-EML-2021.02> (accessed 2022-03-23).
- [3] Snead, D. R.; McQuade, D. T.; Ahmad, S.; Krack, R.; Stringham, R. W.; Burns, J. M.; Abdiaj, I.; Gopalsamuthiram, V.; Nelson, R. C.; Gupton, B. F. *Org. Proc. Res. Dev.* **2020**, *24*, 1194–1198.
- [4] The Medicines for All Institute. Process Development Report: 5-Fluorocytosine. **2019**, <https://medicines4all.vcu.edu/our-portfolio/bmgf-projects/5-fluorocytosine/> (accessed 2022-03-23).
- [5] Taghizadeh, M. J.; Malakpouri, G. R.; Javidan, A. *J. Iranian Chem. Soc.* **2019**, *16*, 785–794.
- [6] Capanec, I.; Litvić, M.; Pogorelić, I. *Org. Proc. Res. Dev.* **2006**, *10*, 1192–1198.
- [7] Wang, B.; Hou, Q.; Feng, J. Method for preparing lorazepam. CN 110776473 A, 2019.
- [8] Wang, B.; Hou, Q.; Feng, J. Light-stabilized pharmaceutical composition, and preparation method and pharmaceutical application thereof. CN 110840898 A, 2020.
- [9] Hou, Q.; Wang, B.; Feng, J. New crystal form of lorazepam, preparation method and pharmaceutical applications thereof. CN 110683994 A, 2020.
- [10] Massah, A. R.; Gharaghani, S.; Lordejani, H. A.; Nasakere, A. *Med. Chem. Res.* **2016**, *25*, 1538–1550.
- [11] Adamo, A.; Beingessner, R. L.; Behnam, M.; Chen, J.; Jamison, T. F.; Jensen, K. F.; Monbaliu, J.-C. M.; Myerson, A. S.; Revalor, E. M.; Snead, D. R. Stelzer, T. Weeranoppanant, N.; Wong, S. Y.; Zhang, P. *Science* **2016**, *352*, 61–67.
- [12] Sugasawa, T.; Adachi, M.; Toyoda, T.; Sasakura, K. *J. Heterocyclic Chem.* **1979**, *16*, 445–448.
- [13] Yuwen, L.; Guan, Q.; Zhao, X.; Li, B. Preparation method of alprazolam intermediate. CN 108250091 (A), 2018.
- [14] Orlov, V. Y.; Kotov, A. D.; Bystryakova, E. B.; Kopeikin, V. V.; Mironov, G. S. *Russian J. Org. Chem.*, **1994**, *30*, 1481–1484.

- [15] Aidene, M.; Belkessam, F.; Soulé, J.-F.; Doucet, H. *ChemCatChem* **2016**, *8*, 1583–1590.
- [16] Russell, M. G.; Veryser, C.; Hunter, J. F.; Beingessner, R. L.; Jamison, T. F. *Adv. Synth. Catal.* **2020**, *362*, 314–319.
- [17] Deutsch, C.; Krause, N. *Chem. Rev.* **2008**, *108*, 2916–2927.
- [18] Jordan, A. J.; Lalic, G.; Sadighi, J. P. *Chem. Rev.* **2016**, *116*, 8318–8372.
- [19] Tsai, E. Y.; Liu, R. Y.; Yang, Y.; Buchwald, S. L. *J. Am. Chem. Soc.* **2018**, *6*, 2007–2011.
- [20] Lipshutz, B. H.; Papa, P. *Angew. Chem.* **2002**, *114*, 4762–4764.
- [21] Lipshutz, B. H.; Papa, P. *Angew. Chem., Int. Ed.* **2002**, *41*, 4580–4582.
- [22] Jover, J.; Cirera, J. *Dalton Transactions* **2019**, *48*, 15036–15048.
- [23] Fan, J.; Wan, C.; Sun, G.; Wang, Z. *J. Org. Chem.* **2008**, *73*, 8608–8611.
- [24] Cheng, P.; Zhang, Q.; Ma, Y.-B.; Jiang, Z.-Y.; Zhang, X.-M.; Zhang, F.-X.; Chen, J.-J. *Bioorg. Med. Chem. Lett.* **2008**, *18*, 3787–3789.

Chapter 5

A Call for Increased Focus on Reproductive Health within Lab Safety Culture

5.1 Introduction

Laboratory safety has received increased attention in recent years, evidenced by the declaration of safety as a core value by the American Chemical Society, and subsequent publication of the dedicated chemical safety journal, ACS Chemical Health and Safety.¹ Reports investigating the root cause of safety incidents conclude that a common underlying cause is systemic failure to provide researchers with the resources to properly assess and mitigate risks.²⁻⁴ With an increase in focus on inclusion within chemistry, reproductive health safety should receive increased attention. When reproductive toxins are not handled with proper care within laboratory settings, it can lead to exposure of people that do not know they are pregnant and people undergoing spermatogenesis, as well as bio-accumulation of these toxins and chemical transmission via toxic compounds remaining on lab clothes that are worn home.⁵ Unintended exposure to reproductive toxins can lead to serious negative outcomes for all individuals. Exposure of laboratory workers to reproductive toxins can lead to infertility,

reduced fertility and genetic damage to germ cells.⁵⁻⁷ Specifically, genetic damage to sperm can lead to pre-term birth, low birth weight, as well as central nervous system malformation in the fetus. Exposure to reproductive toxins during pregnancy can lead to transmission of chemicals through the placenta which can cause stillbirth, spontaneous abortion, as well as diseases or congenital abnormalities in the fetus.^{5,7} During lactation, exposure to reproductive toxins can transmit these chemicals to the child via human milk.⁵ The period encompassing planned or unplanned conception, pregnancy, and lactation amounts to years during which individuals need heightened protection from reproductive toxins. We believe that Chemical Hygiene Plans (CHPs) could serve as an important resource to provide guidance for laboratory workers on the identification of potential reproductive toxins in the workplace.

In this perspective, we evaluate the information provided by CHPs pertaining to reproductive health for university laboratory workers. Generally speaking, we find that the instruction on reproductive health safety in CHPs is absent or minimal, often puts the onus on the pregnant person or person planning to conceive to identify and minimize exposure to reproductive toxins, and generally provides non-private resources or a wide range of recommended resources with no guidance on how to use each one. After this assessment, we evaluate three external resources commonly recommended by CHPs: Safety Data Sheets (SDSs), the NIOSH Pocket Guide (NPG), and the Proposition 65 list (Prop. 65). We then compare how these sources classify chemicals listed as reproductive toxins within CHPs. Finally, we recommend straightforward changes within CHPs and laboratory-level discussions that will lead to improved guidance for reproductive safety of laboratory workers.

5.2 Analysis and Perspective

A way of providing sufficient protection from occupational hazards is to implement a universal or unified protection safety model in which all workers follow the recommended guidelines for protection of the group which is most sensitive to chemical exposure.⁶ An alternative, individualistic safety model, *differentiated protection*,^{6,8}

aims to protect the sensitive group by reducing only the exposure of that group. In the context of reproductive health safety, an example of unified protection is ensuring that all individuals identify substances in their work as possible reproductive toxins and handle these substances accordingly. An example of differentiated protection would be removal of a pregnant worker from the lab environment to minimize their exposure to reproductive toxins. Differentiated protection has been shown to provide insufficient protection from reproductive toxins in the following situations: unplanned conception, bio-accumulation effects, and when pregnancy is not immediately known.⁶ Laboratory safety guidelines should protect the reproductive health of all workers by implementing a unified protection safety model in which all take care to control and minimize exposures to reproductive toxins. A first step towards implementing a unified protection safety model is to effectively communicate that the risk of reproductive toxin exposure within laboratories affects everyone. To evaluate the current messages pertaining to reproductive health that university laboratory workers are receiving, we elected to assess the guidance in university CHPs. Under OSHA's Laboratory Standard, it is recommended that all laboratories using hazardous chemicals inform laboratory workers of chemical dangers and safe-handling practices in a safety manual known as the CHP.⁹ CHPs could serve as a first resource that a laboratory worker references to begin research on reproductive toxin exposure if they are developed to provide thorough guidance on practical aspects of identifying reproductive toxins. To obtain a representative sample of university-level CHPs, we reviewed the CHPs available in 2020 by the 100 top-ranking US graduate chemistry programs¹⁰ for their discussion of reproductive health safety.¹¹ We concluded that the identification of reproductive toxins is nuanced, and that university CHPs vary in the quality of guidance that they provide to researchers for the assessment of risk of exposure to reproductive toxins. Additionally, we found that discussion of reproductive health within university CHPs generally follows a differentiated safety model by specifically advising pregnant workers or workers planning conception to identify and mitigate exposure to reproductive toxins.

While assessing reproductive health guidance, we observed that some CHPs lacked

sufficient discussion of reproductive health safety. We searched for the Top 100 (105) CHPs using a Google search for “[school name] chemical hygiene plan” and found that 87 appeared within the first page of results, 6 were found after further searching, and 12 were not found at all. This led to the inclusion of 93 university CHPs in our assessment. Of the 93 CHPs assessed, only 31 indicated a section on reproductive health safety within the Table of Contents, and only 54 mentioned “pregnan[cy][t]”¹² or “male [reproductive health]” (or both) anywhere in the document.¹³ We view the lack of a reproductive health section within some CHPs as a shortcoming of reproductive health safety guidance in the academic research setting. We believe that all CHPs should contain discussions pertaining to reproductive health to further normalize this topic as an important laboratory safety principle.

In many cases, the language used in CHPs that do include sections on reproductive health implies that reproductive health only affects certain groups, such as pregnant workers or workers planning conception. In our evaluation of 93 CHPs, 17 only mentioned female reproductive health, 9 only mentioned male reproductive health, and 28 mentioned both female and male reproductive health. The mention of only one type of reproductive health in the absence of another suggests that this sensitive group should take on the responsibility of identifying reproductive health risks as well as creating a safe work environment. Unfortunately, this is an unproductive way of protecting individuals from exposure to reproductive toxins and could perpetuate unequal working environments.⁶ It is crucial that language used within CHPs clearly communicates that safety pertaining to reproductive health affects everyone and thus promotes an inclusive safety culture. Next, we evaluated how CHPs inform laboratory workers to utilize resources for the identification of reproductive toxins. Many CHPs recommended that laboratory workers seek advice from the Environmental Health and Safety office, Principal Investigator, or Primary Care Physician. While these resources are indispensable, some laboratory workers may hesitate to take advantage of these resources.¹⁴ For example, the individual could feel that engaging in this discussion would imply to their supervisor that they are planning conception, or they may fear the highly personal nature of the conversation. Due to the private

nature of reproductive health, CHPs should inform laboratory workers about useful discreet resources which they can consult for the identification of reproductive toxins. Improving access to discreet resources should make reproductive health safety guidance available to a broader audience. Our review of CHPs revealed that the discreet resources most commonly recommended by CHPs include SDSs, NPG, and Prop. 65; these resources are open access and provide reproductive health safety guidance without the need for discussion with another individual.

In 48 of the CHPs assessed we found a list of specific examples of reproductive toxins. We compiled a list of all compounds mentioned by CHPs as examples of reproductive toxins, which resulted in 1,087 unique chemicals. Lead and carbon disulfide were the two most commonly listed chemicals, and were given as examples in 23 CHPs. Only 11 CHPs provided a literature reference for the examples, so we decided to carry out our own assessment by investigating how chemicals listed by at least five unique CHPs are classified by SDSs, NPG, and Prop. 65.¹⁵ This assessment revealed inconsistencies in the way these compounds are classified.¹⁵⁻¹⁷ Our findings are depicted in Figure 5-1.

Surprisingly, only 63, 26, and 67 of compounds listed by CHPs as examples of reproductive toxins were classified as reproductive toxins within their respective SDS, NPG, or Prop. 65 entry. Of the 107 compound classifications assessed, only 26 were classified in the same way by all three. Table 5.1 displays the 14 most commonly reported reproductive toxins within CHPs as well as their classification within their respective SDS, NPG, and Prop. 65 entry. The inconsistencies between classifications of these compounds by various sources provides unclear guidance to laboratory workers on the identification of potential reproductive toxins.

To better understand why the classification of compounds as reproductive toxins differs between sources, we investigated the authorship and sources of information for the content provided in CHPs, SDSs, NPG, and Prop. 65. The following information summarizes resources available to laboratory workers containing information on reproductive health safety or identification of reproductive toxins in laboratories. This list highlights the general similarities and differences between these four resources.¹⁶⁻²²

- *Chemical Hygiene Plan (CHP)*

General description of source safety manuals that inform laboratory workers of chemical dangers as well as proper workplace safety practices

Is this a required source? If so, by whom? yes, OSHA

Who writes this? employer (university)

What classifies as a reproductive toxin? discretion of author

How often is this source revised? when there is an updated requirement by OSHA (most recently 2013)

- *Safety Data Sheet (SDS)*

General description of source a source that contains information relating to occupational safety and health for commercially available chemicals

Is this a required source? If so, by whom? yes, OSHA

Who writes this? manufacturer/distributor of the chemical, no legal requirement for authorship

What classifies as a reproductive toxin? discretion of author based on OSHA guidelines for hazard identification and available literature and data concerning the chemical in question

How often is this source revised? within 3 months of new and significant information regarding hazard or ways to protect against hazards, also if there is an audit

- *NIOSH Pocket Guide (NPG)*

General description of source a guide which provides general industrial hygiene information for hundreds of chemicals/classes

Is this a required source? If so, by whom? not required, maintained by CDC

Who writes this? contractors and personnel from various divisions within NIOSH and OSHA

What classifies as a reproductive toxin? compounds for which an REL or PEL has been assigned, based on NIOSH policy documents and references within industrial hygiene, occupational medicine, toxicology, and analytical chemistry

How often is this source revised? periodically to reflect new data regarding the toxicity of various substances and any changes in exposure standards or recommendations

- *Proposition 65 List (Prop. 65)*

General description of source a list which informs Californians of carcinogens and reproductive toxins

Is this a required source? If so, by whom? Yes, State of CA

Who writes this? a team of scientists appointed by the governor of CA

What classifies as a reproductive toxin? compounds known by the state of CA to cause reproductive harm, based on current labor code, states qualified experts, authoritative bodies, and formally required to be labeled

How often is this source revised? annually

These resources have different merits when viewed through the lens of reproductive health safety. We found that the main advantage of CHPs and SDSs is availability. Each is generally available in all university labs and for all commercially available chemicals, respectively. The main drawback for these two documents is their lack of transparency regarding references and authorship. Each university or chemical supplier is responsible for producing their respective CHP or SDSs. Differences in authorship is a possible source of inconsistency which can lead to different interpretations of hazards. For example, when comparing SDSs from different chemical suppliers for *N*-nitrosodimethylamine and 2,4-dichlorophenoxyacetic acid, we find that some companies identify reproductive hazards while others do not (Tables 5.2 and 5.4).²³⁻²⁷ A third example with hexafluoroacetone illustrates how different hydrates of the same molecule contain different reproductive hazard information (Table 5.3).^{28,29} SDSs from different chemical suppliers differ in the information they provide due to differences in literature and data retrieval and interpretation of information by the author.²⁰ Interestingly, an SDS may contain an H340 or H360 hazard statement in Section 2: Hazards Identification but lack a discussion of reproductive toxicity in Section 11: Toxicological Information (or vice versa, Tables 5.2, 5.4, and 5.3). Again, these differences can be attributed to the author's interpretation of guidelines for hazard identification. We present this information to illustrate how a laboratory worker may easily feel overwhelmed or confused in their attempt to identify reproductive toxins. As described in Prudent Practices in the Laboratory, SDSs remain "the best single source for the purpose of evaluating the hazards and assessing the risks of chemical substances". Prudent Practices also highlighting the following important limitations of SDSs: variation in quality depending on chemical supplier, differences in toxicity due to morphology or experimental scale, and overly inclusive lists of hazards which distract from those most likely to cause harm.³⁰

NPG and Prop. 65 communicate that their information is obtained from scientifically credible sources and that these documents are written by experts in the field. Importantly, NPG and Prop. 65 differ in their inclusivity: NPG is exclusive (only includes chemicals that report PELs and RELs) while Prop. 65 is inclusive (includes

all potential reproductive toxins). Prop. 65 stands out in the frequency with which it is revised (annually). SDSs, NPG, and Prop. 65 all contain valuable information which should guide researchers in the identification of chemical reproductive toxins. CHPs should communicate the utility of these resources while also highlighting the important differences and the information one should expect to obtain from each source.

5.3 Conclusion

In conclusion, we have highlighted opportunities for improvement of reproductive health safety guidance provided to university laboratory workers by laboratory CHPs. We recommend the following straightforward changes to CHPs. First, we recommend that all CHPs include a dedicated section on reproductive health safety. Within this section, the language should communicate that all laboratory workers are responsible for safe handling of any potential reproductive toxins. The section should also include recommended resources for laboratory workers to consult for the identification of potential reproductive toxins in their work. Each recommended resource should include an explanation of how it is most effectively utilized. For example, the CHP should suggest NPG and Prop. 65 as reputable resources, and clearly explain the differences between and advantages of each. CHPs should inform laboratory workers that if a compound is not listed as a reproductive toxin within a CHP or SDS, this does not necessarily exclude it as a potential reproductive toxin. While some of the CHPs met many of these criteria, others did not. All laboratory workers need to hear the same message that reproductive health affects everyone. Second, we recommend that all laboratories engage in discussions pertaining to reproductive health. We believe this will help shift the current culture away from a differentiated protection safety model. Specifically, incorporating discussions about reproductive health safety at laboratory group meetings can normalize this topic. The more laboratories are able to discuss reproductive health as a universal safety issue, and create safety plans that will protect everyone, the easier and more habitual these changes will become. Thus, we must

always continue to learn and adapt our behaviors within laboratory settings, which begins with conversations between laboratory colleagues.

We believe the implementation of these changes will lead to the promotion of more inclusive safety models. This type of shift in laboratory safety culture should ultimately provide improved protection for all laboratory workers from reproductive toxins.

5.3.1 Supporting Figures and Tables

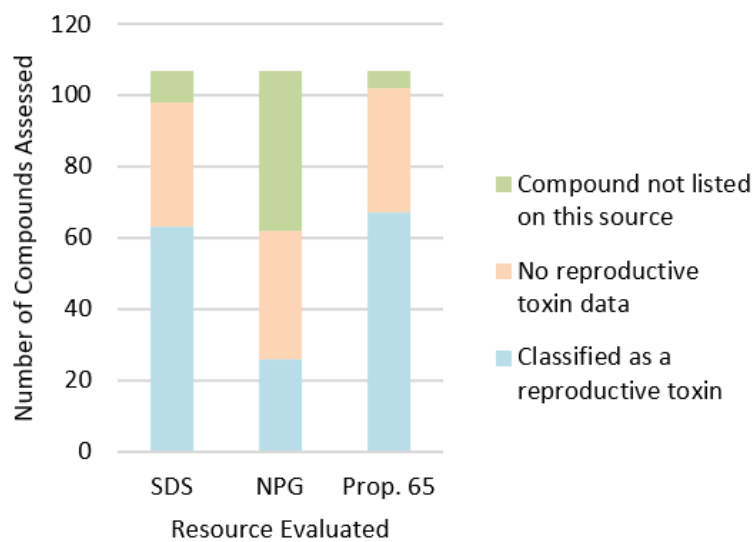


Figure 5-1: The classification by SDSs, NPG, and Prop. 65 of compounds listed as reproductive toxins within 5 or more CHPs.

CAS	Chemical Name ^a	Occurrence in CHPs	Reproductive Information		
			SDS	NPG Prop. 65	
7439-92-1	lead	23	Repr. Tox.	N.D.	Repr. Tox.
75-15-0	carbon disulfide	23	Repr. Tox.	Repr. Tox.	Repr. Tox.
108-88-3	toluene	22	Repr. Tox.	N.D.	Repr. Tox.
71-43-2	benzene	20	N.D.	N.D.	Repr. Tox.
75-21-8	ethylene oxide	20	Repr. Tox.	Repr. Tox.	Repr. Tox.
75-01-4	vinyl chloride	18	N.D.	N.D.	N.D.
96-12-8	1,2-dibromo-3-chloropropane	18	Repr. Tox.	Repr. Tox.	Repr. Tox.
7440-43-9	cadmium	16	Repr. Tox.	N.D.	Repr. Tox.
75-12-7	formamide	16	Repr. Tox.	Repr. Tox.	N.D.
109-86-4	ethylene glycol monomethyl ether	15	Repr. Tox.	Repr. Tox.	Repr. Tox.
1330-20-7	xylene	14	N.D.	N.D.	N.D.
50-00-0	formaldehyde	13	N.D.	N.D.	N.D.
50-18-0	cyclophosphamide	13	Repr. Tox.	Not Listed	Repr. Tox.
67-66-3	chloroform	13	Repr. Tox.	N.D.	Repr. Tox.

^a In total, 1,087 unique reproductive toxins were listed across 93 CHPs, of which 107 compounds were listed in 5 or more CHPs. The compounds in this table are the top 14 examples.

N.D. = no data; Repr. Tox. = classified as a reproductive toxin by this source.

Table 5.1: The 14 chemicals most commonly listed as examples of reproductive toxins within university CHPs and their reproductive toxicity classification by SDSs, NPG, and Prop. 65.



Chemical Substance	<i>N</i> -nitroso-dimethylamine (NDMA)	
	Supplier 1	Supplier 2
SECTION 2: Hazard Identification	–	Germ cell mutagenicity, Category 1B Reproductive toxicity, Category 2 May cause genetic defects Suspected of damaging fertility or the unborn child
GHS Pictograms ³¹		
SECTION 11: Toxicological Information	Germ cell mutagenicity – – –	Germ cell mutagenicity mmo-sat 10 mmol/L (-S9) mmo-sat 50 µL/plate (+S9) msc-hmn-lym 14 mmol/L Reproductive Toxicity orl-mus TDLo: 1940 µg/kg (75D pre/1-22D preg) orl-rat TDLo: 20 mg/kg (20D preg)

Table 5.2: Comparison of SDSs for NDMA from different chemical suppliers.

Chemical Substance	hexafluoroacetone	
SDS Source	Supplier 1 SDS for sesquihydrate	Supplier 2 SDS for trihydrate
SECTION 2: Hazard Identification	–	Reproductive toxicity (Category 2), H361 Suspected of damaging fertility or the unborn child
GHS Pictograms ³¹		
SECTION 11: Toxicological Information	<p>Germ cell mutagenicity Test Type: Ames test Test system: Salmonella typhimurium Result: negative Remarks: (National Toxicology Program)</p> <p>Reproductive Toxicity No data available</p>	<p>Germ cell mutagenicity No data available</p> <p>– – –</p> <p>Reproductive Toxicity Possible risk of congenital malformation in the fetus Suspected human reproductive toxicant No data available No data available</p>

Table 5.3: Comparison of SDSs for hexafluoroacetone from different chemical suppliers.




2,4-dichloro-phenoxyacetic acid			
Chemical Substance	Supplier 1	Supplier 2	Supplier 3
SDS Source	–	Supplier 2	–
SECTION 2: Hazard Identification	–	Toxic to Reproduction [Category 2] Suspected of damaging fertility or the unborn child	–
GHS Pictograms ³¹			
SECTION 11: Toxicological Information	<p>Germ cell mutagenicity No data available</p> <p>–</p> <p>–</p> <p>Reproductive Toxicity Laboratory experiments have shown teratogenic effects No data available</p>	<p>Germ cell mutagenicity dni-ham-ovr 1 mmol/L sce-hmn-lym 10 mg/L mmo-sat 250 µg/plate (-S9)</p> <p>Reproductive Toxicity orl-rat TDLo: 220 µg/kg (1–22D preg) orl-rat TDLo: 500 mg/kg (6–15D preg)</p>	<p>Mutagenic Effects No information available</p> <p>Reproductive Effects No information available</p> <p>Developmental Effects Teratogenicity No information available</p>

Table 5.4: Comparison of SDSs for 2,4-dichloro-phenoxyacetic acid from different chemical suppliers.

5.3.2 Abbreviations

CHP Chemical Hygiene Plan

SDS Safety Data Sheet

NPG NIOSH Pocket Guide

Prop. 65 Proposition 65 list

PEL Permissible Exposure Limit

REL Recommended Exposure Limit

CDC Center for Disease Control and Prevention

OSHA Occupational Safety and Health Administration

NIOSH National Institute for Occupational Safety and Health

CA California.

5.4 References

- [1] Benderly, B. L.; Cautious optimism as society names lab safety a core value. *Science*, October 4, 2017. <https://www.sciencemag.org/careers/2017/10/cautious-optimism-society-names-lab-safety-core-value> (accessed June 17, 2021).
- [2] Ménard, A. D.; Trant, J. F. *Nat. Chem.* **2020**, *12*, 17–27.
- [3] Benderly, B. L.; Déjà vu all over again. *Science*, August 3, 2016. <https://www.sciencemag.org/careers/2016/08/d-j-vu-all-over-again> (accessed June 17, 2021).
- [4] Kemsley, J.; 10 years after Sheri Sangji's death, are academic labs any safer? *Chem. Eng. News*, December 28, 2018. <https://cen.acs.org/safety/lab-safety/10-years-Sheri-Sangjis-death/97/i1> (accessed Apr 7, 2021).
- [5] Selma, A. *Journal of Society for Development in New Net Environment in B&H* **2010**, *4*, 643–651.
- [6] Hansson, S. O.; Schenk, L. *Eur. J. Risk Regul.* **2016**, *7*, 404–412.

- [7] Beyler, R. E.; Meyers, V. K. *J. Chem. Educ.* **1982**, *59*, 759–763.
- [8] Hansson, S. O. *J. Radiol. Prot.* **2009**, *29*, 211–218.
- [9] Occupational Safety and Health Administration, United States Department of Labor. Section 1910.1450 *Occupational exposure to hazardous chemicals in laboratories*. <https://www.osha.gov/laws-regs/regulations/standardnumber/1910/1910.1450> (accessed Mar 26, 2021).
- [10] 105 schools are ranked within the top 100 due to ties in the rankings; thus 105 CHPs were evaluated.
- [11] U.S. News and World Report. Best Chemistry Programs. <https://www.usnews.com/best-graduate-schools/top-science-schools/chemistry-rankings> (accessed Mar 23, 2021).
- [12] For simplification, we used pregnan[t][cy] as a key word to identify female reproductive health within CHPs. We understand that not all pregnant people identify as female, and not all males undergo spermatogenesis.
- [13] The remaining 39 CHPs did not mention these terms anywhere in the document. Determined by searching keywords or reading through the document if not searchable.
- [14] Pain, E.; Pregnancy and the Lab–Feature Index. *Science*, April 7, 2006. <https://www.sciencemag.org/careers/2006/04/pregnancy-and-lab-feature-index> (accessed Apr 7, 2021).
- [15] (a) This resulted in the evaluation of 107 unique compounds. (b) SDSs were obtained for commercially available compounds manufactured by Sigma-Aldrich (MilliporeSigma), TCI America, or Alfa Aesar matching the assigned CAS numbers.
- [16] Center for Disease Control and Prevention. NIOSH Pocket Guide to Chemical Hazards. <https://www.cdc.gov/niosh/npg/default.html> (accessed Mar 26, 2021).
- [17] California Office of Environmental Health Hazard Assessment. The Proposition 65 List. <https://oehha.ca.gov/proposition-65/proposition-65-list> (accessed Mar 26, 2021).
- [18] Occupational Safety and Health Administration, United States Department of Labor. Section 1910.1200 Toxic and Hazardous Substances, revised March 26, 2012. <https://www.osha.gov/laws-regs/regulations/standardnumber/1910/1910.1200> (accessed Mar 26, 2021).
- [19] United States Department of Labor. Hazard Communication. <https://www.osha.gov/hazcom> (accessed Mar 26, 2021).

- [20] Foulke, E. G.; Occupational Safety and Health Administration, United States Department of Labor. Guidance for Hazard Determination for Compliance with the OSHA Hazard Communication Standard. <https://www.osha.gov/hazcom/ghd053107> (accessed Jul 13, 2021).
- [21] Center for Disease Control and Prevention. NIOSH Pocket Guide to Chemical Hazards. Introduction. <https://www.cdc.gov/niosh/npg/pgintrod.html> (accessed Mar 26, 2021).
- [22] California Office of Environmental Health Hazard Assessment. About Proposition 65. <https://oehha.ca.gov/proposition-65/about-proposition-65> (accessed Mar 26, 2021).
- [23] *N*-Nitrosodimethylamine (NDMA), USP Reference Standard; CAS RN 62-75-9; Sigma Product No. 1466674; Revision Date Apr 21, 2021. <https://www.sigmaaldrich.com/US/en/product/usp/1466674?context=product> (accessed Jul 14, 2021).
- [24] *N*-Nitrosodimethylamine (NDMA), >99.0%(GC); CAS RN 62-75-9; TCI Product No. D0761; Revision Date Oct 11, 2018. <https://www.tcichemicals.com/AU/en/p/D0761documentsSectionPDP> (accessed Jul 14, 2021).
- [25] 2,4-Dichlorophenoxyacetic acid, >95%, crystalline; CAS RN: 94-75-7; Sigma-Aldrich Product No. D7299; SDS Revision Date Apr 18, 2021. <https://www.sigmaaldrich.com/US/en/sds/sigma/d7299> (accessed Jul 14, 2021).
- [26] 2,4-Dichlorophenoxyacetic acid, >97.0%(T); CAS RN: 94-75-7; TCI America Product No. D0396; SDS Revision Date Mar 18, 2021. <https://www.tcichemicals.com/US/en/p/D0396documentsSectionPDP> (accessed Jul 14, 2021).
- [27] 2,4-Dichlorophenoxyacetic acid, 98%; CAS RN: 94-75-7; Alfa Aesar Product No. A12467; SDS Revision Date Feb 14, 2020. <https://www.alfa.com/en/msds/?language=ENsubformat=AGHSsku=A12467> (accessed Jul 14, 2021).
- [28] Hexafluoroacetone sesquihydrate for synthesis; CAS RN: 13098-39-0; Sigma-Aldrich Product No. 8.04521; SDS Revision Date Jul 1, 2021. <https://www.sigmaaldrich.com/US/en/sds/mm/8.04521> (accessed Jul 14, 2021).
- [29] Hexafluoroacetone trihydrate, 98%; CAS RN 34202-69-2; Sigma-Aldrich Product No. 139238; SDS Revision Date Jan 15, 2020. <https://www.sigmaaldrich.com/US/en/sds/aldrich/139238> (accessed Jul 14, 2021).

- [30] National Research Council, Prudent Practices in the Laboratory: Handling and Management of Chemical Hazards, Updated Version. Washington, DC: The National Academies Press, 2011.
- [31] United States Department of Labor, Occupational Health and Safety Administration. Hazard Communication: Hazard Communication Pictograms. <https://www.osha.gov/hazcom/pictograms> (accessed Mar 26, 2021).